





# TS SR

Trinity Student  
Scientific Review

Volume V



# TS SR

Trinity Student Scientific Review

Volume V

Published by the Trinity Student Scientific Review  
c/o Faculty of Engineering, Mathematics and Science,  
Trinity College, Dublin 2  
Republic of Ireland.

All rights reserved.  
Copyright © contributors to the  
Trinity Student Scientific Review 2019

All views expressed herein are those of the authors and do  
not necessarily reflect the views of the editors or sponsors.

This journal claims no special rights or privileges.

Print managed by Custodian

Cover by Tigran Simonian

Photography by Tigran Simonian, David Simonian and Dale  
Chen

The TSSR logo created by Ger Walsh at Magnet Design in  
2014.

The Trinity Student Scientific Review is also available online  
at <http://trinityssr.com>

Inquiries at [trinsnr@tcd.ie](mailto:trinsnr@tcd.ie)

# TS SR

**The Trinity Student Scientific Review  
is kindly sponsored by**

The Faculty of Engineering, Mathematics and Science  
Trinity College Dublin

# SPONSORSHIPS

The entire editorial board of TSSR would like to take a moment to convey our profound gratitude in the diligence, patience, and hard work of all the Faculty of the Engineering, Mathematics, and Science in Trinity College Dublin. Without their support, Volume V would not have been possible.



**Trinity College Dublin**  
Coláiste na Tríonóide, Baile Átha Cliath  
The University of Dublin

With Thanks to:  
TCD Association & Trust

# IdentiGEN

With Thanks to:  
IdentiGEN

# TSSR Volume V Committee



*Back Row (L to R): Tigran Simonian, Natalie Ness, Kathryn Yeow, Ciarán Ó Cuív, Maxime Deckers*

*Front Row (L to R): Alva Casey, Danielle Olavario, Aislinn O'Brien*

*Right Insert: Ronan Treanor*

<b>General Manager</b>	Danielle Olavario
<b>Deputy General Manager</b>	Tigran Simonian
<b>Financial Officer</b>	Aislinn O'Brien
<b>Life Sciences Editor</b>	Alva Casey
<b>Assistant Life Sciences Editor</b>	Ronan Treanor
<b>Assistant Life Sciences Editor</b>	Natalie Ness
<b>Chemistry Editor</b>	Kathryn Yeow
<b>Natural Sciences Editor</b>	Ciarán Ó Cuív
<b>Physics Editor</b>	Maxime Deckers

# PRIZE-WINNING REVIEWS

## **Best Overall Review**

**Auroral Radio Emission: A Potential Method for the Direct  
Detection of Exoplanets**

Niamh Feeney

## **Best Natural Sciences Review**

**Not with a Bang but with a Whimper: Plant Evolution  
During Mass Extinctions**

Jessie Dolliver

## **Best Chemistry Review**

**Electrospinning and the Redox Flow Battery: a Fabrication  
Method for Biomass-derived Electrodes**

Lia Grogan

## **Best Life Sciences Review**

**The Gut-Brain Axis in Mental Health and Parkinson's  
Disease**

Áine McCabe

## **Best Fresher Review**

**Structure, Function and Pathogenic Mutations of Mitochondrial  
Complex I: Implications for Human Disease**

Jane Cook

# ACKNOWLEDGEMENTS

Life Sciences Editor	Alva Casey
Assistant Life Sciences Editors	Ronan Treanor Natalie Ness
Life Sciences Peer Reviewers	Chloe Choi, Joseph O'Callaghan, Elaine Dempsey, Niamh Mohan, Arnas Petrauskas, Conor Rossi, Daniel Fortunati
Natural Sciences Editor	Ciarán Ó Cuív
Natural Sciences Peer Reviewers	Fionn Ó Marcaigh, Paula Tierney, Cian White
Chemistry Editor:	Kathryn Yeow
Chemistry Academic Advisor:	Dr. Mike Southern
Chemistry Peer Reviewers:	Mike Southern, Mike Lyons, Isabel Rozas, Peter Dunne, Mathias Senge

Physics Editor:

Maxime Deckers

Physics Academic Advisor:

Dr. David McCloskey

Physics Peer Reviewers:

Dr. David McCloskey,  
Hugh Manning,  
Robert Kavanagh,  
Calin Hrelescu

TS  
SR

# **LIFE SCIENCES**

## **Letter from the Editors**

1

## **STRUCTURE, FUNCTION AND PATHOGENIC MUTATIONS OF MITOCHONDRIAL COMPLEX I: IMPLICATIONS FOR HUMAN DISEASE**

Jane Cook

5

## **A GLIAL PERSPECTIVE: THE ROLE OF ASTROCYTES IN ALZHEIMER'S DISEASE**

Cliona Farrell

17

## **ERADICATION OF MEASLES VIRUS**

Laura Hennelly Mc Carthy

27

## **GLIOBLASTOMA MULTIFORME AND THE CANCER STEM CELL MODEL**

Ellen Tuck

39

## **THE USE OF BIKES AND TRIKES AS A CANCER IMMUNOTHERAPY**

Cathal Keane

51

**THE GUT-BRAIN AXIS IN MENTAL HEALTH AND PARKINSON'S  
DISEASE**

Áine McCabe

63

**POLYGENIC RISK SCORES AND COMPLEX DISEASE**

Iseult Jackson

73

**AN INTEGRATIVE NEUROSCIENTIFIC EVALUATION OF SOCIAL  
MOTIVATION AND REWARD**

Áine Heffernan

83

# NATURAL SCIENCES

**Letter from the Editor**

93

**VENTIFACTS: WHERE FORM MEETS FUNCTION**

Maria Cordero

97

**NOT WITH A BANG BUT WITH A WHIMPER: PLANT EVOLUTION  
DURING MASS EXTINCTIONS**

Jessie Dolliver

105

# CHEMISTRY

## Letter from the Editor

115

## CYCLIC PEPTIDE THERAPEUTICS: A BRIEF OVERVIEW

Susie Calvert

119

## ELECTROSPINNING AND THE REDOX FLOW BATTERY: A FABRICATION METHOD FOR BIOMASS-DERIVED ELECTRODES

Lia Grogan

131

## PT(IV) COMPLEXES AS PRODRUGS FOR TRADITIONAL PT(II) DRUGS

Aoife Donaghy

143

## PHOTON UPCONVERSION BY TRIPLET PHOTSENSITISER COMPLEXES

Luke Doolan

155

# PHYSICS

## Letter from the Editor

169

## FLEXIBLE ELECTRONICS AND THE PRE-STRAIN STRATEGY: A POSITIVE SIDE TO WRINKLING

Lucy Prenderville

173

## AURORAL RADIO EMISSION: A POTENTIAL METHOD FOR THE DIRECT DETECTION OF EXOPLANETS

Niamh Feeney

185

## RECENT RESEARCH ON PHASE CHANGE MATERIAL VANADIUM DIOXIDE

Jill Ivers

195

## WORTH ITS SALT? A STUDY OF SALINITY GENERATED ENERGY AND ITS (ELECTRICAL) CURRENT CHALLENGES

Pierce Sinnott

205

TS  
SR

## Welcome

We live in a scientific golden age. There are breakthroughs almost every day which develop our understanding of every topic imaginable. However, we also live in a new era of antiscience activism. Our society's trust on science and its experts has eroded to the point that fake news and "alternative facts" have become part of our vernacular. Many have become cynical of the scientific process and therefore its discoveries; many climate change deniers, for example, hold political power and determine policy, while the anti-vaccination movement endures, as is reflected by the fact that measles outbreaks have been reported all around the world in the first three months of 2019.

In the very first Trinity Student Scientific Review published in 2015, general managers Johnny Deane & Georgia O'Sullivan said that TSSR aims to "provide Trinity science undergraduates with an opportunity to bridge the gap between their degree and the research-driven world of science." A lot has changed in this publication and in the state of the world since 2015, but this core mission remains the same. In 2019, TSSR aims to allow science to be more accessible not only to science undergraduates but also to the wider college community. TSSR is our attempt to cut through the noise in whatever way we can and allow for science to be more inclusive.

The fifth volume of Trinity Student Scientific Review would not have been possible without a few people. First, our sincerest thanks to Dean Vinny Cahill and the Faculty of Engineering, Maths and Science, for their unwavering support and faith in the TSSR team. We also owe an enormous debt of gratitude to this year's sponsors, Identigen and TCD Trust. I would also like to thank Gemma Mortell, last year's general manager, and the rest of TSSR Volume IV team for their support.

Lastly, this review would not have been achieved without this year's phenomenal team: Tigran Simonian, Aislinn O'Brien, Alva Casey, Natalie Ness, Ronan Treanor, Kathryn Yeow, Maxime Deckers and Ciarán Ó Cuív. Thank you all so much for your hardwork.

It is with immense pride that we bring to you Trinity Student Scientific Review Volume V

Danielle Olavario

General Manager, Trinity Student Scientific Review Vol. V

TS  
SR



# Life Sciences

TS  
SR

## Letter from the Editors

The Life Sciences section consists of a collection of reviews that encompass a broad spectrum of topics. These reviews showcase the diversity of the biological moderatorships that are undertaken by students here in Trinity College. As such, you will find that this section includes reviews on research in areas of microbiology, genetics, immunology and more. The enthusiasm and passion of Trinity students for the life sciences is evident in both the volume of submissions that we received and also in the quality of the reviews, for which the authors should be highly commended.

Research in the life sciences is vital to advances in medicine and continues to improve human health and living standards. The reviews published in this, the fifth year of Trinity Student Scientific Review's life sciences section, is a reflection of this statement. The editorial board for the life sciences section selected reviews that captured the cutting-edge research being conducted in diverse fields of study. The authors have successfully presented comprehensive and informed reviews that are indicative of critical scrutiny of the current scientific thinking and literature. The outstanding quality of the reviews published in this year's life sciences section is a testament to the ability and talent of the authors.

The editorial process was directed by the advice and guidance of a team of peer reviewers. We would like to express our gratitude to all the peer reviewers whose input and support were invaluable in bringing the life sciences section to fruition. We would also like to thank all the students who prepared a submission for publication. The diligence shown by those students who undertook the difficult task of evaluating complex fields of research is admirable. This commitment to and passion for research is a clear reflection of the academic drive that is encouraged in Trinity.

Effective scientific communication is a critical skill for any science graduate regardless of whether or not they pursue a career in scien-

tific research. The ability to convey complex experimental evidence and summarise exciting and every expanding research fields in a short review requires a combination of brevity and clarity that is demonstrated in all the published reviews. There is no doubt that all the authors that took part in the editorial process have improved their scientific writing. This skill will be of great benefit to them in their academic future.

It has been a pleasure to serve on the editorial board for the life sciences section. We have thoroughly enjoyed reading the reviews and we are delighted to share them in this volume of TSSR. We hope that you find them as intriguing and inspiring as we did.

Alva Casey, Natalie Ness and Ronan Treanor

Life Science Editors

Trinty Student Scientific Review 2019

# STRUCTURE, FUNCTION AND PATHOGENIC MUTATIONS OF MITOCHONDRIAL COMPLEX I: IMPLICATIONS FOR HUMAN DISEASE

Jane Cook

Junior Fresh

Biological and Biomedical Sciences

*Mitochondria produce energy in the form of ATP through oxidative phosphorylation via a series of enzyme complexes. The first, largest, and least understood enzyme in this process is NADH:ubiquinone oxidoreductase (complex I). The L-shaped enzyme consists of 14 core subunits and up to 32 supernumerary subunits and its main function is a series of electron transfer processes culminating in proton translocation across the mitochondrial inner membrane in order to power ATP synthesis. Complex I deficiency has been implicated as a cause of several severe mitochondrial disorders and a number of associated DNA mutations have been identified. The enzyme is also known to be a source of deleterious reactive oxygen species which are linked to Parkinson's Disease. The importance of this enzyme in normal cell function cannot be overstated and further study of complex I is crucial to being able to understand and treat a variety of disorders*

## Introduction

Mitochondria are ubiquitous organelles responsible for producing energy in the form of ATP through the process of oxidative phosphorylation (OXPHOS). OXPHOS is powered by five enzyme complexes embedded in the inner mitochondrial membrane, with NADH:ubiquinone oxidoreductase (complex I) being the first and largest enzyme in the respiratory chain<sup>1, 2</sup>. Complex I is an L-shaped molecule, with one arm embedded in the mitochondrial membrane and a peripheral arm protruding into the matrix<sup>2</sup>. Though a few papers describe mammalian complex I as being composed of 44 subunits<sup>3, 4</sup>, it is typically understood that the mammalian enzyme is composed of 45 subunits<sup>1, 4, 5</sup>. There does not appear to be a well-defined reason for this discrepancy, but given the fact that bacterial complex I consists

of a mere 14 subunits while human complex I consists of 45, it is possible that some slight variation may occur even between mammal species. 7 of the subunits are encoded in the mitochondrial DNA (mtDNA) and the remaining subunits are encoded in the nuclear DNA (nDNA)<sup>4,5</sup>. Recent research has uncovered a number of assembly factors required for the correct biosynthesis of complex I, adding another piece to the puzzle of understanding this complicated enzyme. For the purpose of consistency, human nomenclature will be used throughout this review. nDNA-encoded subunits have the prefix “NDU,” mtDNA subunits have the prefix “ND” and assembly factors are denoted “NDUFAF” or given their common name, all with their corresponding numbers.

It is vital that the structure, function and assembly of complex I be fully understood as a deficiency of the fully-functioning enzyme can cause severe disorders. Approximately 1 in 5000 adults suffer from mitochondrial diseases<sup>7</sup>, with a deficiency of complex I being the most common single enzyme cause<sup>5</sup>. Complex I deficiency has been linked to numerous disorders, including Leber’s Hereditary Optic Neuropathy (LHON), Mitochondrial Encephalomyopathy, Lactic Acidosis and Stroke-like episodes (MELAS), Leigh Syndrome (LS) and Parkinson’s<sup>1</sup>. It has also been suggested that complex I is a source of deleterious reactive oxygen species (ROS), which have been implicated as a cause of some neurodegenerative diseases<sup>8</sup>.

Despite their relative frequency, there are few effective treatments and no known cure for mitochondrial diseases<sup>9</sup>. This is partly due to the sheer number and diversity of genetic mutations that result in decreased mitochondrial function, as well as the variety of clinical presentations. For example, the same mtDNA point mutation can result in two different complex I deficiency disorders in two different patients<sup>1,9</sup>. In addition, pathogenic mutations have been identified in both mtDNA and nDNA encoded complex I subunits as well as in enzyme assembly factors<sup>5</sup>. The involvement of two genomes combined with the complex relationship between genotype and phenotype for complex I deficiency disorders makes diagnosis and therefore research a formidable task.

This review aims to summarize the current understanding of the structure and function of mammalian complex I, disorders related to complex I, and ultimately, call for further investigation of this essential enzyme.

## Structure and Function of Complex I

The characteristic L-shaped structure of complex I was first identified by electron microscopy, and all but one of the published reconstructions of the enzyme exhibit this shape<sup>10, 11</sup>. Though the existence and approximate number of individual enzyme subunits had been discovered, their relative positions and relation to function were unknown until later studies. Baradaran et. al reported the first crystal structure of the entire, intact complex in *Thermus thermophilus* in 2013,

identifying the locations of the individual subunits in the enzyme as well as the locations of the functional modules<sup>12</sup>. The detailed model they developed was consistent with the accepted models at that time, like that determined from the yeast *Yarrowia lipolytica* by Radermacher et. al in 2006<sup>11</sup>. Efforts have been made to extrapolate these findings to human complex I through study of the extremely similar mammalian enzyme in bovine complex I, as the bovine complex comprises 45 subunits<sup>13</sup>. Across species, complex I consists of 14 “core” subunits that house the enzyme’s catalytic machinery and can form the minimal structure necessary to perform the bioenergetic functions of the enzyme<sup>4</sup>. Seven of these subunits are hydrophobic and encoded by mtDNA (ND1, ND2, ND3, ND4, ND4L, ND5 and ND6), while the other seven are hydrophilic and encoded by nDNA (NDUFB1, NDUFB2, NDUFB3, NDUFB4, NDUFB5, NDUFB6 and NDUFB7)<sup>12, 14</sup>. Up to 32 supernumerary subunits may also be present, and it is suggested that they are involved in regulation and/or stability of the enzyme. A model of mammalian complex I can be seen in Figure 14. Prokaryotic complex I consisting of just the 14 core subunits has a mass of about 550 kDa, while the 45 subunit mitochondrial complex I in mammals has a combined mass of over 980 kDa<sup>16</sup>.

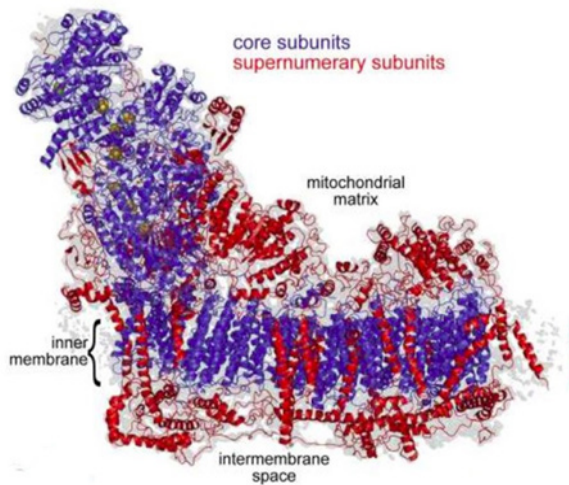


Figure 1: Figure and information in description from Zhu et. al unless stated otherwise<sup>4</sup>. A cryoelectron microscopy (cryoEM) map of mammalian complex I from *Bos taurus* from Zhu et. al. The 14 core subunits are identified in blue, the 31 supernumerary subunits are labeled in red and the cryoEM density is presented as grey.

Complex I can be divided into three functional modules: the N or electron input module that oxidizes NADH, the Q or electron output module that reduces ubiquinone, and the P module which translocates protons across the inner membrane<sup>14</sup>. The N and Q modules are located in the hydrophilic, peripheral arm

of the enzyme, as shown by both Baradaran et. al and Sazanov et. al<sup>12, 17</sup>. These two modules contain all of the redox centers of the enzyme: non-covalently bound flavin mononucleotide (FMN) and up to nine iron-sulfur (Fe-S) clusters<sup>12</sup>. The electrons from NADH oxidation are passed to FMN and then, via a series of Fe-S clusters, reach ubiquinone (also referred to as coenzyme Q) which is subsequently reduced<sup>4</sup>. This series of electron transfer reactions generates enough energy, through conformational changes in the membrane arm (P module) of the enzyme, to pump four protons into the intermembrane space<sup>4</sup>. Approximately 40% of the electrochemical gradient that drives ATP synthesis comes from these four protons, demonstrating the crucial role of complex I in OXPHOS<sup>18</sup>.

## Assembly of Complex I

The correct biogenesis of complex I relies on coordinated assembly of its subunits, a largely unknown process<sup>19</sup>. Mutations in the subunit-encoding genes often cause errors in the assembly process thus resulting in disease<sup>20</sup>. This has become the subject of intense research interest, with studies leading to models for assembly as well as the identification of numerous assembly factors involved in the process<sup>6</sup>. Conflicting models have been proposed for the mechanism of complex I assembly. Antonicka et. al investigated stalled intermediates of the complex in muscle mitochondria from patients with complex I deficiency using blue native polyacrylamide gel electrophoresis (BN-PAGE)<sup>21</sup>. From their results, they proposed a model of assembly where subunits of both the membrane and peripheral arms were found together in early intermediates<sup>21</sup>. In a conflicting investigation, Hofhaus and Attardi studied a human cell line lacking the ND4 subunit due to a frameshift mutation in the mtDNA<sup>22</sup>. Their results showed that while ubiquinone reduction, which occurs extremely close to the membrane arm P module, ceased completely, NADH:Fe(CN)<sub>6</sub> oxidoreductase activity, another electron transfer process in the peripheral arm, was normal<sup>22</sup>. This demonstrated that the membrane arm lacking the ND4 subunit did not form correctly but that the peripheral arm did, suggesting that the two arms are formed independently<sup>22</sup>. Subsequently, Bai and Attardi achieved a very similar result studying complex I lacking the ND6 subunit, where the function of the membrane arm ceased entirely but function in the peripheral arm was normal<sup>23</sup>. Following further study, the role of assembly factors was introduced and some commonality emerged among the conflicting models. McKenzie and Ryan combined existing research and models to propose a consensus for human complex I assembly including the aid of assembly factors identified at that point (Fig. 2)<sup>6</sup>.

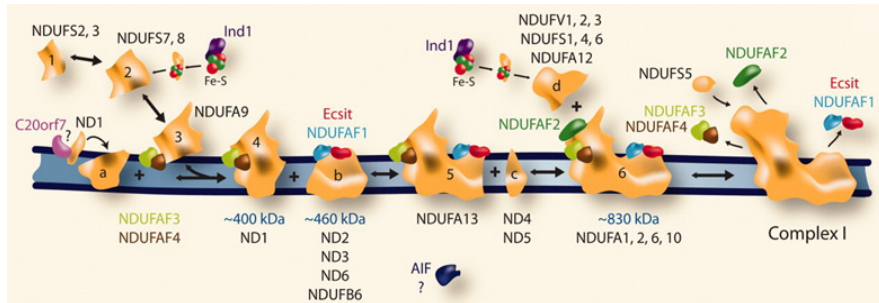


Figure 2: Figure and information in description from McKenzie and Ryan unless stated otherwise<sup>6</sup>. Proposed model for human complex I assembly from McKenzie and Ryan. Entry points of structural subunits are indicated by black arrows, mitochondrial membrane is indicated by horizontal blue stripe. Subunits NDUFS2, 3, 7 and 8 form the Q module during the early stages of assembly. NDUFA9 is added and the resulting intermediate is then anchored to the membrane by the assembly factors Ndufaf3 (C3orf60) and Ndufaf4 (C6orf66). ND1 is then added while the membrane arm subunits ND2, ND3, ND6 and NDUFB6 assemble with the aid of assembly factors Ndufaf1 and Ecsit. The two large intermediates then join with ND4 and ND5 and assemble together. Assembly factors Ndufaf1, Ndufaf2, Ecsit, Ndufaf3 and Ndufaf4 are involved in assembly from this point until the addition of an intermediate containing the N module completes the enzyme.

Though this linear model of complex I assembly is widely accepted, it should be noted that the precise mechanism is still under some debate and will require further research. However, even with a limited understanding of assembly, exciting new studies have begun exploring cross-linking subunits while maintaining function of the enzyme, which could have potential for future therapy development<sup>24</sup>.

## Clinical Phenotypes of Complex I Deficiency

Symptoms of complex I deficiency typically arise early in life, and can affect just one organ in the body but are frequently multisystemic in nature<sup>9</sup>. Pathogenic mutations have been identified in 20 nDNA-encoded subunits, ten nDNA-encoded assembly factors, and all seven of the mtDNA-encoded subunits<sup>25</sup>. The variety of severe diseases resulting from complex I deficiency emphasizes the need for more research into effective treatments and cures of these disorders. It should be noted that the following is not a list of all known disorders, just those that are relatively well-documented with some studies of note.

### *Disorders Associated with nDNA and Assembly Factor Mutations*

#### *Leigh Syndrome*

Leigh syndrome (LS) is one of the most common complex I-linked disorders, as

disease-causing mutations have been identified in nDNA-encoded subunits, assembly factors and mtDNA-encoded subunits<sup>5</sup>. In fact, LS is the most common clinical presentation of mitochondrial disease in children, with nearly 80% of pediatric patients exhibiting complex I deficiency developing the syndrome<sup>26</sup>. LS is a severe neurological disorder characterized by brain lesions that develop on the basal ganglia, cerebellum and brainstem of affected patients<sup>27</sup>. Affected individuals typically experience progressive loss of mental and movement abilities until death within two to three years, usually because of respiratory failure<sup>27</sup>. A number of specific nDNA mutations that cause LS have been identified, with some studies also identifying the specific effect resulting from a given mutation. In 2017, Baertling et. al identified a homozygous missense variant of the assembly factor NDUF4F that prevented the Q module of the enzyme from forming<sup>28</sup>. Earlier, in 2013, four novel, pathogenic mutations in NDUFV1 and NDUF52 were identified by Marin et. al through study of six patients with LS<sup>29</sup>. Mutations have also been identified in the subunits NDUF51, 3, 4, 6, 7 and 8, NDUF41, 2, 10 and 12 as well as assembly factors C8orf38, FOXRED1, and NUPBL<sup>18</sup>.

### *Lactic Acidosis*

Lactic acidosis has been linked to nDNA mutations in subunits NDUFV1, NDUF51, 2, 4, 6 and 7, NDUF410 and 11, and seven assembly factors<sup>18</sup>. This congenital disease is rapidly progressive and can present in conjunction with other mitochondrial disorders<sup>30</sup>. It is caused by a buildup of lactate in the body that eventually leads to multiple organ failure and death<sup>30</sup>.

### *Leukoencephalopathy*

Leukoencephalopathy is a condition characterized by developmental abnormalities or degeneration of white matter in the brain<sup>31</sup>. Ferreira et. al identified a mutation in NDUF51 causing leukoencephalopathy associated with complex I deficiency<sup>32</sup>. Their findings were supported by introducing the same mutation in the fungus *Neurospora crassa*, where severe complex I deficiency was also observed<sup>32</sup>. Nearly all complex I-related leukoencephalopathy is linked to mutations either in NDUF51 or NDUFV1<sup>18</sup>.

### *Cardiomyopathy*

Cardiomyopathy is a term for diseases of the heart, often causing the muscle to become thicker or rigid and subsequently weakened<sup>33</sup>. Fassone et. al identified two heterozygous missense mutations in the NDUF4F1 assembly factor gene as the cause of fatal cardiomyopathy in patients with isolated complex I deficiency<sup>34</sup>. Mutations in the subunits NDUFV2, NDUF54 and 8, NDUF42 and 11 as well as five assembly factors have also been implicated as causes of cardiomyopathy<sup>18</sup>.

## *Disorders Associated with mtDNA Mutations*

### *Leigh Syndrome*

As previously mentioned, mutations causing complex I specific LS have been identified in both nDNA encoded subunits and assembly factors as well as mtDNA encoded subunits. Pathogenic mutations have been identified in the genes for ND1, 2, 3, 4, 5 and 6<sup>10</sup>.

### *Mitochondrial Encephalomyopathy, Lactic Acidosis and Stroke-like Episodes (MELAS)*

MELAS is a multisymptomatic, multisystemic condition that particularly affects the brain, nervous system and muscles<sup>35</sup>. Lactic acidosis and stroke and seizure-like episodes are characteristic symptoms of the disease<sup>35</sup>. Pathogenic mutations in both ND1 and ND5 have been identified, but the ND5 gene appears to be a particular “hot-spot” for mutations causing MELAS<sup>36</sup>.

### *Leber’s Hereditary Optic Neuropathy (LHON)*

LHON was one of the first conditions definitively linked to complex I deficiency, and mutations of distinct complex I genes are a central pathogenic feature of the disease<sup>37</sup>. A mutation in the ND4 gene has been linked to a significant number of LHON cases, while mutations in ND1, 2 and 5 also appear significant<sup>37</sup>.

## **Neurodegenerative Disorders and Reactive Oxygen Species (ROS)**

Reduced OXPHOS function has long been linked to neurodegenerative diseases like Parkinson’s Disease (PD) and Alzheimer’s Disease (AD), but the exact relationship between the two and the possible implications of ROS in the ageing process have recently rendered the topic extremely controversial<sup>38</sup>. In 1983, Langston et. al discovered that the use of 1-methyl-4-phenyl-1,2,5,6-tetrahydropyridine (MPTP) inhibited complex I function and resulted in an acute parkinsonism syndrome that was indistinguishable from PD, leading to the conclusion that pathogenesis of PD was directly related to complex I deficiency<sup>39</sup>. However, the subsequent research was inconclusive, as complex I mutations were not consistently identified in PD or AD patients, and it was unclear whether the reduced function caused the diseases or resulted from the diseases<sup>38</sup>. Mitochondrial dysfunction cannot be ignored, however, as it and oxidative stress have been implicated in cell ageing which is the greatest risk factor for neurodegenerative diseases like PD and AD<sup>40, 41</sup>. ROS are suggested to be causes of oxidative stress, and research has shown that complex I produces ROS<sup>42, 43</sup>. Recent studies uncovered a plant extract, Salidroside, that exhibits neuronal cell protection from parkinsonism by inhibiting an ROS and nitric

oxide pathway<sup>40</sup>. Although previous hypotheses focused on OXPHOS deficiency as a cause of PD and AD, these results suggest that ROS may play a much bigger role in their pathogenesis than was previously realized. If cells can be protected from parkinsonism by inhibition of a single ROS and nitric oxide pathway, that indicates that ROS are far bigger factors in PD pathogenesis than previously known. Once researched more thoroughly, a comprehensive understanding of ROS produced by complex I and their effect on cells could be the next step towards understanding and treating PD.

## Concluding Remarks

Since its initial discovery, tremendous progress has been made in understanding the structure, function and pathogenic mutations of mitochondrial complex I. Advances in techniques like BN-PAGE and genetic sequencing have revealed the complexity of this enzyme and begun to decipher its role in cell function and disease, but a massive knowledge gap remains. This review summarized the current research on complex I in order to highlight how much research still needs to be done. The handful of disorders mentioned, with the exception of Parkinson's and Alzheimer's, are early-onset, rapidly progressive and often fatal. For all these disorders, treatment is limited and there is no cure. Thus, it will be important to pursue investigations into the exact defects in the complex caused by a given mutation, and to examine the role of ROS in pathogenesis of Parkinson's and Alzheimer's in order to begin developing effective therapies. Exploration of the effects of cross-linking subunits to one another while maintaining enzyme function is an emerging field of study, along with studies like the use of a plant extract to uncover the relationship between complex I, ROS and PD. Novel approaches like these and comprehensive knowledge of the structure and function of complex I are the key to eventually understanding the largest and most complicated enzyme in the respiratory chain.

## References

1. McKenzie M. Mitochondrial DNA mutations and their effects on complex I biogenesis: implications for metabolic disease. In: St. John JC, editor. *Mitochondrial DNA, mitochondria, disease and stem cells*. New York: Springer Science + Business Media; 2013. p. 25-47
2. Sharma LK, Lu J, Bai Y. Mitochondrial respiratory complex I: Structure, function and implication in human disease. *Curr Med Chem* [Internet]. 2009
3. Sánchez-Caballero L, Gerrero-Castillo S, Nijtmans L. Unraveling the complexity of mitochondrial complex I assembly: a dynamic process. *Biochim Biophys Acta* [Internet]. 2016 Mar [cited 2019 Jan 02];1857(7):980-90.
4. Zhu J, Vinothkumar KR, Hirst J. Structure of mammalian respiratory complex I. *Nature* [Internet]. 2016 Aug [cited 2019 Jan 03];536(7616):354-58.
5. Rodenburg RJ. Mitochondrial complex

- I-linked disease. *Biochim Biophys Acta* [Internet]. 2016 Feb [cited 2019 02 Jan];1857(7):938-45.
6. McKenzie M, Ryan MT. Assembly factors of human mitochondrial complex I and their defects in disease. *IUBMB Life* [Internet]. 2010 April [cited 2019 Jan 24];62(7):497-502.
7. Ng YS, Turnbull DM. Mitochondrial disease: genetics and management. *J Neurol* [Internet]. 2015 Aug [cited 2019 Jan 25];263:179-91.
8. Hunte C, Zickermann V, Brandt U. Functional modules and structural basis of conformational coupling in mitochondrial complex I. *Science* [Internet]. 2010 Jul [cited 2019 Jan 24];329(5990):448-51.
9. Gorman GS, Schaefer AM, Ng Y, Gomez N, Blakely EL, Alston CL, et al. Prevalence of nuclear and mitochondrial DNA mutations related to adult mitochondrial disease. *Ann Neurol* [Internet]. 2015 Feb [cited 2019 Jan 02];77(5):753-59.
10. Fassone E, Rahman S. Complex I deficiency: clinical features, biochemistry and molecular genetics. *J Med Genet* [Internet]. 2012 Oct [cited 2019 Jan 03];49(9):578-90.
11. Radermacher M, Ruiz T, Clason T, Benjamin S, Brandt U, Zickermann V. The three-dimensional structure of complex I from *Yarrowia lipolytica*: A highly dynamic enzyme. *J Struct Bio* [Internet]. 2006 Jun [cited 2019 Jan 24];154(3):269-79.
12. Baradaran R, Berrisford JM, Minhas GS, Sazanov LA. Crystal structure of the entire respiratory complex I. *Nature* [Internet]. 2013 Feb [cited 2019 Jan 25];494(7438):443-48.
13. Carroll J, Fearnley IM, Skehel JM, Shannon RJ, Hirst J, Walker JE. Bovine complex I is a complex of 45 different subunits. *J Bio Chem* [Internet]. 2006 Jul [cited 2019 Jan 25];281(43):32724-27.
14. Brandt U. Energy converting NADH:quinone oxidoreductase (complex I). *Annu. Rev. Biochem.* [Internet]. 2006 Mar [cited 2019 Jan 03];75:69-92.
15. Wirth C, Brandt U, Hunte C, Zickermann V. Structure and function of mitochondrial complex I. *Biochim Biophys Acta* [Internet]. 2016 Jul [cited 2019 Jan 25];1857(7):902-14.
16. Efremov RG, Baradaran R, Sazanov LA. The architecture of respiratory complex I. *Nature* [Internet]. 2010 May [cited 2019 24 Jan];465:441-45.
17. Sazanov LA, Hinchliffe P. Structure of the hydrophilic domain of respiratory complex I from *Thermus thermophilus*. *Science* [Internet]. 2006 Mar [cited 2019 Jan 24];311(5766):1430-36.
18. Saada (Reisch) A. Complex subunits and assembly genes: Complex I. In: Wong LJC, editor. *Mitochondrial disorders caused by nuclear genes*. New York: Springer Science + Business Media; 2013. p. 185-202.
19. Vogel RO, Dieteren CEJ, van den Heuvel LPWJ, Willems PHGM, Smeitink JAM, Koopman WJH et al. Identification of mitochondrial complex I assembly intermediates by tracing tagged NDUFS3 demonstrates the entry point of mitochondrial subunits. *J Bio Chem* [Internet]. 2007 Jan [cited 2019 Jan 25];282:7582-90.
20. Lazarou M, McKenzie M, Ohtake A, Thorburn DR, Ryan MT. Analysis of the assembly profiles for mitochondrial- and nuclear-DNA-encoded subunits into complex I. *Mol Cell Biol* [Internet]. 2007 Jun [cited 2019 Jan 25];27(12):4228-37.
21. Antonicka H, Ogilvie I, Taivassalo T, Anitori RP, Haller RG, Vissing J et al. Identification and characterization of a common set of complex I assembly intermediates in mitochondria from patients with complex I deficiency. *J Biol Chem* [Internet]. 2003 Aug [cited 2019 Jan 25];278:43081-88.
22. Hofhaus G, Attardi G. Lack of assembly of mitochondrial DNA-encoded subunits of respiratory NADH dehydrogenase and loss of enzyme activity in a human cell mutant lacking the mitochondrial ND4 gene product. *EMBO J* [Internet]. 1993 Aug [cited 2019

Jan 11];12(8): 3043-48.

23. Bai Y, Attardi G. The mt-DNA-encoded ND6 subunit of mitochondrial NADH dehydrogenase is essential for the assembly of the membrane arm and the respiratory function of the enzyme. *EMBO J* [Internet]. 1998 Aug [cited 2019 Jan 11];17(16): 4848-58.

24. Zhu S, Canales A, Bedair M, Vik SB. Loss of Complex I activity of the *Escherichia coli* enzyme results from truncating the C-terminus of subunit K, but not from cross-linking it to subunits N or L. *J Bioenerg Biomembr* [Internet]. 2016 Jun [cited 2019 Jan 02];48(3):325-33.

25. Alston CL, Rocha MC, Lax NZ, Turnbull DM, Taylor RW. The genetics and pathology of mitochondrial disease. *J Pathol* [Internet]. 2017 Jan [cited 2019 Jan 25];241(2): 236-50.

26. Rahman S, Blok RB, Dahl HHM, Danks DM, Kirby DM, Chow CW et. al. Leigh syndrome: Clinical features and biochemical and DNA abnormalities. *Ann Neurol* [Internet]. 1996 Mar [cited 2019 Jan 25];39(3): 343-51.

27. Genetics Home Reference [Internet]. Bethesda: *U.S. National Library of Medicine*; c2019. Leigh syndrome; 2016 Jun [cited 2019 Jan 25].

28. Baertling F, Sánchez-Caballero L, van den Brand MAM, Wintjes LT, Brink M, van den Brandt FA et. al. NDUF4 variants are associated with Leigh syndrome and cause a specific mitochondrial complex I assembly defect. *Eur J Hum Genet* [Internet]. 2017 Aug [cited 2019 Jan 25];25(11): 1273-77.

29. Marin SE, Mesterman R, Robinson B, Rodenburg RJ, Smeitink J, Tarnopolsky MA. Leigh syndrome associated with mitochondrial complex I deficiency due to novel mutations in NDUFV1 and NDUF52. *Gene* [Internet]. 2013 Mar [cited 2019 Jan 25];516(1): 162-67.

30. *National Organization for Rare Disorders* [Internet]. Bethesda: National Institutes of Health, c2019. Congenital lactic acidosis; 2017 Mar [cited 2019 Jan 25].

31. Filley CM. Leukoencephalopathy, disconnection and cognitive neuroscience. *Touch Neurology* [Internet]. Updated 2019 [cited 2019 Jan 25].

32. Ferrerira M, Torraco A, Rizza T, Fattori F, Meschini MC, Castana C et. al. Progressive cavitating leukoencephalopathy associated with respiratory chain complex I deficiency and a novel mutation in NDUF51. *Neurogen* [Internet]. 2011 Feb [cited 2019 Jan 25];12(1): 9-17.

33. *American Heart Association* [Internet]. Dallas: American Heart Association, c2019. What is cardiomyopathy in adults?; 2016 Mar [cited 2019 Jan 25].

34. Fassone E, Taanman JW, Hargreaves IP, Sebire NJ, Cleary MA, Burch M et. al. Mutations in the mitochondrial complex I assembly factor NDUF4F1 cause fatal infantile hypertrophic cardiomyopathy. *J Med Genet* [Internet]. 2011 Oct [cited 2019 Jan 25];48(10): 691-97.

35. *Genetics Home Reference* [Internet]. Bethesda: U.S. National Library of Medicine; c2019. Mitochondrial encephalomyopathy, lactic acidosis, and stroke-like episodes; 2013 Dec [cited 2019 Jan 02].

36. Liolitsa D, Rahman S, Benton S, Carr LJ, Hanna MG. Is the mitochondrial complex I ND5 gene a hot-spot from MELAS causing mutations? [Internet]. *Ann Neurol*. 2002 Dec [cited 2019 Jan 25];53(1): 128-32.

37. Johns DR, Berman J. Alternative, simultaneous complex I mitochondrial DNA mutations in Leber's hereditary optic neuropathy. *Biochem Biophys R Comm* [Internet]. 1991 Feb [cited 2019 Jan 25];174(3): 1324-30.

38. Area-Gomez E, Guardia-Laguarta C, Schon EA, Przedborski. Mitochondria, OXPHOS, and neurodegeneration: cells are not just running out of gas. *J Clin Invest* [Internet]. 2019 Jan [cited 2019 Jan 25];129(1): 34-45.

39. Langston JW, Ballard P, Tetrud JA, Irwin I. Chronic parkinsonism in humans due to a product of meperidine-analog synthesis. *Science* [Internet]. 1983 Feb [cited 2019 Jan

25];219(4587): 979-80.

40. Wang S, He H, Chen L, Zhang W, Zhang X, Chen J. Protective effects of salidroside in the MPTP/MPP<sup>+</sup>-induced model of Parkinson's disease through ROS-NO-related mitochondrion pathway. *Mol Neurobio* [Internet]. 2015 Apr [2019 Jan 25];51(2): 718-28.

41. Lin MT, Beal MF. Mitochondrial dysfunction and oxidative stress in neurodegenerative diseases. *Nature* [Internet]. 2006 Oct [cited 2019 Jan 25];443(7113): 787-95.

42. Hirst J, Roessler MM. Energy conversion, redox catalysis and generation of reactive oxygen species by respiratory complex I. *Biochim Biophys Acta* [Internet]. 2016 Jul [cited 2019 Jan 25];1857(7): 872-883.

43. Vinogradov AD, Grivennikova VG. Oxidation of NADH and ROS production by respiratory complex I. *Biochim Biophys Acta* [Internet]. 2016 Jul [cited 2019 Jan 25];1857(7): 863-71.



# A GLIAL PERSPECTIVE: THE ROLE OF ASTROCYTES IN ALZHEIMER'S DISEASE

Cliona Farrell  
Senior Sophister  
Neuroscience

*Glia cells are the non-neuronal cells of the nervous system, acting in a supportive capacity to the neurons. Astrocytes are the most abundant glial cells, representing up to 40% of the cells of the adult human brain. Knowledge of astrocytes is limited. The intensive study into their functions, interactions with neurons, and role in disease has only begun in recent times. Moving away from the typical neuron-centric view of neurodegeneration, the aim of this review is to elucidate the roles played by astrocytes in Alzheimer's disease (AD). Astrocytes contribute to neurodegeneration through their reactivity and their secretion of apolipoprotein E (ApoE). Reactive astrocytes secrete inflammatory modulators and neurotoxic factors, contributing to many degenerative diseases. ApoE is a major risk factor of AD but ApoE expression/secretion in astrocytes has not been well considered. Furthermore, recent developments in induced pluripotent stem cell technology have allowed investigations into astrocytes to become more patient- and disease-specific. The ability to culture large populations of cells from a living patient offers a new way to examine the causative factors of neurodegenerative disease.*

## Introduction

Glia are the supporting cells of the nervous system, maintaining homeostasis, forming myelin and providing protection for the neurons. Astrocytes, like all glia, have a wide range of functions in the central nervous system (CNS) which play a critical neuroprotective role, maintaining the optimal neuronal environment. Astrocytes are heterogeneous throughout all regions of the brain in both their morphology and physiological functions<sup>1</sup> and this heterogeneity is key in understanding how astrocytes may react differently to varying insults.

Astrocytes play a vital role during development, being necessary for neurogenesis, synaptogenesis and axonal guidance<sup>2</sup>. In the developed brain, astrocytes are involved in maintaining the blood-brain barrier (BBB)<sup>3</sup>. They establish a diffusion barrier which prevents the exchange of many molecules between the brain parenchyma and the blood travelling from the periphery due to the tight junctions created between adjacent endothelial cells, giving the brain a significant level of immune segregation from the rest of the body<sup>3</sup>. Astrocytes function in neuronal homeostasis, supplying energy to neurons through the production of lactate, uniquely used by neurons instead of glucose in periods of energy deprivation<sup>4</sup>. As well as this, astrocytes uptake glutamate from the synapse, preventing excitotoxicity, maintain the extracellular K<sup>+</sup> ion concentration through passive uptake, active uptake or spatial buffering<sup>5</sup>, act as gliotransmitters at the tripartite synapse<sup>6-7</sup>, and play a vital role in the formation, maturation and elimination of synapses through the secretion of regulatory signals and contact of neurons and astrocytes<sup>8</sup>.

This review investigates how these homeostatic astrocytic functions become altered in neurodegeneration. AD is a neurodegenerative disease that is phenotypically associated with cognitive decline and dementia, a neurochemical hallmark of which is the degeneration of cholinergic neurons of the basal forebrain<sup>9</sup>. The pathological features of AD are the aggregation of extracellular amyloid- $\beta$  plaques, the accumulation of the hyperphosphorylated tau protein in the form of neurofibrillary tangles and the accumulation of these plaques and tangles ultimately leading to neurodegeneration<sup>10</sup>. The main treatments for AD have ultimately focused on increasing the activity of cholinergic neurons, but little progress has been made in slowing the progression of the disease<sup>11</sup>. However, as outlined above, astrocytes play a huge role in the protection of vulnerable neurons. For this reason, recent investigations suggest that an inability of astrocytes to maintain these protective functions may be implicated in neurodegenerative diseases such as AD.

## Reactive Astrocytes

An alteration in the astrocytic functions outlined above is now being considered as one of the primary contributing factors to a large variety of neurological disorders<sup>12</sup>. Astrocytes become reactive in response to toxic materials and change their morphological, functional and protein expression properties<sup>13</sup>. The discovery of different reactive phenotypes in astrocytes in response to immune attack, chronic neurodegenerative disease or acute trauma has been termed "reactive astrogliosis"<sup>14</sup>. Purified and genetically profiled mouse astrocytes were stimulated with either lipopolysaccharide, to induce an inflammatory response, or with middle cerebral artery occlusion as a method of simulating ischemia<sup>15</sup>. Two reactive phenotypes were seen in the astrocyte population in response to these conditions. The reactive astrocytes which respond to inflammation were shown to upregulate

the expression of factors, such as C1q, which have previously been shown to be involved in synapse elimination<sup>16</sup>. These astrocytes also secrete neurotoxins which can induce cell death in neurons and oligodendrocytes, however, the nature of this neurotoxin is not confirmed. In comparison, reactive astrocytes induced by ischemia, were shown to upregulate expression of neurotrophic factors which promote neuronal outgrowth, including thrombospondins<sup>15</sup>, which play a role in synapse formation/repair<sup>8</sup>. It is highly unlikely that only these two phenotypes of reactive astrocytes exist. What is more likely is that the heterogeneity seen in astrocytes under normal conditions is also seen in reactive astrocytes.

Astrocytes become reactive in response to signals secreted by microglia, the primary immune responding cells in the brain<sup>17</sup>. These microglial factors, IL-1 $\alpha$ , TNF $\alpha$  and C1q, are released in response to neuroinflammation. Increased expression of GFAP was originally used as a descriptor for the increase in reactivity of astrocytes<sup>18</sup>, however, it was later discovered that reactive astrocytes are not proliferating, and thus, increased GFAP is not due to the presence of more astrocytes, but likely due to higher protein concentrations and cortical atrophy<sup>19</sup>.

## Reactive Astrocytes in Alzheimer's Disease

Reactive astrocytes have been closely linked to the pathology of AD in recent years<sup>20</sup>. Astrocytes become activated in the early stages of AD, a state in which they can phagocytose material and is morphologically characterised by a hypertrophic somata and ramified processes<sup>21</sup>. These activated astrocytes become reactive in late stage AD4. Amyloid Beta (A $\beta$ ) aggregates are the main inducer of astrogliosis in AD, by chronic stimulation of astrocytes<sup>13</sup>. Specifically, microglia respond to A $\beta$  by secreting inflammatory mediators, now known to be IL-1 $\alpha$ , TNF $\alpha$  and C1q<sup>17</sup>, which induce astrogliosis. The repulsive factor for axonal growth (RGMa) has been identified as a neurotoxin that may be furthering neurodegeneration<sup>22</sup>.

However, it appears that astrocytes play a dual role in AD, exerting both beneficial and detrimental effects. The elicited effect depends on a multitude of factors, including the molecules or insult which stimulate their reactivity<sup>15</sup>. Altered gliotransmission has been seen in AD, which effects neuronal activity<sup>23</sup>. An increase in  $\gamma$ -aminobutyric acid (GABA) synthesis and release in astrocytes surrounding A $\beta$  plaques has been seen, due to elevation of putrescine and monoamine oxidase B which are necessary for GABA production<sup>21</sup>. Increase in GABA levels at the synapse inhibits neuronal activity and was shown to impair the memory abilities in mouse models of AD<sup>24</sup>. The protective versus detrimental role of GABA in AD is still being debated however, and it is suggested that GABA may be protecting neurons from over-excitation, at the expense of memory impairment<sup>21</sup>. Other studies have shown protective effects of reactive astrocytes in AD, whereby astrocytic processes infiltrated plaques surrounding synapses and used their end-feet to form a protective barrier for these neurons(1). This display of both

neurotoxic and neuroprotective actions of reactive astrocytes in AD alludes to the possible heterogeneity seen in astrogliosis and the different reactive phenotypes that may exist.

Recent studies show that the JAK2-STAT3 pathway is a necessary pathway involved in the induction and maintenance of reactive astrogliosis<sup>25</sup>. Inhibiting the JAK2-STAT3 pathway in mouse models of AD led to the reduction of amyloid deposits, the improvement in spatial learning and the restoration of synaptic deficits; hallmark features of AD<sup>9, 25</sup>. These findings show the key role reactive astrocytes play in the propagation of the disease and offer a potential therapeutic target for AD, moving away from neuron-based therapies.

## Reactive Astrocytes and Aging

It has also recently been shown that it is not just disease, but normal aging, and the level of cognitive decline associated with aging, that can induce reactive astrogliosis<sup>26</sup>. RNA sequencing of astrocytes identified both age- and brain region-dependent transcriptional changes that caused aged astrocytes to develop a reactive phenotype, typical of what has been characterised in disease and inflammation<sup>26-28</sup>. Not only this, but in the absence of the microglial factors that have been shown to induce reactive astrocytes (IL-1 $\alpha$ , TNF $\alpha$  and C1q)<sup>17</sup>, age-induced upregulation of reactive astrocytes was significantly decreased. This finding is critical in understanding that reactive astrogliosis is not confined to disease but can also be associated in age-related decline. Furthermore, downregulating the microglial factors involved in the reactive response offers a potential therapeutic avenue in neurodegenerative disease.

## ApoE, Astrocytes and Alzheimer's Disease

As well as astrocyte reactivity playing a role in neurodegeneration, apolipoprotein E is a major genetic risk factor in AD<sup>29</sup>. ApoE is a lipoprotein, which is plays a role in the catabolism of triglyceride rich lipoproteins<sup>30</sup>. In the CNS, ApoE acts to transport cholesterol to neurons for repair, by binding to ApoE receptors which are members of the low-density lipoprotein receptor family<sup>31</sup>. In the brain, astrocytes are the primary producers of ApoE; neurons have only been shown to secrete ApoE in cases of injury, such as excitotoxicity<sup>32</sup>. The ApoE gene has three single-nucleotide polymorphisms, with variants on the  $\epsilon$ 2,  $\epsilon$ 3, and  $\epsilon$ 4 alleles at only two positions<sup>33</sup>, and have distributions in the population of 8.4%, 77% and 13.7% respectively<sup>34</sup>. The structural differences between the three isoforms influences their ability to bind lipids and receptors. The aggregation of A $\beta$  plaques is more abundant in ApoE  $\epsilon$ 4 carriers than in the other two isoforms because it is less effective at clearing soluble A $\beta$  in the extracellular space, due to its poorly lipidated structure<sup>35</sup>. The binding abilities of ApoE3 and ApoE4 have been compared and ApoE3 has a five-fold higher

binding affinity than ApoE4 for both A $\beta$ -40 and A $\beta$ -42, the two most common A $\beta$  species seen in AD<sup>36</sup>. Homozygosity for the  $\epsilon$ 4 allele has been shown to increase an individual's likelihood of developing late-onset AD to 91% by the age of 68 years, compared to individuals who are homozygous for the E3 isoform<sup>29</sup>. Furthermore, it has been shown that the less common E2 isoform of ApoE is involved in a reduced risk for the development of AD<sup>37</sup>. Although a well-established contributing factor of the disease, the importance of ApoE secretion by astrocytes has not been well considered. Could astrocytes homozygous for ApoE4 be susceptible to a higher level of reactivity than astrocytes homozygous for ApoE3? If so, this could indicate that glial cells play a larger role in neurodegeneration than once thought.

In cognitively normal individuals, and in transgenic mice, a differential rate of clearance and synthesis of A $\beta$  in early life was shown to result in an ApoE isoform-dependent rate of A $\beta$  aggregation in later life, with ApoE4 showing the poorest ability to remove soluble A $\beta$  from the interstitial fluid<sup>38</sup>. Following on from studies showing that the ApoE4 isoform leads to A $\beta$  pathology, recent studies have shown that ApoE4 is also implicated in non-A $\beta$  pathology surrounding AD, including its effects on BBB permeability<sup>39</sup>, altering synapse integrity<sup>40</sup> and involvement in exacerbating tau-mediated phosphorylation<sup>41</sup>. Interestingly, these defects involve the breakdown of crucial homeostatic astrocytic functions. Using tau transgenic mice with knock-in or knock-out for ApoE2, E3 or E4, a marked increase in the tau accumulation of ApoE4 mice, which led to heightened brain atrophy and neurodegeneration, was shown<sup>41</sup>. In vitro, co-culturing tau-expressing neurons with astrocytes expressing ApoE4 led to a significant increase in TNF $\alpha$  secretion, decreasing the viability of these neurons<sup>41</sup>. Notably, TNF $\alpha$  is one of the three factors shown to evoke reactivity in astrocytes<sup>17</sup> and so it is likely that reactive astrogliosis is a contributing factor to this pathology in AD. In this case, ApoE is conferring a toxic gain-of-function that is independent to the involvement of ApoE in A $\beta$  plaque aggregation.

Additionally, reactive glial cells have been shown to surround A $\beta$  plaques in AD brains. In a study comparing all three ApoE isoforms, E4 mice had significantly more and denser plaques than E2 or E3 mice, but more interestingly, cortical level of IL-1 $\beta$  were nearly twofold greater in E4 mice due to increased levels of microglial reactivity<sup>42</sup>. This study noted dystrophic astrocytes being prominent in the brains of this mouse model of AD and it is possible that this reactivity contributed to the increased secretion of the inflammatory cytokine. More recently, it has been shown that glia maturation factor (GMF), a brain-specific neuroinflammatory protein which is upregulated in AD brains and induces neurodegeneration, is predominantly expressed in reactive astrocytes surrounding A $\beta$  plaques<sup>43,44</sup>. Not only this, GMF and ApoE4 are strongly co-localised in A $\beta$  plaques themselves. This co-localisation suggests a dual contribution to the pathological changes of AD<sup>45</sup>.

From these investigations, it is clear that the altered phenotype of astrocytes in neurodegeneration must be considered in the pathology of AD. Reactive astrocytes

offer a future therapeutic target for the combat of degenerative diseases.

## iPSC Technology as a Path Forward

Experiments up to this point have primarily used primary cultures isolated from animals, specifically rodents. However, the use of non-human models for human diseases presents barriers to the depths of knowledge we can obtain from them, because human diseases, such as AD, are not developed in the same way by other animals. Furthermore, rodent astrocytes differ greatly from human astrocytes in morphology, such as number and thickness of branches, in their ratio to neurons and in their gene expression patterns<sup>4</sup>. The development of induced pluripotent stem cell (iPSC) technology gives an experimental medium for studying patient-specific cells and, in theory, provides a human-specific disease model<sup>46</sup>. iPSCs are embryonic stem cell (ESC)-like; they express the same set of pluripotency genes, have the same karyotype, the same morphology and can generate cells with three germ layers in vitro and produce teratomas in immunosuppressed mice<sup>47, 48</sup>. However, iPSC lack the ethical controversy surrounding ESC. iPSC are derived from somatic cells of living patients (usually fibroblasts) in a relatively non-invasive way<sup>46</sup>. Since their discovery, the procedure for iPSC generation is being continuously updated to improve the efficiency and efficacy of generation<sup>49, 50</sup>. Specific regionality can be introduced to these cells by treatment with developmental factors that recapitulate the signals seen during CNS development, including Sonic Hedgehog to induce transcription factors specific to the ventral forebrain cells<sup>51</sup>. Furthermore, it is possible to induce a reactive phenotype in astrocytes by the addition of three microglial factors, IL-1 $\alpha$ , TNF $\alpha$  and C1q<sup>17</sup>.

iPSC technology provides a huge leap forward in the development of disease-specific models. The use of iPSC to derive patient-specific astrocyte cell lines can allow the closer examination of the role of reactivity and the ApoE genotype in AD. The ability to generate astrocytes which also have a regional identity will allow the further investigation into disease-specific effects in different brain regions, particularly in diseases like AD that have a prominent genetic aspect.

## Conclusion

It is only recently that glial cells are being acknowledged for the huge part they play in all aspects of brain function. Glia primarily act to support the neurons, however, there are aspects of astrocyte dysfunction that can lead to, or significantly contribute to, degeneration of neurons. Neuronal death in degenerative diseases is just a quantifiable manifestation of a whole brain phenomena. Neurodegenerative disease is having a major effect on the glia, specifically astrocytes, and inducing a reactive phenotype in these cells<sup>55</sup>. Reactive astrocytes can further neurodegeneration through the secretion of inflammatory mediators

and neurotoxins which disable neurons. This contribution of astrocytes to the pathology of AD, on top of A $\beta$  plaques and phosphorylated tau, offers a potential therapeutic avenue that moves away from targeting genetic markers, which confer the disease in only 10% of AD patients. Furthermore, ApoE is long established as a strong risk factor for late-onset AD. Research into reactive ApoE4 astrocytes is limited<sup>45</sup> but offers a prominent clinical route of investigation. The development of iPSC technology has been a vital step forward in the ability to investigate human astrocytes and their functions and is a promising tool for the development of neurodegenerative disease-specific models in human cells and in the development of therapeutic targets.

## Acknowledgements

This work was adapted from a literature review "The role of reactive astrocytes and apolipoprotein E in Alzheimer's disease: using iPSC as a tool for investigation" for course NSU44490.

## References

1. Ben Haim L, Rowitch DH. Functional diversity of astrocytes in neural circuit regulation. *Nat Rev Neurosci.* 2017;18(1):31-41.
2. Kanski R, van Strien ME, van Tijn P, Hol EM. A star is born: new insights into the mechanism of astrogenesis. *Cell Mol Life Sci.* 2014;71(3):433-47.
3. Abbott NJ, Rönnbäck L, Hansson E. Astrocyte-endothelial interactions at the blood-brain barrier. *Nat Rev Neurosci.* 2006;7(1):41-53.
4. Chandrasekaran A, Avci HX, Leist M, Kobilák J, Dinnyés A. Astrocyte Differentiation of Human Pluripotent Stem Cells: New Tools for Neurological Disorder Research. *Front Cell Neurosci.* 2016;10:215.
5. Gee JR, Keller JN. Astrocytes: regulation of brain homeostasis via apolipoprotein E. *Int J Biochem Cell Biol.* 2005;37(6):1145-50.
6. Rossi D, Martorana F, Brambilla L. Implications of gliotransmission for the pharmacotherapy of CNS disorders. *CNS Drugs.* 2011;25(8):641-58.
7. Allen NJ, Eroglu C. Cell Biology of Astrocyte-Synapse Interactions. *Neuron.* 2017;96(3):697-708.
8. Clarke LE, Barres BA. Emerging roles of astrocytes in neural circuit development. *Nat Rev Neurosci.* 2013;14(5):311-21.
9. Wang J, Gu BJ, Masters CL, Wang YJ. A systemic view of Alzheimer disease - insights from amyloid- $\beta$  metabolism beyond the brain. *Nat Rev Neurol.* 2017;13(11):703.
10. Hardy J, Selkoe DJ. The amyloid hypothesis of Alzheimer's disease: progress and problems on the road to therapeutics. *Science.* 2002;297(5580):353-6.
11. Selkoe DJ. Defining molecular targets to prevent Alzheimer disease. *Arch Neurol.* 2005;62(2):192-5.

12. Ben Haim L, Carrillo-de Sauvage MA, Ceyzériat K, Escartin C. Elusive roles for reactive astrocytes in neurodegenerative diseases. *Front Cell Neurosci.* 2015;9:278.
13. Osborn LM, Kamphuis W, Wadman WJ, Hol EM. Astrogliosis: An integral player in the pathogenesis of Alzheimer's disease. *Prog Neurobiol.* 2016;144:121-41.
14. Pekny M, Pekna M. Astrocyte reactivity and reactive astrogliosis: costs and benefits. *Physiol Rev.* 2014;94(4):1077-98.
15. Zamanian JL, Xu L, Foo LC, Nouri N, Zhou L, Giffard RG, et al. Genomic analysis of reactive astrogliosis. *J Neurosci.* 2012;32(18):6391-410.
16. Stevens B, Allen NJ, Vazquez LE, Howell GR, Christopherson KS, Nouri N, et al. The classical complement cascade mediates CNS synapse elimination. *Cell.* 2007;131(6):1164-78.
17. Liddelow SA, Guttenplan KA, Clarke LE, Bennett FC, Bohlen CJ, Schirmer L, et al. Neurotoxic reactive astrocytes are induced by activated microglia. *Nature.* 2017;541(7638):481-7.
18. Sofroniew MV, Vinters HV. Astrocytes: biology and pathology. *Acta Neuropathol.* 2010;119(1):7-35.
19. Liddelow SA, Barres BA. Reactive Astrocytes: Production, Function, and Therapeutic Potential. *Immunity.* 2017;46(6):957-67.
20. Perez-Nievas BG, Serrano-Pozo A. Deciphering the Astrocyte Reaction in Alzheimer's Disease. *Front Aging Neurosci.* 2018;10:114.
21. Chun H, Lee CJ. Reactive astrocytes in Alzheimer's disease: A double-edged sword. *Neurosci Res.* 2018;126:44-52.
22. Satoh J, Tabunoki H, Ishida T, Saito Y, Arima K. Accumulation of a repulsive axonal guidance molecule RGMA in amyloid plaques: a possible hallmark of regenerative failure in Alzheimer's disease brains. *Neuropathol Appl Neurobiol.* 2013;39(2):109-20.
23. Agulhon C, Sun MY, Murphy T, Myers T, Lauderdale K, Fiacco TA. Calcium Signaling and Gliotransmission in Normal vs. Reactive Astrocytes. *Front Pharmacol.* 2012;3:139.
24. Jo S, Yarishkin O, Hwang YJ, Chun YE, Park M, Woo DH, et al. GABA from reactive astrocytes impairs memory in mouse models of Alzheimer's disease. *Nat Med.* 2014;20(8):886-96.
25. Ceyzériat K, Ben Haim L, Denizot A, Pommier D, Matos M, Guillemaud O, et al. Modulation of astrocyte reactivity improves functional deficits in mouse models of Alzheimer's disease. *Acta Neuropathol Commun.* 2018;6(1):104.
26. Clarke LE, Liddelow SA, Chakraborty C, Münch AE, Heiman M, Barres BA. Normal aging induces A1-like astrocyte reactivity. *Proc Natl Acad Sci U S A.* 2018;115(8):E1896-E905.
27. Boisvert MM, Erikson GA, Shokhirev MN, Allen NJ. The Aging Astrocyte Transcriptome from Multiple Regions of the Mouse Brain. *Cell Rep.* 2018;22(1):269-85.
28. Heimann G, Sirko S. Investigating Age-Related Changes in Proliferation and the Cell Division Repertoire of Parenchymal Reactive Astrocytes. *Methods Mol Biol.* 2019;1938:277-92.
29. Corder EH, Saunders AM, Strittmatter WJ, Schmechel DE, Gaskell PC, Small GW, et al. Gene dose of apolipoprotein E type 4 allele and the risk of Alzheimer's disease in late onset families. *Science.* 1993;261(5123):921-3.
30. Mahley RW. Central Nervous System Lipoproteins: ApoE and Regulation of Cholesterol Metabolism. *Arterioscler Thromb Vasc Biol.* 2016;36(7):1305-15.
31. Liu CC, Kanekiyo T, Xu H, Bu G. Apolipoprotein E and Alzheimer disease: risk, mechanisms and therapy. *Nat Rev Neurol.* 2013;9(2):106-18.
32. Xu Q, Bernardo A, Walker D, Kanegawa

- T, Mahley RW, Huang Y. Profile and regulation of apolipoprotein E (ApoE) expression in the CNS in mice with targeting of green fluorescent protein gene to the ApoE locus. *J Neurosci.* 2006;26(19):4985-94.
33. Kim J, Basak JM, Holtzman DM. The role of apolipoprotein E in Alzheimer's disease. *Neuron.* 2009;63(3):287-303.
34. Liu S, Breitbart A, Sun Y, Mehta PD, Boutajangout A, Scholtzova H, et al. Blocking the apolipoprotein E/amyloid  $\beta$  interaction in triple transgenic mice ameliorates Alzheimer's disease related amyloid  $\beta$  and tau pathology. *J Neurochem.* 2014;128(4):577-91.
35. Hauser PS, Ryan RO. Impact of apolipoprotein E on Alzheimer's disease. *Curr Alzheimer Res.* 2013;10(8):809-17.
36. Tokuda T, Calero M, Matsubara E, Vidal R, Kumar A, Permanne B, et al. Lipidation of apolipoprotein E influences its isoform-specific interaction with Alzheimer's amyloid beta peptides. *Biochem J.* 2000;348 Pt 2:359-65.
37. Serrano-Pozo A, Qian J, Monsell SE, Betensky RA, Hyman BT. APOE $\epsilon$ 2 is associated with milder clinical and pathological Alzheimer disease. *Ann Neurol.* 2015;77(6):917-29.
38. Castellano JM, Kim J, Stewart FR, Jiang H, DeMattos RB, Patterson BW, et al. Human apoE isoforms differentially regulate brain amyloid- $\beta$  peptide clearance. *Sci Transl Med.* 2011;3(89):89ra57.
39. Bell RD, Winkler EA, Singh I, Sagare AP, Deane R, Wu Z, et al. Apolipoprotein E controls cerebrovascular integrity via cyclophilin A. *Nature.* 2012;485(7399):512-6.
40. Klein RC, Mace BE, Moore SD, Sullivan PM. Progressive loss of synaptic integrity in human apolipoprotein E4 targeted replacement mice and attenuation by apolipoprotein E2. *Neuroscience.* 2010;171(4):1265-72.
41. Shi Y, Yamada K, Liddelov SA, Smith ST, Zhao L, Luo W, et al. ApoE4 markedly exacerbates tau-mediated neurodegeneration in a mouse model of tauopathy. *Nature.* 2017;549(7673):523-7.
42. Rodriguez GA, Tai LM, LaDu MJ, Rebeck GW. Human APOE4 increases microglia reactivity at A $\beta$  plaques in a mouse model of A $\beta$  deposition. *J Neuroinflammation.* 2014;11:111.
43. Thangavel R, Kempuraj D, Stolmeier D, Anantharam P, Khan M, Zaheer A. Glia maturation factor expression in entorhinal cortex of Alzheimer's disease brain. *Neurochem Res.* 2013;38(9):1777-84.
44. Thangavel R, Kempuraj D, Zaheer S, Raikwar S, Ahmed ME, Selvakumar GP, et al. Glia Maturation Factor and Mitochondrial Uncoupling Proteins 2 and 4 Expression in the Temporal Cortex of Alzheimer's Disease Brain. *Front Aging Neurosci.* 2017;9:150.
45. Thangavel R, Bhagavan SM, Ramaswamy SB, Surpur S, Govindarajan R, Kempuraj D, et al. Co-Expression of Glia Maturation Factor and Apolipoprotein E4 in Alzheimer's Disease Brain. *J Alzheimers Dis.* 2018;61(2):553-60.
46. Takahashi K, Yamanaka S. Induction of pluripotent stem cells from mouse embryonic and adult fibroblast cultures by defined factors. *Cell.* 2006;126(4):663-76.
47. Takahashi K, Tanabe K, Ohnuki M, Narita M, Ichisaka T, Tomoda K, et al. Induction of pluripotent stem cells from adult human fibroblasts by defined factors. *Cell.* 2007;131(5):861-72.
48. Yamanaka S, Takahashi K. Induction of pluripotent stem cells from mouse fibroblast cultures. *Tanpakushitsu Kakusan Koso.* 2006;51(15):2346-51.
49. Okita K, Matsumura Y, Sato Y, Okada A, Morizane A, Okamoto S, et al. A more efficient method to generate integration-free human iPSCs. *Nat Methods.* 2011;8(5):409-12.
50. Serio A, Bilican B, Barmada SJ, Ando DM, Zhao C, Siller R, et al. Astrocyte pathology and the absence of non-cell autonomy in an induced pluripotent stem cell model of TDP-43 proteinopathy. *Proc Natl*

*Acad Sci U S A.* 2013;110(12):4697-702.

51. Krencik R, Weick JP, Liu Y, Zhang ZJ, Zhang SC. Specification of transplantable astroglial subtypes from human pluripotent stem cells. *Nat Biotechnol.* 2011;29(6):528-34.

TS  
SR

# ERADICATION OF MEASLES VIRUS

Laura Hennelly Mc Carthy  
Senior Sophister  
Microbiology

*This review highlights the current difficulties facing global eradication of Measles Virus (MV). There are several difficulties with the current measles and rubella global strategic plan 2012 – 2020 which hinder the successful eradication of MV. The main factors that hinder global eradication of MV include difficulties in implementation of current vaccination strategies, limited healthcare resources, social unrest and political conflict in the developing world where MV has still not achieved elimination status. Coupled with the issues of the ambitious measles and rubella global strategic plan 2012 – 2020 which aimed to eradicate MV by 2020, a herd immunity threshold between 85% - 95% or higher is required to protect a susceptible population against the disease. The herd immunity threshold for MV is significantly higher in comparison to other diseases such as Rubella or Mumps. Inward and outward migration from developing, war-torn nations has been suggested as one of the reasons for the resurgence of measles prevalence in Europe. There is a complacency regarding the importance of the safe and efficacious MMR (Measles, Mumps and Rubella) trivalent vaccine and an over-reliance on herd immunity. Vigorous awareness campaigns promoting the importance of the MMR vaccine as safe and efficacious and vaccination awareness is urgently required in order for the successful eradication of MV.*

## Introduction

Measles virus (MV) is a highly contagious, infectious and severe disease prevalent in young children and immunocompromised individuals worldwide<sup>1</sup>. It remains as a high cause of morbidity and mortality in the developing world, despite global vaccination campaigns and the wide availability of an effective, safe and inexpensive vaccine<sup>2</sup>. MV is a member of the genus *Morbillivirus*, the subfamily *Paramyxovirinae* and the family *Paramyxoviridae*. MV is an enveloped virus with a

single-strand, non-segmented negative sense RNA genome<sup>3</sup>. It contains a single serotype and can be classified into different genotypes depending upon their genetic sequences<sup>4</sup>. MV is the sole human virus of the *Morbillivirus* genus and is closely related to the rinderpest virus, another *Morbillivirus* which infects cattle. MV is an aerosol-borne virus as it is predominantly transmitted via respiratory droplets. Once MV is inhaled by a susceptible host and a primary target cell is infected, signs and symptoms of MV will begin to appear after a 9–19-day period. Symptoms of MV include; high fever, cough, sore throat, conjunctivitis (inflamed eyes) and a classic maculopapular rash associated with the disease.

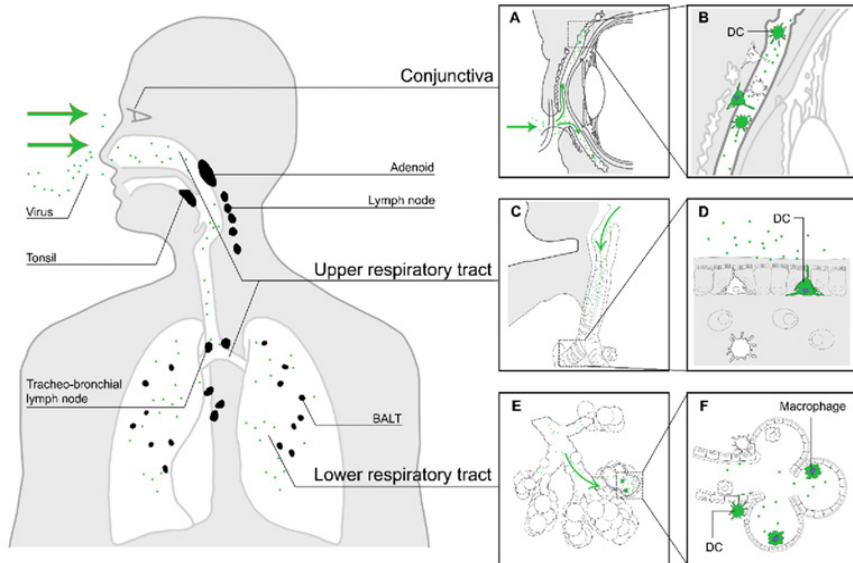


Figure 1: The route of transmission employed by MV during the first stage of infection into a susceptible individual. MV gains entry into the host via the nose, eyes or mouth indicated via the green arrows on the left side of the image. Images C and E show the primary site of infection where MV enters the respiratory tract and infects dendritic cells or CD150<sup>+</sup> macrophages. Image A indicates another entry site utilised by MV through conjunctiva, an area enriched with dendritic cells and CD150<sup>+</sup> lymphocytes. Image D shows MV invasion of dendritic cells on the alveolar lumina of the respiratory tract. Both image E and F convey the infection of macrophages or dendritic cells in the lower respiratory tract. After successful infection of the alveolar immune cells, the infected immune cells migrate to the lymph nodes and lymph tissue (black in figure on the left). Image adapted from <sup>3</sup>.

As a result of successful measles control and mass vaccination programs, the WHO (World Health Organisation) has examined the feasibility and potential to eradicate MV. Previous eradication campaigns lead by the WHO include the eradication of smallpox and rinderpest viruses<sup>7</sup>. Since the start of 2017, measles were officially declared eradicated from North America, South America, 24 countries in Europe

and seven countries in the Western Pacific<sup>8</sup>. MV is still a common disease of concern in developing world countries within regions of Asia and Africa<sup>9</sup>. The WHO has set targets for the global elimination of MV by 2020<sup>4</sup> where measles elimination is defined as the absence of endemic measles virus transmission in a region or other defined geographic area for more than 12 months<sup>10</sup>. Eight out of a previous 24 known MV genotypes have been detected since 2009 which implies that the other genotypes are no longer in circulation<sup>5</sup>. The herd immunity protection threshold for measles is among the highest of all vaccine preventable diseases and ranges in various regions from approximately 85% to exceeding 95%<sup>11</sup>.

## **Characteristics of Measles Vaccine and Vaccination Control Campaigns**

Measles mortality rates have declined during the past century largely due to the implementation of vaccination programmes as well as improvements in socioeconomic backgrounds, nutrition and healthcare<sup>5</sup>. It was estimated that approximately 7 - 8 million children died annually due to MV infection during the pre-vaccination programmes era. Before the MMR vaccine was introduced in 1963, measles epidemics occurred every 2 – 3 years<sup>11</sup>. MV is a vaccine preventable disease, one of the biological reasons that eliminating the virus can be considered.

The measles vaccine is generally administered as part of the MMR (Measles, Mumps and Rubella) live attenuated virus vaccines or it can also be given as a monovalent vaccine. The addition of various mutations during the procedure of vaccine production has led to the establishment of a very stable vaccine, where reversion to MV pathogenicity has been rarely observed<sup>14</sup>. An inactive vaccine was developed but subsequently withdrawn due to the development of a severe atypical form of measles upon a subsequent MV infection<sup>11</sup>. A single dose of MMR vaccine is approximately 93% effective for MV, while two doses of the vaccine is approximately 97% effective. In Ireland, the first dose of the MMR vaccine (MMR1) is given at 12 months and the second dose of the vaccine (MMR2) can be given between the ages of 4 – 5 years old. It is strongly recommended that the vaccine is given to a child before they begin primary school. Some countries may offer supplementary MMR vaccines if an individual fails to respond to previously administered MMR vaccination doses<sup>11, 15-18</sup>. Epidemiological and serological evidence reveals that vaccine-induced measles immunity provides long-term if not lifelong immunity in most individuals<sup>4</sup>.

There have been several mass measles immunisation campaigns led by organisations such as the WHO, Centre for Disease Control and Prevention (CDC), United Nations Foundation (UNF) and the American Red Cross (ARC). Such campaigns include “catch-up” or “booster” vaccination programmes where individuals in target age groups missed vaccination of MMR due to inaccessibility or general concerns regarding the vaccine<sup>21</sup>. The measles and rubella global

strategic plan 2012 – 2020 was employed which sought to eliminate measles and rubella in five WHO regions by 2020. The strategic plan was considered ambitious by critics with the midterm report stating that some of the goals have still not been fully implemented<sup>21-23</sup>.

Previous controversies regarding the vaccine can be traced back to religious and ethical concerns or objections to immunisation programmes and campaigns. Although such controversies were disproven, global support for anti-vaccination campaigns for diseases including MV can contribute significantly to lapses in vaccination coverage<sup>19, 24</sup>. As a result of its near eradication status, there has been a reduction in uptake of getting the MMR vaccine or monovalent MV vaccine amongst global populations. It appears that a complacency has emerged regarding measles elimination and eradication<sup>13, 25</sup>. Uninformed minority groups in Europe, low immunisation in African nations and degrading healthcare in Venezuela all threaten the global eradication target employed by the WHO. Several lapses in vaccination coverage of MV have led to a rise in individuals presenting with measles coupled with the belief that measles is a harmless childhood disease<sup>17, 25</sup>. WHO regions which have eliminated MV are still at risk of imported measles from nations where the prevalence of measles is still in circulation<sup>5</sup>.

Recent Ebola virus outbreaks in the Democratic Republic of the Congo has contributed to the interruption of MV vaccination programmes in the developing world<sup>13, 26</sup>. Such outbreaks are capable of limiting the distribution of other childhood vaccinations including the MMR vaccine which are deemed not to be as important. The Ebola virus outbreaks in West African countries and its reoccurrence since 2014, MV susceptibility has increased in the region due to disruptions in vaccination programmes for measles as the other Ebola outbreaks took priority<sup>27</sup>. The problems associated with the current measles and rubella global strategic plan 2012 – 2020 highlights the difficulties in implementation of current strategies, political and social unrest, and limited healthcare resources in developing nations<sup>5</sup>. Setbacks in vaccination control campaigns question the efficiency of current existing vaccination programmes<sup>13</sup>.

## **The Role of Population Immunity in the Eradication of Measles Virus**

For the eradication of MV to be achieved, MMR vaccine induced immunity for MV should be sustained for a long period of time<sup>7, 29</sup>. High vaccination coverage rates as well as vaccine efficacy required for population immunity is characteristically a lot higher for MV in comparison to other diseases<sup>28</sup>. Herd immunity is considered successful when a sufficient level of a population are immune to a disease, usually via vaccination. High levels of herd immunity required to interrupt MV transmission are not achieved with a single dose of the vaccine<sup>12</sup>. As MV is a highly contagious and infectious disease, a herd immunity threshold between 85% - 95%

or higher is required to protect a susceptible population against the disease.

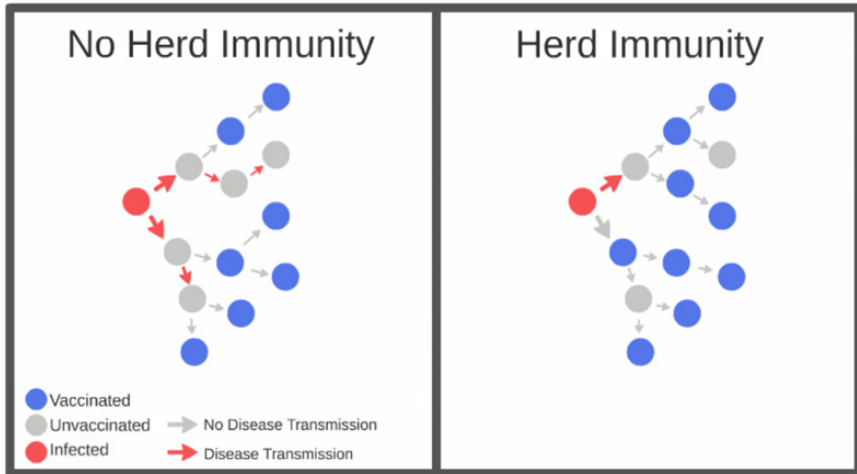


Figure 2: Illustration on the concept of herd immunity in disease transmission. Image titled “No Herd Immunity”, shows how an infected individual (red) is capable of infecting an unvaccinated individual (grey) thus spreading a disease. Image titled “Herd Immunity”, illustrates that a vaccinated individual (blue) does not contract the disease. Herd immunity occurs when a high proportion of vaccinated individuals (blue) provides a measure of protection for individuals who have not acquired immunity from a disease. Image adapted from <sup>30</sup>.

Countries can utilise the basic reproduction number,  $R_0$  which describes transmissibility within a population to aid in the understanding of the characteristics of MV transmission and the importance of herd immunity in MV.  $R_0$  is highly dependent on a particular population and the method of calculation.  $R_0$  is defined as the average number of secondary cases generated by a primary case in a completely susceptible population.  $R_0$  is a vital epidemiological summary measure of biological and sociodemographic variables providing a threshold parameter for the spread of disease<sup>31</sup>.  $R_0$  can also be used in determining herd immunity thresholds, the likelihood of an outbreak occurring and detecting gaps in vaccination coverage rates<sup>31</sup>. The  $R_0$  of MV is estimated to be 9 – 18 in various settings. This contagious and infectious nature of MV is a major challenge in eradication of MV. Nations can estimate herd immunity by using the  $R_0$  of MV to give a full estimation of how many people need to be immunised to limit to spread of the disease. For example, MV which has an  $R_0$  of 12 (9– 18 depending on circumstances), vaccine efficacy  $E$ , which for MV is approximately 97%, countries can estimate the vaccine coverage ( $V_c$ ) necessary for herd immunity ( $q_c$ ), using the following formulae;

$$\begin{aligned}
 \text{Herd Immunity} & \qquad \qquad \qquad qc = 1 - \frac{1}{12} = 0.916 \\
 \text{Vaccine Coverage} = \text{Herd Immunity} / \text{Vaccine Efficacy} & \qquad Vc = qc/E \\
 \text{Vaccine Coverage} & \qquad \qquad \qquad Vc = (1 - \frac{1}{12}) / 0.97 = 0.945
 \end{aligned}$$

Thus, approximately 94.5 % measles vaccine coverage is necessary to stop the spread of MV in a population (30).

Infection	Basic reproduction number*	Herd immunity threshold
Diphtheria	6–7	83–85%
Measles	12–18	92–94%
Mumps	4–7	75–86%
Pertussis	5–17	92–94%
Polio	2–20	50–95%
Rubella	6–7	83–85%
Smallpox	5–7	80–85%

\* Basic reproduction number is a measure of transmissibility and is calculated as the number of people who will be infected on average by a single case. ♦

Figure 3: Herd immunity threshold for selected vaccine-preventable diseases. The table includes the  $R_0$  for vaccine-preventable diseases along with the herd immunity threshold necessary for the successful immunisation within a population. It is evident that the herd immunity for measles is higher compared to the other diseases selected. Data adapted from <sup>32</sup>.

High herd immunity thresholds are necessary in limiting the spread or occurrence of MV as well as achieving the goal of elimination of MV<sup>33</sup>. Herd immunity gives an indirect immunity or protection to vulnerable individuals who cannot receive the MMR vaccines<sup>33, 34</sup>. Populations must be vaccinated to achieve the necessary herd immunity threshold required to eliminate MV. A decrease in MMR vaccination rates can contribute and lead to a falling herd immunity level within a region. This has contributed to recent outbreaks across the world, with particular outbreaks prevalent across Europe. Although globally the measles mortality rate has dropped by an astonishing 98% , recent epidemics have put a halt on certain regions achieving an MV “eradication” status<sup>13, 17</sup>. Intensifying vaccination control campaigns to increase awareness about the necessary MV herd immunity

threshold and highlighting the important role it has in MV elimination should be employed<sup>28, 33</sup>.

## **A Surge in Outbreaks and Measles Virus Surveillance.**

During 2018 there has been a significant increase in reported MV cases which has led to several outbreaks across the world and 85 reported cases of the disease in the Republic of Ireland<sup>20, 35</sup>. This poses immediate threats to neighbouring countries (25). It is capable of hindering some countries successful elimination of MV status and can aid in the reestablishment of endemic measles within those nations<sup>24</sup>. It is estimated that in 2017, 110,000 people died as a result of MV with children under the age of five years old predominantly affected<sup>9</sup>.

Global coverage of the first dose of the measles vaccine remains at 85% which is far from the 95% immunity protection rate required to prevent sporadic outbreaks<sup>17</sup>. Dose coverage of the second vaccine lies at approximately 65 % - 70% which leaves many individuals worldwide susceptible to the disease. A resurgence of MV with endemic outbreaks in regions with almost complete elimination of the disease is of grave concern and can lead to successful reestablishment of measles<sup>24, 37</sup>. Travel including inward and outward migration to Europe from developing, war-torn nations has been suggested as one of the possibilities of the resurgence of measles coupled with a complacency regarding the importance of the MMR vaccination and an over reliance on herd immunity<sup>25, 36</sup>. Refugees who have immigrated from war-torn countries to Europe had low and insufficient vaccination coverage rates in comparison to the native European populations<sup>25</sup>. It is vital to show that although a country may have eliminated measles, imported MV cases can still occur and cause outbreaks in a susceptible population<sup>36</sup>.

In the developing world, measles vaccination control campaigns are usually a successful strategy employed for protecting susceptible individuals (mainly children) who do not have access to healthcare services<sup>11</sup>. The knowledge of various recent outbreaks and advances in research have highlighted the importance of not only having elimination level coverage greater than 95% to ensure population immunity levels reach 95%, but also ensuring that there is no lapse in vaccination coverage<sup>17</sup>. However, more tailored campaigns targeting socioeconomically disadvantaged or vaccination sceptical groups showing the importance of MV vaccination using evidence-based information should be employed<sup>25</sup>. A recent study has shown the trends between a population which has no immunity (unvaccinated) against MV and their social status. This implies that vaccination campaigns may not be reaching susceptible individuals or "target" populations depending on their socioeconomic background<sup>28</sup>.

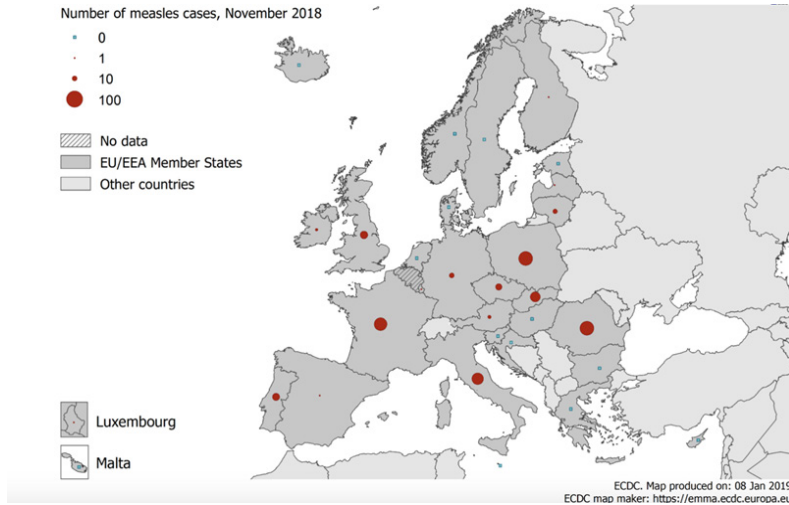


Figure 4: Measles cases and incidence by country across EU/EEA, November 2018. 29 countries reported measles data for November 2018 with a total of 385 cases in 16 countries. 13 countries reported no cases of measles. According to the map, Poland (74 cases), France (60 cases), Italy (51 cases), United Kingdom (22 cases) and Portugal (21 cases) had the highest number of measles cases during November 2018. Measles continues to spread across European countries as vaccination coverage in many countries is not reaching the sufficient herd immunity threshold. Data adapted from <sup>39</sup>.

One of the main features in the eradication of smallpox was not only due to vaccination but also as a result of an effective worldwide surveillance system. Actively reporting cases of smallpox virus as part of a wide surveillance network of the disease contributed in the successful eradication of the virus<sup>13</sup>. However, in contrast to smallpox, MV does not cause permanent visible disfiguring which may contribute to a misunderstanding of the serious implications and consequences of measles disease in a public domain<sup>19</sup>. Exact measurements of MV occurrence and mortality are lacking in under developed countries due to poor MV surveillance systems and lack of knowledge on MV<sup>5, 20</sup>.

To achieve successful eradication of MV, countries must integrate and engage with effective surveillance systems and/or serosurvey information gathered to enhance vaccination campaigns thus targeting susceptible individuals within a population<sup>11, 21</sup>. Serosurveys are capable of determining population immunity and aid in the identification of vaccination coverage flaws or lapses. They are conducted in a manner using serum samples i.e. blood or oral fluids from diagnostic public health laboratories. Countries such as Australia, Japan and South Korea have employed the usage of serosurveys which in turn have provided them with vital information regarding immunity gaps in specific age groups. Serosurveys can supply important information necessary to maintain MV elimination, thus progressing to the eradication of measles. In the developing world, serosurveys aided in identifying a serious lack of immunity against MV in Cambodia which resulted in the supply

of supplementary vaccination dosages for that particular age cohort<sup>12</sup>. As well as serosurveys, vigorous vaccination laws enforced in Australia known as, “No Jab, No Play” and “No Jab, No Pay” have contributed enormously to the high MV immunisation rates in the country. Such legislation requires all schoolchildren to be fully vaccinated in New South Wales, Queensland and Victoria. The Australian Government introduced legislation where parents of unvaccinated children would lose benefits and welfare payments<sup>32</sup>. Australian legislation poses the question as to whether other nations should adopt a similar stance regarding the necessity of vaccination in the elimination of MV and other vaccine-preventable diseases. Global outbreak investigations can provide vital information regarding the flaws of measles immunisation programmes and examine the fundamental reasons how and why outbreaks of MV can occur<sup>21</sup>.

## Future Prospects and Concluding Remarks

Despite targets employed by various healthcare organisations such as the WHO and CDC, it is unlikely that MV will be eliminated by 2020 as ambitiously desired. Using the current vaccination strategy shows that MV elimination is not on target as a result of recent surges in global outbreaks<sup>21,24</sup>. Vigorous and enhanced awareness campaigns in a public domain regarding MMR vaccination is urgently required to combat controversies posed by anti-vaccination groups and vaccination sceptics<sup>25</sup>.

There has been extensive progress in reducing the prevalence of measles morbidity and mortality through vaccination campaigns and programmes predominantly led by the WHO and CDC. However, urgent action is required to improve and increase vaccine coverage rates worldwide via immunisation programmes to exceed the 95 % herd immunity threshold required to achieve successful elimination of measles<sup>5</sup>.<sup>12</sup>. Research will be vital in achieving measles elimination goals within regions and progression to eradication of the disease worldwide. A systematic approach should be employed when responding to outbreaks, enhancing surveillance, strengthening immunisation services and maintaining the herd immunity required to achieve eradication of the disease<sup>5,11,18</sup>.

The eradication of MV would achieve several health accolades such as strengthening healthcare systems worldwide and would leave scope for the potential eradication of other life-threatening diseases such as Rubella, Hepatitis B and Yellow Fever. The eradication of measles virus is possible. However, it would be premature to determine when the eradication of the virus will or may occur.

## References

1. Kulkarni RD, Ajantha GS, Kiran AR, KR. P. Global eradication of measles: Are we poised? *Indian J Med Microbiol.* 2017;35(1):10-6.
2. Furuse Y, Oshitani H. Global Transmission Dynamics of Measles in the Measles Elimination Era. *Viruses* 2017;9(82).

3. Laksono BM, de Vries RD, McQuaid S, Duprex WPa, de Swart RL. Measles Virus Host Invasion and Pathogenesis. *Viruses*. 2016;8(210).
4. Cosby SL, Weir L. Measles vaccination: Threat from related veterinary viruses and need for continued vaccination post measles eradication. *Human Vaccines & Immunotherapeutics*. 2018;14(1):229-33.
5. Moss WJ. Measles. *Lancet*. 2017;390:2490–502.
6. Bellini WJ, Rota PA. Biological feasibility of measles eradication. *Virus Research*. 2011;162 72–9.
7. McKee A, Ferrari MJA, Shea K. Correlation between measles vaccine doses: implications for the maintenance of elimination. *Epidemiology and Infection*. 2018;146:468 – 75.
8. WHO. *Measles 2018* [Available from: <http://www.who.int/news-room/fact-sheets/detail/measles>].
9. Dabbagh A, Patel MK, Dumolard L, Gacic-Dobo M, Mulders MN, Okwo-Bele J-M, et al. Progress Toward Regional Measles Elimination – Worldwide, 2000–2016. *Morbidity and Mortality Weekly Report (MMWR)*. 2017;66(42).
10. WHO. Measles vaccines: WHO position paper. *WEEKLY EPIDEMIOLOGICAL RECORD*. 2017.
11. Durrheim DN, Orenstein WA, Schluter WW. Assessing population immunity for measles elimination – The promise and peril of serosurveys. *Vaccine* 2018;36:4001-3.
12. Holzmann H, Hengel H, Tenbusch M, Doerr HW. Eradication of measles: remaining challenges. *Med Microbiol Immunol*. 2016;205:201–8.
13. Rauch S, Jasny E, and SK, Petsch B. New Vaccine Technologies to Combat Outbreak Situations. *Front Immunol*. 2018;9(1963).
14. ECDC. Vaccine Scheduler Ireland Recommended Vaccines Stockholm 2018
15. Finnegan G. FRANCE MEASLES OUTBREAK: BABIES HIT HARDEST 2018
16. Lindmeier C, Rowland A, Fulker J, Sidhu S. Measles cases spike globally due to gaps in vaccination coverage Geneva/Atlanta/ New York: WHO; November 2018
17. WHO. Measles vaccines: WHO position paper. *WEEKLY EPIDEMIOLOGICAL RECORD*. 2017.
18. Plemper RK, Hammond AL. Will Synergizing Vaccination with Therapeutics Boost Measles Virus Eradication? *Expert Opin Drug Discov* 2014;9(2):201–14.
19. Ryan Ó. The number of reported measles cases in Ireland more than trebled this year. *The Journal*. 2018.
20. Orenstein WA, Cairns L, Hinman A, Nkowane B, Olivé J-M, Reingold AL. Measles and Rubella Global Strategic Plan 2012–2020 midterm review report: Background and summary. *Vaccine*. 2018;36:A35–A42.
21. Hinman AR. Measles and rubella eradication. *Vaccine*. 2018;36:1 - 3.
22. WHO. Measles and Rubella Global Strategic Plan 2012-2020 Midterm Review. 2016.
23. Doyle L. Measles outbreak: 'Anti-vax' movement could cost DECADES of progress according to WHO 2018
24. Storr C, Sanftenberg L, Schelling J, Heining U, Schneider A. Measles status—barriers to vaccination and strategies for overcoming them. *Dtsch Arztebl Int* 2018;115:723–30.
25. WHO. Disease Outbreak News (DONs) 2018
26. Takahashi SC, Metcalf JE, Ferrari MJ, Moss WJ, Truelove SA, Tatem AJ, et al. The growing risk from measles and other childhood infections in the wake of Ebola. *Science*. 2015;13(6227):1240-2.
27. Kien VD, Van Minh H, Giang KB, Mai VQ, Tri Tuan N, Quam MB. Trends in childhood measles vaccination highlight

- socioeconomic inequalities in Vietnam. *Int J Public Health*. 2017;62:S41–S9.
28. Grobusch MP, Rodriguez-Morales AJ, Wilson ME. Measles on the move. *Travel Medicine and Infectious Disease*. 2017;18:1 - 2.
29. Hart R, Patel K. What the anti-vaxxers are getting dangerously wrong. *USC-BROOKINGS SCHAEFFER ON HEALTH POLICY*; 2015.
30. Guerra FM, Bolotin S, Lim G, Heffernan J, Deeks SL, Li Y, et al. The basic reproduction number ( $R_0$ ) of measles: a systematic review. *Lancet Infect Dis* 2017. 2017;17:e420–28.
31. Beard FH, Leask J, McIntyre PB. No Jab, No Pay and vaccine refusal in Australia: the jury is out. *Med J Aust* 2017. 2017;206(9):381-3.
32. Jent P, Trippel M, Frey M, Pöllinger A, Berezowska S, Langer R, et al. Fatal Measles Virus Infection After Rituximab-Containing Chemotherapy in a Previously Vaccinated Patient. *Open Forum Infectious Diseases*. 2018;5(11).
33. Bowes J. Measles, misinformation, and risk: personal belief exemptions and the MMR vaccine. *Journal of Law and the Biosciences*. 2016:718–25.
34. Times TI. The Irish Times view on the measles outbreak: An unnecessary exposure. *The Irish Times*. 2018.
35. Bester JC. Measles Vaccination is Best for Children: The Argument for Relying on Herd Immunity Fails. *Bioethical Inquiry*. 2017;14:375 – 84.
36. View TIT. The Irish Times view on the measles outbreak: An unnecessary exposure. *The Irish Times*. 2018.
37. Durrheim DN, Crowcroft NS, Strebel PM. Measles – The epidemiology of elimination. *Vaccine*. 2014;32:6880–3.
38. ECDC. European Centre for Disease Prevention and Control, Monthly measles and rubella monitoring report. Stockholm 2018.
39. Eom H, Park Y, Kim J, Yang J-S, Kang H, Kim K, et al. Occurrence of measles in a country with elimination status: Amplifying measles infection in hospitalized children due to imported virus. *PLoS ONE*. 2018;13(2).
40. Hübschen JM, Bork SM, Brown KE, Mankertz A, Santibanez S, Ben Mamou M, et al. Challenges of measles and rubella laboratory diagnostic in the era of elimination. *Clinical Microbiology and Infection*. 2017;23:511 - 5.

TS  
SR

# GLIOBLASTOMA MULTIFORME AND THE CANCER STEM CELL MODEL

Ellen Tuck  
Senior Sophister  
Human Genetics

*Glioblastoma Multiforme is a high-grade brain tumour with a dismal prognosis and 5-year survival rate of just 5%. Over the past decade, great effort has been put into elucidating the genetic basis of this lethal disease. However, efforts to translate this molecular understanding into clinical practice have been generally disappointing. Vast genetic heterogeneity contributes to this lack of success, as well as cancer cells that gain stem cell-like properties, aiding their proliferation and resistance to treatment. This review presents an overview of glioblastoma genetics and the Cancer Stem Cell model, highlighting the relevance of this model to understanding and defeating this fatal cancer.*

## Introduction

Glioblastoma Multiforme (GBM) is the most common and lethal brain cancer in adults. It affects approximately 3 in 100,000 people with an average age of onset of ~60 years. The prognosis for a GBM patient is on average 15 months with treatment, or 3 months without<sup>1</sup>. Treatment consists of surgical resection of the tumour followed by radiation therapy (RT) and chemotherapy with an alkylating agent such as Temozolomide (TMZ) or Carmustine. Recurrence of the tumour after treatment occurs nearly universally and is the main cause of mortality in GBM patients<sup>1</sup>.

Investigations into the genetic basis of GBM have revealed it to be a very complex cancer with a diverse spectrum of genetic mutations underlying the disease in different patients. Different mutational profiles are even found in different cells within the same tumour<sup>2</sup>. This genetic heterogeneity may contribute to the failure of targeted therapies<sup>3</sup>. Furthermore, the precise cellular origin of GBM remains elusive. Different tumours and even different cells within the same tumour can present genetic profiles representative of different nervous system cell types, for example neuronal, glial or mesenchymal<sup>2</sup>.

It has been proposed that considering GBM tumours in the light of the cancer stem cell model may improve our understanding of these aggressive tumours and direct future therapeutic strategies<sup>4</sup>.

## Cancer Stem Cell Model

Stem cells are rare cells which have the unique ability to self-renew and to produce all differentiated cells of a particular tissue. For example, haematopoietic stem cells in the bone marrow produce differentiated blood and immune cells of the myeloid and lymphoid lineages<sup>5</sup>.

The cancer stem cell (CSC) hypothesis arose from the observation that only a small proportion of acute myeloid leukaemia (AML) cells isolated from an affected mouse and transplanted into an immune deficient mouse could reproduce the leukaemia in the recipient mouse<sup>6</sup>. Most AML cells were found to have limited proliferative potential and did not produce a leukemic phenotype upon transplantation. The leukaemia-initiating cells were found to present cell surface markers also found on normal blood stem cells and they were negative for markers of differentiated blood lineage cells (CD34+;CD38-)<sup>6</sup>. This led to the emergence of a model in which cancers are maintained by a rare population of stem-like cells. The model has since been extended to solid tumours, with putative tumour-initiating 'stem' cells having been isolated from many types of tumour including breast, pancreatic and brain cancers<sup>7</sup>. The model proposes a hierarchical organisation of cells within the tumour, with tumour growth being sustained by a small population of rare cancer stem cells. Thus, the cancer can be viewed as an abnormal organ to which the principles of normal stem cell renewal and differentiation can apply<sup>8</sup>.

The CSC model has implications for therapeutic approach. If true, whole tumours could be eliminated by targeting only this small population of CSCs. However, if any single CSC remains after therapy, the tumour would survive and proliferate again<sup>8</sup> (Figure 1).

Vagotomies have proven useful in establishing when gut-brain crosstalk occurs through the vagus nerve. In one study, mice exhibiting anxiety- and depressive-like symptoms were found to improve and to exhibit alterations in their GABAergic systems after treatment with *Lactobacillus rhamnosus* (JB-1)<sup>23</sup>. However, these neurochemical and behavioural changes did not occur in mice that underwent vagotomy, indicating that the vagus nerve was important in communicating the change in microbial composition to the brain. It has been suggested that a truncal vagotomy confers some protection against PD, suggesting that the vagus nerve plays a role in some, but not all, cases of PD<sup>24</sup>.

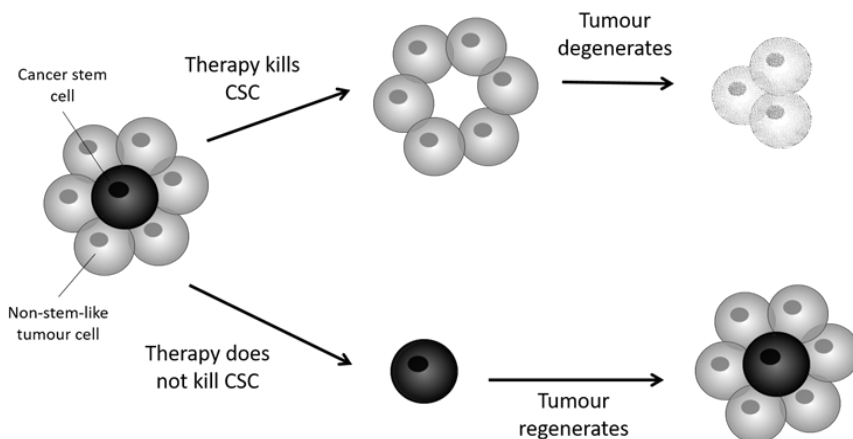


Figure 1: Implications of therapeutic targeting with respect to cancer stem cells. In a tumour maintained by a self-renewing and proliferating cancer stem cell (CSC), therapies targeting the main tumour mass but not eliminating the CSC will ultimately allow for the recurrence of the tumour once the treatment is withdrawn. Conversely, a therapy targeting the CSC, even without ablating the main tumour cell mass, may lead to degeneration of the tumour by removing its core proliferative source.

## Complex Genetics of Glioblastoma Multiforme

GBM was the subject of the first pilot study by the The Cancer Genome Atlas (TCGA). TCGA performs multi-platform, integrative genetic analyses on large, statistically powered cohorts to provide unprecedented insights into the genomic basis of cancers. In 2008, TCGA and another independent, smaller scale study integrated exome sequencing, gene expression and DNA copy number data to identify recurrent mutations characterising primary GBM. The mutations observed in both studies converged on three main cellular signalling pathways: the RB1, TP53 and receptor tyrosine kinase (RTK) signalling pathways<sup>9,10</sup>. A follow-up study was carried out in 2013 on a larger sample cohort ( $n > 500$ ). Disruptions to the same three pathways were highlighted as key events in the development of glioblastoma, with the RB1, TP53 and RTK pathways incurring a mutation in 79%, 86% and 90% of samples, respectively<sup>11</sup>. These putative core glioblastoma pathways are found disrupted in many cancers as they are involved in cell cycle control, DNA damage response, cell growth and proliferation (Figure 2A-C).

Whole genome sequencing revealed widespread mutations in the promoter of the Telomerase Reverse Transcriptase (TERT) gene in glioblastoma cells<sup>11</sup>. TERT maintains telomere sequences present at the end of chromosomes, contributing towards increased longevity of cells. TERT is not normally expressed in somatic

cells but TERT promoter mutations observed in GBM upregulate its expression in these tumour cells. In tumours with wild-type TERT promoter, mutations in the ATRX1 gene were present. Mutation or loss of ATRX1 contributes to activation of alternative lengthening of telomeres (ALT)<sup>12</sup>. Therefore, it is suggested that aberrant maintenance of telomeres is another event required for gliomagenesis<sup>11</sup> (Figure 2D).

Recurrent missense mutations in Isocitrate Dehydrogenase 1 (IDH1) were discovered in a relatively small proportion of patients<sup>9,13</sup>. IDH1 normally catalyses the production of  $\alpha$ -ketoglutarate which stimulates enzymes involved in DNA and histone demethylation. The observed IDH1 mutations always affect the same codon and result in the R132H amino acid change within the active site of the enzyme. The R132 mutation confers neomorphic enzymatic activity on IDH1<sup>14</sup>. The product of this new catalytic activity inhibits enzymes involved in demethylation of DNA and histone proteins. Inhibition of such enzymes leads to higher levels of DNA and histone methylation in IDH1-mutated glioma cells (Figure 2E). These epigenetic changes may influence gene expression and maintain glioma cells in a less differentiated state<sup>15,16</sup>.

The diverse mutational spectrum of GBM has been probed in attempts to identify molecular subtypes of GBM. Gene expression data produced by TCGA was subject to unsupervised linkage hierarchical clustering revealing four clusters – Classical, Mesenchymal, Proneural and Neural. Each subtype is defined by a particular genetic signature, including gene loss or amplification, protein-coding mutations and expression of particular CNS cell-type markers<sup>17</sup> (Table 1).

Considering GBM in the light of molecular subtypes seemed a promising strategy to provide a better understanding of its origin and to help in developing a more targeted approach to therapy design<sup>17</sup>. In 2016 the World Health Organisation released new classification guidelines for tumours of the central nervous system, including glioblastoma, based on the tumour genome as opposed to purely histological differences. This includes a distinction between IDH-wildtype and IDH-mutated glioblastoma<sup>18</sup>. However, there has been very limited translation of the molecular subtyping of GBM beyond this.

A confounding factor may be the subsequently discovered, vast intratumoral heterogeneity present in GBM. The full extent of genetic diversity within a glioblastoma tumour cannot be captured by the whole-tumour profiling discussed thus far<sup>19</sup>. In fact, there have been multiple reports of tumours containing populations of cells with different glioblastoma subtype genetic signatures<sup>2,19</sup>.

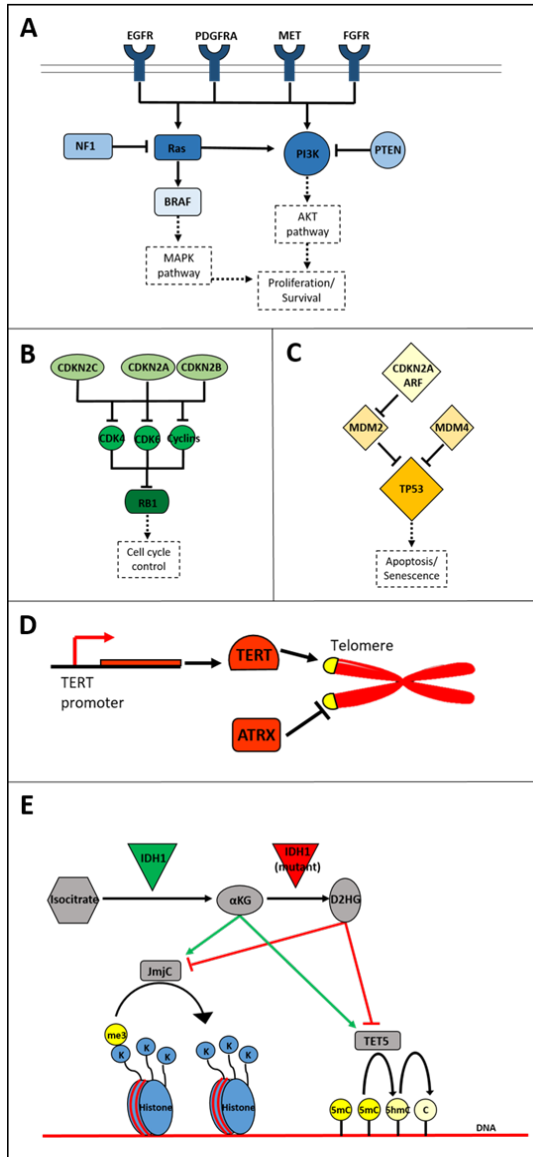


Figure 2: Cellular pathways affected in Glioblastoma Multiforme. (A) RTK signalling pathway. These cell-surface receptors and intra-cellular proteins are the most frequently altered constituents of the RTK pathway in GBM and their mutation leads to aberrant proliferation of cells. (B) RB1 pathway. These cell-cycle regulators are mutated in GBM, leading to uncontrolled entry into an active cell cycle. (C) TP53 pathway. These proteins are often activated in response to DNA damage and induce cell death or senescence. Failure to do so in GBM leads to accumulation of genetic damage and uncontrolled

proliferation. (D) Maintenance of telomeres in GBM. Upregulation of TERT contributes to maintenance of telomeres. Mutation to ATRX abolishes its inhibitory effect on alternative lengthening of telomeres. (E) IDH1 metabolic pathway. The effect of IDH1 and its mutant inhibitory activity on histone and cytosine demethylation. (JmJc – histone demethylase; TET5 – DNA demethylase; 5mC – 5-methyl cytosine).

Table 1. Glioblastoma Multiforme Subtypes		
Subtype	Chromosomes/Genes affected	Cell-type markers
Classical	Chr7 amplification	Neural/Stem
	Chr10 loss	
	EGFR amplification/mutation	
	9p21.3 (CDKN2A) homozygous deletion	
Mesenchymal	NF1 deletion/mutation/lower expression	Astrocytic/Microglial
	Inflammatory pathways upregulated	Mesenchymal
Proneural	IDH mutations	Oligodendrocytic
	PDGFRA mutations	
	TP53 mutations/LOH	

Table 1: *Glioblastoma Multiforme Subtypes*. Above are the four subtypes of GBM proposed by Verhaak et al. (2010) and the genetic markers defining their classification.

Intratumoral heterogeneity of GBM may be at the root of treatment resistance and tumour recurrence. Soeda et al. demonstrated differential response to an EGFR inhibitor in subclones isolated from a glioblastoma patient. This may be explained by mosaic amplification of different RTKs in different cells<sup>3</sup>. The intratumoral heterogeneity and redundancy in proliferative signalling pathways likely allow for evasion of therapies targeted at one specific, putative driver RTK<sup>19</sup>.

Any cell unreached by therapy may itself be tumorigenic, resulting in the recurrence of the glioblastoma after treatment. Johnson et al. sequenced the exome of 23 gliomas and recurrent tumours in the same patients. Comparison of the paired mutational profiles revealed that cells in the recurrent tumours did not contain all the same mutations as the initial resected tumour, but they did share some early mutational events<sup>20</sup>. This again points to the clonal evolution of glioblastoma and to selection, in the context of treatment, for clone-specific mutations which lend resistance to this treatment.

## Cancer stem cells in Glioblastoma Multiforme

The cellular origin of glioblastoma has yet to be conclusively determined. The subtypes proposed by Verhaak et al. express markers of certain CNS lineages, hinting at a cell of origin. However, this classification cannot account for the presence of multiple subtypes within one tumour<sup>2</sup>.

The cancer stem cell (CSC) hypothesis has been proposed as a model which can account for the heterogeneity and cellular hierarchies found in GBM<sup>21</sup>. CSCs can undergo self-renewal and differentiation processes akin to those of normal stem cells, giving rise to tissues composed of heterogeneous cell populations with different proliferative potential<sup>8</sup>.

In support of this model, only a subset of cells within glioblastoma tumours are capable of tumorigenesis when transplanted into the brains of mice and these tumour initiating cells express the stem cell marker CD133<sup>22, 23</sup>. Furthermore, it was demonstrated that knockout of tumour suppressor genes in neural stem and progenitor cells (NSPCs) could generate 'glioblastoma stem cells' (GSCs) which drive glioblastoma formation in mice. These tumours underwent differentiation processes during proliferation, apparently producing differentiated cells of different CNS lineages<sup>24</sup>.

The cancer stem cell model does not necessitate the tumour origin being a normal stem cell, but rather that the mutated tumorigenic cell assumes stem-like properties. Dedifferentiation of normal cells has been observed to occur, producing tumorigenic neural stem-like cells. Silencing of the tumour suppressor genes NF1 and p53 with short hairpin RNAs in neural stem cells, astrocytes or even mature neurons resulted in malignant glioma formation in mice via dedifferentiation to a stem-like state<sup>25</sup>.

Suva et al. identified a set of four transcription factors that are sufficient to transform differentiated GBM cells into stem-like cells capable of *in vivo* tumour propagation. The transcription factors (POU3F2, SOX2, SALL2, and OLIG2) were found to reprogram the epigenetic landscape of the differentiated cells, recapitulating that of tumour-initiating, stem-like cells<sup>26</sup>. This study, and others, highlight a bidirectional plasticity in cancer stem cell differentiation, in contrast to the unidirectional dogma of stem cell biology<sup>26, 27</sup>.

It is proposed that GSCs are stuck in a proliferative state, unable to effectively escape the cell cycle and undergo terminal differentiation. Carén et al. found that GSCs exposed to Bone Morphogenic Protein (BMP) differentiation factor did generate more differentiated astrocyte- or oligodendrocyte-like cells. However, these cells displayed a propensity to re-enter the cell cycle and revert to a stem-like state. Differentiation-related chromatin remodelling and DNA methylation did not occur in these cells in response to BMP, possibly limiting commitment to a differentiated lineage<sup>28</sup>.

This inability to terminally differentiate and the expression of neural stem cell markers may be mechanistically linked to the underlying cancer-driving mutations that arise in the cell. For example, it was discovered that the mutant EGFR variant found commonly in GBM, EGFRvIII, stimulates expression of FOXG1<sup>29</sup>. FOXG1 had previously been found to be overexpressed in GSCs compared to normal neural stem cells<sup>30,31</sup>. FOXG1 is a transcription factor expressed in NSPCs associated with maintenance of a stem-like state and inhibiting differentiation. It achieves this by controlling expression of cell cycle regulators such as FoxO3 and epigenetic regulators such as some DNA and histone methyltransferases<sup>32</sup>. Thus, oncogenic mutations in glioblastoma cells may be hijacking existing developmental systems, therein immortalising the cells in which they are present.

GBM therapies developed in the future may be designed to target GSCs and induce their differentiation in order to reduce their proliferative potential. An early preclinical experiment has investigated the anti-tumorigenic potential of the BMP9 differentiation factor. Treatment of GBM xenografts in mice with BMP9 directly counteracted tumour growth by inducing differentiation. It also inhibited tumour angiogenesis – the development of new blood vessels within the tumour, which normally aids its proliferation<sup>4</sup>. These promising results must be weighed up against previous *in vitro* studies like that of Carén and colleagues which found this BMP-induced GSC differentiation to be incomplete and prone to reversion<sup>28</sup>. However, further research may improve and refine such approaches, opening a new frontier in glioblastoma treatment.

## Conclusion

The understanding of the genetic basis of GBM has advanced enormously in the past decade thanks to large-scale integrative studies like TCGA initiative. Despite this progress the survival of GBM patients has not seen much improvement in decades, especially in comparison to many other cancers. Death rates declined during the 2011-2015 period for 14 of the top 20 cancers in women and 11 of 18 for men but the death rate of brain cancers, including glioblastoma, increased for both women and men, highlighting the lack of progress in therapy development for brain tumours<sup>33</sup>.

The future of GBM treatment may involve focussing therapies on the finite number of tumour-initiating 'glioblastoma stem cells' remaining after initial resection. Further understanding of these cancer stem cells and their aberrant exploitation of normal neurodevelopmental processes may elucidate ways to control this invasive tumour. Reversal of their stem-like state through differentiation therapies may revolutionise treatment of this resilient tumour. However, this approach is in very early, mainly theoretical, phases of development with much validation and drug design to be completed before it can be translated to clinical trials.

As a mainly sporadic cancer with no strongly associated risk factors, diagnosis of GBM comes as a devastating shock and still entails a dismal prognosis. Hopefully

with the growing understanding of GBM pathogenesis, cancer stem cells and barriers to therapeutic response, newly developed therapies will have a positive outcome for patients.

## Acknowledgements

This work was adapted from an essay “The Genetic Basis of Glioblastoma Multiforme” for course GEU44201.

## References

1. Stupp R, Mason WP, van den Bent MJ, Weller M, Fisher B, Taphoorn MJB, et al. Radiotherapy plus Concomitant and Adjuvant Temozolomide for Glioblastoma. *N Engl J Med* [Internet]. 2005 Mar 10 [cited 2018 Oct 26];352(10):987–96.
2. Sottoriva A, Spiteri I, Piccirillo SGM, Touloumis A, Collins VP, Marioni JC, et al. Intratumor heterogeneity in human glioblastoma reflects cancer evolutionary dynamics. *Proc Natl Acad Sci* [Internet]. 2013 Mar 5 [cited 2018 Oct 13];110(10):4009–14.
3. Soeda A, Hara A, Kunisada T, Yoshimura S, Iwama T, Park DM. The Evidence of Glioblastoma Heterogeneity. *Sci Rep* [Internet]. 2015 Jul 27 [cited 2018 Oct 22];5(1):7979.
4. Porcù E, Maule F, Boso D, Rampazzo E, Barbieri V, Zuccolotto G, et al. BMP9 counteracts the tumorigenic and pro-angiogenic potential of glioblastoma. *Cell Death Differ* [Internet]. Nature Publishing Group; 2018 Oct 5 [cited 2018 Oct 26];25(10):1808–22.
5. Baum CM, Weissman IL, Tsukamoto AS, Buckle AM, Peault B. Isolation of a candidate human hematopoietic stem-cell population. *Proc Natl Acad Sci U S A* [Internet]. 1992 Apr 1 [cited 2019 Jan 25];89(7):2804–8.
6. Lapidot T, Sirard C, Vormoor J, Murdoch B, Hoang T, Caceres-Cortes J, et al. A cell initiating human acute myeloid leukaemia after transplantation into SCID mice. *Nature* [Internet]. 1994 Feb 17 [cited 2019 Jan 21];367(6464):645–8.
7. Visvader JE, Lindeman GJ. Cancer stem cells in solid tumours: accumulating evidence and unresolved questions. *Nat Rev Cancer* [Internet]. 2008 Oct 11 [cited 2019 Jan 21];8(10):755–68.
8. Reya T, Morrison SJ, Clarke MF, Weissman IL. Stem cells, cancer and cancer stem cells. *Nature* [Internet]. 2001 Nov 1 [cited 2018 Oct 7];414(6859):105–11.
9. Parsons DW, Jones S, Zhang X, Lin JC-H, Leary RJ, Angenendt P, et al. An Integrated Genomic Analysis of Human Glioblastoma Multiforme. *Science* (80- ) [Internet]. 2008 Sep 26 [cited 2018 Oct 13];321(5897):1807–12.
10. TCGA, McLendon R, Friedman A, Bigner D, Van Meir EG, Brat DJ, et al. Comprehensive genomic characterization defines human glioblastoma genes and core pathways. *Nature* [Internet]. 2008 Oct 23 [cited 2018 Sep 25];455(7216):1061–8.
11. Brennan CW, Verhaak RGW, McKenna A, Campos B, Nounshmehr H, Salama SR, et al. The Somatic Genomic Landscape of Glioblastoma. *Cell* [Internet]. 2013 Oct 10 [cited 2018 Sep 12];155(2):462–77.
12. Pickett HA, Reddel RR. Molecular mechanisms of activity and derepression of alternative lengthening of telomeres. *Nat Struct Mol Biol* [Internet]. 2015 Nov 4 [cited 2018 Oct 24];22(11):875–80.
13. Yan H, Parsons DW, Jin G, McLendon

- R, Rasheed BA, Yuan W, et al. IDH1 and IDH2 Mutations in Gliomas. *N Engl J Med* [Internet]. 2009 Feb 19 [cited 2018 Sep 23];360(8):765–73.
14. Dang L, White DW, Gross S, Bennett BD, Bittinger MA, Driggers EM, et al. Cancer-associated IDH1 mutations produce 2-hydroxyglutarate. *Nature* [Internet]. NIH Public Access; 2009 Dec 10 [cited 2018 Sep 23];462(7274):739–44.
15. Miller JJ, Shih HA, Andronesi OC, Cahill DP. Isocitrate dehydrogenase-mutant glioma: Evolving clinical and therapeutic implications. *Cancer* [Internet]. 2017 Dec 1 [cited 2018 Sep 10];123(23):4535–46.
16. Rohle D, Popovici-Muller J, Palaskas N, Turcan S, Grommes C, Campos C, et al. An Inhibitor of Mutant IDH1 Delays Growth and Promotes Differentiation of Glioma Cells. *Science* (80- ) [Internet]. 2013 May 3 [cited 2018 Sep 23];340(6132):626–30.
17. Verhaak RGW, Hoadley KA, Purdom E, Wang V, Qi Y, Wilkerson MD, et al. Integrated Genomic Analysis Identifies Clinically Relevant Subtypes of Glioblastoma Characterized by Abnormalities in PDGFRA, IDH1, EGFR, and NF1. *Cancer Cell* [Internet]. 2010 Jan 19 [cited 2018 Sep 22];17(1):98–110.
18. Louis DN, Perry A, Reifenberger G, von Deimling A, Figarella-Branger D, Cavenee WK, et al. The 2016 World Health Organization Classification of Tumors of the Central Nervous System: a summary. *Acta Neuropathol* [Internet]. 2016 Jun 9 [cited 2018 Oct 21];131(6):803–20.
19. Patel AP, Tirosh I, Trombetta JJ, Shalek AK, Gillespie SM, Wakimoto H, et al. Single-cell RNA-seq highlights intratumoral heterogeneity in primary glioblastoma. *Science* (80- ) [Internet]. 2014 Jun 20 [cited 2018 Oct 13];344(6190):1396–401.
20. Johnson BE, Mazar T, Hong C, Barnes M, Aihara K, McLean CY, et al. Mutational Analysis Reveals the Origin and Therapy-Driven Evolution of Recurrent Glioma. *Science* (80- ) [Internet]. 2014 Jan 10 [cited 2018 Sep 23];343(6167):189–93.
21. Lathia JD, Mack SC, Mulkearns-Hubert EE, Valentim CLL, Rich JN. Cancer stem cells in glioblastoma. *Genes Dev* [Internet]. Cold Spring Harbor Laboratory Press; 2015 Jun 15 [cited 2018 Sep 17];29(12):1203–17.
22. Singh SK, Hawkins C, Clarke ID, Squire JA, Bayani J, Hide T, et al. Identification of human brain tumour initiating cells. *Nature* [Internet]. 2004 Nov 18 [cited 2018 Oct 7];432(7015):396–401.
23. Brescia P, Ortensi B, Fornasari L, Levi D, Broggi G, Pelicci G. CD133 Is Essential for Glioblastoma Stem Cell Maintenance. *Stem Cells* [Internet]. Wiley-Blackwell; 2013 May 1 [cited 2018 Oct 15];31(5):857–69.
24. Alcantara Llaguno S, Chen J, Kwon C-H, Jackson EL, Li Y, Burns DK, et al. Malignant Astrocytomas Originate from Neural Stem/Progenitor Cells in a Somatic Tumor Suppressor Mouse Model. *Cancer Cell* [Internet]. 2009 Jan 6 [cited 2018 Oct 15];15(1):45–56.
25. Friedmann-Morvinski D, Bushong EA, Ke E, Soda Y, Marumoto T, Singer O, et al. Dedifferentiation of Neurons and Astrocytes by Oncogenes Can Induce Gliomas in Mice. *Science* (80- ) [Internet]. 2012 [cited 2018 Oct 15];338(6110):1080–4.
26. Suvà ML, Rheinbay E, Gillespie SM, Patel AP, Wakimoto H, Rabkin SD, et al. Reconstructing and reprogramming the tumor-propagating potential of glioblastoma stem-like cells. *Cell* [Internet]. NIH Public Access; 2014 Apr 24 [cited 2018 Sep 29];157(3):580–94. Available from: <http://www.ncbi.nlm.nih.gov/pubmed/24726434>
27. Chaffer CL, Brueckmann I, Scheel C, Kaestli AJ, Wiggins PA, Rodrigues LO, et al. Normal and neoplastic nonstem cells can spontaneously convert to a stem-like state. *Proc Natl Acad Sci U S A* [Internet]. National Academy of Sciences; 2011 May 10 [cited 2018 Oct 15];108(19):7950–5.
28. Carén H, Stricker SH, Bulstrode H, Gargra S, Johnstone E, Bartlett TE, et al. Glioblastoma Stem Cells Respond to Differentiation Cues but Fail to Undergo Commitment and Terminal Cell-Cycle Arrest. *Stem Cell Reports* [Internet]. 2015 Nov 10 [cited 2018 Oct 16];5(5):829–42.

29. Liu F, Hon GC, Villa GR, Turner KM, Ikegami S, Yang H, et al. EGFR Mutation Promotes Glioblastoma through Epigenome and Transcription Factor Network Remodeling. *Mol Cell* [Internet]. 2015 Oct 15 [cited 2018 Sep 25];60(2):307–18.
30. Engström PG, Tommei D, Stricker SH, Ender C, Pollard SM, Bertone P. Digital transcriptome profiling of normal and glioblastoma-derived neural stem cells identifies genes associated with patient survival. *Genome Med* [Internet]. 2012 [cited 2018 Oct 16];4(10):76.
31. Verginelli F, Perin A, Dali R, Fung KH, Lo R, Longatti P, et al. Transcription factors FOXG1 and Groucho/TLE promote glioblastoma growth. *Nat Commun* [Internet]. 2013 Dec 20 [cited 2018 Oct 16];4(1):2956.
32. Bulstrode H, Johnstone E, Marques-Torres MA, Ferguson KM, Bressan RB, Blin C, et al. Elevated FOXG1 and SOX2 in glioblastoma enforces neural stem cell identity through transcriptional control of cell cycle and epigenetic regulators. *Genes Dev* [Internet]. Cold Spring Harbor Laboratory Press; 2017 [cited 2018 Oct 16];31(8):757–73.
33. Cronin KA, Lake AJ, Scott S, Sherman RL, Noone A-M, Howlader N, et al. Annual Report to the Nation on the Status of Cancer, part I: National cancer statistics. *Cancer* [Internet]. 2018 Jul 1 [cited 2018 Oct 29];124(13):2785–800.

TS  
SR

# THE USE OF BiKEs AND TriKEs AS A CANCER IMMUNOTHERAPY

Cathal Keane  
Junior Sophister  
Biochemistry

*Natural killer (NK) cells identify and kill tumour cells. There are certain disadvantages to their use against malignancy, including: strong inhibitory interactions and inability to survive and proliferate for long periods of time. Immunomodulators called bispecific killer engagers (BiKEs) and trispecific killer engagers (TriKEs), were recently developed to overcome these problems and sustain NK cells for long periods of time, while simultaneously improving their cytotoxicity.*

## Introduction

Cancer immunotherapy is based on the principle of using the body's immune system to treat cancer and prevent its recurrence. Many cells of our immune system can destroy cancer cells and convey long term memory preventing recurrent malignancies<sup>1</sup>. The major benefit of cancer immunotherapy is its specificity to attack cancer cells while minimizing the effect to surrounding healthy tissue<sup>2</sup>. This feature of immunotherapy is what makes it preferential to current cancer therapeutics, such as chemotherapy and radiation therapy. These therapies have an inability to differentiate between healthy and malignant tissue.

NK cells were initially recognised by their ability to kill tumour cells without any prior exposure to tumour antigens. They are cells of the innate immune system that, once activated, can release cytotoxic molecules including granzymes and perforin to lyse cells<sup>3</sup>. This makes them suitable targets for immunotherapy<sup>4</sup>.

Unlike T-cells, NK cells do not recognise tumour antigens. Instead, they recognise stress induced ligands characteristic to tumour transformation on the surface of tumour cells. They recognise these ligands via receptors encoded by genes inherited through the germline<sup>5</sup>. This characterises them to the innate immune system and differentiates them from cytotoxic T-cells. Therefore, NK cells reduce the number of steps before killing, as they do not require recognition of tumour antigen by antigen processing cells, making them suitable for cancer treatment. This innate nature of NK cells means that their activity must be extremely tightly regulated to

prevent the killing of healthy cells. The method by which NK cells are regulated is called the 'missing self hypothesis.' This states that inhibitory receptors on the surface of NK cells will recognise self-MHC molecules and prevent an immune response against self-cells<sup>6</sup>. Activating receptors like CD16, for example, recognise the fragment crystallisable (Fc) region of IgG antibodies, which are molecules that are only produced in response to infection. This ligation is just strong enough to overcome inhibitory signals allowing NK cells to become activated<sup>7</sup>. This is the basis for BiKE and TriKE therapy, as illustrated in Figure 1.

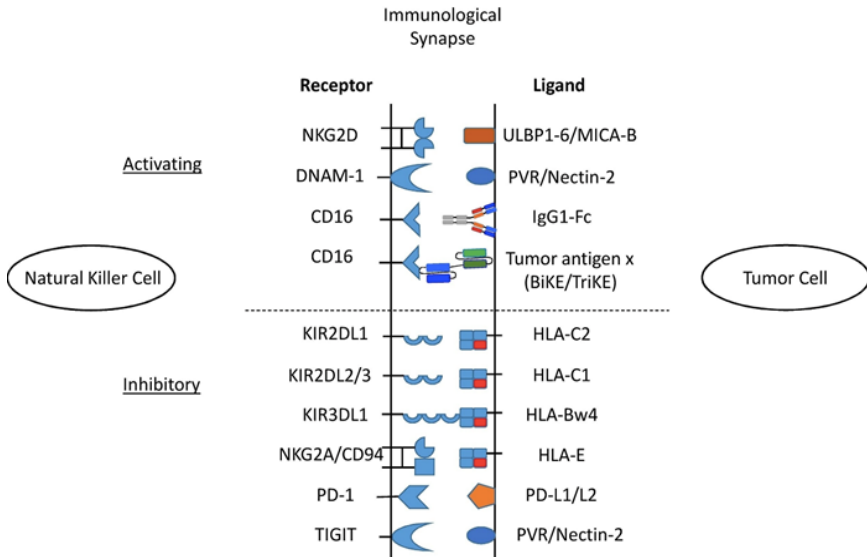


Figure 1: *Activating and inhibitory interactions between NK cells and tumour cells. Figure taken from Davis, et al.<sup>14</sup>.*

## CD16 (Fc $\gamma$ RIII)

In addition to the activation of NK cells via target cell-expressed ligands, CD16 also mediates antibody-dependent cellular cytotoxicity (ADCC). Two isoforms of the receptor exist: CD16a and CD16b. CD16a is a transmembrane receptor on the surface of NK cells, macrophages and placental trophoblasts, while CD16b is a GPI-anchored receptor on the surface of neutrophils<sup>8</sup>. The two isoforms have 90% homology, however, only CD16a will result in ADCC against tumour targets<sup>9</sup>. NK cells make up roughly 15% of the body's lymphocytes, and of this amount, 90% express CD16a. There are two distinct NK cell subsets in humans that are characterised by differences in CD56 expression<sup>10</sup>. NK cells that express CD16a are called CD56<sup>dim</sup>, meaning they have low expression of CD56 and high expression of CD16. The other subset, accounting for 10% of NK cells, is called CD56<sup>bright</sup>. These NK cells show very little cytotoxicity because of their low expression of CD16a<sup>10</sup>. By performing flow cytometric analysis, de Maria et al.<sup>11</sup>, were able to observe

cytokine production in NK cells over a period of 16 hours. After stimulation with monoclonal antibodies (mAb), it was observed that IFN $\gamma$  was produced much earlier in CD56<sup>dim</sup> NK cells. This was between 2 and 4 hours after stimulation, coinciding with cytotoxic activity. CD16a is a low affinity receptor for the fragment crystallizable (Fc) region of IgG antibodies. While the antigen binding (Fab) fragment recognises its target, CD16a will bind to the Fc region of the antibody via its FcR $\gamma$  subunit, which contains an immunoreceptor tyrosine-based activation motif (ITAM)<sup>12</sup>. Binding induces positive signalling through the ITAM, that will result in the production of cytokines such as IFN $\gamma$  and TNF $\alpha$  which are essential anti-tumour agents<sup>9</sup>.

## Bispecific killer engagers (BiKEs)

The limitation of NK cells for cancer therapy is the absence of cancer cell specificity<sup>13</sup>. This led to the initial development of an immunomodulator called a BiKE. BiKEs consist of two antibody fragments; one that recognises the tumour, while the other antibody recognises CD16a on NK cells. The CD16a antibody is an anti-human anti-CD16 single chain variable fragment (scFv)<sup>14</sup>. Variable regions of antibodies consist of heavy (VH) and light (VL) chains. However, these chains have inadequate stability and will dissociate from one another. Therefore, links between the two chains have been developed to stabilise the interaction<sup>15</sup>. The second antibody fragment is an scFv for a tumour antigen. Vallera et al.<sup>14</sup>, created a BiKE with an antibody fragment for CD33, a tumour antigen associated with acute myeloid lymphoma (AML) and myelodysplastic syndromes. The result was a 1633 BiKE which could enhance the action of NK cells to CD33<sup>+</sup> AML blasts and formed a cytolytic synapse between the NK cell and the target cell.

The effectiveness of BiKEs for tumour elimination *in vivo* was also studied by Vallera et al.<sup>14</sup>, using mouse xenograft models. This experiment showed that even though there was a large amount of initial recruitment and activation of NK cells, tumour growth ultimately persisted. While ADCC was observed initially, NK cell survival was the barrier to the potency of BiKEs as an immunotherapy<sup>16</sup>.

## IL-15

Interleukin-15 (IL-15) is an important cytokine involved in function of NK cells, natural killer T (NKT) cells and memory CD8<sup>+</sup> T cells expressing IL-15 receptor  $\beta$  (IL-15R $\beta$ ). It is trans-presented, meaning that it is secreted bound to its receptor (receptor  $\alpha$ ) forming the complex IL-15/IL-15R $\alpha$ <sup>17</sup>. In this form, IL-15R $\alpha$  can present IL-15 to IL-15R $\beta$ , triggering a response in target cells. This involves activation of genes associated with promoting cell survival and proliferation and preventing cell death<sup>18</sup>. As well as stimulating NK cell growth and proliferation, treatment with IL-15 can induce faster NK cell priming<sup>19</sup>. NK cells treated with IL-15 have

a higher rate of production of  $\text{IFN}\gamma$  after re-exposure to the cytokine, suggesting that 'innate memory' is conveyed onto these cells<sup>19</sup>.

In a clinical trial in the US, IL-15 was being administered to AML patients<sup>20</sup>. The main issue with these studies was that treatment with large amounts of IL-15 can cause autoimmune toxicity, so dose levels must be kept low. However, correlation between IL-15 levels and NK cell regeneration was positive, indicating that IL-15 can be associated with tumour regression.

Another promising IL-15 treatment involves the introduction of 'memory' into NK cells. Cytokine-induced memory-like NK cells differentiate after treatment with IL-12, IL-15 and IL-18, and have enhanced anti-tumour activity<sup>21</sup>. The first in-human clinical trial showed that these cells have increased expression of  $\text{IFN}\gamma$  and showed heightened proliferation in AML patients, leading to a more aggressive response<sup>21</sup>.

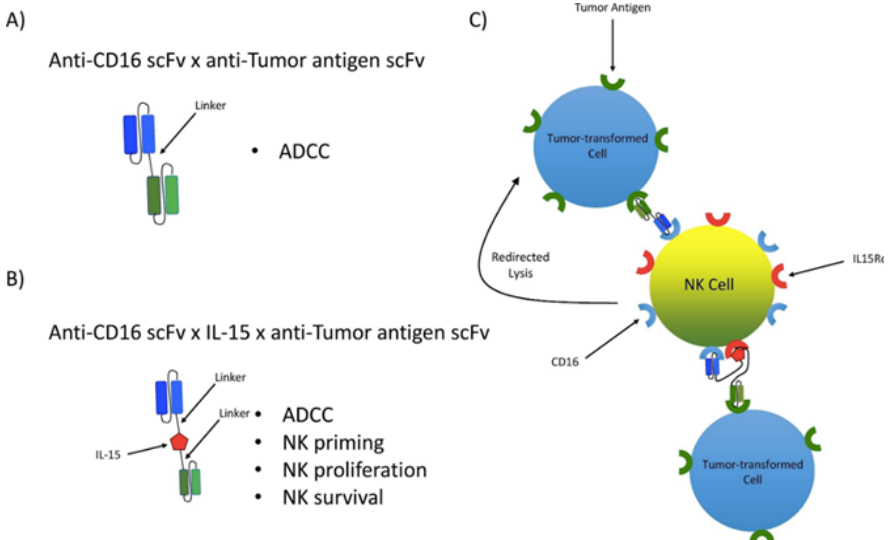


Figure 2: (A) Basic design of BiKE. (B) Basic design of TriKE. (C) Function of BiKE and TriKE. Figure taken from Davis, et al.<sup>16</sup>.

## Expression and Purification of BiKEs and TriKEs

The following method of expression was used by Vallera et al.<sup>14</sup>, to develop the initial trispesic killer engager (TriKE). TriKEs are a further development on BiKEs as they include human IL-15 as a linker between the CD16a scFv and the tumour antibody forming a 161533 TriKE (Fig. 2). The final configuration of the gene was spliced into the pET21d expression vector. This was then transformed into the *Escherichia coli* strain BL21 and expression was induced using isopropyl-

b-D-thiogalactopyranoside (IPTG). Subsequent purification by ion exchange chromatography, left a sample of 161533 TriKE for *in vivo* studies.

Interestingly the presence of IL-15 made purification easier, when compared to the 1633 TriKE. This is because addition of IL-15 reduced the isoelectric point by two units of pH. This enhanced purification meant that there was nearly twice the yield of 161533 TriKE compared to 1633 BiKE<sup>14</sup>.

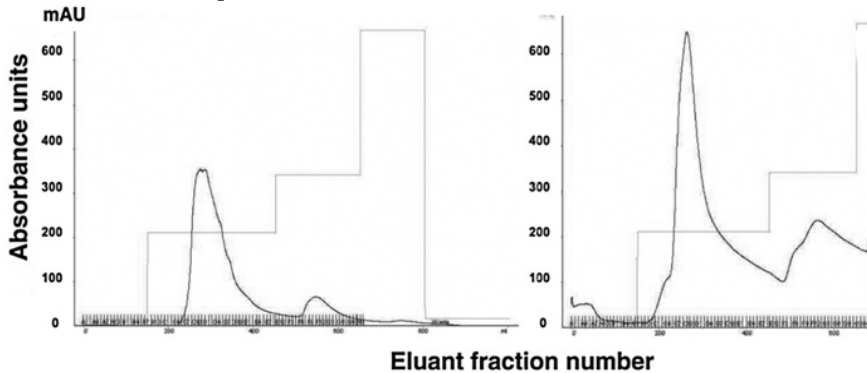


Figure 3: Absorbance readings for BiKE (left) and TriKE (right) eluted from an ion exchange column, showing a higher yield of TriKE. The first peak in both graphs indicates the product. Taken from Vallera, et al.<sup>14</sup>

## Effects of BiKEs and TriKEs on NK cell anti-tumour activity

Because NK cells treated with BiKEs showed high levels of ADCC, tests were carried out to ensure that the same result was observed in NK cells treated with TriKEs. This was done *in vitro*, using CD33<sup>+</sup> targets from the human leukemia cell line, HL-60, in a 4-hour chromium-51 release assay<sup>14</sup>. The result was that the cells treated with 161533 TriKE had much greater levels of cytotoxicity, degranulation and cytokine production, than the cells treated with 1633 BiKE. TriKE treated cells resulted in killing of 58.3% of radiolabelled HL60 while BiKE treated cells killed 33.0% of the cells<sup>14</sup>. In order to determine if the presence of IL15 is the primary cause for this cytotoxicity, Vallera et al.<sup>14</sup>, performed a similar assay with BiKE and IL15 present. The observed cytotoxicity was similar to that of the 161533 TriKE. Presence of IL-15 has always been associated with enhanced cytotoxic activity. It is clearly the combination of the specificity of the BiKE for CD33<sup>+</sup> targets and the activity of IL-15 that enhances NK cell toxicity<sup>14</sup>.

However, the ultimate test of TriKE's anti-tumour activities is an *in vivo* demonstration. This was done in mouse xenograft models, using human CD33<sup>+</sup> myeloma cells. Transfer of NK cells and subsequent treatment with BiKE and TriKE enabled studies on tumour regression<sup>14</sup>. The *in vivo* experiment consisted of three mouse groups, each containing five mice injected with CD33<sup>+</sup> myeloma cells. The

control group were not given any drug or NK cells. The second group were given 1633 BiKE and human NK cells. The third group were given 161533 TriKE and human NK cells<sup>14</sup>. The results showed that significant tumour regression, at day 21, was only observed in the 161533 TriKE group. While initial tumour regression was observed in the 1633 BiKE group, control of the tumour was not maintained by day 21. Although mice in this group had prolonged survival in comparison to the control group, in which two mice had died, the TriKE showed superior anti-tumour activity to the BiKE<sup>14</sup>.

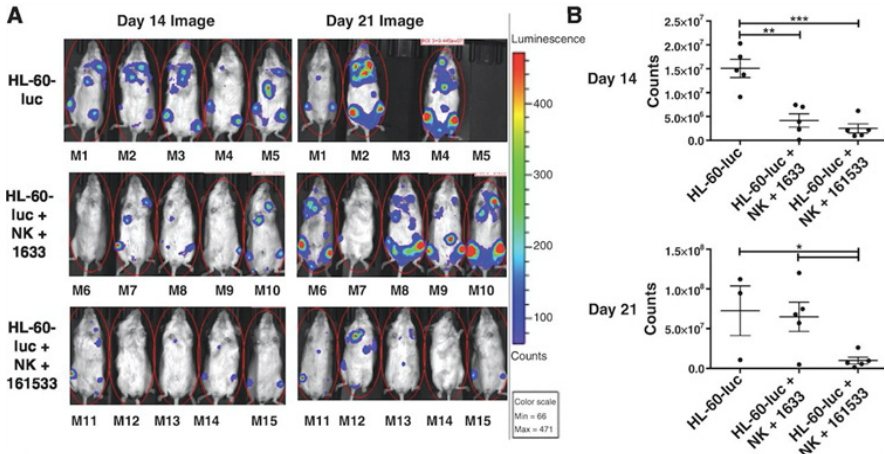


Figure 4: There are three mouse groups, each containing five mice injected with CD33<sup>+</sup> myeloma cells of the HL-60-luc cell line. These cells contain a luciferase reporter gene that enables imaging because of bioluminescence characteristic of luciferase. The control group only received HL-60-luc cells, whereas the treatment groups received NK cell infusions followed by treatment with 1633 BiKE or 161533 TriKE. (A) Bioluminescence imaging of mice from the three groups on day 14 and day 21. M refers to mouse. (B) Graphical representation of luminescence in mice. The dots represent individual mice and the bars denote mean  $\pm$  SEM. Taken from Vallera, et al.<sup>14</sup>.

## Effects of BiKEs and TriKEs on survival and proliferation of NK cells

Schmohl et al.<sup>26</sup> further investigated the effects of TriKEs on proliferation of NK cells, using another form of TriKE called the 1615EpCAM TriKE. This immunomodulator targets the carcinoma-specific ligand: EpCAM (epithelial cell adhesion molecule). In order to eliminate all other sources of proliferation inducers, five groups of NK cells were each treated with one of the following: TriKE, BiKE, anti-CD16 scFv, IL-15 and anti-EpCAM scFv. After 7 days of incubation and LIVE/DEAD staining, it was determined that only the TriKE and IL-15 groups triggered proliferation and prolonged survival as most NK cells in the other groups were

dead. Subsequent flow cytometry and trypan blue staining showed that NK cells in the TriKE group were superior in preservation of NK cells when compared to the group containing IL-15 alone. This verified the hypothesis that presence of an IL-15 moiety in TriKEs enables enhanced survival of NK cells as well as enhanced anti-tumour effects.

## Further developments of BiKEs and TriKEs

The possibility of generating BiKEs and TriKEs with specificity to a number of varying ligands makes them a useful means of treating cancer for two reasons. Firstly, they can be used to target a wide variety of different tumour ligands, making it possible to redirect NK cells towards a multitude of tumours. Secondly, this feature means that the problem of tumour immunoediting can be overcome. Some cancer cells can evade immune surveillance as their phenotype will not trigger an immune response. These cells have the capacity to do this as they are rapidly mutating in a process called immunoediting<sup>22</sup>. By identifying a new tumour ligand that can be targeted by an NK cell, a new scFv can be expressed specific to that ligand<sup>23</sup>. This feature means that BiKEs and TriKEs are immunotherapies that could bear long-term success. Many cancers express ligands also found on healthy cells. This means that the ligands chosen must be unique to tumour cells. If not, immune toxicity would result which is a major issue when developing cancer therapies.

Interestingly, the main obstacle to the lasting success of BiKEs and TriKEs is not immunoediting of cancer ligands but shedding of CD16 on NK cells<sup>24</sup>. After NK cell activation, CD16 is lost from the cell surface because of cleavage of the extracellular domain by A disintegrin and metalloprotease-17 (ADAM17)<sup>24</sup>. This will disassemble the NK cell immune synapse and prevent excessive immune response<sup>24</sup>. ADAM17 is a potent target in cancer therapies as it is overexpressed in many tumours. This enables the tumour itself to prevent continuous ADCC by NK cells<sup>25</sup>. Inhibition of ADAM17 in NK cells leads to increased ADCC due to the preservation of CD16 on the cell surface. This can be done by incubating NK cells in the presence of the ADAM17 inhibitor: BMS566394. Subsequent assays revealed increased cytotoxicity due to increased expression of IFN- $\gamma$  and TNF- $\alpha$ <sup>26</sup>.

It is also possible to simultaneously target two cell surface proteins. The TriKE synthesised by Schmohl, et al.<sup>28</sup>, was specific to a tumour transmembrane glycoprotein called EpCAM<sup>27</sup>. By incorporating another scFv into a pre-existing TriKE, the resulting killer engager is known as a tetra specific killer engager (TetraKE). The initial investigation of the viability of TetraKEs was carried out on cultured Caco-2 colon carcinoma cells, which express EpCAM and CD133 on their surface<sup>28</sup>. The results showed that 1615EpCAM133 TetraKEs were more successful at killing the carcinoma cells than EpCAM16 BiKEs and 1633BiKEs<sup>28</sup>. This was in part due to heightened expression of perforin and granzyme as well as greater

degrees of degranulation<sup>28</sup>.

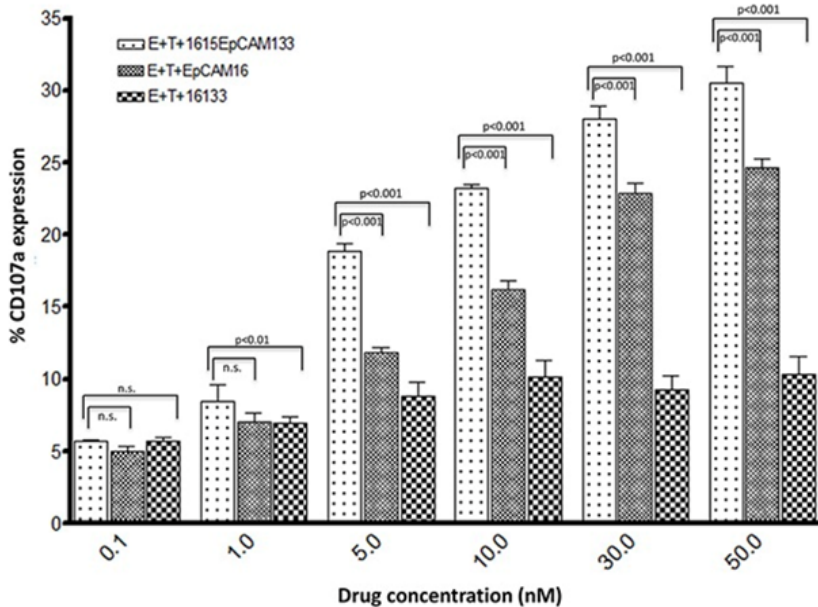


Figure 5: Quantifying degranulation in a 1615EpCAM TetraKE, an EpCAM16 BiKE and a 1633 BiKE. To quantify dose dependent degranulation a flow cytometry based CD107a assay was performed. CD107a surface expression serves as a marker for NK cell degranulation. E (effector), refers to NK cells and T (target), refers to Caco-2 colon carcinoma cells. Taken from Schmohl, et al.<sup>28</sup>.

As previously mentioned, EpCAM is highly expressed on carcinomas, however, it is also highly expressed on the basolateral membrane of normal epithelia<sup>29</sup>. This is reason for concern, as BiKEs, TriKEs and TetraKEs that have an anti-EpCAM scFv may result in severe side-effects such as severe inflammation of the gastrointestinal tract. Even though EpCAM is mainly expressed on the basolateral membrane and may not be accessible to immunotherapies, this is still a major cause for concern<sup>30</sup>. Other immunotherapies, may be able to use molecules downstream of EpCAM in its signalling pathway, but this is not a possibility for killer engagers as they are reliant on molecules present on the cell surface.

Because NK cells only target tumour-specific ligands, it is possible for the tumour to evade NK cells by immunoediting. This is done by inhibiting expression of adhesion molecules and activating ligands, promoting expression of class I MHC and shedding of soluble activation ligands from the surface<sup>31</sup>. By promoting expression of class I MHC, the distribution of the molecules on the surface of the tumour cell will resemble a normal cell, resulting in an inhibitory signal to the NK cell. In addition, shedding of soluble ligands, such as MICA can prevent tumour detection by NKG2D<sup>32</sup>. Tumours can also suppress NK cell function by

the release of inhibitory factors such as IL-10 or TGF- $\beta$ <sup>33</sup>. Concurrent treatment of inhibitors of IL-10 and TGF- $\beta$ , with TriKEs, could overcome this obstacle, just as ADAM17 inhibitors are used to prevent CD16 shedding. Another interesting development could be the incorporation of an scFv that will block ADAM17, IL-10 or TGF- $\beta$ , into an immunomodulator.

## Risks associated with BiKEs and TriKEs

While a number of different types of killer engagers have been developed showing promise for future treatment, studies have only been carried out in mouse xenograft models. For this reason, the safety of these treatments cannot be properly assessed. The main reason for concern regarding TriKEs is their incorporation of IL-15, which will stimulate NK cell NKT cells and CD8<sup>+</sup> cytotoxic T cells. If IL-15 is present in abundance, a prolonged cytokine cascade could cause an immune response that is too aggressive and may cause harm to the patient<sup>34</sup>. However, a reduction in administration of TriKEs may not be sufficient for potent killing of tumour cells. In the xenograft model done by Vallera et al.<sup>14</sup>, 20  $\mu$ g of TriKE was administered for two weeks, without any detectable adverse side effects. Considering the high level of ADCC observed, this is very promising, but a lot more work must be done to determine if killer engagers containing IL-15 are safe.

While some risks such as autoimmune toxicity can be predicted, extensive investigation into dosage is required. Currently there is one clinical trial that is expected to begin this year, using the 161533 TriKE to treat 60 patients with myelodysplastic syndrome and AML. There are six dosage levels ranging from 5  $\mu$ g/kg/day to 200  $\mu$ g/kg/day to determine the optimal dose in terms of safety and effectiveness<sup>35</sup>. Once these studies are carried out and physiological responses are determined, it will then be possible to consider the use of TriKEs as an adequate cancer therapy.

## Conclusion

Targeted antibody therapies, such as BiKEs and TriKEs, are promising cancer immunotherapies because of their ability to add ligand specificity and enhance survival and cytotoxicity of NK cells against tumours. They also have the potential of becoming a potent 'off-the-shelf' therapy which holds many major benefits over personalised medicine, such as CAR T-cell therapy. These therapies can pose a number of risks, including systemic inflammation resulting from the release of pro-inflammatory cytokines<sup>36</sup>. Although their development is in early stages, the use of the 161533 BiKE in xenograft mouse models in the study by Vallera, et al.<sup>14</sup>, shows their ability to promote tumour regression. They provide an excellent platform for versatility because of the ease at which scFv portions can be changed and added. This feature shows their ability to overcome checkpoint signalling,

tumour immunoediting and receptor shedding on NK cells. The use of these immunomodulators in cancer therapy is in very early stages and substantial research must be undertaken to ensure that they are safe for use. Many features, such as non-tumour-specific target ligands and the presence of IL-15, suggest that an autoimmune cytotoxic response is possible for some models. Although the in vivo studies didn't show any detectable negative reactions to the therapy, the true indicator will be the results of the first clinical trial which is due to start in January 2020.

## References

1. Finn, O.J. Immuno-oncology: understanding the function and dysfunction of the immune system in cancer. *Ann Oncol.* 2012; 23(8):6-9
2. Lowry, L.E., Zehring, W.A. Potentiation of Natural Killer Cells for Cancer Immunotherapy: A Review of Literature. *Front Immunol.* 2017; 8
3. Herberman, R.B., Nunn, M.E., Lavrin, D.H. Natural cytotoxic reactivity of mouse lymphoid cells against syngeneic acid allogeneic tumors. I. Distribution of reactivity and specificity. *Int J Cancer.* 1975; 16(2):216-229
4. Morvan, M.G., Lanier, L.L. NK cells and cancer: you can teach innate cells new tricks. *Nat Rev Cancer.* 2015; 16(1):7-19
5. Raulet, D.H., Guerra, N. Oncogenic stress sensed by the immune system: role of NK cell receptors. *Nat Rev Immunol.* 2009; 9(8):568-580
6. Raulet, D.H. Missing self-recognition and self-tolerance of natural killer (NK) cells. *Sem Immunol.* 2006; 18(3):145-150
7. Anegón, I., Cuturi, M.C., Trinchieri, G., Perussia, B. Interaction of Fc receptor (CD16) ligands induces transcription of interleukin 2 receptor (CD25) and lymphokine genes and expression of their products in human natural killer cells. *J Exp Med.* 1988; 167(2):452-472
8. Ravetch, J.V., Perussia, B. Alternative membrane forms of Fc gamma RIII(CD16) on human natural killer cells and neutrophils. Cell type-specific expression of two genes that differ in single nucleotide substitutions. *J Exp Med.* 1989; 170(2):481-497
9. Lanier, L.L., Ruitenberg, J.J., Phillips, J.H. Functional and biochemical analysis of CD16 antigen on natural killer cells and granulocytes. *J Immunol.* 1988; 141(10):3478-3485
10. Cooper, M.A., Fehniger, T.A., Caligiuri, M.A. The biology of human natural killer-cell subsets. *Trends Immunol.* 2001; 22(11):633-640
11. De Maria, A., Bozzano, F., Cantoni, C., Moretta, L. (2011) Revisiting human natural killer cell subset function revealed cytolytic CD56dim CD16+ NK cells as rapid producers of abundant IFN- $\gamma$  on activation. *Proc Natl Acad Sci USA*, 108, 728-732
12. Scholl, P.R., Ahern, D., Geha, R.S. Protein tyrosine phosphorylation induced via the IgG receptors Fc gamma R1 and Fc gamma R2 in the human monocytic cell line THP-1. *The J Immunol.* 1992; 149(9):1751-1757
13. Rubnitz, J.E., Inaba, H., Ribeiro, R.C., Pounds, S., Rooney, B., Bell, T., Pui, C.H., Leung, W. NKAML: a pilot study to determine the safety and feasibility of haploidentical natural killer cell transplantation in childhood acute myeloid leukemia. *J Clin Oncol.* 2010; 28(6):955-959
14. Vallera, D.A., Felices, M., McElmurry, R., McCullar, V., Zhou, X., Schmohl, J.U., Zhang, B., Lenvik, A.J., Panoskaltis-Mortari, A., Verneris, M.R., Tolar, J., Cooley, S., Weisdorf, D.J., Blazar, B. (2016) IL15 Trispecific Killer Engagers (TriKE) Make Natural Killer Cells Specific to CD33+ Targets While Also Inducing Persistence, In Vivo Expansion and Enhanced Function. *Clin Cancer*

Res. 2016; 22(14):3340-3350

15. Feng, J., Xie, Z., Guo, N., Shen, B. Design and assembly of anti-CD16 ScFv antibody with two different linker peptides. *J Immunol Methods*. 2003; 282(1):33-43

16. Davis, Z.B., Vallera, D.A., Miller, J.S., Felices, M. Natural killer cells unleashed: Checkpoint receptor blockade and BiKE/TriKE utilisation in NK-mediated anti-tumor immunotherapy. *Sem Immunol*. 2017; 31:64-75

17. Castillo, E.F., Schluns, K.S. Regulating the immune system via IL-15 transpresentation. *Cytokine*. 2012; 59(3):479-490

18. Lodolce, J.P., Burkett, P.R., Koka, R.M., Boone, D.L., Ma, A. Regulation of lymphoid homeostasis by interleukin-15. *Cytokine Growth Factor Rev*. 2002; 13(6):429-439

19. Romee, R., Schneider, S.E., Leong, J.W., Chase, J.M., Keppel, C.R., Sullivan, R.P., Cooper, M.A., Fehniger, T.A. Cytokine activation induces human memory-like NK cells. *Blood*. 2012; 120(11):4751-4760

20. Haploidentical Donor Natural Killer Cell Infusion With IL-15 in Acute Myeloid Leukemia (AML). 2015; Retrieved from <https://clinicaltrials.gov/ct2/show/NCT01385423> Identification No. NCT01385423

21. Romee, R., Rosario, M., Berrien-Elliott, M.M., Wagner, J.A., Jewell, B.A., Schappe, T., Leong, J.W., Abdel-Latif, S., Schneider, S.E., Willey, S., Neal, C.C., Yu, L., Oh, S.T., Lee, Y.S., Mulder, A., Claas, F., Cooper, M.A., Fehniger, T.A. Cytokine-induced memory-like natural killer cells exhibit enhanced responses against myeloid leukemia. *Sci Transl Med*. 2016; 8(357):357ra123

22. Dunn, G.P., Koebel, C.M., Schreiber, R.D. Interferons, immunity and cancer immunoediting. *Nat. Rev. Immunol*. 2006; 6:836-848

23. Tay, S.S., Carol, H., Biro, M. TriKEs and BiKEs join CARs on the cancer immunotherapy highway. *Hum Vaccin Immunother*. 2016; 12(11):2790-2796

24. Srpan, K., Ambrose, A., Karampatzakis, A., Saeed, M., Cartwright, A.N.R., Guldevall, K., Dos Santos Cruz De Matos, G., Onfelt, B., Davis, D.M. Shedding of CD16 disassembles the NK cell immune synapse and boosts serial engagement of target cells. *J Cell Biol*. 2018; 217(9):3267

25. Wiernik, A., Foley, B., Zhang, B., Verneris, M.R., Warlick, E., Gleason, M.K., Ross, J.A., Luo, X., Weisdorf, D.J., Walcheck, B., Vallera, D.A., Miller, J.S. Targeting Natural Killer cells to Acute Myeloid Leukemia in vitro with a CD16x33 bispecific killer cell engager (BiKE) and ADAM17 inhibition. *Clin Cancer Res*. 2013; 19(14):3844-3855

26. Romee, R., Foley, B., Lenvik, T., Wang, Y., Zhang, B., Ankarlo, D., Luo, X., Cooley, S., Verneris, M., Walcheck, B., Miller, J. NK cell CD16 surface expression and function is regulated by a disintegrin and metalloprotease-17 (ADAM17). *Blood*. 2013; 121(18):3599-3608

27. Went, P.T.H., Lugli, A., Meier, S., Bundi, M., Mirlacher, M., Sauter, G., Dirnhofer, S. Frequent EpCam protein expression in human carcinomas. *Hum Pathol*. 2004; 35(1):122-128

28. Schmohl, J.U., Felices, M., Todhunter, D., Taras, E., Miller, J.S., Vallera, D.A. Tetra-specific scFv construct provides NK cell mediated ADCC and self-sustaining stimuli via insertion of IL-15 as a cross-linker. *Oncotarget*. 2016(45); 7:73830-73844

29. Trzpis, M., McLaughlin, P.M.J., de Leij, L.M.F.H., Harmsen, M.C. Epithelial Cell Adhesion Molecule: More than a Carcinoma Marker and Adhesion Molecule. *American J Pathol*. 2007; 171(2):386-395

30. Balzar, M., Winter, M.J., de Boer, C.J., Litvinov, S.V. The biology of the 17-1A antigen (Ep-CAM). *J Mol Med*. 1999; 77(10):699-712

31. Ljunggren, H.G., Karre, K. In search of the 'missing self': MHC molecules and NK cell recognition. *Immunol Today*. 1990; 11(7):237-244

32. Deng, W., Gowen, B.G., Zhang, L., Wang, L., Lau, S., Iannello, A., Xu, J., Rovis, T.L., Xiong, N., Raulet, D.H. A shed NKG2D

ligand that promotes natural killer cell activation and tumor rejection. *Science*. 2015; 348(6230):136-139

33. Ostrand-Rosenberg, S., Myeloid-derived suppressor cells: linking inflammation and cancer. *J Immunol*. 2009; 182(8):4499-4506

34. Zhang, J.M., An, J. Cytokines, Inflammation and Pain. *Int Anaesthesiol Clin*. 2007; 45(2):27-37

35. CD16/IL-15/CD33 Tri-Specific Killer Engagers (TriKEs) for High Risk Heme Malignancies. (2017) Retrieved from <https://clinicaltrials.gov/ct2/show/NCT03214666> Identification No. NCT03214666

36. Brudno, J.N., Kochenderfer, J.N. Toxicities of chimeric antigen receptor T cells: recognition and management. *Blood*. 2016; 127(26):3321-3330

TS  
SR

# THE GUT-BRAIN AXIS IN MENTAL HEALTH AND PARKINSON'S DISEASE

Áine McCabe  
Senior Sophister  
Biochemistry

*This review explores how events that occur in the gut, often modulated by the microbiota, affect the brain and can lead to the breakdown of homeostasis. It explores emerging research on the role played by the gut microbiota modulating brain function in relation to depression and anxiety and it goes on to consider the gut-brain axis in the context of a common protein misfolding disease, Parkinson's Disease. Gut-brain axis signalling, potential biomarkers and possible therapeutic avenues are considered.*

## Introduction

The gut-brain axis is a very interesting aspect of science at the forefront of much emerging research. It is increasingly referred to as the gut-brain-microbiota axis in recognition of the importance of the role played by the 200 g of bacteria, viruses, archaea and eukaryotes that colonise the gut from birth until after death<sup>1</sup>. This topic lies at the interface of neuroscience, microbiology, physiology and biochemistry. The gut-brain-microbiota axis is thought to play an important role in health, including in mental health and Parkinson's disease (PD) which will be discussed in this review.

Gut-brain cross-talk refers to the bidirectional communication that occurs between the gastrointestinal tract and the brain<sup>2</sup>. Gut-brain cross-talk occurs through the autonomic and enteric nervous systems as well as endocrine, immune, and metabolic pathways, with cytokines as well as hormones and neurotransmitters released from the gut and intestinal bacteria and all playing important roles<sup>3</sup>. The gut is considered to be the largest endocrine organ in mammals due to the multiplicity of the signalling molecules, including peptides, that it secretes: the microbiota is considered to be a virtual endocrine organ in its own right<sup>4,5</sup>. The gut-brain-microbiota axis plays an important role in the maintenance of homeostasis.

## Gut Microbiota and its Impact on the Brain

Until recently, the microbiota was considered to be unimportant and difficult to study because many of the bacteria are strict anaerobes and were difficult to culture outside of the body. Recently, with the development of high throughput gene sequencing technologies and the Human Microbiome Project (2008-2012), the gut microbiota has gained a lot of attention and has now been described as a key regulator of the brain, behaviour and immunity<sup>6</sup>.

It has been found that the distinctive combination of microbes in a person's gut, combined with the stability of those microbial populations affects their predisposition towards numerous illnesses including metabolic and neurological diseases. Animal studies have shown that the microbiota can affect anxiety- and depressive-like behaviours, but the mechanism through which it does this remains unknown<sup>7</sup>. Hoban et al. performed an experiment in which intestinal dysbiosis was induced in rats by administration of antibiotics, and the rats were shown to have deficits in spatial memory, increased visceral sensitivity, more depressive-like behaviours, and altered central nervous system serotonin and BDNF concentrations and hypothalamus-pituitary-adrenal axis receptors<sup>8</sup>. Bailey et al. examined the gut microbiome of infant monkeys, and observed that three days after maternal separation, significantly lower numbers of *lactobacilli* were present in stool samples, and low numbers of *lactobacilli* correlated with the highest stress-indicative behaviours<sup>9</sup>. Galley et al. found that, in mice, just two hours of social defeat was sufficient to significantly alter the composition of the intestinal microbiota<sup>10</sup>. Building on that, a study involving post-weaning social isolation in mice suggested that stress at a young age may produce changes in the gut microbiota that affect the development of neuronal and endocrine function<sup>11</sup>.

Davari et al. found that probiotic administration in rats that had diabetes mellitus and subsequent metabolic changes in memory and learning reversed a decline in synaptic activity<sup>12</sup>. The mechanism of action of gut microbiota remains unclear: it may competitively exclude gut pathogens; it may stimulate the immune system by providing anti-inflammatory cytokines or it may communicate with the central nervous system through the vagus nerve<sup>13</sup>. Studies in humans are beginning to emerge to support the hypothesis that altering the microbiota in patients can alter brain function and therefore improve health. Benton et al. found that a significant portion of participants with low baseline mood scores who drank a fermented milk drink containing *Lactobacillus casei* probiotic supplement scored their mood as happy, compared to those who consumed a placebo<sup>14</sup>. Interestingly, the same trend did not manifest itself in people whose baseline mood scores were considered normal to begin with. Probiotics, usually containing lactic-acid producing bacteria from the genera *Lactobacillus* and *Bifidobacterium*, are increasingly used as food supplements and are linked to the relief of irritable-bowel syndrome, inflammatory bowel disease, the amelioration of lactose intolerance, prevention of bowel cancer and general benefits to the immune system<sup>15-20</sup>.

Diverse forms of neuroimmune and neuropsychiatric disorders are related to or modulated by the microbiome and it is thought that, through gut-brain cross-talk, microbiota can affect brain plasticity and cognitive function<sup>13</sup>. There are many ways through which this cross-talk could occur: some of these are explored in Figure 1. In an interesting study, faecal microbial transplant (FMT) was performed on two groups of germ-free mice: one group were colonised with bacteria from patients with depression and the control group was colonised with bacteria from healthy individuals<sup>21</sup>. The mice colonised with the bacteria from the depressed patients exhibited depressive-like symptoms, compared to the control group. The study suggests that depression-like behaviours stemming from gut dysbiosis are transmissible and it reasserts that the microbiome may work as a valuable target for depression therapy.

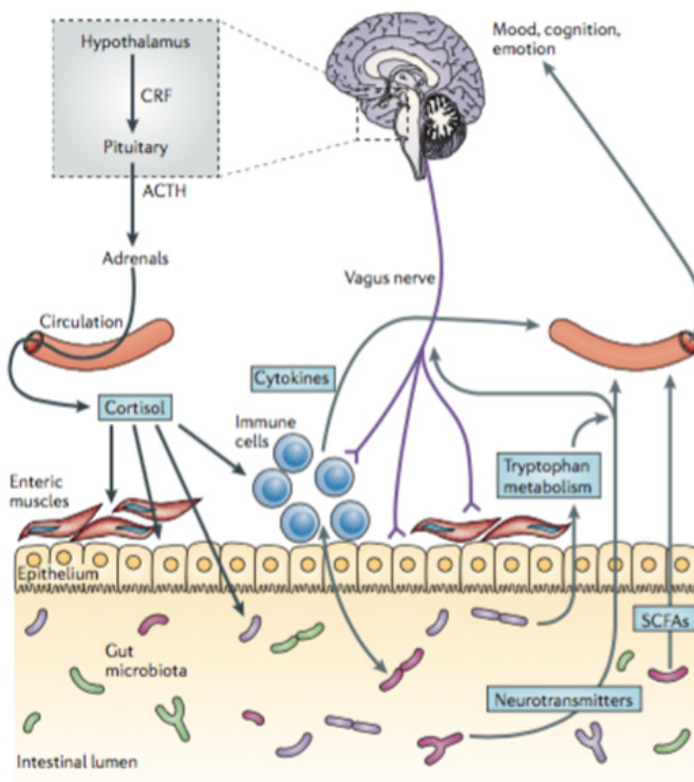


Figure 1: *Methods of Gut-Brain Interaction*, taken from Cryan and Dinan, 2012<sup>22</sup> demonstrates the many ways in which the gut microbiota and the brain can interact. The vagus nerve, hormone transport in circulation and conveyance of signals via the immune system all play critical roles, further emphasizing the multidisciplinary nature of the gut-brain-microbiota axis.

Vagotomies have proven useful in establishing when gut-brain crosstalk occurs through the vagus nerve. In one study, mice exhibiting anxiety- and depressive-like symptoms were found to improve and to exhibit alterations in their GABAergic systems after treatment with *Lactobacillus rhamnosus* (JB-1)<sup>23</sup>. However, these neurochemical and behavioural changes did not occur in mice that underwent vagotomy, indicating that the vagus nerve was important in communicating the change in microbial composition to the brain. It has been suggested that a truncal vagotomy confers some protection against PD, suggesting that the vagus nerve plays a role in some, but not all, cases of PD<sup>24</sup>.

## General Therapies Targeting the Microbiota

The newly emerging role of the microbiota presents potential therapeutic solutions. FMT is a practice that dated back to ancient China<sup>25</sup> but it is currently used clinically as a treatment for persistent *Clostridium difficile* infection. When more concrete, mechanistic evidence becomes available regarding the impact of the microbiota on the brain and health in general, FMT may prove to be an easy and cheap element of therapy for certain conditions, with inflammatory bowel disease, metabolic syndrome and obesity being proposed as candidates. Psychobiotics are a new therapeutic strategy which aim to improve mental health by affecting the gut microbiome through adding strains of bacteria that have been found to have a positive correlation with mental health, on the basis that it has been found that modulating gut microbiota influences brain function<sup>26</sup>.

## Parkinson's Disease Models and the Gut-Brain Axis

PD is a progressive, neurodegenerative disease characterised by a loss of dopamine neurons in the substantia nigra in the midbrain, which results in manifestation of the commonly recognised motor symptoms such as muscular rigidity, tremor and dyskinesia. There are a multitude of models of PD, many of which involve the gut-brain axis. Recent reviews conclude the factors that initiate the pathophysiological cascade in PD remain unknown, but an environmental factor likely plays a key role<sup>27</sup> probably against a background of genetic vulnerability<sup>28</sup>. The manifestation of symptoms first in the gut lends support to the hypothesis that this environmental factor exerts its influences primarily via the gut<sup>28, 29</sup>. The olfactory system is also of particular interest, as it also has a large surface area which is exposed to environmental factors, and defects of the olfactory system are also frequently implicated early in PD pathology<sup>30, 31</sup>.

The theory of molecular mimicry suggests that bacterial proteins from the nose and/or the gut may affect the brain through nerves including the vagus nerve and elicit cross-seeded misfolding, inflammation and oxidative stress and cellular toxicity, thereby initiating or influencing neurodegeneration in PD and other

conditions<sup>32</sup>. This is somewhat in line with the “Dual Hit Hypothesis”, which proposes that PD may be initiated by one of two routes: nasal, through the olfactory bulb to the temporal lobe; or gastric, through the enteric nervous system, caused by swallowing nasal secondary secretion in saliva<sup>33</sup>. Evidence, both clinical and pathological, shows that misfolded  $\alpha$ -synuclein is found in enteric nerves before it is found in the brain, thereby supporting the hypothesis that PD pathology may originate in the gut and spread to the central nervous system via cell-to-cell prion-like propagation through the vagus nerve<sup>34</sup>.

The gut and the brain have a strong connection in the context of PD, as explored in Figure 2. The gut microbiota induces dopamine synthesis in the brain via dopamine producing enzymes that travel along the microbiota-gut-brain axis<sup>35</sup>. The enteric nervous system and parasympathetic nerves are often affected by  $\alpha$ -synuclein pathology very early in the progression of PD<sup>28</sup>. Gastrointestinal symptoms are very common amongst patients with PD, with 80% experiencing chronic constipation<sup>36</sup>. This is thought to be caused by  $\alpha$ -synuclein deposition and associated neurodegeneration in the enteric nervous system, which gives rise to increased intestinal permeability and an inflammatory response<sup>37</sup>. These symptoms are thought to manifest themselves up to years in advance of the onset of the motor symptoms of PD, supporting the hypothesis that the disease pathogenesis might have primary connections with the gut<sup>35</sup>. Holmqvist et al. showed that  $\alpha$ -synuclein injected into the intestine is transported to the brain via the vagus nerve to the dorsal motor nucleus of the vagus nerve in the brainstem<sup>38</sup>. This finding reasserts the strength of the connection between the gut and the brain and it presents a possible way through which PD can spread from non-motor symptoms in the gastrointestinal system to the brain, from which it causes its characteristic motor deficits.

Nair et al. commented that it is possible that the trigger that causes blood-brain barrier leakage, immune cell activation and inflammation and ultimately neuroinflammation in the central nervous system may possibly be due to the chronic, low-grade inflammation in the gut<sup>35</sup>. Pro-inflammatory factors associated with chronic gastrointestinal diseases induce brain inflammation and death of dopaminergic neurons, which lead to PD<sup>39</sup>. Studies have indicated that people with PD have increased intestinal permeability, although it remains unclear whether this contributes to the causation or is caused by PD<sup>40</sup>.

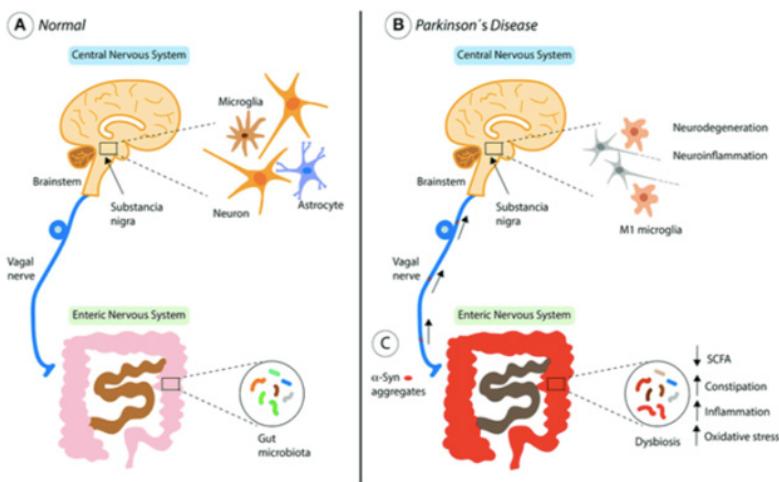


Figure 2: *The Gut-Brain Axis in Health and Parkinson's Disease: This figure is taken from Troncoso-Escudero, P. et al. (2018)<sup>41</sup>. It shows how dysbiosis can lead to a reduction in short chain fatty acid (SCFA) production and a rise in levels of constipation, inflammation and oxidative stress. It also suggests that  $\alpha$ -synuclein aggregates may travel to the brain through the vagus nerve and potentially result in an increase in pro-inflammatory M1 microglia, causing neurodegeneration and neuroinflammation.*

## The Involvement of the Microbiota in Parkinson's Disease

The intestinal microbiomes of people suffering from PD have been found to have differences to those of the general population. It was found that the abundance of *Prevotellaceae* in faeces of PD patients was reduced by 77.6% as compared with controls and that the relative abundance of *Enterobacteriaceae* was positively associated with the severity of postural instability and gait difficulty<sup>28</sup>. In the same study, using logistic regression based on the severity of constipation and the relative abundance of four bacterial families, PD patients were identified with 66.7% sensitivity and 90.3% specificity<sup>28</sup>. The prevalence of small intestine bacterial overgrowth was also found to be elevated in patients suffering from PD, at 25-54.5% compared to 8.3-20% in normal controls<sup>42</sup>.

## Treatment of Parkinson's disease

Existing treatments for PD can only somewhat alleviate the symptoms: the disease cannot be reversed. Current treatment involves increasing dopamine levels in the brain or – failing this – surgery can be an option to remove damaged brain regions.

Earlier diagnosis through identification of biomarkers could enable earlier and potentially novel treatment options.

There seems to be consensus on the fact that the non-motor symptoms of PD should be explored as potential indicators of risk or early biomarkers of disease. The focus need not be on the brain: to date, abnormal  $\alpha$ -synuclein accumulation has been identified in biopsies of the salivary glands, stomach, duodenum, colon and rectum of patients with PD<sup>35</sup>. The major drawback of the conventional treatment of PD is that, while it may alleviate symptoms, it cannot reverse them or prevent disease progression. Also, the conventional diagnosis of PD relies on motor symptoms, but by the time that these have manifested themselves, significant damage may have already occurred. The potential of immunohistochemical detection of  $\alpha$ -synuclein in the gut to act as a biomarker for PD was investigated, with a view to its use as a tool that would enable pre-symptomatic diagnosis of PD or, failing that, a diagnostic test that would help to confirm PD diagnoses in patients presenting atypical symptoms<sup>34</sup>. Methodological differences between studies makes comparison difficult, but ultimately it was concluded that, while it may have potential, that method does not currently give an accurate diagnosis. Detection of risk-factors might open the door to the discovery of preventative therapies and the discovery early biomarkers would facilitate early detection. The microbiota may be useful in this regard.

The intersection of PD and the microbiota appears to hold serious potential in terms of discovery of biomarkers or therapeutic targets for PD. For example, the data obtained in the experiment referred to above would suggest that a person with a high abundance of *Prevotellaceae* is very unlikely to suffer from PD, whereas low *Prevotellaceae* is associated with autism and type-1 diabetes as well as PD<sup>28</sup>. While a high proportion of *Prevotellaceae* may therefore prove useful to rule out PD, more biomarkers are needed and a more comprehensive analysis of the composition of the gut microbiota would increase accuracy. In terms of therapies, companies such as Enterin currently have compounds in clinical trials which are designed specifically to target the gut-brain axis in PD<sup>43</sup>. The possibility of food-based therapies has also been considered<sup>44</sup>. PD therapies are likely to see significant investment and, hopefully, some breakthroughs over the coming years.

## Conclusion

Gut-brain crosstalk and proteostasis are highly interrelated processes that leave much room for expansion of knowledge. Further research will require continued cooperation between the various disciplines that study various aspects of the gut-brain-microbiota axis. For mental health and PD, elucidation of the mechanisms through which the gut, the brain and the microbiome interact would bring greater understanding as well as increased interest and therapeutic potential to this exciting and rapidly-evolving field.

## References

1. Sender R, Fuchs S, Milo R. Revised Estimates for the Number of Human and Bacteria Cells in the Body. *PLoS Biol.* 2016;14(8):e1002533.
2. Mayer EA. Gut feelings: the emerging biology of gut-brain communication. *Nat Rev Neurosci.* 2011;12(8):453-66.
3. de Weerth C. Do bacteria shape our development? Crosstalk between intestinal microbiota and HPA axis. *Neurosci Biobehav Rev.* 2017;83:458-71.
4. Clarke G, Stilling RM, Kennedy PJ, Stanton C, Cryan JF, Dinan TG. *Mol Endocrinol.* 2014;28(8):1221-38
5. O'Callaghan TF, Ross RP, Stanton C, Clarke G. The gut microbiome as a virtual endocrine organ with implications for farm and domestic animal endocrinology. *Domest Anim Endocrinol.* 2016;56 Suppl:S44-55.
6. Bailey MT, Cryan JF. The microbiome as a key regulator of brain, behavior and immunity: Commentary on the 2017 named series. *Brain Behav Immun.* 2017;66:18-22.
7. Lach G, Schellekens H, Dinan TG, Cryan JF. Anxiety, Depression, and the Microbiome: A Role for Gut Peptides. *Neurotherapeutics.* 2017.
8. Hoban AE, Moloney RD, Golubeva AV, McVey Neufeld KA, O'Sullivan O, Patterson E, et al. Behavioural and neurochemical consequences of chronic gut microbiota depletion during adulthood in the rat. *Neuroscience.* 2016;339:463-77.
9. Bailey MT, Coe CL. Maternal separation disrupts the integrity of the intestinal microflora in infant rhesus monkeys. *Dev Psychobiol.* 1999;35(2):146-55.
10. Galley JD, Bailey MT. Impact of stressor exposure on the interplay between commensal microbiota and host inflammation. *Gut Microbes.* 2014;5(3):390-6.
11. Doherty FD, O'Mahony SM, Peterson VL, O'Sullivan O, Crispie F, Cotter PD, et al. Post-weaning social isolation of rats leads to long-term disruption of the gut microbiota-immune-brain axis. *Brain Behav Immun.* 2018;68:261-73.
12. Davari S, Talaei SA, Alaei H, Salami M. Probiotics treatment improves diabetes-induced impairment of synaptic activity and cognitive function: behavioral and electrophysiological proofs for microbiome-gut-brain axis. *Neuroscience.* 2013;240:287-96.
13. Solas M, Milagro FI, Ramirez MJ, Martinez JA. Inflammation and gut-brain axis link obesity to cognitive dysfunction: plausible pharmacological interventions. *Curr Opin Pharmacol.* 2017;37:87-92.
14. Benton D, Williams C, Brown A. Impact of consuming a milk drink containing a probiotic on mood and cognition. *Eur J Clin Nutr.* 2007;61(3):355-61.
15. Gorbach SL. Probiotics and gastrointestinal health. *Am J Gastroenterol.* 2000;95(1 Suppl):S2-4.
16. Martini MC, Kukielka D, Savaiano DA. Lactose digestion from yogurt: influence of a meal and additional lactose. *Am J Clin Nutr.* 1991;53(5):1253-8.
17. Jiang T, Mustapha A, Savaiano DA. Improvement of lactose digestion in humans by ingestion of unfermented milk containing *Bifidobacterium longum*. *J Dairy Sci.* 1996;79(5):750-7.
18. Michetti P, Dorta G, Wiesel PH, Brassart D, Verdu E, Herranz M, et al. Effect of whey-based culture supernatant of *Lactobacillus acidophilus* (johnsonii) La1 on *Helicobacter pylori* infection in humans. *Digestion.* 1999;60(3):203-9.
19. Varcoe JJ, Krejcarek G, Busta F, Brady L. Prophylactic feeding of *Lactobacillus acidophilus* NCFM to mice attenuates overt colonic hyperplasia. *J Food Prot.* 2003;66(3):457-65.
20. Kopp-Hoolihan L. Prophylactic and

- therapeutic uses of probiotics: a review. *J Am Diet Assoc.* 2001;101(2):229-38; quiz 39-41.
21. Zheng P, Zeng B, Zhou C, Liu M, Fang Z, Xu X, et al. Gut microbiome remodeling induces depressive-like behaviors through a pathway mediated by the host's metabolism. *Mol Psychiatry.* 2016;21(6):786-96.
22. Cryan JF, Dinan TG. Mind-altering microorganisms: the impact of the gut microbiota on brain and behaviour. *Nat Rev Neurosci.* 2012;13(10):701-12.
23. Bravo JA, Forsythe P, Chew MV, Escaravage E, Savignac HM, Dinan TG, et al. Ingestion of Lactobacillus strain regulates emotional behavior and central GABA receptor expression in a mouse via the vagus nerve. *Proc Natl Acad Sci U S A.* 2011;108(38):16050-5.
24. Liu G, Men P, Perry G, Smith MA. Nanoparticle and iron chelators as a potential novel Alzheimer therapy. *Methods Mol Biol.* 2010;610:123-44.
25. de Groot PF, Frissen MN, de Clercq NC, Nieuwdorp M. Fecal microbiota transplantation in metabolic syndrome: History, present and future. *Gut Microbes.* 2017;8(3):253-67.
26. Dinan TG, Cryan JF. Melancholic microbes: a link between gut microbiota and depression? *Neurogastroenterol Motil.* 2013;25(9):713-9.
27. Kiebertz K, Wunderle KB. Parkinson's disease: evidence for environmental risk factors. *Mov Disord.* 2013;28(1):8-13.
28. Scheperjans F, Aho V, Pereira PA, Koskinen K, Paulin L, Pekkonen E, et al. Gut microbiota are related to Parkinson's disease and clinical phenotype. *Mov Disord.* 2015;30(3):350-8.
29. Poirier AA, Aube B, Cote M, Morin N, Di Paolo T, Soulet D. Gastrointestinal Dysfunctions in Parkinson's Disease: Symptoms and Treatments. *Parkinsons Dis.* 2016;2016:6762528.
30. Attems J, Walker L, Jellinger KA. Olfactory bulb involvement in neurodegenerative diseases. *Acta Neuropathol.* 2014;127(4):459-75.
31. Rahayel S, Frasnelli J, Joubert S. The effect of Alzheimer's disease and Parkinson's disease on olfaction: a meta-analysis. *Behav Brain Res.* 2012;231(1):60-74.
32. Friedland RP. Mechanisms of molecular mimicry involving the microbiota in neurodegeneration. *J Alzheimers Dis.* 2015;45(2):349-62.
33. Hawkes CH, Del Tredici K, Braak H. Parkinson's disease: a dual-hit hypothesis. *Neuropathol Appl Neurobiol.* 2007;33(6):599-614.
34. Ruffmann C, Parkkinen L. Gut Feelings About alpha-Synuclein in Gastrointestinal Biopsies: Biomarker in the Making? *Mov Disord.* 2016;31(2):193-202.
35. Nair AT, Ramachandran V, Joghee NM, Antony S, Ramalingam G. Gut Microbiota Dysfunction as Reliable Non-invasive Early Diagnostic Biomarkers in the Pathophysiology of Parkinson's Disease: A Critical Review. *J Neurogastroenterol Motil.* 2018;24(1):30-42.
36. Ueki A, Otsuka M. Life style risks of Parkinson's disease: association between decreased water intake and constipation. *J Neurol.* 2004;251 Suppl 7:vIII18-23.
37. Devos D, Lebouvier T, Lardeux B, Biraud M, Rouaud T, Pouclet H, et al. Colonic inflammation in Parkinson's disease. *Neurobiol Dis.* 2013;50:42-8.
38. Holmqvist S, Chutna O, Bousset L, Aldrin-Kirk P, Li W, Bjorklund T, et al. Direct evidence of Parkinson pathology spread from the gastrointestinal tract to the brain in rats. *Acta Neuropathol.* 2014;128(6):805-20.
39. Sui YT, Bullock KM, Erickson MA, Zhang J, Banks WA. Alpha synuclein is transported into and out of the brain by the blood-brain barrier. *Peptides.* 2014;62:197-202.
40. Salat-Foix D, Tran K, Ranawaya R, Meddings J, Suchowersky O. Increased in-

testinal permeability and Parkinson disease patients: chicken or egg? *Can J Neurol Sci.* 2012;39(2):185-8.

41. Troncoso-Escudero P, Parra A, Nassif M, Vidal RL. Outside in: Unraveling the Role of Neuroinflammation in the Progression of Parkinson's Disease. *Front Neurol.* 2018;9:860.

42. Fasano A, Bove F, Gabrielli M, Petracca M, Zocco MA, Ragazzoni E, et al. The role of small intestinal bacterial overgrowth in Parkinson's disease. *Mov Disord.* 2013;28(9):1241-9.

43. Perni M, Flagmeier P, Limbocker R, Cascella R, Aprile FA, Galvagnion C, et al. Multistep Inhibition of alpha-Synuclein Aggregation and Toxicity in Vitro and in Vivo by Trodusquemine. *ACS Chem Biol.* 2018;13(8):2308-19.

44. Perez-Pardo P, Kliet T, Dodiya HB, Broersen LM, Garssen J, Keshavarzian A, et al. The gut-brain axis in Parkinson's disease: Possibilities for food-based therapies. *Eur J Pharmacol.* 2017;817:86-95.

TS  
SR

# POLYGENIC RISK SCORES AND COMPLEX DISEASE

Iseult Jackson  
Senior Sophister  
Human Genetics

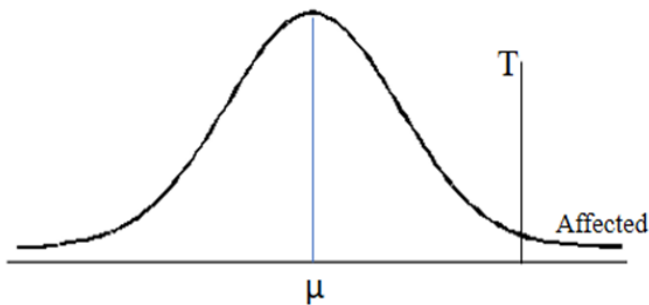
*Many common diseases are caused by both heritable and non-genetic factors. These are termed polygenic diseases and constitute a major healthcare burden. Patient stratification according to genetic risk factors may play a major role in clinical decision making. However, substantial barriers to the understanding and translation of polygenic disease genetics remain. In this review, the concept of polygenic disease and approaches for studying it are introduced. Then, the development and application of polygenic risk scores (PRS) in complex diseases and issues with the lack of diversity in genomics and its implications for PRS are discussed. Although there are still substantial limitations to polygenic disease research, recent developments in PRS suggest there is promise for the future of precision medicine.*

## Introduction

A central goal of human genetic research is to characterise disease, identify risk factors and develop therapeutic strategies. Mendelian disorders have straightforward genetic aetiology but are rare due to selective pressure against penetrant, disease-causing mutations<sup>1</sup>. Polygenic diseases have a heritable component and are influenced by environmental factors. For example, smoking influences age-related macular degeneration risk, but genetic variants also have a substantial effect<sup>2</sup>. Research into the genetic architecture of complex disorders could help identify disease mechanisms and potential therapeutic targets. However, the complexity of disease genetics is a substantial barrier to the understanding of disease mechanisms and clinical implementation of genetic knowledge<sup>3</sup>. This review focuses on progress made using genome-wide association study (GWAS) data in generating polygenic risk scores for complex diseases, their potential in precision medicine and challenges associated with them.

A key concept in polygenic disease genetics is the liability scale (Figure 1). Formalised by DS Falconer, this was used to justify the use of quantitative genetic

theory to investigate complex disease<sup>4</sup>. Incidence of certain diseases is higher among relatives of affected individuals than the general population, suggesting a genetic component to disease risk<sup>5</sup>. Although disease is thought of as a binary trait (i.e. individuals have a disease or do not), Falconer proposed a latent liability variable, which conferred disease above a certain threshold ( $T$  in the figure). This includes both environmental and genetic contributions to liability and is transformed to follow a normal distribution. This transformation allowed comparisons between groups and heritability estimations. Heritability is the proportion of trait variance accounted for by genetic variance. It reveals how much disease genetics has been explained and how much remains to be discovered<sup>6</sup>. Enrichment of heritability can also be used to dissect functional contributions to disease<sup>7</sup>.



### Liability conferred by risk variants and environmental components

Figure 1: *Liability scale in polygenic disease (adapted from Falconer and MacKay, 1996). Risk is conferred by genetic and environmental risk components. Threshold ( $T$ ) inferred from incidence in population (affected area on distribution). Mean liability ( $\mu$ ) can shift in high-risk groups (e.g. relatives). Difference in means can be used to estimate heritability.*

This model relies on assumptions that may not hold for all diseases: variance of liability must be the same between groups, and liability should be a continuous variable. There must be a reasonable number of risk factors to approximate this. Finally, the distribution of liability must be unimodal to allow transformation to a normal distribution. When there is one gene or environmental exposure with a large effect on risk compared to other contributors, this may not be true<sup>4</sup>. Although these assumptions may not be valid for all polygenic diseases<sup>8</sup>, it is a useful way of thinking about genetic contributions to disease risk, and insights gained from approaches based on this model are of clinical value.

## Detecting risk variants: GWAS

Identifying risk variants for polygenic disease is challenging because variants are not fully penetrant and do not segregate with disease. GWAS has made a major contribution to the understanding of polygenic disease genetics<sup>3</sup>. These studies investigate associations between common SNPs and a trait in an unrelated case/control population<sup>9</sup>. This contrasts with previous approaches for understanding polygenic disease, such as candidate gene-based approaches (reliant on prior assumptions about disease mechanism) and linkage analyses (which are not well-powered to detect common variants)<sup>10</sup>. GWAS allows the discovery of a larger number of associated variants so new hypotheses can be made about disease mechanisms, leading to clinically actionable data<sup>1</sup>.

The common disease/common variant (CD/CV) model of polygenic disease underlies GWAS. This model states that for a disease to be common, most of the genetic variance should be caused by the contribution of common variants<sup>11</sup>. These variants would likely have a small effect size due to purifying selection (influenced by variant effect size)<sup>12</sup>. It has recently been discovered that more recent variants explain a greater proportion of heritability, implying negative selection on disease-associated variants<sup>13</sup>. Although this model stipulates that most heritability comes from common variants, it does not exclude the contribution of rarer alleles<sup>3</sup>. Therefore, alternative approaches probing rare variant contribution may also be valuable.

GWAS uses the principle of linkage disequilibrium (LD) to identify variants associated with disease. LD is the non-random co-inheritance of alleles (located near each other on a chromosome)<sup>14</sup>. Cohorts are genotyped for a panel of common SNPs which tag most genomic variation. Associated variants must surpass a stringent p-value to minimise false discovery. These SNPs tag causative variants and generally don't play a causative role themselves. Strength of LD between a tagging SNP and a causal variant is affected by the frequency of both the SNP and causal variant, so GWAS SNP panels are powered to detect common variants<sup>9</sup>. Therefore, validity of the CD/CV model is essential to most polygenic disease research.

Variants tagged can be imputed from haplotype data, for example from the 1000 Genomes Project. This has led to major advancements in the understanding of polygenic disease. Despite this, one study has demonstrated the ability of genotyped SNPs to tag causal variants is error-prone in simulations in a range of populations<sup>15</sup>. However, this focused on the performance of two SNPs only, and investigated efficacy in cohorts with diverse ancestry. Limitations to GWAS translation due to the use of European imputation panels and the lack of diversity in genomics is discussed below and it is important to be aware of limitations to imputation when considering GWAS results. This is particularly relevant when considering polygenic models such as in PRS, which look at a large number of risk variants so error can be compounded<sup>15</sup>.

The ability of GWAS to explain variance in diverse populations is another major limitation. The majority of GWAS are performed on populations with European ancestry<sup>16</sup>. Standard GWAS arrays are designed to detect more variation in common reference (European) populations and do not perform as well in populations of different ancestries<sup>17</sup>. Although there is less variation in genomes of non-African populations, variants genotyped in standard GWAS are more polymorphic in European and Latino populations than in African ones<sup>18</sup>. One approach to attempt to tackle this is to include populations with diverse ancestry in imputation panels<sup>19</sup>. Multi-ancestry GWAS have also had some success. A GWAS for atopic dermatitis was performed on a cohort consisting of individuals of European, Japanese, African and Latino ancestry, and found variants associated across all populations, and population-specific variants<sup>20</sup>. This shows that although GWAS can be useful across populations, some disease-associated variants are population-specific. This may be a barrier to understanding a common disease mechanism and therefore to translation<sup>20</sup>. Differences in allele frequency between patient and study populations and differences in LD also influence variant discovery, even if underlying disease biology and causal variants are the same<sup>21</sup>. The challenge of translating GWAS in diverse populations is discussed in the section “Population Diversity and PRS”.

## Polygenic Risk Scores: Calculations

It had been predicted that GWAS would reveal variants explaining a large proportion of variance which might be clinically targetable<sup>9</sup>. With rare exceptions, this has not proven to be the case, meaning variants identified by GWAS may not be actionable on their own<sup>22</sup>. Thinking about disease quantitatively has allowed the development of polygenic risk scores (PRS), which capture disease liability from GWAS variants<sup>23</sup>. PRS are a weighted sum of the variants individuals carry associated with disease<sup>24</sup>. GWAS requires a stringent p-value threshold ( $P_T$ ) to assign significance to individual associated variants, but PRS generally use more relaxed thresholds. This is because the proportion of variance explained by genome-wide significant variants is not high, and analyses using LD score regression and genomic inflation statistics have revealed there is a reasonable amount of polygenicity not captured by GWAS<sup>25</sup>. Less stringent  $P_T$  aims to capture more of this variance, but must balance the risk of inflation due to random associations<sup>23</sup>.

Euesden et al. (2015) developed software to calculate PRS using a high-throughput method to obtain optimal  $P_T$ . Although this “best-fit” PRS may be better than those obtained by investigating broad  $P_T$  intervals, it involves multiple testing, so there is some inflation of the PRS p-value<sup>24</sup>. Other approaches include leveraging genetic correlation between diseases to improve prediction<sup>26</sup>. For example, there is a correlation between variants associated with schizophrenia and bipolar disorder<sup>27</sup>, and joint modelling of these diseases can increase sample size and power of risk score calculations. Functional annotation is also used to prioritise shared causal variants and improve prediction accuracy. This was validated in Crohn’s disease,

coeliac disease and type 2 diabetes, suggesting that greater knowledge of related architectures of complex disease can improve risk prediction accuracy<sup>26</sup>. A major limitation is that there may be sample overlap between GWAS leading to spurious correlations, but approaches have been developed to tackle this<sup>28</sup>.

Bayesian approaches have also been developed to estimate PRS<sup>29</sup>. Speed and Balding (2018) adopt this approach when investigating a new method of estimating heritability and its effect on a number of measures, including PRS. This method involves weighting the per-SNP effect size using a prior distribution that estimates heritability tagged by that SNP. “Classical” approaches weight PRS with the correlation between genotype and phenotype. The bayesian approach was shown to improve the performance of PRS under some models of heritability but not others. Improved approaches in calculating PRS are sure to be developed in the coming years, and there are now some PRS which are likely to be clinically useful in some cases<sup>30</sup>. However, limitations in non-European populations mean there are major ethical barriers to their immediate implementation<sup>21</sup>.

## Population Diversity and PRS

Although previous critiques of PRS accuracy involved limitations due to GWAS sample size, these issues are largely resolved<sup>31</sup>. A major limitation of PRS is that accuracy varies between populations<sup>15</sup>. In practice, this means that prediction accuracy is much lower in non-Europeans than Europeans (Figure 2)<sup>17,32</sup>. As well as being a major limitation to PRS utility in diverse populations, it also raises ethical questions about inequalities in access to precision medicine<sup>33</sup>. Martin et al. (2017) demonstrate major inconsistencies in PRS between populations and that the most commonly used GWAS SNP array is not optimal in non-European populations. There is a bias in PRS in different populations depending on the ancestry of the GWAS training set. To avoid this, the authors suggest PRS should be normalised for each group if data is not available from a similar population<sup>17</sup>. However, the over-representation of Europeans in GWAS leads to systematic bias in PRS in non-European individuals because prediction accuracy decreases proportionally to genetic distance from the study population<sup>17,34</sup>. This is compounded by the fact that variants genotyped for GWAS are chosen because of their variability and frequency in European populations, and panels used to impute genomic variance are disproportionately European<sup>18,35</sup>. This means Europeans (who already benefit from health service disparities) disproportionately benefit from “precision healthcare”. Further efforts to resolve the diversity problem in genomics is necessary to allow precision medicine to deliver on its promises.

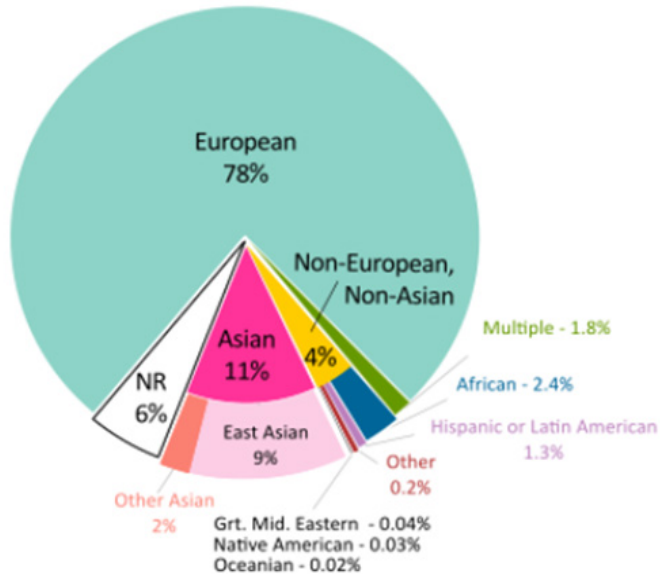


Figure 2: Ancestry of GWAS participants (from Morales et al 2018). Individuals of European descent account for a disproportionate number of GWAS participants. NR= ancestry not reported.

Márquez-Luna et al. (2017) propose a method of integrating training data from large, European GWAS and smaller GWAS from different populations to combat inaccuracies<sup>16</sup>. Although this led to >70% improvement in prediction in Latino and South Asian populations, variance explained remained small, and there was only a 30% relative improvement in prediction in the African population. This may be compounded by the fact that there is much more variation in African populations, which may make GWAS more challenging<sup>36</sup>.

Genomics is expensive and infectious disease research is the priority in African countries<sup>18</sup>. However, the legacy of European colonialism has led to mistrust of non-African scientists, and a fear of exploitation<sup>37</sup>. Funding from bodies such as the NIH and the Wellcome Trust has allowed investment of more than \$216 million in genomics projects led by African scientists in 2015 and it has been noted that a disproportionate number of associations have been found in GWAS with individuals of African ancestry<sup>18,32</sup>. Differences in population structure, including less homogeneity means that population genetic methodologies need to be adjusted for these analyses<sup>18</sup>. These issues should be addressed more thoroughly with increased investment.

## Clinical Application of PRS

PRS performance has been improved by the integration of epidemiological and genomic data<sup>38,39</sup>. This can be useful in clinical decision making and in motivating patients to make healthy lifestyle choices<sup>23</sup>.

Many medical interventions have associated risks, and the benefit of intervention must be balanced with potential harms. PRS can stratify patients to high- and low-risk groups to assess treatment options. For example, statins are an effective cholesterol-lowering therapy that may prevent heart attack, but there is no definitive consensus about statin therapy dosage and timing<sup>23</sup>. Mega et al. (2015) investigated the relative benefit of statin therapy in the highest and lowest PRS quintiles for coronary heart disease. It was found that there was a gradient in risk reduction, with a 48% reduction in high-risk patients after statin therapy, 29% reduction in intermediate-risk patients, and 13% reduction in low-risk patients<sup>39</sup>. A similar gradient was found by Natarajan et al. (2017), who also found high-risk individuals had more sub-clinical atherosclerosis, demonstrating an underlying liability trait increases with disease risk<sup>40</sup>. These studies show that PRS can stratify patients to identify those who would gain the most benefit from therapeutic intervention.

Breast cancer offers another example of the potential for PRS in decision making. Maas et al. (2016) stratified women according to PRS combined with epidemiological risk factors<sup>38</sup>. Average lifetime risk is approximately 11%, but ranged between 4.4%- 23.5% in individuals at the extremes of liability. However, if individuals in the highest PRS decile were low-risk for modifiable factors such as BMI and menopausal hormone therapy (MHT), their risk was comparable to the population average. PRS could help make decisions about MHT, and could motivate people to engage in lower-risk behaviours<sup>38,41</sup>. In addition, discrimination between high- and low-risk individuals may be useful in decisions about when screening should begin to minimise risks associated with false-positive scans<sup>23</sup>.

Although the above examples use a combination of clinical and genetic risk factors, Khera et al. (2018) used genetic information alone to calculate risk predictions for coronary artery disease, with accuracy comparable to predictions in monogenic forms of disease<sup>30</sup>. In addition, it was found that genetic data was more successful in discriminating individuals with three-fold increased risk of disease than conventional risk data. This suggests that it is time to consider the use of PRS in the clinic, as polygenic forms of disease account for more of the patient population than monogenic<sup>30</sup>. However, Khera et al. note that their PRS was applied in individuals of mainly European ancestry, and, as discussed above, significant challenges remain in PRS translation to diverse populations<sup>30</sup>.

## Conclusion

Polygenic diseases account for a large proportion of the healthcare burden in the

world today. However, the complex aetiology of these disorders mean there are significant challenges to understanding pathology and developing treatments. Identifying patients at higher risk so as to instigate preventative measures leads to greater efficiency in reducing healthcare burden. This review has discussed the development of polygenic risk scores in complex diseases, the challenges associated with them and their potential clinical utility.

PRS prediction accuracy must be improved in diverse populations before their potential can be realised. As well as equity considerations, diverse populations are useful in genomics studies because new, important variants for a particular trait can be discovered due to differences in allele frequency and LD structure. Martin et al (2018) suggest that the two main actions that should be taken to improve the diversity problem in genomics is to prioritise the inclusion of diverse participants in studies and to have open access to the resulting summary statistics so they can be used in PRS generation<sup>21</sup>. The development of accurate PRS by Khera et al (2018) suggests a dawn of precision medicine for complex disorders, and the implementation of suggestions from Martin and others should help to usher in this new era in healthcare.

## References

1. Timpson NJ, Greenwood CMT, Soranzo N, Lawson DJ, Richards JB. Genetic architecture: The shape of the genetic contribution to human traits and disease. *Nat Rev Genet* 2018; 19: 110–124.
2. Chen Y, Bedell M, Zhang K. Age-related macular degeneration: genetic and environmental factors of disease. *Mol Interv* 2010; 10: 271–81.
3. Visscher PM, Wray NR, Zhang Q, Sklar P, McCarthy MI, Brown MA et al. 10 Years of GWAS Discovery: Biology, Function, and Translation. *Am J Hum Genet* 2017; 101: 5–22.
4. Falconer DS, Mackay TFC. Introduction to quantitative genetics. *Longman*, 1996.
5. Falconer DS. The inheritance of liability to certain diseases, estimated from the incidence among relatives. *Ann Hum Genet* 1965; 29: 51–76.
6. Witte JS, Visscher PM, Wray NR. The contribution of genetic variants to disease depends on the ruler. *Nat Rev Genet* 2014; 15: 765–776.
7. Finucane HK, Bulik-Sullivan B, Gusev A, Trynka G, Reshef Y, Loh P-R et al. Partitioning heritability by functional annotation using genome-wide association summary statistics. *Nat Genet* 2015; 47: 1228–1235.
8. Génin E, Clerget-Darpoux F. Revisiting the Polygenic Additive Liability Model through the Example of Diabetes Mellitus. *Hum Hered* 2016; 80: 171–177.
9. Visscher PM, Brown MA, McCarthy MI, Yang J. Five years of GWAS discovery. *Am J Hum Genet* 2012; 90: 7–24.
10. Price AL, Spencer CCA, Donnelly P. Progress and promise in understanding the genetic basis of common diseases. *Proc R Soc B Biol Sci* 2015; 282: 20151684.
11. Reich DE, Lander ES. On the allelic spectrum of human disease. *Trends Genet* 2001; 17: 502–10.
12. Park J-H, Gail MH, Weinberg CR, Carroll RJ, Chung CC, Wang Z et al. Distribution of allele frequencies and effect sizes and their interrelationships for common genetic susceptibility variants. *Proc Natl*

- Acad Sci U S A* 2011; 108: 18026–31.
13. Gazal S, Finucane HK, Furlotte NA, Loh PR, Palamara PF, Liu X et al. Linkage disequilibrium-dependent architecture of human complex traits shows action of negative selection. *Nat Genet* 2017; 49: 1421–1427.
  14. Gibson G. Rare and common variants: Twenty arguments. *Nat Rev Genet* 2012; 13: 135–145.
  15. Scheinfeldt LB, Schmidlen TJ, Gerry NP, Christman MF. Challenges in translating GWAS results to clinical care. *Int J Mol Sci* 2016; 17: 6–8.
  16. Márquez-Luna C, Loh P-R, Price AL. Multiethnic polygenic risk scores improve risk prediction in diverse populations. *Genet Epidemiol* 2017; 41: 811–823.
  17. Martin AR, Gignoux CR, Walters RK, Wojcik GL, Neale BM, Gravel S et al. Human Demographic History Impacts Genetic Risk Prediction across Diverse Populations. *Am J Hum Genet* 2017; 100: 635–649.
  18. Martin AR, Teferra S, Möller M, Hoal EG, Daly MJ. The critical needs and challenges for genetic architecture studies in Africa. *Curr Opin Genet Dev* 2018; 53: 113–120.
  19. The Haplotype Reference Consortium, McCarthy S, Das S, Kretzschmar W, Delaneau O, Wood AR et al. A reference panel of 64,976 haplotypes for genotype imputation. *Nat Genet* 2016; 48: 1279–1283.
  20. Paternoster L, Standl M, Waage J, Baurecht H, Hotze M, Strachan DP et al. Multi-ancestry genome-wide association study of 21,000 cases and 95,000 controls identifies new risk loci for atopic dermatitis. *Nat Genet* 2015; 47: 1449–1456.
  21. Martin AR, Kanai M, Kamatani Y, Okada Y, Neale BM, Daly MJ. Hidden ‘risk’ in polygenic scores: clinical use today could exacerbate health disparities. *bioRxiv* 2018. doi:10.1101/441261.
  22. Boyle EA, Li YI, Pritchard JK. An Expanded View of Complex Traits: From Polygenic to Omnigenic. *Cell* 2017; 169: 1177–1186.
  23. Torkamani A, Wineinger NE, Topol EJ. The personal and clinical utility of polygenic risk scores. *Nat Rev Genet* 2018; 19: 581–590.
  24. Euesden J, Lewis CM, O’Reilly PF. PRSice: Polygenic Risk Score software. *Bioinformatics* 2015; 31: 1466–1468.
  25. Bulik-Sullivan BK, Loh P-R, Finucane HK, Ripke S, Yang J, Patterson N et al. LD Score regression distinguishes confounding from polygenicity in genome-wide association studies. *Nat Genet* 2015; 47: 291–295.
  26. Hu Y, Lu Q, Liu W, Zhang Y, Li M, Zhao H. Joint modeling of genetically correlated diseases and functional annotations increases accuracy of polygenic risk prediction. *PLOS Genet* 2017; 13: e1006836.
  27. Purcell SM, Wray NR, Stone JL, Visscher PM, O’Donovan MC, Sullivan PF et al. Common polygenic variation contributes to risk of schizophrenia and bipolar disorder. *Nature* 2009; 460: 748–752.
  28. LeBlanc M, Zuber V, Thompson WK, Andreassen OA, Schizophrenia and Bipolar Disorder Working Groups of the Psychiatric Genomics Consortium S and BDWG of the PG, Frigessi A et al. A correction for sample overlap in genome-wide association studies in a polygenic pleiotropy-informed framework. *BMC Genomics* 2018; 19: 494.
  29. Speed D, Balding DJ. Better estimation of SNP heritability from summary statistics provides a new understanding of the genetic architecture of complex traits. *Nat Genet* 2018. doi:10.1038/s41588-018-0279-5.
  30. Khera A V, Chaffin M, Aragam KG, Haas ME, Roselli C, Choi SH et al. Genome-wide polygenic scores for common diseases identify individuals with risk equivalent to monogenic mutations. *Nat Genet* 2018; 50: 1219–1224.
  31. Knowles JW, Ashley EA. Cardiovascular disease: The rise of the genetic risk score. *PLOS Med* 2018; 15: e1002546.

32. Morales J, Welter D, Bowler EH, Cerezo M, Harris LW, McMahon AC et al. A standardized framework for representation of ancestry data in genomics studies, with application to the NHGRI-EBI GWAS Catalog. *Genome Biol* 2018; 19: 21.
33. Petrovski S, Goldstein DB. Unequal representation of genetic variation across ancestry groups creates healthcare inequality in the application of precision medicine. *Genome Biol* 2016; 17: 157.
34. Scutari M, Mackay I, Balding D. Using Genetic Distance to Infer the Accuracy of Genomic Prediction. *PLOS Genet* 2016; 12: e1006288.
35. McCarthy S, Das S, Kretzschmar W, Delaneau O, Wood AR, Teumer A et al. A reference panel of 64,976 haplotypes for genotype imputation. *Nat Genet* 2016; 48: 1279–1283.
36. Gravel S, Henn BM, Gutenkunst RN, Indap AR, Marth GT, Clark AG et al. Demographic history and rare allele sharing among human populations. *Proc Natl Acad Sci* 2011; 108: 11983–11988.
37. Munung NS, Mayosi BM, de Vries J. Equity in international health research collaborations in Africa: Perceptions and expectations of African researchers. *PLoS One* 2017; 12: e0186237.
38. Maas P, Barrdahl M, Joshi AD, Auer PL, Gaudet MM, Milne RL et al. Breast Cancer Risk From Modifiable and Nonmodifiable Risk Factors Among White Women in the United States. *JAMA Oncol* 2016; 2: 1295–1302.
39. Mega JL, Stitzel NO, Smith JG, Chasman DI, Caulfield MJ, Devlin JJ et al. Genetic risk, coronary heart disease events, and the clinical benefit of statin therapy: An analysis of primary and secondary prevention trials. *Lancet* 2015; 385: 2264–2271.
40. Natarajan P, Young R, Stitzel NO, Padmanabhan S, Baber U, Mehran R et al. Polygenic risk score identifies subgroup with higher burden of atherosclerosis and greater relative benefit from statin therapy in the primary prevention setting. *Circulation* 2017; 135: 2091–2101.
41. Khera A V., Emdin CA, Drake I, Natarajan P, Bick AG, Cook NR et al. Genetic Risk, Adherence to a Healthy Lifestyle, and Coronary Disease. *N Engl J Med* 2016; 375: 2349–2358.

# AN INTEGRATIVE NEUROSCIENTIFIC EVALUATION OF SOCIAL MOTIVATION AND REWARD

Áine Heffernan  
Junior Sophister  
Neuroscience

*Humans are constantly described as being social creatures but what is it that is responsible for driving this behaviour in our species and what is it that causes this drive to differ among individuals? These questions largely remain unanswered but in recent years progress has been made using an interdisciplinary scientific approach, which has given an insight into the neuroscientific basis of social motivation and reward. This review will focus on our current understanding of the field and discuss the importance of increasing our knowledge of the neural circuitry involved in social motivation and reward especially in terms of clinical relevance for individuals with autism spectrum disorder (ASD). This review also outlines where future research should be directed to gain a greater understanding of social motivation and reward.*

## Introduction

Social interaction has long been classified as one of an animal's fundamental motivational drives<sup>1</sup>. The incentive theory of motivation explains this phenomenon by stating that rewarding experiences drive motivated behavior<sup>2</sup>. In this instance it implies that animals find social interaction rewarding resulting in a strong desire to seek social contact. If an animal finds something rewarding this means that it can like and/or want the reward as liking and wanting are two separate aspects of motivation<sup>2</sup>. In this context, liking reflects the hedonic impact of a social encounter whereas wanting refers to the incentive salience associated with an interaction<sup>2</sup>. It is thought that the positive, rewarding aspects of social interactions may have evolved to promote cooperative and fruitful interactions between members of the group to further the group's survival<sup>3</sup>.

In recent years integrative behavioural studies have shown that the ventral tegmental area (VTA) and nucleus accumbens (NAcc) are areas of the brain

required for social motivation and reward and that dopamine (DA), oxytocin (OT) and  $\mu$ -opioid receptors are involved at a molecular level<sup>3, 4, 5</sup>. However, the neural mechanisms encoding the social reward of same-sex, same-age non-aggressive social interaction still remain largely unknown.

Early behavioural studies first showed that social interaction is highly rewarding. It was observed that during social interaction rats emit high frequency vocalizations, at approximately 50kHz, which they also emit during other known rewarding activities such as sexual behaviour<sup>6</sup>. Place conditioning experiments are another means of measuring social motivation and reward<sup>7</sup>. Using this technique, it was shown that an individual rat would prefer to interact with a conspecific than be isolated and that interactive social encounters are more rewarding than interaction with a sedentary conspecific<sup>8, 9</sup>. Play, a form of social interaction, could be used as an incentive for operant lever pressing and maze learning as well as for conditioned place preference (CPP) showing the relationship between reward and motivation for such social interactions<sup>10, 11</sup>.

## Neural Mechanisms Involved in Social Motivation and Reward

DA is a key neurotransmitter involved in motivation and reward in general and has important roles in motivation and reward of same-sex affiliative interactions<sup>12</sup>. DA neurons in the VTA are involved in processing stimuli of both positive and negative valence and predicting the associated reward<sup>13</sup>. The VTA is composed of diverse cell types which play different roles in modulating reward and aversion based on connectivity and projections to different structures. These cells project broadly throughout the brain to limbic regions such as the medial prefrontal cortex (mPFC), NAcc and amygdala which mediate both appetitive and aversive processes<sup>14</sup>. In a recent study fibre photometry was used to record VTA DA neurons to determine their relationship specifically in social motivation and reward and this showed that the VTA neuron's activity increased in mice during social interaction<sup>4</sup>. In the same study, optogenetic activation of DA cells with VTA-NAcc projections was shown to increase social interaction whereas optogenetic activation of VTA-mPFC projections had no effect on social interaction<sup>4</sup>. The NAcc is a key structure involved in social reward processing and NAcc multiunit firing rate is significantly higher when a test mouse is in a social chamber compared to a neutral chamber (see Figure 1)<sup>4, 15</sup>. Fibre photometry shows stronger encoding of novel social rather than novel object interactions by the VTA-NAcc projection which allows for dissociation of social activity from general novelty-related activity<sup>2</sup>. This information has led to the current hypothesis that increased activity in VTA DA neurons, especially in their projections to the NAcc, promotes positive reinforcement of social interaction and plays a causal role in social reward and motivation<sup>2</sup>.

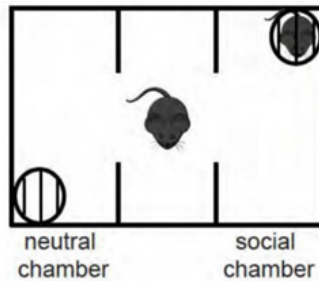


Figure 1: *Social Test Chamber. Mice were habituated in the central chamber. During testing, mice could explore both the neutral chamber or the chamber with an unfamiliar mouse which they could enter through doorways in the dividing walls. Adapted from Gunaydin et al. 2014<sup>4</sup>.*

OT is another molecule with a crucial role in social motivation and reward and it is already known to be important in maternal and pair bonding in prairie voles<sup>3, 16, 17</sup>. However, it is only in more recent years that the role of OT in peer interactions has been studied. In one study OT antagonist infused mice displayed a significantly increased latency to begin responding to access to the target mouse compared to control mice which suggested reduced motivation for social reward in these mice<sup>18</sup>. In line with this idea, OT receptor knockout mice exhibit a range of social deficits, including fewer vocalizations in response to social isolation<sup>19</sup>.

Following on from this, a recent study by Dölen et al.<sup>3</sup> examined the role of OT in non-aggressive peer interactions. The study showed that in mice OT acts as a social reinforcement signal within the NAcc where it elicits a presynaptically expressed long-term depression (LTD) of excitatory synaptic transmission in medium spiny neurons (MSNs) of the NAcc. This study revealed that the oxytocin receptor was localized in the NAcc, and locomotor or cocaine CPP was not affected, showing how OT was specific to social reward. Social reward requires OT receptors in presynaptic boutons in the NAcc as both OT receptor antagonist and selective deletion of the receptor respectively prevented normal social CPP occurring<sup>3</sup>. Through further testing it was established that presynaptic OT receptors activation on dorsal raphe axon terminals in the NAcc co-ordinates with 5-hydroxytryptamine (5-HT) activity<sup>3</sup>. Activation of OT receptors in the terminals of dorsal raphe axons within the NAcc is hypothesised to lead to 5HT1b receptor dependent form of LTD<sup>3</sup>. 5-HT is needed for social reward as blocking the 5HT1b receptors with an antagonist, prevented social CPP<sup>3</sup>. Coordinated activity of OT and 5-HT is required for reward associated with social interactions and this modifies the mesocorticolimbic circuit properties by generating LTD of excitatory synapses onto MSNs in the NAcc<sup>3</sup>.

More recent research has examined the relationship that OT has with DA and the VTA<sup>20</sup>. Parvocellular paraventricular nucleus (PVN) OT neurons project to the VTA (see Figure 2)<sup>20</sup>. These PVN neurons projecting to the VTA are necessary for social reward as reduced CPP occurs when these neurons were inhibited<sup>20</sup>. Mice lacking OT receptors in the VTA also exhibited no social CPP<sup>20</sup>. The VTA projecting PVN

neurons activity increased during social interaction compared to when a mouse interacted with a toy mouse<sup>20</sup>. Sociability is reduced when OT inputs in the VTA are optogenetically inhibited<sup>20</sup>. Optogenetic activation of PVN OT neurons alone is not rewarding and it only enhances sociability when activation of these OT axons occurs during social interactions<sup>20</sup>. This is thought to happen because OT is released in the VTA early in the course of social interaction which amplifies the excitability of dopaminergic neurons projecting to the NAc<sup>20</sup>. Based on these findings, it is thought that OT enhances DA release which imparts social reward via the NAc which reinforces social interaction<sup>20</sup>.

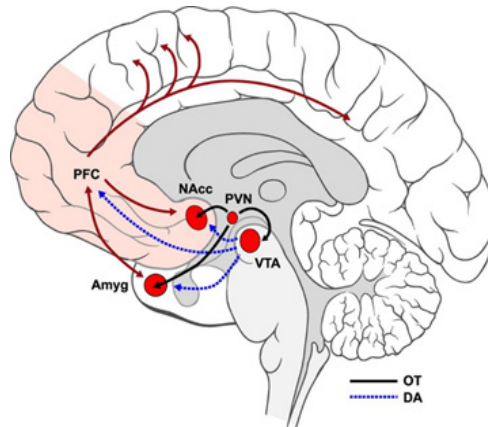


Figure 2: Schematic overview of dopaminergic and oxytocinergic pathways in the human brain. Dopamine (DA; dashed blue) neurons in the ventral tegmental area (VTA) project to the nucleus accumbens (NAcc), amygdala (Amyg) and prefrontal cortex (PFC). Paraventricular nucleus (PVN) oxytocin (OT; solid black) neurons projects to sites on the DA pathway (VTA, NAcc, and Amyg), potentially allowing it to modulate DA activity such as that involved in social motivation and reward.

Adapted from Gordon et al., 2016<sup>21</sup>

$\mu$ -opioid receptors in the NAcc join OT and DA in playing a role in social motivation and reward. The brain opioid theory of social attachment states that opioids are responsible for the enjoyment and satisfaction felt from achieving a social connection, the liking aspect of motivation<sup>22</sup>. A recent study demonstrated that infusion of  $\mu$ -opioid receptor selective agonist DAMGO ([D-Ala2, N-MePhe4, Gly-ol]-enkephalin) increased pinning and pouncing showing how  $\mu$ -opioid receptors specifically affect social play<sup>5</sup>. Pinning and pouncing are two prominent behaviours of social play in mice and indicate that the social interaction is rewarding<sup>5</sup>. CTAP(Cys-Tyr-D-Trp-Arg-Thr-Pen-Thr-Nh2), a  $\mu$ -opioid receptor antagonist reduced pinning and pouncing<sup>5</sup>. B-endorphin is the endogenous ligand for the receptor and its infusion in the NAcc increases pouncing and pinning behaviour<sup>5</sup>. In all the experiments social exploration behaviour was not changed demonstrating how these receptors are not involved in general social behaviours

but have more specific functions in motivation and reward<sup>5</sup>.  $\mu$ -opioid receptors in the NAcc mediate social play induced CPP as CTAP infused in the NAcc before conditioning saw animals spend an equal amount of time in both compartments<sup>5</sup>. This provides evidence that  $\mu$ -opioid receptor stimulation mediates social reward<sup>5</sup>.

The absence of social contact as well as positive rewarding social encounters triggers a strong desire to seek social interaction<sup>23</sup>. The mesolimbic system has been implicated in, and perturbations in DA signalling have been reported, following chronic social isolation<sup>24</sup>. Following on from this, a recent study by Matthews et al.<sup>25</sup> looked at the role of dorsal raphe (DRN) DA neurons in isolation. In this study, calcium imaging revealed dorsal raphe neurons show increased activity upon social contact following isolation. The study also showed that optogenetic activation of DRN DA neurons increases social preference but causes place avoidance when there is no social stimulus. Furthermore, these neurons are necessary for promoting social motivation following an acute period of isolation. In socially isolated mice a significant increase in fluorescence signal was observed in response to first contact with another mouse, compared with group housed mice<sup>25</sup>. There was also a greater response when a live mouse was introduced compared with a toy mouse showing the differing effects of a social target on DRN DA activity<sup>25</sup>. Optogenetic inhibition of DRN DA neurons prevented the typical restoration of social contact following periods of isolation<sup>25</sup>. It can then be concluded that DRN DA motivates sociability after a negative state of isolation<sup>25</sup>. It is important to understand the differences in this type of social motivation after isolation in comparison with the social motivation associated with positive valence and reward discussed earlier. It has recently been established that distinct neural circuits motivate food consumption related to the rewarding value of food and the need to obtain food to relieve hunger<sup>26, 27</sup>. In a similar manner, distinct neural circuits may be involved in social motivation driven by reward and isolation. More research needs to be carried out to determine if these two circuits are completely independent as the current literature suggests or if some overlap exists between the two circuits.

## Areas of Further Study

There is a need for further studies to be undertaken in this area of neuroscience to provide a more comprehensive understanding of the neural circuitry underlying social motivation and reward as many fundamental questions need to be answered. Further research needs to be carried out to find what differences exists between the different types of social motivation and reward neural circuits such as peer, maternal and pair-bond and if there is any overlap. There is also a need to understand how social and non-social reward stimuli are encoded, and if they are encoded in the same or different ways. A more coherent study needs to analyse all the anatomical areas of the brain involved in social motivation and reward using more sophisticated neuroimaging, axonal tracing, neuronal labelling and

optogenetic techniques. It is also important to determine how molecules such as opioids, OT, DA and 5-HT may interact and coordinate or work independently in each area. More clarity needs to be brought to the role OT has in peer interactions as recent studies highlight the complexity of the neural circuitry associated with motivation and reward involving OT in different roles. The relationship between the coordination of OT and 5HT and their role in LTD of excitatory synapses onto MSNs needs to be more thoroughly investigated to see the exact implications both have on social motivation and reward and whether their activity is dependent as hypothesised or if their activity is independent and other unknown factors need to be considered. A possible explanation of the different roles of OT may be due to DA and 5-HT giving social reward on different timescales. While 5-HT has a role in delayed gratification of rewards, there is a decrease in dopamine response following reward delay suggesting a decrease in reward value<sup>28, 29</sup>. How these timescales would be implicated in social motivation and reward is yet to be understood.

Future studies also need to examine the role of  $\mu$ -opioid receptors in other types social interaction besides play. It is important to determine if the neural mechanisms underlying the different classes of social motivation are distinct or if any links exist between them. Other behavioural tests which would give a clearer indication of social reward and motivation need to be developed. Such tests would give a more exhaustive classification and quantification of behavioural patterns associated with peer social interactions. Furthermore, there is a huge variation in interpreting behavioural data. Behavioural tests need to be designed to give quantitative and objective behavioural measurement. There is also a need for behavioural analysis tests to integrate multiple pieces of information due to the complex nature of neural circuitry. Current tests are restrictive as often they can only be carried out in a laboratory environment due to technological limits. In addition, animals may not be able to display their full behavioural repertoire due to invasive devices, such as those used in optogenetics. When improvements in neural activity recording technologies occur this issue will be rectified. This will lead to more comprehensive, less ambiguous findings. Most of the current studies in the field are based on experiments carried out on mice, future studies should shift to focusing on social motivation and reward in rats as they are more social animals than mice<sup>30</sup>. In a study examining differences in social behaviour between the two species, it was shown that during a fifteen minute period rats engaged in social encounters for 79% of the time whereas mice only spent 22% of their time interacting with conspecifics<sup>30</sup>. This suggests that results obtained from experiments using rats as their model species would be more beneficial in terms of extracting information that could have clinical relevance for human treatments.

## Clinical Relevance

More scientific studies are focusing on social motivation because it is hypothesized

that a lack of motivation for social interactions occurs in individuals with ASD. The social motivation hypothesis of autism states that individuals with ASD do not find social interactions inherently rewarding and they show a deficit in assigning value to social stimuli resulting in social dysfunction<sup>31</sup>. A greater understanding of the underlying neural circuitry behind social motivation could lead to an insight into ASD and other neuropsychiatric disorders hypothesised to have a lack of social motivation associated with them. While a study showed that OT can modulate sociability via the VTA, the clinical value of administering more OT to individuals with ASD remains unclear<sup>20</sup>. However, OT treatment has improved social behaviour deficits in mouse models of autism<sup>32</sup>. Unfortunately, mouse models of autism fail to map to the human disorder due to the difficulty of examining all the social deficits associated with human ASD in mice. This happens because of the difficulty in classifying symptoms in humans, the lack of biomarkers and knowledge of neurobiology and genetics underpinning the disorder<sup>19</sup>. Currently most animal models are based on loss-of-function mutations of genes associated with the disorder and focus on the particular molecular mechanism attributed to that specific gene<sup>19</sup>. It would therefore be important in future studies to focus on general patterns involved in circuitry modulation of social motivation and reward. Understanding the circuit-specific mechanisms by which OT contributes to social reward is a critical step in bridging this gap and may eventually lead to novel therapies for social disorders.

Enhanced NAcc activity with  $\mu$ -opioid receptors has been observed in rewarding interactions in humans including social interaction with friends in young adults and during social cooperation<sup>33,34</sup>. Thus, dysfunction of  $\mu$ -opioid receptor functions may play a role in social dysfunction in humans and a greater understanding of the receptor's role in social reward may lead to treatments for ASD. In  $\mu$ -opioid knockout mice reared by their mother and an additional lactating female showed increased social motivation<sup>19</sup>. These results are encouraging as they suggest a potential practical therapy for individuals with ASD, which would increase social contact from a young age. Further research investigating if and how the circuitries of the social brain are affected in animal models of the disorder will help identify a common pathophysiology, which is essential to translate to a clinical setting.

## Conclusions

The neural mechanisms of social motivation and reward are still largely unknown despite several promising studies in this field, particularly in relation to the VTA and the NAcc and the roles of OT, opioids, DA and 5-HT in these structures. More comprehensive studies using this new information need to be carried out to assess how all the components are integrated into the neural circuitry. It is an area of neuroscience that is extremely interesting and due to its hypothesised connection to social dysfunction disorders will be an area that continues to expand in the future. It is important to identify molecular mechanisms that are specific for social

motivation and reward as this will have an impact on developing treatments aimed at restoring underlying neuropathophysiology.

## Acknowledgements

This work was adapted from an essay “An Integrative Neuroscientific Evaluation of Social Motivation and Reward”, for course BIU33465.

## References

1. Reiss S. Who Am I? the 16 basic desires that motivate our actions and define our personalities. New York: Tarcher/Putnam; 2000.
2. Berridge KC. Evolving Concepts of Emotion and Motivation. *Front Psychol.* 2018;9:1647.
3. Dölen G, Darvishzadeh A, Huang KW, Malenka RC. (2013) Social reward requires coordinated activity of nucleus accumbens oxytocin and serotonin. *Nature.* 2013;501(7466):179-84.
4. Gunaydin LA, Grosenick L, Finkelstein JC, Kauvar IV, Fenno LE, Adhikari A, Lamme S, Mirzabekov JJ, Airan RD, Zalocusky KA, Tye KM, Anikeeva P, Malenka RC, Deisseroth K. Natural neural projection dynamics underlying social behavior. *Cell.* 2014;157(7):1535-51.
5. Trezza V, Damsteegt R, Achterberg EJM, Vanderschuren MJM. Nucleus Accumbens  $\mu$ -Opioid Receptors Mediate Social Reward. *J. Neurosci.* 2011;31(17):6362-6370.
6. Burgdorf J, Kroes RA, Moskal JR, Pfau JG, Brudzynski SM, Panksepp J. Ultrasonic vocalizations of rats (*Rattus norvegicus*) during mating, play, and aggression: Behavioral concomitants, relationship to reward, and self-administration of playback. *J Comp Psychol.* 2008;122(4):357-67.
7. Martin L, Iceberg E. Quantifying Social Motivation in Mice Using Operant Conditioning. *J Vis Exp.* (102), e53009, doi:10.3791/53009 (2015).
8. Moy SS, Nadler JJ, Perez A, Barbaro RP, Johns JM, Magnuson TR, Piven J., Crawley JN. Sociability and preference for social novelty in five inbred strains: an approach to assess autistic-like behavior in mice. *Genes Brain Behav.* 2004;3(5):287-302.
9. Calcagnetti DJ, Schechter MD. Place conditioning reveals the rewarding aspect of social interaction in juvenile rats. *Physiol Behav.* 1992;51(4):667-72.
10. Mason WA, Saxon SV, Sharpe LG. Preferential responses of young chimpanzees to food and social rewards. *Psychol Rec.* 1963;13(3):341-345.
11. Humphreys AP, Einon DF. Play as a reinforcer for maze-learning in juvenile rats. *Animal Behaviour* 1981;29(1):259-270.
12. Robinson DL., Heien ML, Wightman RM. Frequency of dopamine concentration transients increases in dorsal and ventral striatum of male rats during introduction of conspecifics. *Journal Neurosci.* 2002;22(23):10477-86.
13. Matsumoto M, Hikosaka O. Two types of dopamine neuron distinctly convey positive and negative motivational signals. *Nature.* 2009;459(7248):837-41.
14. Tye KM, Mirzabekov JJ, Warden M, Ferenczi EA, Tsai HC, Finkelstein J, Kim SY, Adhikari A, Thompson KR, Andalman AS, Gunaydin LA, Witten IB, Deisseroth K. Dopamine neurons modulate neural encoding and expression of depression-related

- behavior. *Nature*. 2012;493(7433):537-541.
15. Lammel S, Lim BK, Ran C, Huang KW, Betley MJ, Tye KM, Deisseroth K, Malenka RC. Input-specific control of reward and aversion in the ventral tegmental area. *Nature*. 2012;491(7423):212-217.
16. Pedersen CA, Prange AJ Jr. Induction of maternal behavior in virgin rats after intracerebroventricular administration of oxytocin. *Proc Natl Acad Sci U S A*. 1979;76(12):6661-5.
17. Williams JR, Insel TR, Harbaugh CR, Carter CS. Oxytocin administered centrally facilitates formation of a partner preference in female prairie voles (*Microtus ochrogaster*). *J Neuroendocrinol*. 1994;6(3):247-50.
18. Matthews TJ, Abdelbaky P, Pfaff DW. Social and sexual motivation in the mouse. *Behav Neurosci*. 2005;119(6):1628-39.
19. Garbugino L, Centofante E, D'Amato FR. Early Social Enrichment Improves Social Motivation and Skills in a Monogenic Mouse Model of Autism, the *Oprm1* (-/-) Mouse. *Neural plasticity*. 2016;2016: 5346161.
20. Hung LW, Neuner S, Polepalli JS, Beier KT, Wright M, Walsh JJ, Lewis EM, Liqun L, Deisseroth K, Dölen G, Malenka RC. Gating of social reward by oxytocin in the ventral tegmental area. *Science*. 2017;357(6358):1406-1411.
21. Gordon I, Jack A, Pretsch CM, Wyk BV, Leckman JF, Feldman R, Pelphrey KA. Intranasal Oxytocin Enhances Connectivity in the Neural Circuitry Supporting Social Motivation and Social Perception in Children with Autism. *Sci Rep*. 2016;6:35054.
22. Panksepp J, Herman B, Conner R, Bishop P, Scott JP. The biology of social attachments: opiates alleviate separation distress. *Biol Psychiatry*. 1978;13(5):607-18.
23. Panksepp J, Beatty WW. Social deprivation and play in rats. *Behav Neural Biol*. 1980;30(2):197-206.
24. Hall FS, Wilkinson LS, Humby T, Inglis W, Kendall DA, Marsden CA, Robbins TW. Isolation rearing in rats: pre- and postsynaptic changes in striatal dopaminergic systems. *Pharmacol Biochem Behav*. 1998;59(4):859-72.
25. Matthews GA, Nieh EH, Vander Weele CM, Halbert SA, Pradhan RV, Yosafat AS, Globber GF, Izadmehr EM, Thomas RE, Lacy GD, Wildes CP, Ungless MA, Tye KM. Dorsal Raphe Dopamine Neurons Represent the Experience of Social Isolation. *Cell*. 2016;164(4):617-31.
26. Nieh EH, Matthews GA, Allsop SA, Presbrey KN, Leppla CA, Wichmann R, Neve R, Wildes CP, Tye KM. Decoding neural circuits that control compulsive sucrose seeking. *Cell*. 2015;160(3):528-41.
27. Chen Y, Lin YC, Kuo TW, Knight ZA. Sensory detection of food rapidly modulates arcuate feeding circuits. *Cell*. 2015;160(5):829-841.
28. Miyazaki KW, Miyazaki K, Tanaka KF, Yamanaka A, Takahashi A, Tabuchi S, Doya K. Optogenetic activation of dorsal raphe serotonin neurons enhances patience for future rewards. *Curr Biol*. 2014;24(17):2033-40.
29. Fiorillo CD, Newsome WT, Schultz W. The temporal precision of reward prediction in dopamine neurons. *Nat Neurosci*. 2008;11(8):966-73.
30. Kummer KK, Hofhansel L, Barwitz CM, Schardl A, Prast JM, Salti A, El Rawas R, Zernig G. Differences in social interaction vs. cocaine reward in mouse vs. rat. *Front Behav Neurosci*. 2014;8:363.
31. Scott-Van Zeeland AA, Dapretto M, Ghahremani DG, Poldrack RA, Bookheimer SY. Reward processing in autism. *Autism Res*. 2010;3(2):53-67.
32. Peñagarikano O, Lázaro MT, Lu XH, Gordon A, Dong H, Lam HA, Peles E, Maidment NT, Murphy NP, Yang XW, Golshani P, Geschwind DH. Exogenous and evoked oxytocin restores social behavior in the *Cntnap2* mouse model of autism. *Sci Transl Med*. 2015;7(271):271ra8.
33. Güroğlu B, Haselager GJ, van Lieshout

CF, Takashima A, Rijpkema M, Fernández G. Why are friends special? Implementing a social interaction simulation task to probe the neural correlates of friendship. *NeuroImage*. 2008;39(2):903-10.

34. Rilling J, Gutman D, Zeh T, Pagnoni G, Berns G, Kilts C. A neural basis for social cooperation. *Neuron*. 2002;35(2):395-405.

TS  
SR



# Natural Sciences

TS  
SR

## Letter from the Editor

The two articles selected for publication in the Natural Sciences section for this year's edition of TSSR highlight how understanding past geological and biological events can inform our understanding of contemporary developments. This approach to learning about the natural world and its processes brings to mind the phrase 'the past is the key to the present' attributed to Scottish geologist Charles Lyell in the 19th Century. It is evident that both papers are the fruit of authors with a rigorous scientific mindset seeking to provide a balanced evaluation of the many, and sometimes even contradictory findings which have been made in each respective field. Through their commentary, the writers show us that in both geological and biological contexts, the underlying drivers of change remain largely static through time. By looking at geological formations and the fossil record we can, as the authors show us, identify how both are capable of recording vital information of the environmental conditions under which they were formed. Through such a system not only can we begin to infer how it is changes occurred in the past but we also begin to predict how future changes will take place.

Not with a bang but with a whimper examines the fossil record of terrestrial land plants and why it is that mass extinction events within this major and important plant group do not in general correlate with those recorded in the overall fossil record. The author explores the unique qualities which have led to this paleontological phenomenon, but also expands to investigate the plant traits which have in the past been associated with more pronounced and severe extinctions. By applying this understanding the author highlights how important it is to understand factors which have affected extinction rates in the past if we are to employ effective conservation measures.

Ventifacts: where form meets function reviews the research which has been done so far on geological formations known as ventifacts which are shaped by wind processes. These formations can be found both on Earth and also Mars. On Mars, the presence of ventifacts

act as important records of changes in the atmosphere over time, ultimately allowing us to reconstruct and deduce important information on how the martian atmosphere works. Indeed a number of robotic expeditions to Mars were used to take photographs and gather information on Martian ventifacts for this very reason. Ventifacts on the earth's surface also act as record keepers and here too they act as important records of the palaeoenvironments.

Although on paper, the topics covered by each of these papers seem to be a world apart, I hope that they will help the reader to appreciate that like all other scientific disciplines the natural sciences too have at their foundation a common set of governing rules which make it possible for us to reconstruct past environments and predict future environments by filling in gaps of direct knowledge by extracting knowledge derived indirectly, be it from the fossil record, or from a ventifact. Ultimately, I trust that the reader will find the papers engaging, accessible and enjoyable as did I.

Ciarán Ó Cuív

Natural Sciences Editor

Trinity Student Scientific Review 2019

# VENTIFACTS: WHERE FORM MEETS FUNCTION

Maria Cordero  
Junior Sophister  
Geography

*Often referred to as “natural sculptures”, ventifacts have always been captivating to researchers because of their striking appearance. The study of these geological formations goes beyond the aesthetic however, and has uncovered much crucial information about the environmental history of not just Earth, but in recent decades, Mars as well. This review outlines the research done on these features on both planets and briefly examines what the future holds for this field of study. Understanding the process of formation of these geological formations can help us to uncover the properties of the Martian atmosphere and the various changes it has undergone through time. On Earth, the study of their formation is particularly useful in reconstructing palaeoclimates which in turn are essential for our understanding of contemporary Earth surface processes since it is only by understanding the principles behind past changes that we can begin to make accurate predictions of future change.*

## Introduction

Ventifacts are rocks which have been abraded by wind carrying particles such as dust or ice. Many abrasion patterns can be seen in these features, for example faceted edges, elongated pits, grooves, and rills. The physics of abrasional processes require that all rocks tend towards an equilibrium shape which can have no further abrasion<sup>1,2</sup>. This ideal shape is rarely realised however, and the final appearance of a ventifact is dependent on a range of variables: the wind direction, wind speed, material supply, material composition, and the composition of the rock itself. For this reason, it can be difficult to model the exact conditions in which they have been formed, however recent models have led to great advances in the study of ventifacts.

To date, ventifacts have only been observed on the surfaces of Mars and Earth. They have not been discovered on any other bodies, and these bodies would

need to meet a range of criteria for them to form. Firstly, there must be rocks on the surface of the body to be abraded. Secondly, there must be a supply of loose material (e.g. sand or ice particles). Lastly there must be an aeolian system at play (a system wind shapes the landscape), which in turn requires the planet to have a sufficient atmosphere. Therefore the presence of ventifacts on a planet's surface tells us a significant amount about that planet and its weathering systems. Analytical studies by Laity et al<sup>3</sup> confirmed that sand is the "principal abrasive agent" on both Earth and Mars, and both planets are known for their recorded aeolian processes.

There are three general modes of aeolian weathering, characterised by the size of the carried grains: suspension, saltation, and surface creep. For the purpose of this essay, saltation is the relevant process, occurring when grains (60 to 2000  $\mu$  in diameter) "hop" across the surface, and simultaneously bring other small particles into suspension and push larger particles across the surface<sup>4</sup>. When particles strike the surface of rocks, they erode the surface as a function of their size (e.g. smaller grains will cause pitting or fluting of rocks while larger particles will cause larger facets). Therefore the appearance of these rocks can tell us a great deal about the materials responsible for their formation.

## What Martian Ventifacts Tell Us

Ventifacts have been a source of fascination since the first photographs of the Martian surface were obtained by the Viking 1 mission whose lander transmitted information over a period of 6 years from its landing in 1976. Their presence on the planet is not surprising, as according to Wells and Zimbelman<sup>5</sup> wind is "currently the dominant agent of surface modification" on Mars. Some aeolian features are in fact still active, such as the active dunes outlined by Edgett and Malin<sup>6</sup> in 2000.



Figure 1: *Martian ventifact which garnered attention due to its resemblance to a spoon. Image Credit: Curiosity Rover, NASA/JPL-Caltech/Malin Space Science Systems*

*In situ* observations at the Gale Crater suggest that saltation could be possible in the current low-density Martian atmosphere<sup>7</sup>, however wind speeds need to be approximately  $30 \text{ ms}^{-1}$  or more to induce saltation, which they rarely are on Mars<sup>8</sup>. This suggests that the majority of Martian ventifacts were created in the geological past. There is still ongoing debate around whether aeolian features would have been formed gradually over time in abrasive “episodes”, or whether Mars experienced a previous era of stronger paleowinds.

Extensive wind tunnel experiments by Bridges et al. which modelled both Earth and Martian conditions found that the direction of the maximum velocity winds has the greatest control over the orientation of flutes on ventifacts<sup>2</sup>. This is because the dominant wind will carry the most saltating particles. The challenges in interpreting the formation processes of Martian ventifacts were highlighted by NASA’s Mars Pathfinder, whose roving probe reached Mars in 1997. For example, In 2001, Greeley et al.<sup>4</sup> stated that ventifacts and the edges of some small craters observed at the Pathfinder landing site had features whose formation could not be explained even by the strongest of current wind speeds estimated by the Mars General Circulation Model, a model which sought to improve our understanding on the inner workings of the Martian atmosphere. These findings hint at the existence of a palaeoclimate which would have featured considerably more extreme winds. Other aeolian features on the surface of Mars do align with the current wind regime, such as wind tails, wind streaks and intercrater deposits<sup>9</sup>. The fact that the orientation of the observed ventifacts seen on the surface doesn’t match the current Martian wind regime suggests that there was likely a different predominant wind direction in the past.

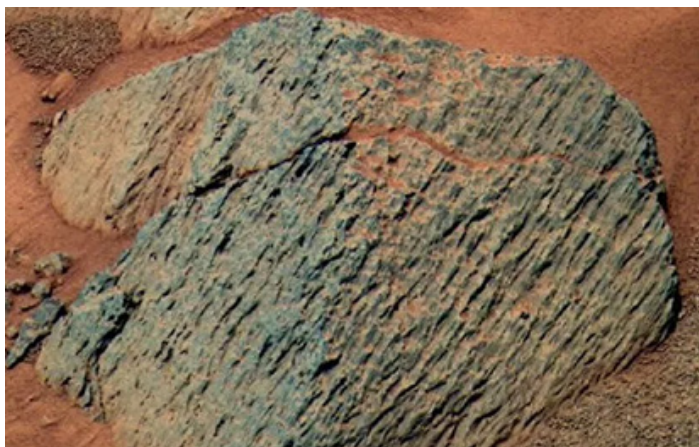


Figure 2: Ventifacts on Mars showing a clear formational wind direction. Image source: Spirit Mission, NASA/JPL/Cornell

## Ventifacts as Witnesses of Change

The Pathfinder mission was crucial to this field, with approximately 50% of the rocks at this site being ventifacts. Golombek and Bridges<sup>10</sup> have suggested that many of these were formed after a catastrophic flood when a large supply of sand-size particles were widely available across the plain. The collection of dunes within the Big Crater were also likely formed at the same time with this material, as the Northwesterly wind pattern suggests both features were formed at the same time.

This idea of palaeowinds having changed direction is supported by other similar studies using the weathered rims of craters. One study on the craters at the Mars Pathfinder landing site suggested that the palaeowinds responsible for the weathering were likely coming from the southeast, which is 90° from the current wind regime in the area (NE to SW)<sup>9</sup>. The same study also suggests that this previous wind regime would have been stronger than that modelled for today.

Thomson and Bridges<sup>11</sup> also suggest that the ventifacts found at the MER Spirit landing site within the Gusev Crater may imply that the past density of the atmosphere was different to that seen today. The superposition of ripples over ventifacts at this site indicates that the latter were formed by a previous wind regime, which was affected by different atmospheric conditions.

These findings all present us with the question of why the direction of these palaeowinds changed at all. One suggestion is that the obliquity of Mars was responsible; since Mars lacks the stabilising pull that Earth experiences from our Moon, it is more prone to changes in obliquity and therefore weather conditions. As a result Mars' spin axis may tilt 15 - 35° over a 124,000 year cycle, with an increased tilt resulting in warmer summers<sup>12</sup>. This theory is not perfect however, and computational models based on the General Circulation Model (GCM) and the Geophysical Fluid Dynamics Laboratory show that the wind direction does not vary significantly as a function of obliquity<sup>13</sup>. Harberle et al.<sup>14</sup> also refuted this theory using the NASA/Ames GCM. The likely flaw with this spin axis theory is that obliquity changes don't alter the nature of the Hadley circulation on Mars.

Schultz and Lutz<sup>15</sup> proposed that the planet's spin pole was in a different location than it is currently, and that at some point in the past it experienced a "polar wander". Recent work by Bouley et al.<sup>16</sup> suggests that this may have been due to the formation of the Tharsis volcanic dome which was so large that its mass may have caused a rotation in the outer layers of the planet around the core. Alternatively, Malin et al.<sup>17</sup> suggest that the change in palaeowind direction may be attributable to changes in the season when the planet is at perihelion, the point in its orbit at which it is closest to the sun, a phenomenon which occurs approximately once every 51,000 years.

## Ventifacts on Earth

Overall, it can be seen that these features have led us to several questions surrounding the palaeoenvironment of Mars, even if we currently lack the answers to these questions. Ventifacts are not just applicable to Martian geomorphology however, and have been studied at length here on Earth. One particular region of the world where ventifacts have been crucial to research is Stewart Island, New Zealand.

Research at Mason Bay off the west coast of the island studied widespread ventifacts in the area, interbedded with peat and gravels and overlain by more recent sand dunes<sup>18</sup>. Palynology and radiocarbon dating used on the peat indicated it was formed approximately 10,000 years ago. There is evidence of a strong westerly airstream which caused dunefield migration and, more strikingly, the formation of ventifacts bearing this wind direction. Closer investigation of the ventifacts showed that they actually bore evidence of two distinct palaeo-windflows: one before and one after the peat layer was deposited. Researchers also determined that the sand used to form the ventifacts came from the exposed coastal plains in the region during low sea level periods. As with the Martian research, we can infer the presence and nature of past wind systems. This research, however, also touches on the nature of the material used to abrade the ventifacts, which is not generally possible on Mars due to technological restrictions.

Another, more recent, study of ventifacts by Petersen et al.<sup>19</sup> on Stewart Island focused on the northeast coast of the island at Lee Bay. This study focused on pyrite-coated granite cobbles in the region, which have been shaped by aeolian processes. The material source responsible for their formation was also found to date back to a period of lowered sea level during the Quaternary Period, as did those from Mason Bay. In this case, however, it is the composition of the ventifacts which shed more light on the region's past. Isotope analysis found that the granite is very similar to that found in other areas of Lee Bay found by Watters<sup>20</sup>, meaning the rocks were domestic to the area. After the ventifacts were shaped, they were then coated in a layer of pyrite. This likely happened at a point when the sea level had risen, as the presence of pyrite requires the presence of sulphur, which is sourced from organic material such as seawater. The pyrite coating was deemed to have been formed in a foreign area, for example a peat swamp, due to the presence of black sand grains which are consistent with the nearby Awarua Bay. These clasts must then have been transported back to Lee Bay. The dissolved iron and sulphide in the layering is indicative of an anoxic environment and the lack of any alteration in any observed feldspars suggests formation during a period of low temperature. These compositional studies of ventifacts can be used to draw conclusions on the palaeoenvironment which is currently impossible to do for Mars.

## Conclusion

While there is still more to learn about the palaeoenvironments within which ventifacts have formed, their appearance, location and composition shed a huge amount of light on the conditions under which they were formed. Both on Earth and on Mars, we can use the direction of their features to infer the direction of the wind that formed them, and compare this to current wind regimes to study past climate changes. Unfortunately, only on Earth can we accurately study composition using isotopic and spectroscopic techniques, as we lack access to extraterrestrial samples.

While analogues from Earth can be useful in the study of Martian features, they must be used conservatively. There are too many variables to truly account for: wind tunnel experiments on ventifacts can take into account the difference in gravity and wind speed on Mars, however they are only so accurate. For example, the composition of the sand involved in aeolian processes on Mars is not definitively known, with our closest supposition being that it is composed mostly of soft mafic minerals according to Smalley and Krinsley<sup>21</sup>, unlike the erosional sand seen on Earth which is mostly quartz-based. Therefore we cannot use ventifacts on Earth to draw conclusions about similar features on Mars. Even ventifacts on Earth are not always comparable, for example some studied in Sweden are formed from ice particles rather than sand<sup>22</sup>.

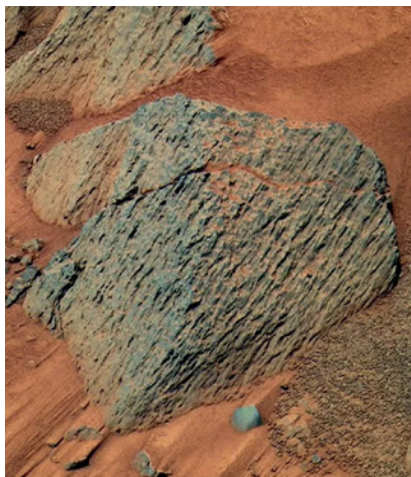


Figure 3: (right to left): Similar appearance of ventifacts found in Death Valley, California and on the surface of Mars. Image credit: Wikimedia Commons and Spirit Mission, NASA/JPL/Cornell

Overall, the study of ventifacts has been crucial to studying the palaeoclimates of both Earth and Mars. Entire discussions have arisen regarding changing Martian wind regimes thanks to the study of these features. Comparing this planetary

research to that on Earth (which has been equally successful in uncovering our geological history) suggests that there is much yet to learn about the Martian features. With improving technology we will soon be able to study Martian ventifacts to the same fine degree as those on Earth and come one step closer to truly understanding the planet's past, and perhaps also our own.

## References

1. Bridges, N., Greeley, R., Haldemann, A., Herkenhoff, K., Kraft, M., Parker, T. and Ward, A. (1999). Ventifacts at the Pathfinder landing site. *Journal of Geophysical Research: Planets*, 104(E4), pp.8595-8615.
2. Bridges, N., Laity, J., Greeley, R., Phoreman, J. and Eddlemon, E. (2004). Insights on rock abrasion and ventifact formation from laboratory and field analog studies with applications to Mars. *Planetary and Space Science*, 52(1-3), pp.199-213.
3. Laity, J. and Bridges, N. (2009). Ventifacts on Earth and Mars: Analytical, field, and laboratory studies supporting sand abrasion and windward feature development. *Geomorphology*, 105(3-4), pp.202-217.
4. Greeley, R., Kuzmin, R. and Haberle, R. (2001). *Space Science Reviews*, 96(1/4), pp.393-404.
5. Wells, G.L. and Zimbleman, F. R. (1997). Extraterrestrial Arid Surface Processes. *Arid Zone Geomorphology: Process Form and Change in Drylands*, 2nd Edition, John Wiley & Sons
6. Malin, M. and Edgett, K. (2000). Sedimentary Rocks of Early Mars. *Science*, 290(5498), pp.1927-1937.
7. Bridges, N., Sullivan, R., Newman, C., Navarro, S., van Beek, J., Ewing, R., Ayoub, F., Silvestro, S., Gasnault, O., Le Mouélic, S., Lapotre, M. and Rapin, W. (2017). Martian aeolian activity at the Bagnold Dunes, Gale Crater: The view from the surface and orbit. *Journal of Geophysical Research: Planets*, 122(10), pp.2077-2110.
8. Schofield, J., Barnes, J., Crisp, D., Haberle, R., Larsen, S., Magalhães, J., Murphy, J., Seiff, A. and Wilson, G. (1997). The Mars Pathfinder Atmospheric Structure Investigation/Meteorology (ASI/MET) Experiment. *Science*, 278(5344), pp.1752-1758.
9. Kuzmin, R. (2001). Wind-Related Modification of Some Small Impact Craters on Mars. *Icarus*, 153(1), pp.61-70.
10. Golombek, M. and Bridges, N. (2000). Erosion rates on Mars and implications for climate change: Constraints from the Pathfinder landing site. *American Geophysical Union*, 105(1), pp.1841-1853
11. Thomson, B. J. and Bridges, N. T. (2006). Ventifact Orientations at the MER Spirit Landing Site: Correlations with Local Topography. *American Geophysical Union*, Fall Meeting 2006
12. Mischna, M., Baker, V., Milliken, R., Richardson, M. and Lee, C. (2013). Effects of obliquity and water vapor/trace gas greenhouses in the early Martian climate. *Journal of Geophysical Research: Planets*, 118(E3), pp.560-576.
13. Fenton, L. and Richardson, M. (2001). Martian surface winds: Insensitivity to orbital changes and implications for aeolian processes. *Journal of Geophysical Research: Planets*, 106(E12), pp.32885-32902.
14. Haberle, R. M., Hollingsworth J.L., Colaprete A., McKay, C.P., Murphy, J. R., Schaeffer J., Freedman R. The NASA/AMES Mars General Circulation Model: Model Improvements and Comparison with Observations. *Journal of Geophysical Research: Planets* Volume 104, Issue E4
15. Schultz, P. and Lutz, A. (1988). Polar wandering of Mars. *Icarus*, 73(1), pp.91-141.

16. Bouley, S., Baratoux, D., Matsuyama, I., Forget, F., Séjourné, A., Turbet, M. and Costard, F. (2016). Late Tharsis formation and implications for early Mars. *Nature*, 531(7594), pp.344-347.
17. Malin, M. (1998). Early Views of the Martian Surface from the Mars Orbiter Camera of Mars Global Surveyor. *Science*, 279(5357), pp.1681-1685.
18. Bishop, D. and Mildenhall, D. (1994). The geological setting of ventifacts and wind-sculpted rocks at Mason Bay, Stewart Island, and their implications for late Quaternary paleoclimates. *New Zealand Journal of Geology and Geophysics*, 37(2), pp.169-180.
19. Petersen, P., Hilton, M. and Wakes, S. (2011). Evidence of aeolian sediment transport across an *Ammophila arenaria*-dominated foredune, Mason Bay, Stewart Island. *New Zealand Geographer*, 67(3), pp.174-189.
20. Watters, W. (1978). Diorite and associated intrusive and metamorphic rocks between Port William and Paterson Inlet, Stewart Island, and on Ruapuke Island. *New Zealand Journal of Geology and Geophysics*, 21(4), pp.423-442.
21. Smalley, I. and Krinsley, D. (1979). Eolian sedimentation on Earth and Mars: Some comparisons. *Icarus*, 40(2), pp.276-288.
22. Schlyter, P. (1994). Paleo-Periglacial Ventifact Formation by Suspended Silt or Snow—Site Studies in South Sweden. *Geografiska Annaler: Series A, Physical Geography*, 76(3), pp.187-201.

# NOT WITH A BANG BUT WITH A WHIMPER: PLANT EVOLUTION DURING MASS EXTINCTIONS

Jessie Dolliver  
Senior Sophister  
Botany

*Mass extinctions involve ecosystem wide effects but the extent to which different groups of organisms are affected varies substantially. Terrestrial plants in particular exhibit interesting extinction and speciation patterns in the fossil record which are largely out of the sync with mass extinction events. This review paper explores how the presence of convergently evolved K-selected and r-selected survival strategies paints a picture of extinction in the fossil record which has occurred not at broad taxonomic levels but rather on the strategies employed by individual taxa. By differentiating plant groups between those who exhibit greater tendencies for a certain strategy it may be possible identify which species run the greatest risk of extinction under anthropogenic change. This in turn would allow for the implementation of targeted conservation measures which reduce costs and improve conservation outcomes*

## Introduction

There have been five mass extinctions during the history of Earth<sup>1,2</sup> (see Table 1). All five of these extinctions were characterized by “a profound loss of biodiversity during a relatively short period”<sup>3</sup>. The most devastating mass extinction was the Permian–Triassic extinction in which 95% of all global species went extinct<sup>1,2</sup>. Mass extinctions eliminate diverse and dominant groups of species, effectively releasing resources; these resources are subsequently consumed in the radiative diversification of those surviving lineages<sup>4</sup>. Palaeobotanical studies of past extinctions provide an opportunity to examine plants’ capacity to adapt to global change, and can help to determine the limits of ecosystems’ tolerance to environmental shifts<sup>5</sup>.

Past Mass Extinction	Cause of Extinction	Loss of global biodiversity
Ordovician–Silurian extinction ( $\approx$ 439 MYA)	Two extinction pulses, about 1 million years apart. Great fluctuations in sea level, which resulted from glacial, interglacial cycles, marine transgressions and regressions, uplift and weathering of Appalachians causing atmospheric and ocean chemistry changes, and CO <sub>2</sub> sequestration. Followed by a period of great global warming.	Approximate 25% of the families and nearly 60% of the genera of marine organisms were lost
Late Devonian extinction ( $\approx$ 364 MYA)	Several extinctions over 3 million years. Cause is unclear but may include global cooling after bolide impacts, spread of anoxic waters, oceanic volcanism, or an extra-terrestrial impact	22% of marine families and 57% of marine genera, including nearly all jawless fishes, disappeared
Permian-Triassic extinction ( $\approx$ 250 MYA)	Causes are debated, but the leading candidate is flood volcanism emanating from the Siberian Traps, which led to profound climate change. Volcanism may have been initiated by a bolide impact, which led to loss of oxygen in the sea. The atmosphere at that time was severely hypoxic, which likely acted synergistically with other factors.	95% of all species (marine as well as terrestrial) were lost, including 53% of marine families, 84% of marine genera, and 70% of land plants, insects, and vertebrates
End Triassic extinction ( $\approx$ 49-214 MYA)	Opening of the Atlantic Ocean by sea floor spreading related to massive lava floods that caused significant global warming. Occurred quickly, in less than 10ky.	Marine organisms were most strongly affected (22% of marine families and 53% of marine genera were lost), but terrestrial organisms also experienced much extinction. Allowed dinosaurs to flourish
Cretaceous-Tertiary extinction ( $\approx$ 65 MYA)	Causes continue to be debated. Leading candidates include diverse climatic changes (e.g., temperature increases in deep seas) resulting from volcanic floods in India (Deccan Traps) and consequences of a giant asteroid impact in the Gulf of Mexico	16% of families, 47% of genera of marine organisms, and 18% of vertebrate families were lost. Marked by the extinction of the non-avian dinosaurs and the beginning of the age of mammals.

Table 1: *An Overview of Earth's Five Past Mass Extinctions Table sourced from* <sup>1,2</sup>

An anthropogenically-induced, 6th mass extinction is currently underway, with many species threatened with extinction as a result of environmentally destructive human activities<sup>3,6-12</sup>. There are an estimated 5 ( $\pm$ 3) million species, with 1.5 million of these described by science<sup>13</sup>. 5% of described species have been assessed for risk of extinction and of these, approximately 6000 species are currently categorised as critically endangered or extinct in the wild, and some have already gone extinct<sup>14</sup>. Within the assessed species, 26% of mammals, 41% of amphibians, 31% of cacti, 63% of cycads (a group of plants), 39% of chameleons, 34% of conifers, 33% of reef-forming coral, 13% of birds, 31% of sharks and rays, 31% of freshwater crabs, and

28% of freshwater shrimps are threatened with extinction<sup>14</sup>. The devastating mass extinctions of the fossil record provided opportunities for the radiative evolution and diversification of existing clades. However, the numerous synergistic effects of humanity have created a mass extinction which, although comparatively great in scale, is utterly dissimilar to any prior event and thus entails unknown ecological and evolutionary consequences<sup>13</sup>. One example of the dissimilarity between this mass extinction and others is that the rate of extinction is much higher. The extinction rates of the past 500 years (22% in mammals and 47–56% in gastropods and bivalves) far exceed those recorded in the fossil record for the five major extinctions of the past 540 million years<sup>15</sup>. Similarly, it is difficult to compare current anthropogenic global warming and associated vegetation responses to past mass extinctions because warming is occurring much faster than in any other episode of Earth's existence.

## A Paleontological Puzzle

Remarkably, broad-scale studies on the stratigraphic ranges of terrestrial land plant species do not indicate a correlation between major declines in diversity and the five mass extinctions described in the geological record<sup>16, 17, 18</sup> (see Figure 1). In stark contrast to the fundamental changes in marine fauna diversity, most major plant groups survived the Permian-Triassic extinction event; widely considered to be the most pronounced biotic and ecological crisis in the history of the Earth<sup>19</sup>. However, small-scale, local studies of the Permian-Triassic and Cretaceous-Tertiary boundaries do document plant extinctions at the taxonomic levels of family and order<sup>16, 21-26</sup>. It is possible that these localised extinctions were not recorded in global studies simply because they were exceptions, or represented a range shift. In this case, dramatic global changes would be manifested in plant community composition and dominance patterns rather than absolute extinction<sup>27-29</sup>. Alternatively, long time intervals and taxonomic inconsistencies could mask extensive transitions in global biodiversity.

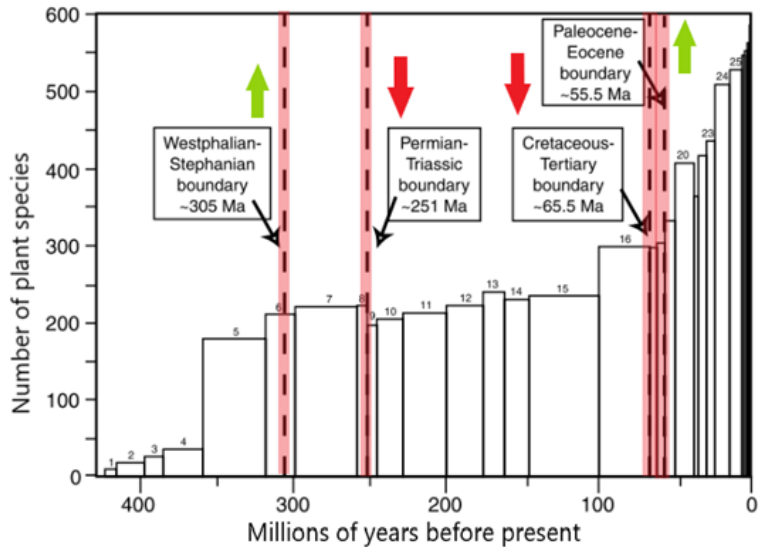


Figure 1: After Niklas and Tiffney<sup>16</sup>; species diversity of embryophytes (terrestrial plants) through time, from the temporal ranges of 8688 species. Notice the absence of major declines in species diversity. Two of the largest mass extinctions span the Permian--Triassic (estimated 80% species extinction among marine animals) and Cretaceous--Tertiary boundaries (estimated 60%). In comparison, there is only a ~10% decrease in plant species biodiversity at the Permian--Triassic boundary, and almost no decrease in plant biodiversity at the Cretaceous--Tertiary boundary whatsoever. Each bar represents an interval of geological time: 1, Late Silurian; 2, Early Devonian; 3, Middle Devonian; 4, Late Devonian; 5, Mississippian (Early Carboniferous); 6, Pennsylvanian (Late Carboniferous); 7, Early Permian; 8, Late Permian; 9, Early Triassic; 10, Middle Triassic; 11, Late Triassic; 12, Early Jurassic; 13, Middle Jurassic; 14, Late Jurassic; 15, Early Cretaceous; 16, Late Cretaceous; 17, early Paleocene; 18, late Paleocene; 19, early Eocene; 20, middle Eocene; 21, late Eocene; 22, early Oligocene; 23, late Oligocene; 24, early Miocene; 25, late Miocene; 26, early Pliocene; 27, late Pliocene; 28, early Pleistocene; 29, late Pleistocene. <sup>2</sup>

## Out of Sync

In the past there have been periods in which global plant extinction rates rose above background levels, although not at the scale of mass extinctions, and interestingly they did not often result in decreases in overall biodiversity. In total, there were 9 of these periods, with the earliest dating as far back as the Early Devonian and the most recent ones taking place in the Oligocene and Miocene respectively<sup>30</sup>. For each of these periods, except the Pennsylvanian-Permian and the Early Triassic, the speciation rate among some plant lineages rose to compensate for the extinction rate. None of these intervals coincided with the mass extinctions for marine or terrestrial fauna that characterize the start and end of eras; they are much more

protracted and more difficult to place in geological history<sup>10, 16</sup>. Indeed it is worth noting that while the evolution of tracheophytes (vascular plants) over the past 420 million years can be subdivided into the Paleophytic (old plants), Mesophytic (middle plants), and Cenophytic (young plants), their respective geological boundaries are still unclear<sup>10</sup>. It is for this reason that the plant kingdom has not been used to define the eras known in geological time.

The apparent resilience of plants to cope with mass extinction events, known as taxonomic resilience, has been noted by numerous papers<sup>17, 31, 32</sup>. Knoll<sup>31</sup> proposed three aspects of the biology of plants which would lend themselves to this resistance to extinction:

1) Resistance to physical stress and destruction. The modular development of plants means that damaged parts can be re-grown. Seeds or spores of plants can lie dormant in the soil for hundreds of years until favourable conditions are detected<sup>33</sup>.

2) Plant populations can disperse long distances in order to adapt to changing environments. Although individual plants are sessile (do not move as adults), this exerts a strong selection pressure on those species which can escape bad conditions through dispersing seeds or spores. Some plant populations have been observed to disperse at rates greater than 1 km/year<sup>34</sup>.

3) Plants make their own food through photosynthesis (with the exception of some parasites and saprophytes), whereas animals have specialized feeding habits. There is thus larger overlap in the resources used by plants, and more competition between species. Extinction as a result of competition is thus observed more in plants, and somewhat diminishes the role played by mass extinctions<sup>31</sup>.

## Vulnerability to Extinction

The tendency for plant speciation to rise in concurrence with extinction may be due to the fierce competition for resources in the plant kingdom mentioned above. As a niche is vacated by an extinct species, another group will radiate to fill it. This compensation may not be ecologically balanced, however. In plant extinctions, large 'K-selected' plants appear to be the most vulnerable; many conifer species went extinct at the Permian-Triassic boundary, as did large angiosperms at the Cretaceous-Tertiary boundary<sup>25, 26</sup>. After each of these events, small, 'r-selected' plants with fast life cycles and good dispersal mechanisms proliferated, and in some cases evolved to occupy the vacated niches of their then-extinct congeners or confamilials<sup>8, 19, 35</sup>. This ecological selectivity seems not to have translated to taxonomic selectivity, perhaps as a result of the diversity of life histories contained within each major clade of plant. The dynamic relationship between K- and r-selected groups may be a major contributing factor to the rapid recovery of the plant kingdom after mass extinctions<sup>35, 36</sup>. Take for example, the forested,

gymnosperm-dominated ecosystems at Astartekløft, East Greenland, a typical late-Triassic locality which transformed through rapid compositional shifts during the Triassic-Jurassic mass extinction. Although only one plant family suffered global extinction, an 85% species-level turnover was observed coincident with a dramatic increase in atmospheric CO<sub>2</sub> by more than 1,500 parts per million (ppm)<sup>37, 38</sup>. Extinction was marked at the species and generic levels only, based on study of macrofossils and of palynomorphs (fossil pollen and spores)<sup>39-41</sup>. In fact, the general response of global vegetation to periods of super-elevated CO<sub>2</sub> consists of a loss of evenness<sup>42</sup> and local-to-regional-scale species turnover<sup>43, 44</sup>, but notably little global extinction at higher taxonomic ranks such as family<sup>45, 46</sup>.

## Learning from the Past

It remains to be seen whether these aspects of plant biology which have protected the kingdom from mass extinction in the past, will also buffer the Plantae from the effects of the anthropogenic sixth mass extinction. This will depend upon the causes of mass extinction. The major human activities causing the 6th mass extinction are, in order: (a) habitat transformation, fragmentation and destruction; (b) overexploitation of species, especially overfishing; (c) biotic exchange leading to the spread of invasive species and genes; (d) nutrient loading of nitrogen, phosphorus, sulphur, and other nutrient-associated pollutants; and (e) anthropogenic climate change<sup>8</sup>. The capacity of plants for dormancy and rapid dispersal is likely to give plants some resistance to these damaging activities, although dispersal will prove more difficult in fragmented habitats, and is of little use if the expansion of human land use tracks that of valuable populations attempting to disperse. Furthermore, for the reasons above, if some extinction-resistant, weedy lineages within each large plant group can be conserved, each is likely to survive and radiate. Human activity as a cause of mass extinction is unprecedented given that the principal driver is a biotic one, as opposed to an abiotic one as was the case in previous mass extinctions. Indeed, through our exponentially growing population and consumption rates, humans have become the greatest geophysical<sup>2</sup> and evolutionary force on Earth<sup>47</sup>.

Despite the resistance of overall plant biodiversity to extreme events and climates, the dynamics of plant communities during mass extinctions is of great relevance in the question of current biodiversity loss. Much can be learned, and the importance of plant communities in the stability of ecosystems cannot be overstated. Over the Permian-Triassic extinction period, volcanogenic greenhouse gases lead to rapid global warming and the drought-induced death of vegetation communities<sup>26, 48</sup>. This damage then propagated up the food chain, resulting in the functional collapse of most terrestrial ecosystems<sup>48</sup>. Additionally, the difference in response to mass extinction between animals and plants has resulted in widespread, severely unbalanced food webs in the past<sup>49</sup>. This variation in capacity for recovery from mass extinction, which results in drastically simplified ecological landscapes is

already becoming common in the sixth mass extinction 8. Differential responses may also have major implications for future macroevolutionary patterns. For example, the global destruction of forests and predominance of smaller plants in the aftermath of the end-Cretaceous Chicxulub impact may have forced the early evolution of modern birds<sup>50</sup>. This would have been through ecological selection against any flying dinosaurs (Avialae) with arboreal ecologies, resulting in a post-extinction neornithine avifauna which rapidly diversified, forming the range of avian ecologies which we know today.

## Conclusion

Mass extinctions have great importance in defining the geological record, but the prevailing paradigm of their singular importance has begun to be questioned<sup>51</sup>. It is now being argued more often, that it is not primarily the extinctions which define macroevolutionary history, but the innovations which occur between them<sup>52</sup>. This has always been obvious in the history of the plant kingdom, such as during the Cretaceous, when angiosperm plants radiated on land and rose to dominance<sup>53-55</sup>. When speaking of extinctions therefore, the wider evolutionary consequences should always be kept in mind.

The plant kingdom has faced off against asteroids and volcanoes to survive previous mass extinctions, demonstrating incredible resistance to extreme events and climate change. Many of the climate shifts in geological time far surpass, in magnitude, both current and projected global warming<sup>10, 16, 56-58</sup>. The rate of change, however, is the unknown variable as we head into the Anthropocene; anthropogenic climate change, habitat destruction, and alteration of geochemical cycles are all occurring at rates which far exceed anything characterized in the deep geological past<sup>58</sup>. Although plant family-level extinctions are rare in the fossil record, it now appears that humans are a very different, efficient type of extinction vector, and so the future of plants on earth remains uncertain<sup>13</sup>. Future directions for palaeobotanical research could include studies on extinctions caused by interacting and diverse forcings, in order to better predict the vegetation response to the current, complex mass extinction which we have created. In the areas of conservation, strong evidence for the ecologically selective nature of plant extinctions in the past gives us an idea of which plant groups are at greatest risk of extinction. Given the vast ecological diversity present within individual taxonomic plant groups, it may ultimately be strategic for groups such as the IUCN to prioritise risk assessment of K selected species whose ecological strategy has in the past and will continue into the future to make them more vulnerable to extinction when faced with rapid changes.

## References

1. Erwin DH (2001) Lessons from the past: Biotic recoveries from mass extinctions. *Proceedings of the National Academy of Sciences* 98: 1399–1403.
2. Jablonski D (1995) In: May RM and Lawton JH (eds.) *Extinction rates*, pp. 25–44, Oxford: *Oxford University Press*.
3. Wake DB and Vredenburg VT (2008) Are we in the midst of the sixth mass extinction? A view from the world of amphibians. *Proceedings of the National Academy of Sciences* 105: 11466–11473.
4. Wing SL. (2004) Mass extinctions in plant evolution. In *Extinctions in the History of Life*, ed. PD Taylor, pp. 61–97. Cambridge, UK: *Cambridge Univ. Press*
5. McElwain, J. C. (2018) Paleobotany and Global Change: Important Lessons for Species to Biomes from Vegetation Responses to Past Global Change, *Annual Review of Plant Biology*, 69(1), pp. 761–787.
6. Jackson JBC (2008) Ecological extinction and evolution in the brave new ocean. *Proceedings of the National Academy of Sciences* 105: 11458–11465.
7. Lewis SL (2006) Tropical forests and the changing earth system. *Philosophical Transactions of the Royal Society B* 361: 195–210.
8. McDaniel CN and Borton DN (2002) Increased human energy use causes biological diversity loss and undermines prospects for sustainability. *Bioscience* 52(10): 929–936.
9. Millennium Ecosystem Assessment. (MEA) (2005) *Millennium Ecosystem Assessment: Ecosystems and Human Well-being (Biodiversity Synthesis)*
10. Steffen W, Crutzen PJ, and McNeill JR (2007) The anthropocene: Are humans now overwhelming the great forces of nature? *Ambio* 36: 614–621.
11. World Wide Fund for Nature (WWF) (2014) *Living Planet Report 2014*. (Accessed 4 February 2019).
12. Zalasiewicz J, Williams M, Steffen W, and Crutzen P (2010) The new world of the anthropocene. *Environmental Science & Technology* 44(7): 2228–2231.
13. Braje, T. J. and Erlandson, J. M. (2013) Human acceleration of animal and plant extinctions: A late pleistocene, holocene, and anthropocene continuum, *Anthropocene*. Elsevier B.V., 4, pp. 14–23. doi: 10.1016/j.ancene.2013.08.003.
14. International Union for Conservation of Nature Red List. (IUCN) (2016) *Red list of threatened species*.
15. Pievani, T. (2018) *Earth's Sixth Mass Extinction Even?* Encyclopedia of the Anthropocene. Elsevier Inc.
16. Niklas, K. J. and Tiffney, B. H. (1994) The quantification of plant biodiversity through time. *Philosophical Transactions of the Royal Society, London, Series B* 345: 35--44.
17. Niklas, K. J., Tiffney, B. H. and Knoll, A. H. (1980) Apparent changes in the diversity of fossil plants. *Evolutionary Biology* 12: 1--89.
18. Niklas, K. J., Tiffney, B. H. and Knoll, A. H. (1985) Patterns in vascular land plant diversification: an analysis at the species level. In: J. W. Valentine (Ed.), *Phanerozoic Diversity Patterns: Profiles in Macroevolution*. Princeton: *Princeton University Press*, pp. 97–128
19. Hochuli, P. A. et al. (2010) Rapid demise and recovery of plant ecosystems across the end-Permian extinction event, *Global and Planetary Change*. Elsevier B.V., 74(3–4), pp. 144–155.
20. Payne, J. L. and Clapham, M. E. (2012) End-Permian Mass Extinction in the Oceans: An Ancient Analog for the Twenty-First Century? *Annual Review of Earth and Planetary Sciences*, 40(1), pp. 89–111.
21. Fröbisch J. (2008) Global taxonomic diversity of anomodonts (Tetrapoda, Therapsida) and the terrestrial rock record across the Permian-Triassic boundary. *PLoS*

ONE 3(11):e3733

22. Maxwell WD. (1992) Permian and Early Triassic extinction of non-marine tetrapods. *Palaentology* 35:571–83

23. Rees PM. (2002) Land-plant diversity and the end-Permian mass extinction. *Geology* 30:827–30

24. Xiong CH, Wang Q. (2011) Permian-Triassic land plant diversity in South China: was there a mass extinction at the Permian/Triassic boundary? *Paleobiology* 37:157–167

25. Nimura, T., Ebisuzaki, T. and Maruyama, S. (2016) End-cretaceous cooling and mass extinction driven by a dark cloud encounter, *Gondwana Research*. Elsevier B.V., 37, pp. 301–307. doi:10.1016/j.gr.2015.12.004

26. Cui, Y. and Kump, L. R. (2014) Global warming and the end-Permian extinction event: Proxy and modeling perspectives, *Earth-Science Reviews*. Elsevier B.V., 149, pp. 5–22. doi:10.1016/j.earscirev.2014.04.007.

27. Mander L, Kürschner WM, McElwain JC. (2010) An explanation for conflicting records of Triassic- Jurassic plant diversity. *PNAS* 107:15351–56

28. McElwain JC, Popa ME, Hesselbo SP, Haworth M, Surlyk F. (2007) Macroecological responses of terrestrial vegetation to climatic and atmospheric change across the Triassic/Jurassic boundary in East Greenland. *Paleobiology* 33:547–73

29. McInerney FA, Wing SL. (2011) The Paleocene-Eocene Thermal Maximum: a perturbation of carbon cycle, climate, and biosphere with implications for the future. *Annu. Rev. Earth Planet. Sci.* 39:489–516

30. Niklas, K. J. (1997) *The Evolutionary Biology of Plants*. University of Chicago Press: Chicago and London.

31. Knoll, A. H. (1984) Patterns of extinction in the fossil record of vascular plants. In: M. H. Nitecki (Ed.), *Extinctions*. Chicago: *The University of Chicago Press*, pp. 21–68.

32. Traverse, A. (1988) Plant evolution

dances to a different beat: plant and animal evolutionary mechanisms compared. *Historical Biology* 1: 277–301

33. Shen-Miller, J., Mudgett, M. B., Schopf, J. W., Clarke, S. and Berger, R. (1995) Exceptional seed longevity and robust growth: ancient sacred lotus from China. *American Journal of Botany* 82: 1367–1380

34. Clark, J. S., Fastie, C., Hurtt, G. et al., (1998) Reid's paradox of rapid plant migration. *BioScience* 48: 13–24

35. Vajda, V. and Bercovici, A. (2014) The global vegetation pattern across the Cretaceous-Paleogene mass extinction interval: A template for other extinction events, *Global and Planetary Change*. Elsevier B.V., 122, pp. 29–49.

36. Chen, Z. Q. and Benton, M. J. (2012) 'The timing and pattern of biotic recovery following the end-Permian mass extinction', *Nature Geoscience*. Nature Publishing Group, 5(6), pp. 375–383. doi: 10.1038/ngeo1475.

37. McElwain JC, Beerling DJ, Woodward FI. (1999) Fossil plants and global warming at the Triassic-Jurassic boundary. *Science* 285:1386–90

38. Steinhorsdottir M, Jeram AJ, McElwain JC. (2011) Extremely elevated CO2 concentrations at the Triassic/Jurassic boundary. *Palaeoogeogr. Palaeoclim. Palaeoecol.* 308:418–32

39. McElwain JC, Popa ME, Hesselbo SP, Haworth M, Surlyk F. (2007) Macroecological responses of terrestrial vegetation to climatic and atmospheric change across the Triassic/Jurassic boundary in East Greenland. *Paleobiology* 33:547–73

40. van de Schootbrugge B, Tremolada F, Rosenthal Y, Bailey TR, Feist-Burkhardt S, et al. (2007) End- Triassic calcification crisis and blooms of organic-walled 'disaster species.' *Palaeoogeogr. Palaeoclim. Palaeoecol.* 244:126–41

41. van de Schootbrugge B, Wignall PB. (2016) A tale of two extinctions: converging end-Permian and end-Triassic scenarios. *Geol. Mag.* 153:332–54

42. McElwain JC, Wagner PJ, Hesselbo SP. (2009) Fossil plant relative abundances indicates sudden loss of Late Triassic biodiversity in East Greenland. *Science* 324:1554–56
43. Bonis NR, Kürschner WM. (2012) Vegetation history, diversity patterns, and climate change across the Triassic/Jurassic boundary. *Paleobiology* 38:240–64
44. Lindström S, van de Schootbrugge B, Hansen KH, Pedersen GK, Alsen P, et al. (2017) A new correlation of Triassic-Jurassic boundary successions in NW Europe, Nevada and Peru, and the Central Atlantic Magmatic Province: a time-line for the End-Triassic mass extinction. *Palaeogeogr. Palaeoclim. Palaeoecol.* 478:80–102
45. Cleal CJ, Cascales-Miñana B. (2014) Composition and dynamics of the great Phanerozoic Evolutionary Floras. *Lethaia* 47:469–84
46. Willis KJ, McElwain JC. (2014) The Evolution of Plants. Oxford, UK: *Oxford Univ. Press*
47. Palumbi SR (2001) Humans as the world's greatest evolutionary force. *Science* 293(5536): 1786–1790.
48. Smith, R. M. H. and Botha-Brink, J. (2014) Anatomy of a mass extinction: Sedimentological and taphonomic evidence for drought-induced die-offs at the Permo-Triassic boundary in the main Karoo Basin, South Africa, *Palaeogeography, Palaeoclimatology, Palaeoecology*. Elsevier B.V., 396, pp. 99–118.
49. Wilf, P. et al. (2006) Decoupled plant and insect diversity after the end-cretaceous extinction, *Science*, 313(5790), pp. 1112–1115.
50. Field, D. J. et al. (2018) Early Evolution of Modern Birds Structured by Global Forest Collapse at the End-Cretaceous Mass Extinction, *Current Biology*. Elsevier Ltd., 28(11), pp. 1825–1831.
51. Hull, P. (2015) Life in the aftermath of mass extinctions, *Current Biology*. Elsevier Ltd, 25(19), pp. R941–R952.
52. Raup, D.M. (1994). The role of extinction in evolution. *Proc. Natl. Acad. Sci. USA* 91, 6758–6763
53. Lloyd, G.T., Davis, K.E., Pisani, D., Tarver, J.E., Ruta, M., Sakamoto, M., Hone, D.W.E., Jennings, R., and Benton, M.J. (2008). Dinosaurs and the Cretaceous Terrestrial Revolution. *Proc. R. Soc. B Biol. Sci.* 275, 2483–2490.
54. Alfaro, M.E., Santini, F., Brock, C., Alamillo, H., Dornburg, A., Rabosky, D.L., Carnevale, G., and Harmon, L.J. (2009). Nine exceptional radiations plus high turnover explain species diversity in jawed vertebrates. *Proc. Natl. Acad. Sci. USA* 106, 13410–13414.
55. Crane, P.R., Friis, E.M., and Pedersen, K.R. (1995). The origin and early diversification of angiosperms. *Nature* 374, 27–33.
56. Jaramillo C, Ochoa D, Contreras L, Pagani M, Carvajal-Ortiz H, et al. (2010) Effects of rapid global warming at the Paleocene-Eocene boundary on Neotropical vegetation. *Science* 330:957–61.
57. McElwain JC, Punyasena SW. (2007) Mass extinction events and the plant fossil record. *Trends Ecol. Evol.* 22:548–57
58. Willis KJ, McElwain JC. (2014) The Evolution of Plants. Oxford, UK: *Oxford Univ. Press*



# Chemistry

TS  
SR

## Letter from the Editor

To know and understand our world and its intricate workings through modern chemistry is an exciting pursuit, one which has progressed significantly from the late 17th century with likes of Irish man Robert Boyle (of Boyle's laws) and Antoine de Lavoisier (who named elemental oxygen).

This volume presents to you four new reviews in the Chemical Sciences that span a broad range of the discipline frequently referred as the 'central science'. It is a wonderful showcase of the significant work being done here at Trinity College Dublin, and across the field. Our goal is to invite readers to zoom-out of small spheres of knowledge and paint a panorama picture of where modern chemistry has been, anticipate where it is headed and then, dive into the detailed pages of this volume sparked with curiosity.

Upon flicking through these pages, it is evident that this area of study does not prove simple and '*Eureka!*' moments are not common reality, for the complexity of our universe would not allow its truths to be revealed with such ease. As well as novel discoveries, this volume celebrates the collaborative nature of science, how lifetimes of brains churning and the rhythms of commitment contribute new ideas of relevance and solutions to real problems, and improvements on current technologies allowing us to move forward.

So with that, I invite you to stick on the kettle, put your feet up, with this copy in one hand and perhaps a search engine of choice in the other and go on this whistle stop tour of the Chemistry section which spans two very important fronts. The first tells of new remedies to the damaging consequences our current technologies have in this Anthropogenic era, and development of more sustainable energy storage devices. The use of heavy metal complexes as photosensitizer molecules for more efficient solar cells will be explored, followed by a discussion on the novel synthetic approach to developing biomass derived fibrous mats for electrodes in the now commercialized

redox flow battery. Then the focus will shift towards the role chemistry is playing in advancements in modern medicine, exploring how peptide therapeutics have diversified the pharmaceutical industry and an introduction to another type of platinum-based drug which is competing with the well-known and loved, cis-platin. I have renewed confidence that this generation of minds possess the drive to seek solutions to the big environmental and public health issues faced by mankind in this day and age, and guided by the teaching and experience of current experts, the field of chemistry has a hopeful future.

I would like to extend my immense gratitude to my academic advisor, Professor Mike Southern for his input, guidance and support in the process and the peer reviewers Peter Dunne, Mike Lyons, Isabel Rozas - who have spared their time to provide detailed feedback to all of the authors, ensuring this volume preserves its high quality. My kudos also goes out to all the submission authors, published or not, the time and effort put into writing your review on top of the prescribed college workload is highly commendable, and I wish you all the best. This year's cohort of submissions is an accurate reflection of quality and diverse group of students and academics in the School of Chemistry, with submission's doubling in number from last year's volume, and having to choose between several great reviews. This publication itself is an example of the power of collaboration in science, and without each person's contribution, big or small it simply would not be possible.

It is my hope that you as the reader, are drawn to the significant role played by Chemistry today, with renewed enjoyment for the science and interest in pursuing its study.

Kathryn Yeow

Chemistry Editor

Trinity Student Scientific Review 2019

# CYCLIC PEPTIDE THERAPEUTICS: A BRIEF OVERVIEW

Susie Calvert  
Senior Sophister  
Chemistry

*Peptides are ubiquitous in nature playing a vital role as signalling molecules in all living systems. Therapeutic peptides were brought to the fore with the introduction of insulin therapy in 1922. Through natural selective pressure, the function of peptides in the living world has been optimised far beyond what could be expected on the basis of their simple chemical nature. The introduction of peptide therapeutics has diversified the pharmaceutical industry bridging the gap between small molecule and antibody-based drugs. Peptide therapeutics offer treatments for a large variety of diseases, with the main focus at present being on cancer, metabolic diseases and cardiovascular disease. This review will briefly summarise the chemical basis for peptide therapeutics with a specific focus on cyclic peptides, their synthesis and future challenges and prospects.*

## Introduction

A peptide can be defined as a biomolecule consisting of a chain of amino acid units linked via amide bonds. To distinguish between proteins and peptides, this review will arbitrarily define peptides as polyaminoacids consisting of 50 amino acid residues or less. Peptides have a vital role in human physiology and with involvements in ion channels, hormones and neurotransmitters within this role are recognised for being highly specific and efficient biomolecules<sup>1</sup>. These functions are regulated by protein-protein interactions (PPIs) and deregulation of these interactions can result in many forms of disease such as infection, neurodegeneration and cancer<sup>2,3</sup>. As a result of these qualities, peptides represent a good starting point for the design of novel therapeutics<sup>4</sup>.

Therapeutics that are currently on the market can be split into two distinct categories: traditional 'small molecule' drugs with molecular weights usually lower than 500 Da and the much larger 'biologics', which are therapeutics derived from or containing components derived from living organisms, with molecular

weights generally over 5000 Da<sup>1</sup>. These 'small molecule' drugs are advantageous due to their oral bioavailability, however, they also often exhibit reduced target selectivity causing subsequent side effects. The larger 'biologics' include protein therapeutics such as, but not limited to, antibodies which are extremely selective for their targets and as such display high potency. However, their large size results in low bioavailability, poor membrane permeability and metabolic instability<sup>1</sup>. These two main classes of therapeutics show a significant gap in their molecular weight brackets, which peptide therapeutics could fill. Peptides represent a class of molecules that are a rich natural source of chemical diversity. They are significantly smaller in size than protein biologics, ranging in size between 247 Da and 5135 Da with the majority lying between 1000 and 2000 Da<sup>5</sup>. Despite their smaller size they still exhibit high specificity towards their in vivo protein targets.

As of March 2017, there are 60 peptide-based drugs approved for use in the United States, Europe and Japan, including the antibiotic vancomycin and the immunosuppressant drug Cyclosporin A. Furthermore, there are over 150 in active clinical development and an additional 260 being tested in human clinical trials<sup>2,5</sup>. From a commercial perspective, the peptide drug market was valued in a recent report by Zion Market Research at US \$23.05 billion in 2017 and this value is expected to grow to US \$43.26 billion by 2024<sup>6</sup>.

## The Chemical Basis and Uses of Peptide Therapeutics

Peptides therapeutics can be categorised into three categories with respect to endogenous peptide molecules: native, analogous or heterologous. Native peptide therapeutics are those in which the amino acid sequence is identical to that of the peptide natural product. Analogues can be defined as substituted or modified versions of the native peptide, whereas heterologous peptide therapeutics are discovered independently of the native peptide through methods such as phage display and synthetic library screening<sup>5</sup>.

In the past, the application of native peptide therapeutics has been limited as a result of their unfavourable properties in vivo. These include chemical and physical instability, poor membrane permeability, high clearance rates and negligible oral bioavailability<sup>4,5</sup>. However, this large pool of naturally occurring peptides does offer an excellent starting point for the design of new analogous and heterologous peptide drugs.

The majority of peptide therapeutics on the market at the present time are analogues of native peptides<sup>5</sup>. These drug molecules have been designed to possess improved pharmaceutical properties, such as oral bioavailability and in vivo stability, but retain their intrinsic selectivity<sup>7</sup>. Modifications including the incorporation of unnatural amino acids, such as D-amino acids, N-terminal modification and head-to-tail cyclisation can be employed to synthesize these peptide analogues (Figure 1)<sup>8-11</sup>. These modifications alter the physical and chemical properties of

the peptides and as such can be used overcome the limitations seen with many naturally occurring peptides. For example, N-methylation enables the formation of a cis-peptide bond and prevents hydrogen bonding. As such, it can have a large impact on the backbone conformation of cyclic peptides<sup>12</sup>.

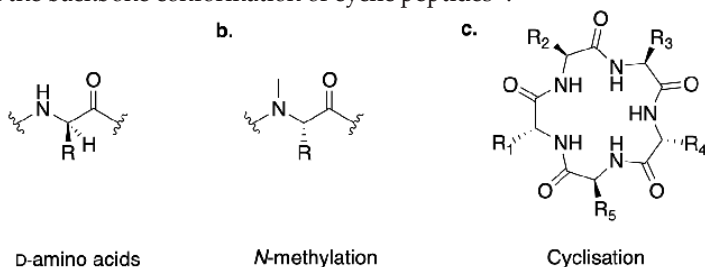


Figure 1: Modifications of peptides

An example of a peptide therapeutic that contains all three of the features shown in Figure 1 is Cyclosporin A (CSA) (sold as Neoral™) (Figure 2). This is a naturally occurring cyclic peptide isolated from cultures of the fungal species *Tolypocladium inflatum* 1, consisting of 11 amino acids. It is orally available and acts as a potent immunosuppressant used for preventing rejection after organ transplant and to treat autoimmune diseases such as psoriasis, uveitis, rheumatoid arthritis and nephrotic syndrome<sup>13,14</sup>. CSA acts as an immunosuppressant through the inhibition of T-cell-dependent biosynthesis of lymphokines, particularly interleukin 2 (IL-2) at the mRNA level. Inhibition of the production of IL-2 prevents T-cell activation and as such the proliferation of cytolytic T-cells<sup>15,16</sup>. The structure consists of a macrocyclic backbone which contains two residues that bear non-canonical side chains, seven N-methylations and a D-alanine residue<sup>17,18</sup>. The large degree of N-methylation largely reduces the number of hydrogen bond donors available and also introduces proteolytic stability<sup>19</sup>. The annual sale of CSA is more than US \$ 1.0 billion in the USA alone.

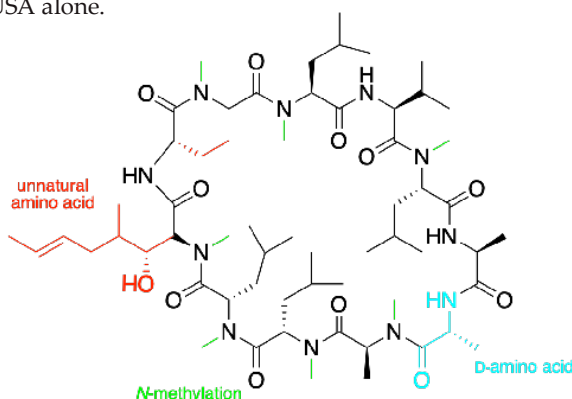


Figure 2: Structure of CSA with key features highlighted<sup>18</sup>

Cyclic peptides have several favourable properties over their linear counterparts including enhanced cell stability, cell membrane permeability and a better resistance to proteolytic degradation<sup>20</sup>. Low permeability results from hydrogen bond donors and acceptors of the peptide participating in hydrogen bonding with the aqueous environment outside the cell. These interactions are disrupted upon entry to the cell, which has a much lower dielectric constant, resulting in an energetic penalty that disfavors permeability<sup>17, 21</sup>. The cyclisation of peptides shields, both conformationally and through the removal of the *N*- and *C*-termini, some of the hydrogen bond donors resulting in a lowering the energetic penalty. Furthermore, cyclisation also results in restriction of the conformational flexibility of the structure and an ability to control the 3D shape<sup>22</sup>. As a result of this, cyclic peptides are less likely to be degraded by peptidases in the blood serum, increasing their *in vivo* half-life, as peptidases show a preference to substrates with extended, flexible conformations and often act by cleaving amino acids from their *N*- and *C*-termini<sup>23, 24</sup>. This restricted flexibility also results in a lowering entropic penalty and improves their binding properties and receptor selectivity<sup>1, 11</sup>.

## Present Outlook on Cyclic Peptide Therapeutics

Over 40 of the 60 peptide therapeutics on the market are cyclic peptides, with approximately one new cyclopeptide therapeutic entering the market each year<sup>25</sup>. For example, in the years between 2006 and 2015 the Food and Drug Administration (FDA) and European Medicines Agency (EMA) approved nine cyclic peptide therapeutics: dalbavancin, telavancin, oritavancin, anidulafungin, lanreotide, romidepsin, pasireotide, linaclotide and peginesatide (later withdrawn), which account for 3% of total number of drugs entering the market during this time<sup>26, 27</sup>. Cyclic peptides have huge potential for disrupting protein-protein interactions and as a result are being pursued as potential therapeutics.

The area of antibiotics presents many examples of cyclic peptide drugs. Colistin and vancomycin (Figure 3) are two of the most famous. Colistin is a cyclic hexapeptide with a tripeptide side chain acylated by a fatty acid amino terminus. It contains cationic residues and two hydrophobic domains which are essential for its antibacterial activity. Colistin selectively binds to lipopolysaccharide (LPS) molecules in the outer membrane of Gram-negative bacteria<sup>28</sup>. This results in the destabilisation of the outer membrane which subsequently leads to the destruction of the phospholipid bilayer that makes up the inner membrane resulting in cell lysis. Vancomycin is a cyclic glycopeptide used to treat serious infections where penicillins and cephalosporins cannot be used. Its antimicrobial properties arise through its inhibition of cell wall synthesis in Gram-positive bacteria. This occurs through the peptide forming 5 hydrogen bonds with the terminal D-alanyl-D-alanine moieties in the backbone strands of the cell wall which prevents cross linking<sup>29, 30</sup>.

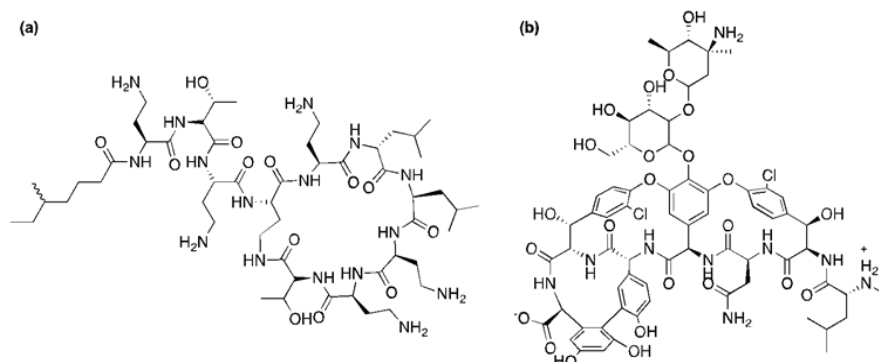


Figure 3: Structures of (a) Colistin and (b) Vancomycin

Many of the cyclic peptide therapeutics that exist on the market are analogues of native cyclic peptide hormones. Examples of these are octreotide, vapreotide, lanreotide and pasireotide (Figure 4) all of which are analogues of somatostatin (Figure 5) and are used to treat patients with neuroendocrine tumours<sup>27, 31, 32</sup>. Somatostatin is a native cyclic tetradecapeptide. It is an endogenous hormone that regulates a large variation of physiological processes in the body including modulation of glucagon secretion, insulin secretion, cell proliferation and neuronal activity<sup>33-35</sup>. These processes are a result of its interaction with 5 G-protein-coupled receptor subtypes ( $sst_1$ - $sst_5$ ) which are widely distributed in the CNS and peripheral tissues<sup>36</sup>. The native form of the peptide has limited clinical use due to its short *in vivo* half-life (1-3 minutes) and its broad biological activity<sup>37</sup>. These analogues have much longer half-lives, for example, octreotide has a half-life of 90 to 120 minutes and lanreotide has a half-life of 25.5 days<sup>38</sup>. Three of the four of these drugs (octreotide, lanreotide and vapreotide) are disulfide cyclised octapeptides which have a high affinity for binding the  $sst_2$  and  $sst_5$ . Pasireotide, on the other hand is a cyclic hexapeptide cyclised through an amide bond. The change in cyclisation method and the smaller macrocycle size results in pasireotide having a 40-fold increased affinity for binding the  $sst_5$  receptor in comparison to the other three analogues<sup>27, 39</sup>. The success of these cyclic peptide analogues of somatostatin can be seen clearly in the sales of octreotide which was one of four peptide therapeutics to have global sales of over US \$1 billion dollars in 2008<sup>37</sup>.

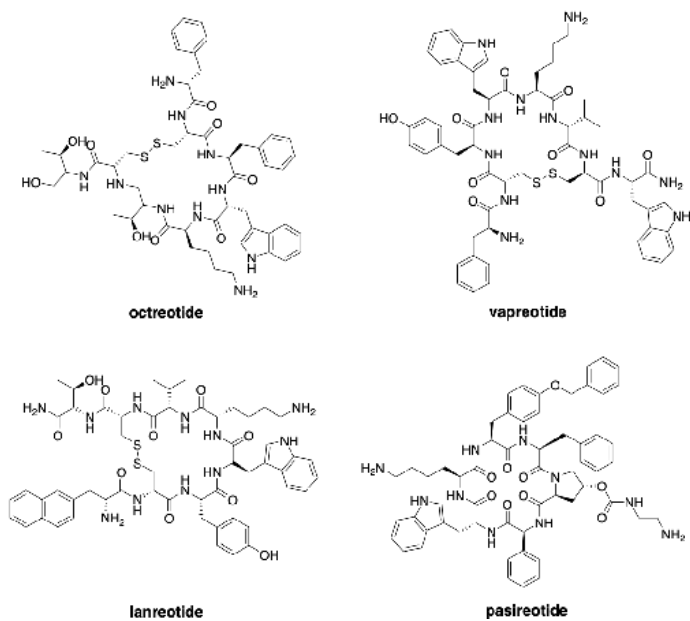


Figure 4: Analogues of Somatostatin

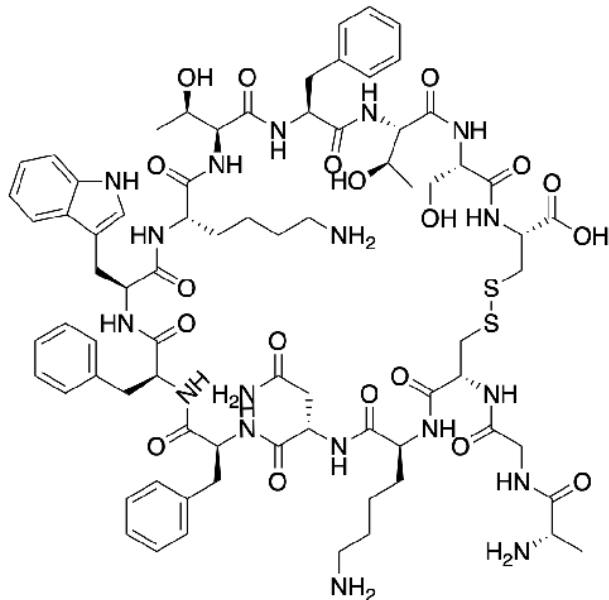


Figure 5: Structure of Somatostatin

## Oral Bioavailability of Cyclic Therapeutics

One of the most important challenges facing the development of cyclic peptide therapeutics is overcoming their poor oral bioavailability and cell permeability. Oral bioavailability can be defined as the proportion of the drug that has been administered orally that reaches systemic circulation<sup>17</sup>. Studies on the properties of therapeutics that result in favourable oral bioavailability carried out by Lipinski<sup>40</sup> and Veber<sup>41</sup> have resulted in the view that peptides are poor candidates as therapeutics. At the present time approximately 75% of peptide therapeutics are presently administered intravenously. Presently, all peptide therapeutics that are orally bioavailable are cyclic peptides of 4-37 amino acid residues<sup>42</sup>. CSA, previously mentioned, has an atypical oral bioavailability of 30% in humans, and breaks 3 of Lipinski's rule of 5<sup>17</sup>. This suggests that in the design of cyclic peptide therapeutics rather than relying on these traditional guidelines improvements should be based on a new set of rules. Research carried out by Nielsen and coworkers<sup>24</sup> suggests that the optimisation of cyclic peptide therapeutic properties should be undertaken solely using NMR to observe amide H-D exchange rates, 3D structure and solvent-exposed polar surface areas.

A recent review published by Nielsen and coworkers<sup>42</sup> has determined a new set of rules resulting in favourable oral bioavailability for cyclic peptides. This review made it clear that it is possible for cyclic peptides to be orally bioavailable and break all of Lipinski and Veber's rules. However, it showed that the number of hydrogen bond donors (HBD), the number of rotatable bonds (RotB) and the LogP are important factors. These findings are likely to prove useful in moving forward in the design of new biologically active cyclic peptides.

The design of therapeutics with high oral bioavailability results in administration of lower doses of the drug and as such fewer side effects as well as higher patient compliance<sup>17</sup>. The introduction of alternative and more patient-friendly routes of administration such as oral and nasal delivery or inhalation would enable a much greater usage of these therapeutics<sup>4</sup>.

## Approaches to Synthesise Cyclic Peptides

As described above, there are a large number of cyclic peptides used for therapeutic use. The most reliable way of synthesising cyclic peptide therapeutics is synthetically using solid phase peptide synthesis. There are biological synthetic methods such as phage display and mRNA display however, the use of these methods is limited and as such will not be covered in this review.

Solid-phase peptide synthesis (SPPS) (Figure 6) was developed by Merrifield [43] in the 1960s, a breakthrough that resulting in him winning the Nobel Prize in 1984<sup>44</sup>. This synthetic strategy has facilitated the synthesis of large quantities of complex peptides. The approach starts with the linking of an *N*-terminal protected amino

acid to a resin via a linker. This is followed by sequential deprotection and peptide coupling steps. Purification consisting of only washing excess reagents off the resin surface with solvents between reactions. Macrocylation can either occur on the resin through side chain-side chain coupling or side chain-C-terminus coupling; or the peptide is cleaved from the resin and macrocylation is carried out through either the head-to-tail coupling of the *N*- and *C*-termini or between the *N*-terminus and a side chain residue. Further improvements to this technique have led to the development of fully automated peptide synthesisers allowing the rapid synthesis of peptides. The feasibility of using this technique on an industrial-scale has been demonstrated by the cost-effective production of the antiretroviral linear peptide therapeutic, enfuvirtide (sold as Fuzeon), at the multi-tonne scale<sup>45</sup>.

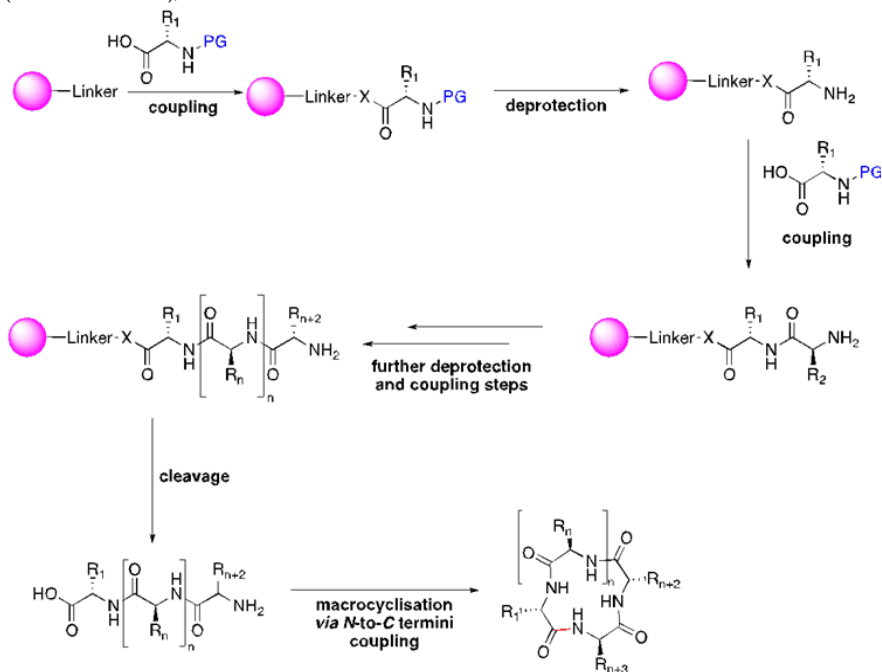


Figure 6: Solid Phase Peptide Synthesis

## Future Prospects and Areas of Research

Throughout the past century, peptide therapeutics have been used to address a variety of biological problems. They have now been established as a distinct area of therapeutics and as such it is clear that they will continue to play a key role in the future of the pharmaceutical market. This is clearly demonstrated upon looking at their success rates in progressing through clinical trials in comparison to small molecule drugs and biologics. Peptide-based therapeutics have an 83% success rate

in progressing through Phase I into Phase II trials in comparison to the 63% and 55% chance small molecule drugs and antibodies have respectively<sup>37</sup>.

It is speculated that peptide therapeutics will play a large role in combating antibiotic resistance. As mentioned previously cyclic peptides have shown excellent efficacy as antibiotics. Antimicrobial resistance (AMR) is a huge problem facing the population. To date, AMR has been observed against all antibiotics used clinically. A 2014 report published by the UK government has estimated that by 2050 antibiotic resistance will cause 300 million premature deaths and will result in a loss of up to US \$100 trillion from the global economy<sup>46</sup>. In recent years, pharmaceutical innovation in this field has been considerably hindered by obstacles. However, antimicrobial peptides (AMPs) offer a strategy for developing novel antibiotics. AMPs are a distinct and diverse group of biomolecules involved in the host innate immunity, whose composition generally ranges between 12 and 50 amino acid subunits<sup>47</sup>. Their physical properties including their cationic nature and high hydrophobic content allows them to selectively target anionic bacterial cell membranes over zwitterionic human cell membranes<sup>48</sup>. Furthermore, many of these peptides are made up on D-amino acids and as such are often resistant to degradation by peptidases as the majority of peptidases selectively cleave L-peptide bonds<sup>49</sup>. These peptides therefore offer an excellent starting point for the structure-based design of novel antibiotics.

However, to facilitate the discovery of novel peptide therapeutics it will be necessary to make improvements in new high through-put peptide screening methods. It is also essential to consider new sources of materials for development of novel therapeutics. Further analysis of the microbiome could give rise to the identification of many new peptides that have arisen from degradation products or signalling molecules. Furthermore, the influence that symbiotic bacteria inhabiting the gut have on the metabolism and absorption of therapeutics has not been considered and it is very likely that this will be an important area of research.

## References

1. Craik, D. J., Fairlie, D. P., Liras, S. & Price, D. The Future of Peptide-based Drugs. *Chem Bio Drug Des* 81, 136–147 (2013).
2. Reichert, J., Pechon, P., Tartar, A. & Dunn, M. K. Development trends for peptide therapeutics: A comprehensive quantitative analysis of peptide therapeutics in clinical development. (2010).
3. Pawson, T. Specificity in Signal Transduction: From Phosphotyrosine-SH2 Domain Interactions to Complex Cellular Systems. *Cell* 116, 191–203 (2004).
4. Fosgerau, K. & Hoffmann, T. Peptide therapeutics: current status and future directions. *Drug Discov. Today* 20, 122–128 (2015).
5. Lau, J. L. & Dunn, M. K. Therapeutic peptides: Historical perspectives, current development trends, and future directions. *Bioorg. Med. Chem.* 26, 2700–2707 (2018).
6. Zion Market Research. Peptide Therapeutics Market by Route of Administration, by Type of Manufacturers, by Type of Molecule, by Technology and by Application: Global Industry Perspective, Compre-

- hensive Analysis and Forecast, 2017 – 2024. (2018).
7. Erak, M., Bellmann-Sickert, K., Els-Heindl, S. & Beck-Sickinger, A. G. Peptide chemistry toolbox – Transforming natural peptides into peptide therapeutics. *Bioorg. Med. Chem.* 26, 2759–2765 (2018).
8. Yin, H. Constrained Peptides as Miniature Protein Structures. *ISRN Biochem.* 2012, 1–15 (2012).
9. Brinckerhoff, L. H. et al. Terminal modifications inhibit proteolytic degradation of an immunogenic mart-127-35 peptide: Implications for peptide vaccines. *Int. J. Cancer* 83, 326–334 (1999).
10. Mandal, D., Nasrolahi Shirazi, A. & Parang, K. Cell-Penetrating Homochiral Cyclic Peptides as Nuclear-Targeting Molecular Transporters. *Angew. Chemie Int. Ed.* 50, 9633–9637 (2011).
11. Joo, S. H. Cyclic Peptides as Therapeutic Agents and Biochemical Tools. *Biomol. Ther.* (Seoul). 20, 19–26 (2012).
12. Chatterjee, J., Gilon, C., Hoffman, A. & Kessler, H. N-Methylation of Peptides: A New Perspective in Medicinal Chemistry. *Acc. Chem. Res.* 41, 1331–1342 (2008).
13. Johnson, K. P. & Belendiuk, G. Use of Cyclosporine in Neurological Autoimmune Disease? *Arch. Neurol.* 42, 1043–1044 (1985).
14. Fathman, C. G. & Myers, B. D. Cyclosporine Therapy for Autoimmune Disease. *N. Engl. J. Med.* 326, 1693–1695 (1992).
15. Wenger, R. M. Cyclosporine and Analogues – Isolation and Synthesis – Mechanism of Action and Structural Requirements for Pharmacological Activity. in *Fortschritte der Chemie organischer Naturstoffe / Progress in the Chemistry of Organic Natural Products* (eds. Herz, W., Grisebach, H., Kirby, G. W. & Tamm, C.) 123–168 (Springer, Vienna, 1986). doi:10.1007/978-3-7091-8888-0\_4
16. Matsuda, S. & Koyasu, S. Mechanisms of action of cyclosporine. *Immunopharmacology* 47, (2000).
17. Wang, C. K. & Craik, D. J. Cyclic Peptide Oral Bioavailability: Lessons From the Past. *Biopolym. Pept. Sci.* 106, 901–909 (2016).
18. Suga, H., Passioura, T. & Ito, K. Technologies for the Synthesis of mRNA-Encoding Libraries and Discovery of Bioactive Natural Product-Inspired Non-Traditional Macrocyclic Peptides. *Molecules* 18, 3502–3528 (2013).
19. Tsomaia, N. Peptide therapeutics : Targeting the undruggable space. *Eur. J. Med. Chem.* 94, 459–470 (2015).
20. Williams, T. M., Sable, R., Singh, S., Vicente, M. G. H. & Jois, S. D. Peptide ligands for targeting the extracellular domain of EGFR: Comparison between linear and cyclic peptides. *Chem. Biol. Drug Des.* 91, 605–619 (2017).
21. Conradi, R. A., Hilgers, A. R., Ho, N. F. H. & Burton, P. S. The Influence of Peptide Structure on Transport Across Caco-2 Cells. *Pharm. Res.* 08, 1453–1460 (1991).
22. Kaspar, A. A. & Reichert, J. M. Future directions for peptide therapeutics development. *Drug Discov. Today* 18, 807–817 (2013).
23. Werle, M. & Bernkop-Schnürch, A. Strategies to improve plasma half life time of peptide and protein drugs. *Amino Acids* 30, 351–367 (2006).
24. Nielsen, D. S. et al. Improving on Nature: Making a Cyclic Heptapeptide Orally Bioavailable. *Angew. Chemie* 126, 12255–12259 (2014).
25. Abdalla, M. & McGaw, L. Natural Cyclic Peptides as an Attractive Modality for Therapeutics: A Mini Review. *Molecules* 23, 2080 (2018).
26. Mullard, A., Hughes, B. & Owens, J. FDA drug approvals 2005-2016. *Nat. Rev. Drug Discov.* 15, 73–76 (2016).
27. Zorzi, A., Deyle, K. & Heinis, C. Cyclic peptide therapeutics: past, present and future. *Curr. Opin. Chem. Biol.* 38, 24–29 (2017).

28. Yu, Z., Qin, W., Lin, J., Fang, S. & Qiu, J. Antibacterial Mechanisms of Polymyxin and Bacterial Resistance. *Biomed Res. Int.* 2015, 1–11 (2015).
29. Knox, J. R. & Pratt, R. F. Different modes of vancomycin and D-alanyl-D-alanine peptidase binding to cell wall peptide and a possible role for the vancomycin resistance protein. *Antimicrob. Agents Chemother.* 34, 1342–7 (1990).
30. Levine, D. P. Vancomycin: A History. *Clin. Infect. Dis.* 42, S5–S12 (2006).
31. Narayanan, S. & Kunz, P. L. Role of Somatostatin Analogues in the Treatment of Neuroendocrine Tumors. *Hematol. Oncol. Clin. North Am.* 30, 163–177 (2016).
32. Rai, U., Thrimawithana, T. R., Valery, C. & Young, S. A. Therapeutic uses of somatostatin and its analogues: Current view and potential applications. *Pharmacol. Ther.* 152, 98–110 (2015).
33. Allen, J. P. et al. Somatostatin receptor 2 knockout/lacZ knockin mice show impaired motor coordination and reveal sites of somatostatin action within the striatum. *Eur. J. Neurosci.* 17, 1881–95 (2003).
34. Cardoso, A. et al. Somatostatin increases mitogen-induced IL-2 secretion and proliferation of human Jurkat T cells via sst3 receptor isotype. *J. Cell. Biochem.* 68, 62–73 (1998).
35. Strowski, M. Z., Parmar, R. M., Blake, A. D. & Schaeffer, J. M. Somatostatin Inhibits Insulin and Glucagon Secretion via Two Receptor Subtypes: An In Vitro Study of Pancreatic Islets from Somatostatin Receptor 2 Knockout Mice 1. *Endocrinology* 141, 111–117 (2000).
36. Günther, T. et al. Somatostatin Receptors: Structure, Function, Ligands, and New Nomenclature. *Pharmacol. Rev.* 70, 763–835 (2018).
37. Rubin, S. J. S. & Qvit, N. Backbone-Cyclized Peptides: A Critical Review. *Curr. Top. Med. Chem.* 18, 526–555 (2018).
38. Astruc, B. et al. Long-Acting Octreotide and Prolonged-Release Lanreotide Formulations Have Different Pharmacokinetic Profiles. *J. Clin. Pharmacol.* 45, 836–844 (2005).
39. Cuevas-Ramos, D. & Fleseriu, M. Pasireotide: a novel treatment for patients with acromegaly. *Drug Des. Devel. Ther.* 10, 227–39 (2016).
40. Lipinski, C. A., Lombardo, F., Dominy, B. W. & Feeney, P. J. Experimental and computational approaches to estimate solubility and permeability in drug discovery and development settings. *Adv. Drug Deliv. Rev.* 46, 3–26 (2001).
41. Veber, D. F. et al. Molecular Properties That Influence the Oral Bioavailability of Drug Candidates. *J. Med. Chem.* 6, 2615–2623 (2002).
42. Nielsen, D. S. et al. Orally Absorbed Cyclic Peptides. *Chem. Rev.* 117, 8094–8128 (2017).
43. Merrifield, R. B. Solid Phase Peptide Synthesis. I. The Synthesis of a Tetrapeptide. *J. Am. Chem. Soc.* 85, 2149–2154 (1963).
44. Merrifield, R. B. Solid Phase Synthesis (Nobel Lecture). *Angew. Chemie Int. Ed. English* 24, 799–810 (1985).
45. Bray, B. L. Large-scale manufacture of peptide therapeutics by chemical synthesis. *Nat. Rev. Drug Discov.* 2, 587–593 (2003).
46. O'Neill, J. The Review of Antimicrobial Resistance (AMR). (2014).
47. Papagianni, M. Ribosomally synthesized peptides with antimicrobial properties: biosynthesis, structure, function, and applications. *Biotechnol. Adv.* 21, 465–499 (2003).
48. Mishra, B., Reiling, S., Zarena, D. & Wang, G. Host defense antimicrobial peptides as antibiotics: design and application strategies. *Curr. Opin. Chem. Biol.* 38, 87–96 (2017).
49. Ballantine, R. D., Li, Y.-X., Qian, P.-Y. & Cochrane, S. A. Rational design of new

cyclic analogues of the antimicrobial lipopeptide tridecaptin A. *Chem. Commun* 54, 10634 (2018).

TS  
SR

# ELECTROSPINNING AND THE REDOX FLOW BATTERY: A FABRICATION METHOD FOR BIOMASS-DERIVED ELECTRODES

Lia Grogan

Senior Sophister

Nanoscience, Physics and Chemistry of Advanced Materials

*Increasing risk of disaster due to anthropogenic climate change has lead to a surge in research relating to clean, renewable power. However, solar and wind energy is generated sporadically, unevenly and in a fashion that is non-compatible with existing electricity grids. Materials science offers a solution to this in the form of electrochemical energy storage systems, a notable example being the redox flow battery (RFB). The discovery of the Vanadium redox flow battery (VRFB) lead to widespread commercial implementation of RFBs. The electrode is a crucial component of the RFB. This review will highlight recent research in optimising these electrodes to improve overall efficiency of the battery. Specically, efforts to develop a fibrous, free-standing electrode mat from various biomass materials will be investigated. Electrospinning, a novel approach for fabrication of fibrous mats, will be specically highlighted.*

## Introduction

A redox flow battery (RFB) is made up of an electrochemical cell and two tanks. The primary components of the cell are two electrodes and a separator, through which an electrolyte solution is circulated<sup>1</sup>. The battery converts chemical energy into electrical energy directly with high energy efficiency<sup>2</sup>. The RFB also holds an advantage over a conventional battery cell by allowing for independent scaling of power and capacity<sup>1</sup>. The structure of the battery is simple and maintenance costs are low<sup>3</sup>.

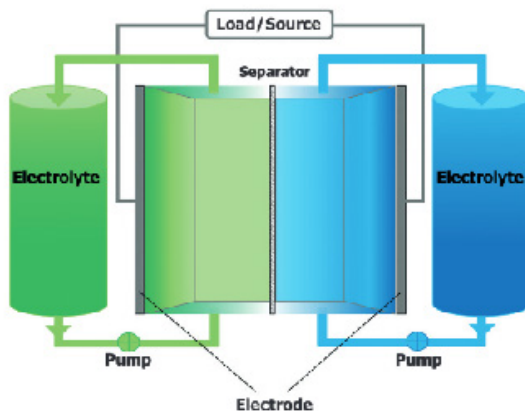


Figure 1: Schematic diagram of RFB. Adapted from Winsberg et al.<sup>1</sup>

The electrochemical performance of the battery may be gauged by the measurement and calculation of several parameters, such as volumetric capacity, energy density, coulombic efficiency (CE) and voltage efficiency (VE)<sup>1</sup>. The volumetric capacity can be expressed as follows, where  $m$  is mass,  $n$  is number of electrons,  $F$  is Faraday's constant,  $M$  is molar mass and  $V$  is volume<sup>1</sup>:

$$C = \frac{m \cdot n \cdot F}{M \cdot V} \quad (1)$$

The energy density may be expressed as follows, where  $U$  is voltage between utilized redox couples<sup>1</sup>:

$$E = C \cdot U \quad (2)$$

The CE relates the charge applied to the battery initially to the charge that is emitted in the discharging process of the same cycle, and may be given as follows<sup>1</sup>:

$$CE = \eta_C = \frac{Q_D}{Q_C} \quad (3)$$

VE may be written as follows:

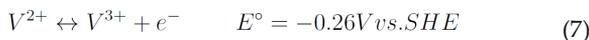
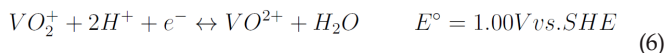
$$VE = \eta_V = \frac{\frac{\int_0^{T_D} E_D(t) dt}{T_D}}{\frac{\int_0^{T_C} E_C(t) dt}{T_C}} = \frac{\overline{E}_D}{\overline{E}_C} \quad (4)$$

This allows us to formulate an expression for energy efficiency (EE)<sup>1</sup>:

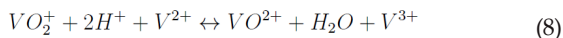
$$EE = \eta_{EE} = \eta_C \cdot \eta_V \quad (5)$$

Constants and subscripts are ascribed the following meanings:  $\eta$  = efficiency,  $C$  = charging,  $D$  = discharging,  $Q$  = charge,  $T$  = time for charging/discharging, and  $E$  = potential.

The Vanadium redox flow battery (VRFB) was famously discovered by Skyllas-Kazacos in 1986. This battery was shown to possess desirable properties such as large power output and storage capacity, rapid response, elongated cycle life and high efficiency<sup>4, 5</sup>. A unique attribute of the VRFB is its' minimisation of cross-contamination, due to the same metal ion being employed in both half-cells<sup>3</sup>. This leads to electrolytes having a longer cycle-life<sup>6</sup>. The VRFB centres around two different reactions of vanadium ions in an acid solution. Vanadium's stability in four different oxidation states enables this ( $V^{2+}$ ,  $V^{3+}$ ,  $V^{4+}$ ,  $V^{5+}$ ) - a characteristic property of transition metals<sup>6, 5</sup>. The cathodic and anodic half-cell reactions are as follows<sup>6</sup>:



This allows for the formation of the total cell reaction:



The electrode is a crucial component of the RFB, it does not take part in the redox reactions, but rather provides an active surface for reactions of redox couples in electrolyte to occur<sup>2</sup>. The system power is determined by the rate of reaction of redox species at each electrode, as power is a time-dependent property of an electrochemical cell. This is expressed in the following formula, where  $P$  is power,  $V$  is electric potential and  $Q$  is electric charge<sup>7</sup>:

$$P = \frac{VQ}{t} \quad (9)$$

Therefore, optimisation of the electrodes in a RFB can hugely improve the efficiency of the system. [3] Thus far, carbon materials have been pinpointed as the most promising electrode material for use in VRFBs. This is due to their high electrical conductivity, good stability, corrosion resistance and wide range of operating potentials<sup>8</sup>. The most commonly used types of carbon material are graphite felts and carbon papers. These materials are usually derived from polyacrylonitrile (PAN)<sup>9</sup> and processed at high temperatures. However, these electrodes have poor electrochemical activity and bad wettability<sup>2</sup>. Issues of high cost for large scale application is also a concern<sup>10</sup>. The need for cost-effective and mass-produced electrodes has turned attention towards biomass-derived materials for VRFBs<sup>8</sup>.

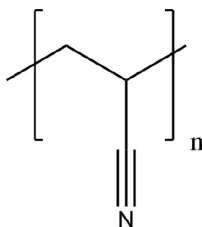


Figure 2: Polyacrylonitrile (PAN) monomer.

An aim in the development of electrode materials has been the improvement of electrocatalytic activity of the electrode. Electrocatalysis may be defined as the heterogeneous catalysis of electrochemical reactions<sup>11</sup>. Carbonised materials act as electrocatalysts in the VRFB due to their abundance of -OH and -COOH groups<sup>12</sup>. The larger the specific surface area of the electrode, the better electrocatalytic properties we would expect to see. Liu et al. previously reported electrospun electrodes with average surface area of  $2.94 \text{ m}^2\text{g}^{-1}$ , with Lai et al. reporting electrospun nanofibres with specific surface area of  $583 \text{ m}^2\text{g}^{-1}$ <sup>14</sup>. Fibrous carbonaceous electrodes were evaluated as a possible electrode material by Liu et al. In a fibrous electrode, a large surface area must be balanced with porosity such that transport properties of the electrode are not diminished<sup>14</sup>. Electrospinning is an efficient, cheap and tunable process with a record of successful implementation in producing nanofibers<sup>15</sup>. This review will lay out developments in the production and analysis of biomass-derived electrodes, and investigate the possibility of producing a lignin-based fibrous electrode mat via a novel method. Possible constituents of a spinnable polymer solution are also discussed, with proposal of synthetic polymers to accompany lignin.

## What makes a good electrode in a VRFB?

An ideal electrode material must provide fast kinetics for the redox couple while inhibiting undesirable side reactions<sup>1</sup>. Zhang et al. were successful in producing an active electrode material from cotton through a pyrolysis process. Their results suggested great promise in the area of biomass-derived electrodes for VRFBs<sup>8</sup>. A renewable precursor for an electrode must be abundant, cheap, and provide the necessary chemical functionalities (-COOH, -OH)<sup>16, 17</sup>. Lignin as a biomaterial presents itself as an appealing precursor for fibrous electrodes, as it fulfills these criteria and is a waste product of the paper manufacturing industry<sup>18, 19</sup>. Lignin is a constituent of plant cell walls, acting to cement cellulose fibres. It is the second most abundant natural raw material and nature's most abundant phenolic polymer<sup>18</sup>.

Lignin-derived fibrous electrodes may be fabricated by electrospinning<sup>14</sup>. Previous studies have sought to improve electrochemical properties of carbonaceous electrodes by metal oxide deposition. Transition metal oxides function as

electrocatalysts as they can change between valence states and absorb reactive species as an active centre<sup>20, 21</sup>. Kim et. al. successfully coated  $Mn_3O_4$  onto carbon felt by hydrothermal method. Cyclic voltammograms showed that following the modification, carbon felts demonstrated better reversibility and electrochemical activity towards both the  $V^{2+}/V^{3+}$  and  $VO_2^+/VO^{2+}$  reactions. They concluded that the improvement in electrochemical performance was due to the better hydrophilicity of the carbon felt surface and lower activation barrier for vanadium redox reactions<sup>22</sup>. Ma et. al. succeeded in producing a graphite felt/ $MnO_2$  composite electrode with good electrocatalytic activity, via a one-step hydrothermal process<sup>23</sup>. In the hydrothermal method, need for high vapour pressure presents difficulties for large scale implementation<sup>2</sup>. A simpler, more scalable approach to transition metal oxide deposition is needed. One possibility would be the decoration of carbon fibres with  $MnO_2$  particles by a simple chemical reaction with  $KMnO_4$ . It is hypothesised that this decoration would improve the electrocatalytic activity of a fibrous electrode.

## Electrocatalysis at the Electrode

The energy efficiency of the VRFB therefore, can be determined almost primarily from the physicochemical properties of the electrode used. Efficiency losses associated with activation polarization originate mainly in the electrode<sup>24</sup>.

An oxygen atom will be transferred during the charge and discharge processes at the positive electrode. This transfer will likely be the limiting step in the reaction mechanism. The increasing of the concentration of oxygen functional groups therefore, will improve the oxygen transfer process<sup>24, 25</sup>. Mechanisms for catalytic half-cell reactions as proposed by Skyllas-Kazacos et al. are as follows<sup>2</sup>.

In operation of the VRFB cell, energy efficiency is determined by activation and concentration polarizations, which are dependent on the electrode material. A VRFB electrode must satisfy a variety of requirements. The electrode itself must not participate in the reaction, merely provide a stable site for the redox reaction to occur. As the supporting electrolyte in a VRFB is normally a strong acid, the electrode must also be stable in highly acidic environments. Additionally, the electrode must be stable within the operating potential window of the VRFB. It must also have excellent electrical conductivity to facilitate rapid charge transfer reactions<sup>24</sup>.

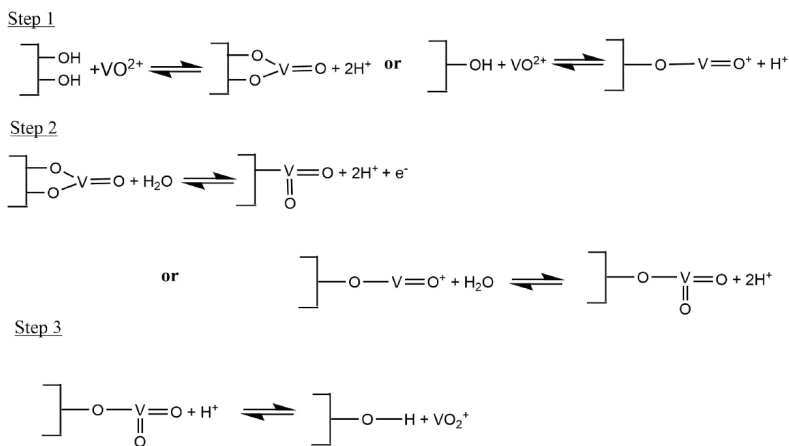


Figure 3: Catalysis mechanism of C-OH groups towards positive side reaction<sup>2</sup>

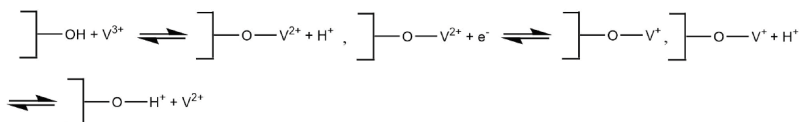


Figure 4: Catalysis mechanism of C-OH groups towards negative side reaction<sup>2</sup>

## Electrospinning

Nanofibres are a class of nanomaterials that have attracted interest due to their high surface area, aspect ratio and flexibility. A variety of methods have been used to produce nanofibres; electrospinning and melt or solution blowing, to mention a few. Electrospinning is the most versatile technique due to its' unique capability in producing nanofibres from materials with different morphologies, patterns and functionalities<sup>26</sup>.

Electrospinning is the process used to produce lignin-based flexible electrode mats<sup>27,28</sup>. It is a spinning fibre forming process based on an electro-hydrodynamic phenomenon which uses electrostatic force to draw continuous fibres in the form of a liquid jet from a polymer solution or melt<sup>29</sup>. In this method, an electric field is applied to a polymer solution held by surface tension at the end of a capillary tube. The application of the electric field induces charge on the surface of the liquid drop at the end of the capillary tube. A force directly opposite to that of the surface tension will be created by mutual charge repulsion<sup>30</sup>.

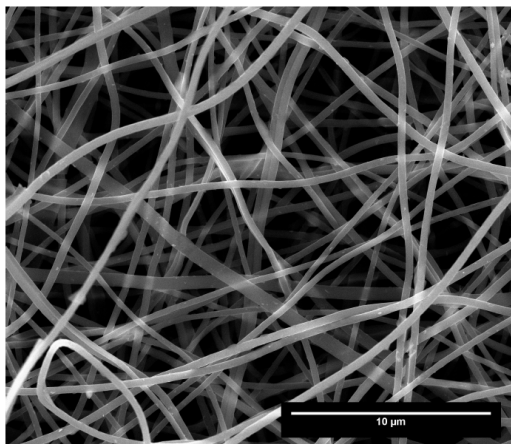


Figure 5: SEM image of electrospun nanofibres.

Increasing intensity of the electric field leads to the elongation of hemispherical surface of solution. A conical shape, known as the Taylor cone, is formed<sup>30</sup>. The principle behind the formation of a Taylor cone is as follows: if electrostatic pressure ( $p_e$ ) exceeds capillary pressure ( $p_c$ ), then a Taylor cone will form<sup>29</sup>. When the electric field reaches a critical value where the repulsive electric force is greater than the surface tension force, a charged jet of solution is ejected from the tip of the Taylor cone. As it travels through the air, solvent must evaporate before reaching the collector, to leave behind a charged polymer fibre<sup>29</sup>. Fibres will be placed randomly on a metal collector. Continuous fibres are laid down which lead to the formation of a non-woven fabric<sup>30</sup>.

A number of parameters have an effect on the electrospinning process. These include solution properties, controlled variables and ambient parameters<sup>30</sup>. The solution properties include viscosity, conductivity and surface tension. Controlled variables are flow rate of solution through capillary, electric potential at the tip, and distance between tip and collection screen. Ambient parameters are temperature, humidity and air velocity in the electrospinning chamber<sup>32</sup>. Fibre morphology is influenced by the competing forces that solution electrospinning jet is subjected to.

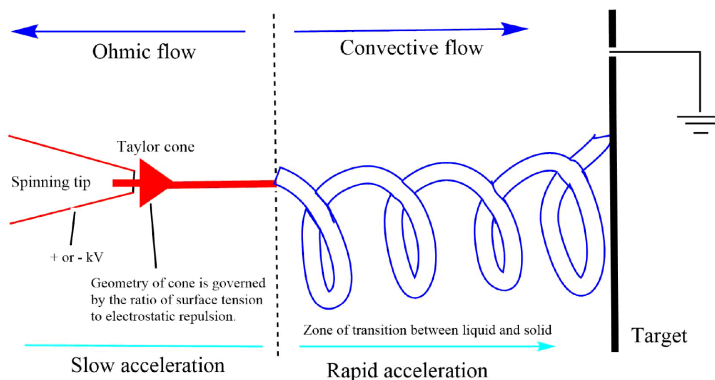


Figure 6: Schematic diagram of electrospinning<sup>31</sup>.

The molecular weight ( $M_w$ ) of the polymer is also a key parameter in electrospinning. Using a high  $M_w$  polymer with a relatively weak electric field ( $E$ ), it may be impossible to develop a Taylor cone and spin a continuous fibre. The higher degree of polymer chain entanglement will lead to high resistance to electrostatic drawing force. Equally, use of a polymer with a low  $M_w$  with high applied  $E$  would result in breakup of the jet stream<sup>29</sup>. One of the primary advantages of electrospinning is the tunability of the method. Fibres produced may be as small as tens of nanometres or as large as several micrometres. This allows for engineering of parameters to achieve optimum balance between surface area fibre diameter. Electrospun mats may be carbonized and utilised as flow-through electrodes in RFBs<sup>33</sup>.

As a carbonised electrospun mat is porous, performance of an RFB becomes dependent on transport in the material. This transport relates strongly to the microstructural properties such as pore size, porosity, tortuosity and connectivity<sup>33</sup>. In this work, focus shall be placed on analysing the porosity of the electrode material and the resulting electrocatalytic performance.

## Optimising the Polymer Solution

Ideal parameters for the electrospinning of a polymer into nanofibres would ensure the diameter of the fibres is held consistent and controllable, the fibre surface being defect-free or defect-controllable, and the continuous single nanofibres be collectable<sup>15, 34</sup>. Doshi demonstrated that there exists an optimum viscosity of polymer solution in order to form fibres by electrospinning. Solutions of poly(ethylene oxide) ( $M_w = 1,450,000$  g/mol) only formed fibres at viscosities in the range 800 - 4000 cP. At viscosity lower than 800 cP, the solution was too dilute to form a stable jet<sup>30</sup>. It has been shown in previous work that viscosity of a solution affects fibre diameter. McKee et al. investigated implications of the entanglement concentration on electrospinning and discovered that fibre diameter and

morphology increased with viscosity and normalised concentration<sup>35</sup>. Molecular weight ( $M_w$ ) and polymer concentration in solution for electrospinning are also important parameters to control. Specific viscosity has previously been found to scale with polymer concentration as a power law, with exponent changing depending on  $M_w$  of polymer<sup>26</sup>.

A combination of three solutes in the polymer solution may be proposed, the first one being polyvinylpyrrolidone (PVP). PVP is soluble in a variety of organic solvents as well as in water<sup>36</sup>. A molecular weight distribution curve of PVP is broad due to transfer reactions which take place during polymerisation. The second solute polymer proposed for use is polyethylene oxide (PEO). PEO, similarly to PVP, is soluble in a number of organic solvents such as ethanol and acetone, as well as in distilled water<sup>15</sup>.

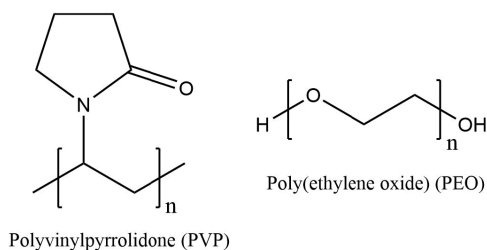


Figure 7: Monomers of synthetic polymers; PVP and PEO.

The third polymer is the biomass-derived polymer, lignin. Lignin is a very abundant biopolymer, second only to cellulose. It is a phenolic macromolecule and a waste product in the paper industry<sup>19</sup>.

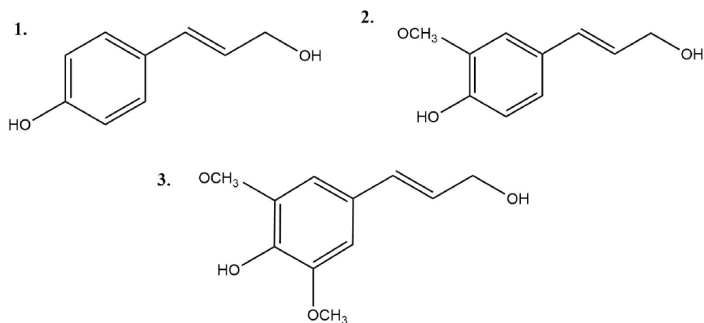


Figure 8: Three common monolignols: paracoumaryl alcohol (1), coniferyl alcohol (2) and sinapyl alcohol (3).

Lignin as used in the production of polymer solution in this experiment is processed and categorised as an organosolved lignin (OSL). In this processing method, organic solvents and acids are applied which degrade and solubilize

lignin to produce pulps. Lignin has a high carbon content of 55-65%<sup>19</sup>. In a proposed method for fabricating fibrous mats a lignin fibre would first be produced by electrospinning then carbonised in a furnace to yield a carbon fibre. OSLs display spinnability, likely due to their low molecular weights. The blending of lignin with low amounts of synthetic polymers such as PVP and PEO can enhance fibre quality by reducing the softening temperature<sup>19</sup>.

## Conclusions

A review of previous work suggests that the use of a lignin precursor would increase the efficiency of an electrode in a VRFB. The abundance of desired chemical functionalities such as -COOH and -CO present in lignin allows for effective catalysis of the redox reaction between four different Vanadium ions. As lignin is abundant and cheap, it presents itself as a novel alternative to entirely synthetic precursors for VRFB electrodes.

It can also be concluded that the decoration of carbonaceous materials with transition metal oxides boosts electrocatalytic activity. These previously established techniques may have application in further improving the electrocatalytic activity of lignin-derived electrodes.

Fibrous electrodes for use in VRFBs have been shown in previous research to be effective. As these materials are very highly porous, ample surface area for redox reactions to occur is available. If the number of redox sites is balanced with the structural properties of the mat in order to allow successful electrolyte transport, optimum efficiency will be achieved.

The merits of electrospinning for producing fibrous mats have been reported. The tunability of the method renders it useful for fabrication of nanofibres from a polymer solution. Therefore, it can be concluded that electrospinning is a cheap and scalable method for making fibrous mats from a lignin-based polymer solution. Future work may allow for the precise tuning of fibre diameters within a mat, based on the molecular weight and wt% of various polymers in a solution.

In conclusion, it can be said that research relating to biomass-derived components of RFBs is likely to surge in the coming years. As global resources deplete and temperatures rise, aims of producing sustainable energy storage devices via sustainable material will become paramount.

## Acknowledgements

This work has been adapted from my final year research project report entitled, "Fabrication and Optimisation of Lignin-derived Electrode for use in the Redox

Flow Battery".

## References

1. Winsberg J, Hagemann T, Janoschka T, Hager MD, Schubert US. Redox-Flow Batteries: From Metals to Organic Redox-Active Materials; 2017.
2. Cao L, Skyllas-Kazacos M, Wang DW. Electrode modification and electrocatalysis for redox flow battery ( RFB ) applications. *Energy Storage Science and Technology*. 2015;4(5):433-457.
3. Flox C, Skoumal M, Rubio-Garcia J, Andreu T, Ramón Morante J. Strategies for enhancing electrochemical activity of carbon-based electrodes for all-vanadium redox flow batteries. *Applied Energy*. 2013;109:344351.
4. Skyllas-Kazacos M, Cao L, Kazacos M, Kausar N, Mousa A. Vanadium Electrolyte Studies for the Vanadium Redox Battery A Review. *Wiley-Blackwell*; 2016.
5. Lu W, Li X, Zhang H. The next generation vanadium flow batteries with high power density-A perspective. *Physical Chemistry Chemical Physics*. 2017;20(1):2335.
6. Cunha Á, Martins J, Rodrigues N, Brito FP. Vanadium redox ow batteries: A technology review. *Wiley-Blackwell*; 2015.
7. Young HD, Freedman RA. Sears and Zemansky's University Physics: with Modern Physics with Mastering Physics; 2004.
8. Zhang ZH, Zhao TS, Bai BF, Zeng L, Wei L. A highly active biomass-derived electrode for all vanadium redox ow batteries. *Electrochimica Acta*. 2017 sep;248:197205.
9. Zhang L, Aboagye A, Kelkar A, Lai C, Fong H. A review: Carbon nanofibers from electrospun polyacrylonitrile and their applications; 2014.
10. Kaneko H, Nozaki K, Wada Y, Aoki T, Negishi A, Kamimoto M. Vanadium redox reactions and carbon electrodes for vanadium redox ow battery. *Electrochimica Acta*. 1991 jan;36(7):11911196.
11. Léger JM, Hahn F. Contribution of In-situ Infrared Reactance Spectroscopy in the Study of Nanostructured Fuel Cell Electrodes. In: In-situ Spectroscopic Studies of Adsorption at the Electrode and Electrocatalysis. *Elsevier Science B.V.*; 2007. p. 6398.
12. Kim KJ, Lee HS, Kim J, Park MS, Kim JH, Kim YJ, et al. Superior electrocatalytic activity of a robust carbon-felt electrode with oxygen-rich phosphate groups for all-vanadium redox flow batteries. *ChemSusChem*. 2016;9(11):13291338.
13. Lai C, Zhou Z, Zhang L, Wang X, Zhou Q, Zhao Y, et al. Free-standing and mechanicallyexible mats consisting of electrospun carbon nanofibers made from a natural product of alkali lignin as binder-free electrodes for high-performance supercapacitors. *Journal of Power Sources*. 2014 feb;247:134141.
14. Liu S, Kok M, Kim Y, Barton JL, Brushett FR, Gostick J. Evaluation of Electrospun Fibrous Mats Targeted for Use as Flow Battery Electrodes. *Journal of The Electrochemical Society*. 2017;164(9):A2038A2048.
15. Huang ZM, Zhang YZ, Kotaki M, Ramakrishna S. A review on polymer nanobers by electrospinning and their applications in nanocomposites. *Composites Science and Technology*. 2003;63(15):22232253.
16. Herou S, Schlee P, Jorge AB, Titirici M. Biomass-derived electrodes for flexible supercapacitors; 2018.
17. Chakrabarti MH, Brandon NP, Hajimolana SA, Tariq F, Yut V, Hashim MA, et al.. Application of carbon materials in redox ow batteries. *Elsevier*; 2014.
18. Suhas, Carrott PJM, Ribeiro Carrott MML. Lignin - from natural adsorbent to

- activated carbon: A review; 2007.
19. Duval A, Lawoko M. A review on lignin-based polymeric, micro- and nano-structured materials. *Reactive and Functional Polymers*. 2014;85:7896.
20. Yao C, Zhang H, Liu T, Li X, Liu Z. Carbon paper coated with supported tungsten trioxide as novel electrode for all-vanadium flow battery. *Journal of Power Sources*. 2012;218:455-461.
21. Wieckowski A. Interfacial electrochemistry : theory, experiment, and applications. In: *Interfacial Electrochemistry: Theory: Experiment, and Applications*. Marcel Dekker; 1999. p. 449461. A
22. Kim KJ, Park MS, Kim JH, Hwang U, Lee NJ, Jeong G, et al. Novel catalytic effects of Mn<sub>3</sub>O<sub>4</sub> for all vanadium redox flow batteries. *Chemical Communications*. 2012;48(44):5455-5457.
23. Ma Q, Deng Q, Sheng H, Ling W, Wang HR, Jiao HW, et al. High electro-catalytic graphite felt/MnO<sub>2</sub> composite electrodes for vanadium redox flow batteries. *Science China Chemistry*. 2018;61(6):732738.
24. Kim KJ, Park MS, Kim YJ, Kim JH, Dou SX, Skyllas-Kazacos M. A technology review of electrodes and reaction mechanisms in vanadium redox flow batteries. *Journal of Materials Chemistry A*. 2015;3(33):1691316933.
25. Sun B, Skyllas-Kazacos M. Modification of graphite electrode materials for vanadium redox flow battery application-I. Thermal treatment. *Electrochimica Acta*. 1992;37(7):12531260.
26. Zdraveva E, Fang J, Mijovic B, Lin T. Electrospun nanobers. In: *Structure and Properties of High-Performance Fibers*; 2016. p. 267300.
27. Greiner A, Wendor JH. Electrospinning: A fascinating method for the preparation of ultrathin fibers; 2007.
28. Wei G, Liu J, Zhao H, Yan C. Electrospun carbon nanobers as electrode materials toward VO<sub>2</sub><sup>+</sup>/VO<sub>2</sub>+redox couple for vanadium flow battery. *Journal of Power Sources*. 2013 nov;241:709717.
29. Brown TD, Dalton PD, Hutmacher DW. Melt electrospinning today: An opportune time for an emerging polymer process. *Progress in Polymer Science*. 2016;56:116166.
30. Doshi J, Reneker DH. Electrospinning Process and Applications of Electrospinning. *Journal of Electrostatics*. 1995;35(2-3):151660.
31. Li D, Xia Y. Electrospinning of nanobers: Reinventing the wheel? *John Wiley & Sons, Ltd*; 2004.
32. Cramariuc B, Cramariuc R, Scarlet R, Manea LR, Lupu IG, Cramariuc O. Fiber diameter in electrospinning process. *Journal of Electrostatics*. 2013;71(3):189198.
33. Kok MDR, Jervis R, Brett D, Shearing PR, Gostick JT. Insights into the Effect of Structural Heterogeneity in Carbonized Electrospun Fibrous Mats for Flow Battery Electrodes by XRay Tomography. *Small*. 2018;14(9).
34. Kok MDR, Gostick JT. Transport properties of electrospun brous membranes with controlled anisotropy. *Journal of Membrane Science*. 2015;473:237244.
35. McKee MG, Wilkes GL, Colby RH, Long TE. Correlations of Solution Rheology with Electrospun Fiber Formation of Linear and Branched Polyesters. *Macromolecules*. 2004;37(5):17601767.
36. Schwarz W. PVP A critical review of kinetics and toxicology of polyvinyl pyrrolidone. *Lewis Publishers*; 1990.

# Pt(IV) COMPLEXES AS PRODRUGS FOR TRADITIONAL Pt(II) DRUGS

Aoife Donaghy  
Senior Sophister  
Medicinal Chemistry

*“For years I’ve been saying this (cisplatin) is the first platinum-based drug we discovered. It can’t possibly be the best one. It’s disappointing that the scientific community has not been able to find better ones.” – Barnett Rosenberg, 1926-2009<sup>1</sup>*

*Cisplatin, along with its derivatives carboplatin and oxaliplatin, are some of the most well-known anti-cancer agents used in clinical practice today. However, they have various disadvantages associated with them, including poor oral availability, toxicity, severe side effects, as well as inherent and acquired immunity<sup>1,2</sup>. In an attempt to combat this, platinum(IV) prodrugs have been developed. With improved oral availability and fewer side effects, they can be combined with other anticancer compounds to act as ‘dual action’ drugs<sup>1,2</sup>. This review will discuss the problems associated with cisplatin and its derivatives, how platinum(IV) prodrugs can overcome these issues and explore some of the recent developments in the field.*

## Introduction

Cisplatin, or CDDP (*cis*-diamminedichloroplatinum (II)), was first discovered by Michele Peyrone in 1845, but its structure was not elucidated until 1893 by Alfred Werner<sup>3</sup>. The confirmation of its square planar geometry differentiated *cis*-platin from its isomer, *trans*-platin and this formed part of the work which was awarded the Nobel Prize for Chemistry<sup>4</sup> in 1913. It was another 52 years before its antineoplastic properties were discovered - scientists at Michigan State University found that a soluble platinum compound generated upon electrolysis of platinum electrodes resulted in the inhibition of binary fission in *E. coli* cells<sup>3,5</sup>. Further testing showed that it was effective at treating sarcomas in rats, but it was a further 10 years before it gained FDA (US Food and Drug Administration) approval. Cisplatin was finally deployed as an anti-cancer agent in 1979 and is still used to treat a wide range of cancers including testicular, ovarian, head and neck tumours<sup>4</sup>

6.

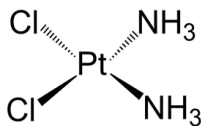


Figure 1: The structure of cisplatin

As relatively simple molecule, cisplatin exerts its activity by binding to the N7 atom in guanine bases in DNA<sup>7</sup>, distorting its overall shape and preventing repair, which ultimately leads to cell death. Upon penetrating the cell membrane intact, one of the chloride ligands is replaced with water, which subsequently binds to a guanine base (see Fig. 2). This process repeats with the second chloride ligand, and intra or inter-strand cross-linking of DNA occurs<sup>7</sup>.

The anti-tumour properties demonstrated by cisplatin are not shared by the trans isomer<sup>8</sup>. Transplatin is highly reactive compared to cisplatin – reactions with H<sub>2</sub>O and NH<sub>3</sub> occur 4 and 30 times faster respectively when compared to cisplatin<sup>9,10</sup>. Transplatin is twice as reactive with the molecule glutathione (GSH)<sup>11</sup> – which leads to rapid deactivation of the compound, through side reactions and conjugation. This increased reactivity means that transplatin is less likely to reach the tumour and exert its anti-cancer activity. However, trans-platin complexes do exhibit weak anti-cancer activity, and are currently under investigation as possible treatments for cisplatin resistant cancers<sup>12,13</sup>.

However, like many drugs, cisplatin is not without side effects; in addition to those associated with nearly all anti-cancer agents (alopecia, myelosuppression, nausea and vomiting) it also causes oral and peripheral neuropathy, and acute nephrotoxicity - the loss of tubular epithelial cells in the proximal and distal tubules and loop of Henle in the kidneys leading to increased loss of fluid and electrolyte imbalance<sup>14, 15, 16</sup>.

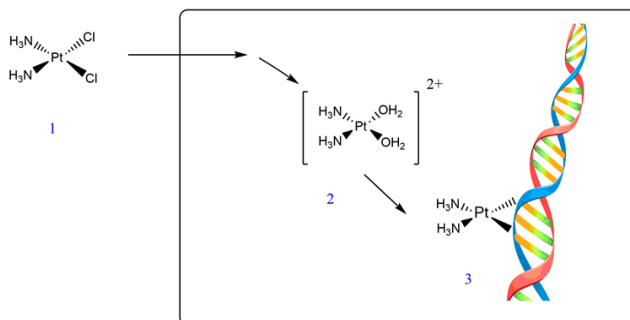


Figure 2: Diagram showing mode of action of cisplatin in cancer cells: 1; Cisplatin penetrates cell membrane, 2; Ligand exchange reactions, 3; Formation of intra- and/or inter-strand linkages with guanine bases in DNA.

Cisplatin, and its derivatives (Fig.4, molecules 1-6), can become conjugated to GSH

or metallothionein (MT) proteins, which in turn are pumped out of the cell via efflux pumps before they have an opportunity to act. This conjugation is an example of Hard Soft Acid Base Theory (HSAB)<sup>4</sup>. Coordination between two 'soft' atoms (the Sulphur of the thiol and the Platinum of cisplatin) is stronger than coordination between Platinum and a hard atom, such as the Nitrogen of the amine ligand, and therefore, the amine is readily displaced by the thiol<sup>4</sup>. Platinum based drugs are also susceptible to resistance via the NER pathway, which both fixes platinum induced DNA damage and removes platinum-DNA adducts<sup>17</sup>. Therefore, it would be helpful if these chemotherapeutic agents could be combined with drugs which can disable these resistance mechanisms and increase the efficacy of the Pt II drugs.

Platinum(IV) prodrugs could be the answer to the problem of cisplatin's resistance and toxicity. A combination of established anti-cancer drugs such as cisplatin, carboplatin or oxaliplatin with small molecules exhibiting anti-tumour activity may result in the discovery of new, more potent and selective anti-cancer agents.

## Platinum(IV) Prodrugs

Platinum(IV) prodrugs are essentially cisplatin (or one of its derivatives) with two additional axial ligands, transforming the square planar ( $d^8$ ) complex into one of octahedral ( $d$ ) geometry. These ligands can be biologically active or inactive; the former are used in dual (two identical axial ligands) and triple (two different axial ligands) threat anti-cancer drugs, whilst the latter are employed to further improve properties such as lipophilicity.

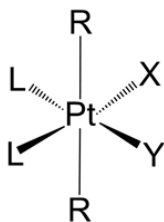


Figure 3: Octahedral structure of Platinum IV complexes. Ligands; R = axial (bioactive or inactive), L = Leaving group (Cl) and X and Y =  $\text{NH}_3$ .

There are numerous advantages of using Pt(IV) prodrugs for administration of cisplatin and its derivatives. Petruzzella<sup>1</sup> and Lippard<sup>7</sup> both identified 'the octahedral geometry and low spin  $d^6$  electronic configuration of Pt(IV) complexes' as being advantageous, as it makes them more kinetically inert than Pt(II). As such, they undergo ligand substitution reactions in the blood a lot less readily than their Pt(II) counterparts, which in turn increases their blood plasma stability and reduces side effects<sup>1,7</sup>. The improved blood stability also means that Pt(IV)

complexes are suitable for oral administration; in contrast to Pt(II) drugs which must be given via injection. The presence of two additional ligands in the axial positions allows for 'fine-tuning' of properties such as lipophilicity.

Dual and triple action anti-cancer drugs are of particular interest, as the use of non-DNA targeting molecules as axial ligands has shown to be effective in lowering levels of drug resistance when compared to cisplatin and its derivatives. The ligands used are usually small molecules, which can be easily attached to the platinum scaffold. Three types of small molecule axial ligands are discussed below; histone deacetylase inhibitors (HDACi), tubulin polymerisation inhibitors and dichloroacetic acid (DCA).

## HDACi Ligands – Histone Deacetylase Inhibitors

Histone deacetylase inhibitors are one of the most common bioactive ligands currently used in Pt(IV) prodrugs. They bring about their anti-cancer effect through deacetylation of the histone proteins around which DNA is wound in the cell: leaving the DNA open to platinum<sup>18, 19</sup>. HDACi ligands also act as epigenetic agents<sup>20, 21</sup>, altering the expression of several genes involved in DNA repair, which further improves the efficacy of Pt(IV) prodrugs.

Two main classes of HDACis exist: Hydroxamic acids and MCFAs (medium chain fatty acids)<sup>19</sup>. The latter are more commonly used, as it is much easier to conjugate MCFAs to the metal core than it is hydroxamic acids. Examples of MCFAs that have been used in Pt(IV) prodrugs include; phenylbutyrate (PhB) (Fig. 4; 7): an orphan drug currently used to treat urea cycle disorders, but which displays good anticancer activity<sup>22</sup>; valproic acid (VPA) (Fig.4; 8): a small molecule anticonvulsant used to treat epilepsy, and which is also being investigated as a possible treatment for HIV and some cancer [23]; and 2-hexyl-4-pentynoic acid (POA)<sup>24</sup> (Fig.4; 9): a potent HDAC inhibitor with IC50 values approximately 10-20 times greater than VPA<sup>25, 26</sup>.

HDACis have been combined with cisplatin in two drugs; satraplatin (Fig. 4; 12) and *cis,cis,trans*-diamminedichlorobisvalproato-platinum(IV), (VAAP) (Fig. 4; 13). VAAP, which combines cisplatin and two molecules of valproic acid, showed similar levels of HDAC inhibition but elevated cytotoxicity in human cancer cell lines when compared with cisplatin. It also displayed lower levels of nephrotoxicity and increased *in vivo* anti-tumour activity when compared with the starting material, ACHP (*cis,cis,trans*-diamminedichlorodihydroxy-platinum (IV))<sup>27, 28</sup>.

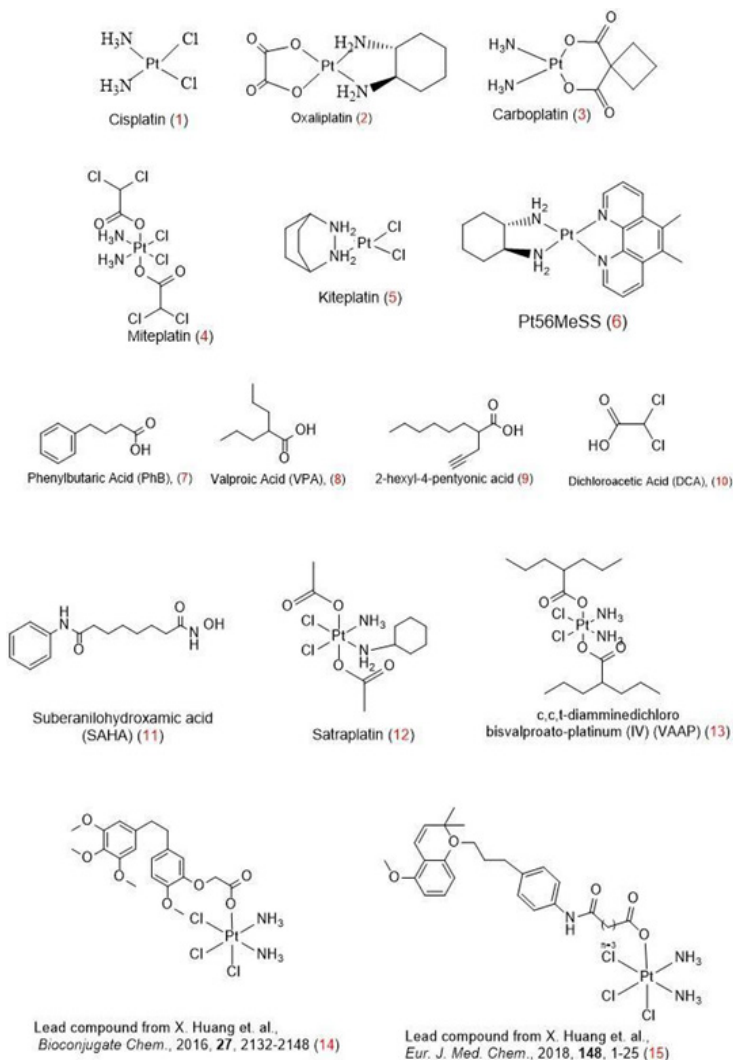


Figure 4: Cisplatin derivatives (1-6), Histone deacetylase inhibitors (7-9, 11), Dichloroacetic acid (10), Histone deacetylase inhibitor-containing prodrugs (12,13), Tubulin polymerisation inhibitor-containing drug candidates (14,15).

However, Osella et. al.<sup>28</sup> hypothesised that cytotoxicity improved not because of the antineoplastic properties of the axial ligands, but that the VPA ligands increased the lipophilicity of the prodrug, which in turn increases accumulation in the target cells. Osella et. al. replaced valproate with its non-HDAC inhibitor isomer, octanoate, and found that it was a very potent anti-cancer drug, despite the

axial ligands having no anti-tumour activity.

In addition, Gibson<sup>29</sup> questioned the use of valproic acid when there are more potent HDAC inhibitors available, such as SAHA (suberanilohydroxamic acid, Fig.4; 11) and POA. For dual action drugs containing cisplatin and HDAC inhibitors, the two components are not active at the same concentrations; the optimum concentration of cisplatin is 'approximately three orders of magnitude lower than that of valproic acid'<sup>29</sup>, whereas SAHA shows better activity at these concentrations. However, SAHA would need significant modification to be conjugated to the central platinum atom.

Satraplatin was first synthesised in the early 1990s<sup>30</sup> and combines cisplatin with two acetic acid axial ligands; in addition, one of the amine ligands is modified to contain a cyclohexyl motif. The drug brings about its anticancer activity through the formation of intra- and inter-strand crosslinks in DNA, which leads to arrest in the G<sub>2</sub> phase of the cell cycle and apoptosis<sup>31</sup>. Similarly to cisplatin, these DNA adducts can be repaired by NER, but are unsusceptible to repair by DNA mismatch repair proteins – this is a significant advantage over previous platinum based anticancer agents<sup>31</sup>.

Satraplatin showed promise in preclinical trials and displayed an improved toxicity profile compared to cisplatin; there was an absence of neurotoxicity and GI toxicities were low and easily managed<sup>31</sup>. However, a plethora of problems were encountered as clinical trials advanced, the most concerning of which was the non-linear pharmacokinetics of the drug<sup>32</sup>. This led to daily oral administration instead of the usual weekly intravenous administration. Satraplatin also demonstrated very complex metabolism, and in some Phase II trials, its anti-tumour activity was not much better than carboplatin<sup>32</sup>. Although it advanced to Phase III trials in combination with prednisone as a potential treatment for Hormone Refractory Prostate Cancer (HRPC)<sup>29</sup>, satraplatin was rejected by the FDA in 2007 as the overall survival rate was not significantly improved on previous platinum anti-cancer agents.

## Tubulin Polymerisation Inhibitors

Tubulin polymerisation inhibitors are another class of compounds which have shown great potential in dual action anti-cancer drugs. These compounds disrupt tubulin polymerisation in the spindle apparatus of dividing cancer cells, preventing replication. There are several different tubulin polymerisation inhibitors: most stop cell division in the G<sub>2</sub>/M phase (vincristine<sup>33</sup>, vinblastine<sup>34</sup> and vinorelbine<sup>35</sup> (Fig. 5; 16, 17, 18 respectively)), but some arrest in the S phase (vindesine<sup>36</sup> (Fig. 5; 19)). Microtubules play an intrinsic role in cell division and make a very attractive non-DNA target for anti-cancer therapies. Several studies<sup>37-42</sup> have combined tubulin polymerisation inhibitors with platinum-based scaffolds, with many reporting lower levels of toxicity and more potent anti-cancer activity.

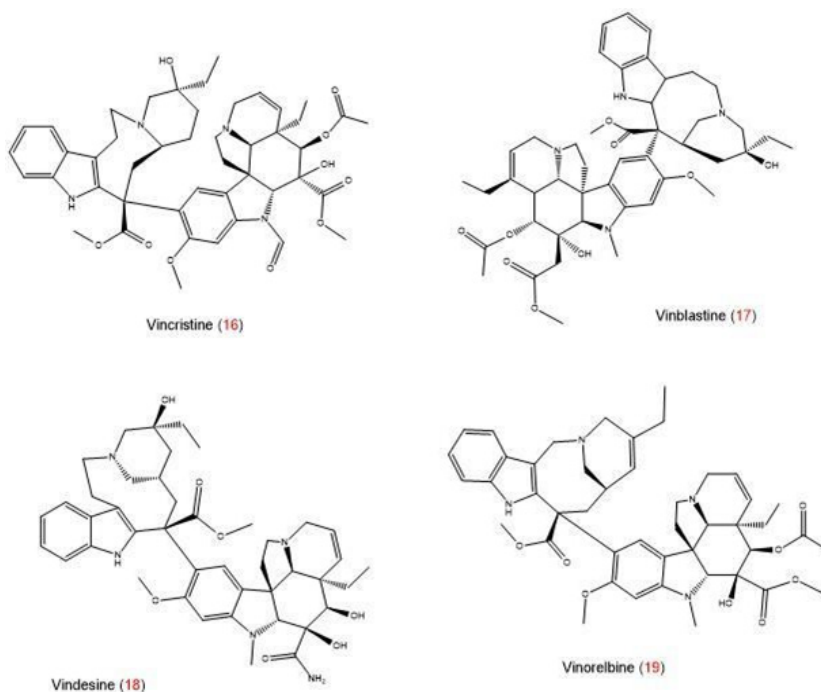


Figure 5: Tubulin polymerisation inhibitors

A lot of the pioneering research in this field has been carried out by Xiaochao Huang and their research team. They have synthesised many novel Pt(IV) prodrugs containing chalcone analogues – molecules containing an aromatic ketone and enone which display various biological activities – which, when released in a tumour cell, bind the chalcone site of microtubules, preventing polymerisation and mitosis<sup>39-41</sup>. For example, a Pt(IV) prodrug containing a combretastatin-A4 analogue displayed a ‘distinct mechanism to kill cancer cells’, which involved arrest at the G<sub>2</sub>/M phase of the cell cycle and inhibition of tubulin assembly (Fig.4; 14). It displayed heightened levels of apoptosis compared to cisplatin, however this may have been due to increased cellular uptake caused by the hydrophobic properties of the axial ligands<sup>40</sup>.

Although this complex showed promise in *in vitro* studies, a more recent paper from this group admitted that its activity *in vivo* couldn’t quite match that of cisplatin<sup>41</sup>. They hypothesised that this depression in activity was due to the difficulty involved in cleaving the strong ether bond binding the chalcone to the platinum core, which resulted in a chalcone derivative being released into the cell, and not the isolated chalcone. To improve on this, Huang et. al. synthesised a series of new millepachine containing compounds which were equally potent towards

cisplatin resistant and non-resistant cells, but most importantly showed very promising *in vivo* activity<sup>41</sup>. The most potent compound, molecule 15 in Fig. 4, was recommended for further investigation with the hope that it could be developed into a new anti-cancer drug.

## Dichloroacetic Acid

Dichloroacetic acid (DCA, Fig.4; 10) is a small molecule drug which exhibits its anti-cancer activity through inhibition of cellular respiration via the Warburg Effect<sup>1</sup>. This phenomenon, discovered in the 1920s by Otto Warburg, shows that glucose uptake in carcinoma cells is much greater than in the surrounding tissue<sup>43</sup>. There are two main processes through which glucose is broken down in cells; oxidative phosphorylation (aerobic) and glycolysis (anaerobic). In healthy cells, the balance is tipped in favour of oxidative phosphorylation, as there is usually an abundance of oxygen with which glucose can be oxidised to CO<sub>2</sub>. In cells starved of oxygen, glucose is partially oxidised to lactate via glycolysis.

However, Warburg and his colleagues noticed that in cancer cells, the balance was tipped in the opposite direction, and glucose was converted to lactate even in aerobic environments. This 'aerobic glycolysis' was termed the 'Warburg Effect'. Many benefits of this effect have been proposed for cancer cells, however none are yet proven<sup>44</sup>. Nevertheless, it is an attractive target for anti-cancer drugs.

DCA inhibits PDK (Pyruvate dehydrogenase kinase), an enzyme which phosphorylates, and subsequently inactivates, PDHC (Pyruvate dehydrogenase complex), another enzyme involved in cellular respiration. Its inactivation results in a preference for aerobic glycolysis: the Warburg Effect, which in turn stops the suppression of apoptosis in mitochondria. Through inhibition of PDK, cellular respiration can continue as normal, the Warburg Effect is reversed, and cancer cells cannot survive<sup>1</sup>.

One of the first compounds to combine DCA and a platinum based anti-cancer drug was mitaplatin, or cis,cis,trans-diamminedichloridobis(dichloroacetato) platinum(IV) (Fig.4; 4)<sup>45</sup>. Upon intracellular reduction, the cisplatin core attacks nuclear DNA whilst the DCA targets mitochondrial DNA, triggering apoptosis. However, in addition to its favourable cytotoxicity profile, there is evidence that mitaplatin is selective for cancer cells, leaving healthy cells untouched<sup>45</sup>.

Studies of dual and triple action anti-cancer drugs have found that the most promising compounds usually contain at least one DCA ligand. Petruzzella et. al<sup>1</sup> found that, in a study of triple action drugs containing HDACi, COXi and PDKi ligands, the drug with the best activity contained one DCA and one PhB ligand. Similarly, in a study on kiteplatin prodrugs containing DCA ligands, Savino et. al<sup>46</sup> found that a drug consisting of a kiteplatin scaffold (Fig. 4; 5) with two axial DCA ligands was most active. In a separate study, Petruzzella et. al. found that

combination of PhB, DCA, cisplatin and Pt56MeSS (a derivative of cisplatin, Fig.4; 6)) was significantly more potent, and showed good activity against highly aggressive cancers, than related dual action prodrugs<sup>48</sup>. This synthesis of a quadruple action platinum anti-cancer drug opens another avenue in cancer research, which has the potential to treat very aggressive cancers by targeting multiple aspects of their mode of action.

## Conclusions

Despite a wealth of studies and the range of potential ligands for these dual action drugs, only a handful are in clinical trials and very few have any real potential as clinical anti-cancer drugs; satraplatin showed initial promise but was halted in Phase III trials as its activity levels showed little improvement on those of cisplatin. In addition to the general disadvantages associated with oral drugs (patient compliance, low or variable oral availability, potential interaction with food and other drugs), many of these bifunctional drugs have been used against Malignant Pleural Mesothelioma (MPM); a cancer which is notoriously difficult to treat<sup>47</sup>. Therefore, dual action drugs may be more successful against less sophisticated cancers; although it is likely that treatments for these diseases already exist.

Although this field of anticancer medicine is incredibly active and shows great promise, further investigation into ligand-platinum interactions are required before a drug to rival cisplatin will emerge. Until then, cisplatin will remain as king of platinum-based cancer therapy.

## References

1. Petruzzella E, Sirota R, Solazzo I, Gandin V, Gibson D. Triple action Pt(IV) derivatives of cisplatin: a new class of potent anticancer agents that overcome resistance, *Chem Sci*, 2018, 9(18), 4299-307
2. Tolan D, Gandin V, Morrison L, El Nahas A, Marzano C, Montagner D, Erxleben A. Oxidative Stress induced by Pt(IV) prodrugs based on the cisplatin scaffold and indole carboxylic acids in axial positions, *Sci Rep*, 2016, 6, 29367-380
3. From Basic Research to Cancer Drug: the story of Cisplatin; <https://www.the-scientist.com/news/from-basic-research-to-cancer-drug-the-story-of-cisplatin-56412> (Accessed 11/7/18)
4. Alderden RA, Hall MD, Hambley TW. The Discovery and Development of Cisplatin, *J. Chem. Edu*, 2006, 83(5), 728-34
5. Rosenberg B, VanCamp L, Trosko JE, Mansour VH. Platinum compounds: A new class of potent antitumour agents, *Nat.*, 1969, 222, 385-386
6. Razaque MS, Taguchi T. Cisplatin Associated Nephrotoxicity and Pathological Events, *Contrib. Nephrol.*, 2005, 148, 106-120
7. Johnstone TC, Suntharalingam K, Lipard SJ. The Next Generation of Platinum Drugs: Targeted Pt(II) agents, nanoparticle delivery and Pt(IV) prodrugs, *Chem Rev.*, 2016, 116(5), 3436-3486
8. Alderden RA, Hall MD, Hambley TW. The Discovery and development of Cisplatin, *J. Chem. Edu*, 2006, 83(5), 728-34

9. Tucker MA, Colvin CB, Martin DS. Substitution reactions of trichloroammine-platinate (II) ion and the trans effect, *Inorg. Chem.*, 1964, 3(10), 1373-83
10. Colvin CB, Gunther RG, Hunter LD, McLean JA, Tucker MA, Martin DS. Kinetics of ammoniation of the chloro-ammine series of Pt (II) complexes, *J. Inorg. Chim. Acta.*, 1968, 2, 486-6
11. Bernen-Price SJ, Kuchel PW. Reaction of cis and trans [PtCl<sub>2</sub>(NH<sub>3</sub>)<sub>2</sub>] with reduced glutathione inside human red blood cells, studied by <sup>1</sup>H and <sup>15</sup>N –(1H) NMR, *J. Inorg. BioChem.*, 1990, 38
12. Eren G, Emerce E, Acik L, Aydin B, Gumus F. A novel Trans-Pt(II) complex bearing 2-acetoxymethylbenimidazole as a non-leaving ligand (trans-[Pt(AMBi)-2Cl<sub>2</sub>]: Synthesis, antiproliferative activity, DNA intercalation and molecular docking studies compared with its cis isomer (cis-[Pt(AMBi)2Cl<sub>2</sub>]), *J. Mol. Struct.*, 2019, 1184, 512-18
13. Jomaa M, Altaf M, Isab A. (2019) Method for inhibiting cancer cell growth with a transplatin complex. 10172823
14. Barbas K, Milner R, Lurie D, Adin C. Cisplatin: a review of toxicities and therapeutic applications, *Vet. Comp. Oncol.*, 2008, 6(1), 1-18
15. Miller RP, Tadagavadi RK, Ramesh G, Reeves WB. Mechanisms of Cisplatin Nephrotoxicity, *Toxins*, 2010, 2(11), 2490-2518
16. Yao X, Panichpisal K, Kurtzman N, Nugent K. Cisplatin Nephrotoxicity: a review, *Am. J. Med. Sci.*, 2007, 334(2), 115-124
17. Longley DB, Johnston PG. Molecular mechanisms of drug resistance, *J. Pathol.*, 2005, 205(2), 275-292
18. Almotiary ARZ, Gandin V, Morrison L, Marzano C, Montagner D, Erxleben A. Antitumour platinum (IV) derivatives of carboplatin and the histone deacetylase inhibitor 4-phenylbutyric Acid, *J. Inorg. BioChem.*, 2017, 177(1), 1-7
19. Gabano E, Ravera M, Zanellato I, Tinello S, Gallina A, Rangone B, Gandin V, Marzano C, Bottone MG, Osella D. An unsymmetric cisplatin based Pt(IV) derivative containing 2-(2-propynyl)octanoate: a very efficient multi-action anti-tumour prodrug candidate, *Dalton Trans.*, 2017, 46(41), 14174-14186
20. Halsall JA, Turner BM. Histone deacetylase inhibitors for cancer therapy: An evolutionary ancient resistance response may explain their limited success, *Bioessays.*, 2016, 38(11), 1102-1110
21. Li Y, Seto E, HDACs and HDAC Inhibitors in Cancer Development and Therapy, *Cold Spring Harb. Perspect. Med.*, 2016, 6(10)
22. DrugBank: Phenylbutyrate [Internet], Canada, 2010 [updated: 2018 November 5; cited January 2019]
23. DrugBank: Valproic Acid/ Valproate [Internet], Canada, 2005 [updated: 2019 March 2; cited January 2019]
24. National Centre for BioTechnology Information: PubChem: 2-hexyl-4-pentynoic acid [Internet], MD, USA, (no date)
25. Leng Y, Marinova Z, Reis-Fernandes MA, Nau H, Chuang DM. Potent neuroprotective effects of novel structural derivatives of valproic acid: potential roles of HDAC inhibition and HSP70 induction, *NeuroSci. Lett.*, 2010, 476(3), 127-132
26. Deubzer H, Busche B, Ronndahl G, Eikel D, Michaelis M, Cinatl J, Schulze S, Nau H, Witt O. Novel valproic acid derivatives with potent differentiation-inducing activity in myeloid leukemia cells, *Leuk. Res.*, 2006, 30, 1167-1175
27. Yang j, Sun X, Mao W, Sui M, Tang J, Shen Y. Conjugate of Pt(IV) – histone deacetylase inhibitor as a prodrug for cancer chemotherapy, *Mol. Pharmaceutics.*, 2012, 9(10), 2793-2800
28. Alessio M, Zanellato I, Bonarrigo L, Gabano E, Ravera M, Osella D. Antiproliferative activity of Pt(IV)-bis (carboxylato) conjugates on malignant pleural mesothelioma

- cells, *J. InOrg. BioChem.*, 2013, 129, 52-57
29. Gibson D. Platinum (IV) anticancer prodrugs – hypotheses and facts, *Dalton. Trans.*, 2016, 45(33), 12983-12991
30. Kelland LR, Abel G, McKeage MJ, Jones M, Goddard PM, Valenti M, Murrer BA, Harrag KR. Preclinical antitumour evaluation of bis-acetato-ammine-dichloro-cyclohexylamine platinum (IV): an orally active platinum drug, *Cancer. Res.*, 1993, 53, 2581-2586
31. Choy H. Satraplatin: an orally available platinum analog for the treatment of cancer, *Expert. Rev. AntiCancer. Ther.*, 2006, 6, 973-982
32. Kelland LR. An update on satraplatin: the first orally available platinum anticancer drug, *Exp. Opin. Invest. Drugs.*, 200, 9, 1373-1382
33. DrugBank: Vincristine [Internet], Canada, 2005, [updated: 2019 March 2; cited January 2019]
34. Drugbank: Vinblastine [Internet], Canada, 2005, [updated: 2019 March 2; cited January 2019]
35. DrugBank: Vinorelbine [Internet], Canada, 2005, [updated: 2019 March 2; cited January 2019]
36. DrugBank: Vindesine [Internet], Canada, 2005, [updated: 2019 March 2; cited January 2019]
37. X. Li, Y. Liu, H. Tain, Current Developments in Pt(IV) prodrugs conjugated with bioactive ligands, *Bio. Chem. Appl.*, 2018
38. Huang X, Huang R, Gou S, Wang Z, Liao Z, Wang H. Platinum (IV) complexes conjugated with phenstatin analogue as inhibitors of microtubule polymerization and reversers of multi-drug resistance, *Bio-organic. Med. Chem.*, 2017, 25(17), 4686-4700
39. Huang X, Huang R, Wang Z, Li L, Gou S, Liao Z, Wang H. Pt (IV) complexes conjugated with chalcone analogue as inhibitors of microtubule polymerization exhibited selective inhibition in human cancer cell lines, *Eur. J. Med. Chem.*, 2018, 146, 435-450
40. Huang X, Huang R, Gou S, Wang Z, Liao Z, Wang H. Combretastatin A-4 analogue: a dual targeting and tubulin inhibitor containing antitumour Pt(IV) moiety with a unique mode of action, *Bioconjugate. Chem.*, 2016, 27(9), 2132-2148
41. Huang X, Hua S, Huang R, Liu Z, Gou S, Wang Z, Laio Z, Wang H. Dual targeting antitumour hybrids derived from Pt(IV) species and millepachine analogues, *Eur. J. Med. Chem.*, 2018, 148, 1-25
42. Patil R, Patil SA, Beaman KD, Patil SA. Indole molecules as inhibitors of tubulin polymerization: potential new anticancer agents; an update (2013-2015), *Future Med. Chem.*, 2016, 8(11), 1291-1316
43. Warburg O, The Metabolism of Carcinoma Cells, *J. Cancer. Res.*, 1925, 9, 148-163
44. Liberti MV, Locasale JW. The Warburg Effect: how does it benefit cancer cells? *Trends. Biochem. Sci.*, 2016, 41(3), 211-218
45. Dhar S, Lippard SJ. Mitaplatin, a potent fusion of cisplatin and the orphan drug dichloroacetate, *Proc. Natl. Acad. Sci.*, 2009, 106(52), 22199-22204
46. Savino S, Gandin V, Hoeschele JD, Marzano C, Natile G, Margiotta N. Dual Action antitumour Pt (IV) prodrugs of kiteplatin with dichloroacetate axial ligands, *Dalton Trans.*, 2018, 47(21), 7144
47. Gabano E., Ravera M., Osella D. Pros and Cons of bifunctional platinum (IV) antitumour prodrugs: two are (not always) better than one, *Dalton Trans.*, 2014, 43(26), 9813-9820
48. Petruzzella E, Braude JP, Aldrich-Wright JR, Gandin V, Gibson D. A Quadruple action Platinum (IV) prodrug with anticancer activity against KRAS mutated cancer cell lines, *Angew. Chem. Int. Ed.*, 2017, 56(39), 11697-11702

TS  
SR

# PHOTON UPCONVERSION BY TRIPLET PHOTOSENSITISER COMPLEXES

Luke Doolan

Junior Sophister

Nanoscience, Physics and Chemistry of Advanced Materials

*Due to the high cost of production of silicon based solar cells, new cheaper forms of solar cells are being investigated. These new forms of solar cells often do not have as low a band gap as silicon based solar cells and so are unable to absorb lower energy light, causing them to be less effective. To counteract this problem photon upconversion is being investigated; that is the conversion of two low energy photons to one photon of higher energy. The most promising method of achieving upconversion within solar cells currently, is by triplet-triplet annihilation, which requires molecules which are referred to as triplet photosensitisers; they can be made using heavy metal complexes as well as metal organic frameworks and complex organic molecules. This review explores the theoretical operation of upconversion by triplet-triplet annihilation and the development of metal complexes for use as triplet photosensitisers, focusing on the use of ruthenium, iridium and dinuclear complexes.*

## Introduction

Due to the large expense incurred in processing silicon a large amount of research is currently being done to create new forms of solar cells and to move away from p-n junction solar cells<sup>1</sup>. One of the most promising forms of these new types of photovoltaic cells are dye sensitised solar cells (DSSC). The main advantage presented by this new form of solar cell is the ability to absorb diffuse light<sup>2</sup> as well as their transparency, allowing them to be used as windows<sup>3</sup>. However, one of the main issues with these cells however is their relatively high band gap, which prevents the absorption of low energy light<sup>4</sup>. In order to counteract this problem, the upconversion of photons is being explored, that is the absorption of two photons by a system and the release of one photon of higher energy<sup>5</sup>. This process would allow for a greater number of photons to be absorbed by the cells, therefore increasing their efficiency<sup>6</sup>. There are four main methods by which photon upconversion can be achieved - two photon absorbing dyes, inorganic crystals, lanthanide ion-doped

$\text{NaYF}_4$ , and triplet photosensitisers which interact with acceptor molecules<sup>7</sup>. Triplet photosensitisers are molecules which can easily convert to their triplet state, and then convert another molecule to its triplet state. The first three of these methods require high light intensities, have low molar absorption coefficients for visible light and have low quantum yields, triplet photosensitisers, can be designed such that they do not suffer from these issues and are therefore the most commonly explored method for upconversion in solar cells<sup>8</sup>.

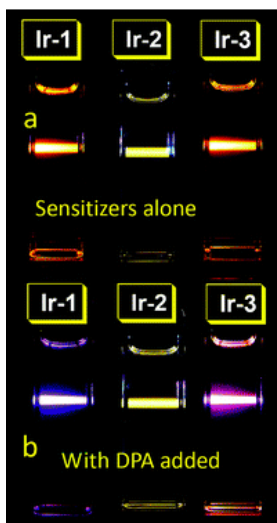
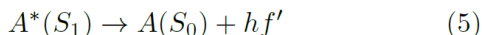
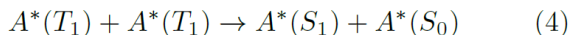
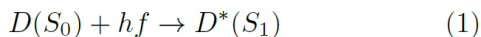


Figure 1: Image of the light emitted by a series of different triplet photosensitisers samples made using iridium complexes with and without an acceptor molecule present. The sample is being excited by 473 nm light<sup>9</sup>

Triplet photosensitisers can achieve upconversion by triplet-triplet annihilation (TTA)<sup>10</sup>. In these interactions the triplet photosensitiser molecule is referred to as the donor molecule and the other molecule which must be involved is referred to as the acceptor molecule. For a molecule to be able to convert to its triplet state a heavy atom or heavy moiety is usually required, heavy metal complexes are often used for this purpose, although organic groups such as fullerenes can also be used<sup>11</sup>. The triplet state is the state in which electrons, which were paired so that their spin was in opposite directions (called the singlet state), are now spinning in the same direction<sup>12</sup>. This is represented diagrammatically in Figure 2, by half arrows pointing up and down, when one arrow points up and one points down the molecule is in its singlet state and when the arrows point in the same direction the molecule is in its triplet state. Due to the change in spin of the electron the orbital it exists in when in its triplet state is different to that it is in when in its singlet state<sup>13</sup>. Conversion to the triplet state occurs by a process called intersystem crossing (ISC)<sup>14</sup>. ISC is caused by the magnetic field due to the relative motion of the nucleus, that the electrons experience. The effect of this field is a mixing of the singlet and triplet orbitals, which allows for the electron to change its spin

direction. The mixing of the orbitals is known as spin orbital coupling (SOC)<sup>15</sup>. It happens predominantly in heavy atoms, as the magnetic field experienced by the electron is dependent on the size of the positive charge in the nucleus to the power of 4<sup>16</sup>. When the donor molecule and the acceptor molecule are in solution together, and the donor molecule is in the triplet state it can collide with an acceptor molecule and the triplet state is exchanged between the molecules, this step is known as triplet-triplet energy transfer (TTET) or a Dexter electron transfer<sup>17</sup>. In a Dexter electron transfer an excited electron is transferred from an excited orbital in one molecule to an excited orbital in another molecule by orbital overlap<sup>18</sup>. The fourth step in this process is known as triplet-triplet annihilation (TTA). It involves the collision of two acceptor molecules causing another Dexter transfer to occur<sup>19</sup>, where one of the acceptor molecules is in its excited singlet state and the other is in its ground state<sup>20</sup>. The acceptor molecule can then decay from its excited singlet state with the release of a photon, if this photon is higher in energy than the originally absorbed photon then upconversion has occurred. An overview of the reaction scheme can be seen in the equations below and a diagrammatic representation can be seen in Figure 2.



Where  $D()$  is the donor molecule and  $A()$  is the acceptor molecule,  $S_0$  is the ground state,  $S_1$  is the first excited singlet state and  $T_1$  is the excited triplet state, \* denotes an excited state. If  $f' > f$  then upconversion is said to have occurred.

The donor molecules are designed so that the first excited singlet state is higher in energy than its first excited triplet state. Decay to the triplet state must occur from the first excited singlet state  $S_1$ , as according to Kasha's rule, a molecule will decay to its first excited state quickly by non-radiative means<sup>16</sup>. Therefore, conversion to the triplet state from any higher energy singlet state, is very unlikely. The molecules are also designed so that the first excited singlet state of the acceptor molecule is higher in energy, than  $S_1$  of the donor molecule, as this means that after the upconversion process has occurred the released electron will be of higher energy<sup>20</sup>.

The quantum yield of a process is the number of photons released by the process relative to the number of photons that would ideally be released by the process, it is therefore the measure of the effectiveness of the upconversion system. The quantum yield of the upconversion process is given by

$$\Phi_{UC} = \Phi_{ISC}\Phi_{TTET}\Phi_F \quad (6)$$

Where  $\Phi_{UC}$  is the quantum yield of the upconversion,  $\Phi_{ISC}$  is the quantum yield of the intersystem crossing,  $\Phi_{TTET}$  is the quantum yield of the triplet-triplet energy transfer and  $\Phi_F$  is the quantum yield of the fluorescence of the acceptor molecule<sup>21</sup>. In order to maximise these terms, the photosensitizer should have high molar absorbance coefficient in the visible and near infrared region<sup>22</sup>, long lived triplet lifetimes  $\tau$  in order to increase the chance of reaction 3 occurring<sup>23</sup> and a high ISC yield<sup>24</sup>. The triplet lifetime of a molecule is defined as the amount of time taken for the number of molecules in the triplet state to decay by  $e^{-1}$ <sup>25</sup>. The molecule also needs to be photochemically stable. One problem that has been encountered is that the acceptor molecule may absorb some of the upconverted photons, this reduces the measured upconversion quantum yield and therefore, the absorption spectrum of the acceptor must be designed to avoid this problem<sup>26</sup>.

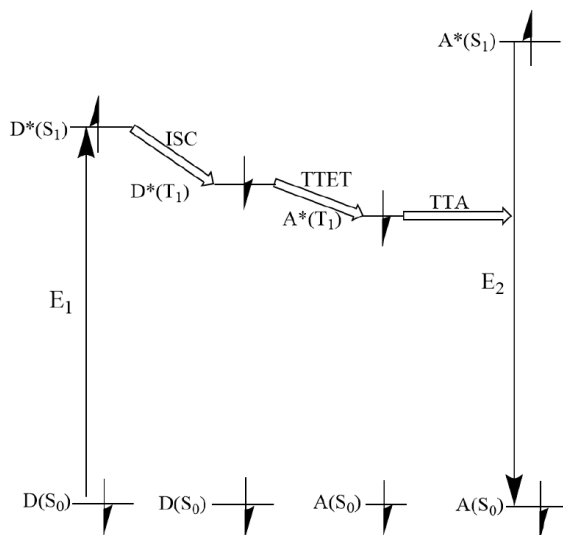


Figure 2: Energy diagram showing the path of an electron during upconversion. If  $E_1 < E_2$  then upconversion can have been said to occur. The half arrows represent the spin of the electrons involved, D is the donor molecule, A is the acceptor molecule, S denotes ground state, T denotes the triplet state and 0 and 1 denote the energy level of the electron relative to the highest occupied molecular orbital which is labelled as 0.

A large variety of donor and acceptor molecules have been synthesised for this process and I will now examine the research that lead to the design of more and more efficient molecules for this process. The donor molecules are predominantly being designed using Ru(II), Pt(II), Pd(II), Re(I) and Ir(III) complexes as these metals are heavy enough for ISC to occur at a useful rate<sup>24</sup>.

## Ruthenium Complexes

Attempts have been made to synthesise triplet photosensitiser systems with the metal centre acting as the donor and one of the ligands carrying an acceptor unit. This was first attempted by Kozlov et al, they reported the synthesis of a Ru(II) complex which can be seen in Figure 3, labelled as M1. This molecule was compared to a system with a ruthenium complex with the same ligands without the acceptor molecule attached to the ligand but instead in solution. The upconversion efficiency of the complex containing the acceptor molecule was 2.9 times lower than the separate donor acceptor system<sup>27</sup>. It was therefore concluded that the attachment of the acceptor molecule to the donor molecule leads to a reduction in the upconversion yield<sup>22</sup>. Both systems demonstrate low molar absorption in the visible region and are therefore not useful for application in photovoltaic cells.

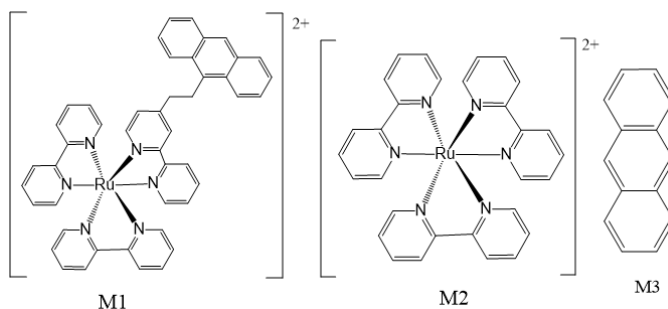


Figure 3: Image of two ruthenium complexes which act as triplet photosensitisers for photon upconversion, synthesised by Kozlov et al<sup>27</sup>, and an anthracene molecule, which acts as the acceptor molecule in the photon upconversion of M2

Tyson et al have found that the use of ethynyl linkers within the ligands can cause a large increase in the triplet lifetime of the molecule. The two ligands shown in Figure 4 were synthesised, in which the only difference between them is a C-C triple bond. These ligands were then used to form ruthenium complexes. The complex without the ethynyl linker (M4) had a triplet lifetime of 148  $\mu\text{s}$ <sup>28</sup>. Upon addition of the ethynyl linker the triplet lifetime of the molecule increased to 270  $\mu\text{s}$ <sup>29</sup>, which was the longest reported triplet lifetime of a Ru(II) based dyad up to 2013<sup>22</sup>. This suggests that the addition of an ethynyl linker increases the triplet lifetime of the molecule considerably. The pyrene groups were attached to the molecule in order to increase its absorption of visible light, the light absorbed by this system however was of a high frequency and absorption of light in the visible region was still weak<sup>22</sup>, therefore these molecules are not useful for applications in upconversion.

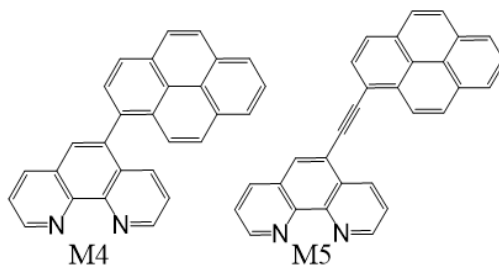


Figure 4: Image of the ligands used in the creation of a triplet photosensitiser, where ruthenium(II) is the metal centre and the ligands act as bidentate ligands which nitrogen as the donor atom, synthesised by Tyson et al. Each ruthenium ion has 3 of these ligands bonded to it in an octahedral geometry and has a charge of +2.

In order to increase the absorption of visible light by the complexes, Galleta et al attached a derivative of the dye boron-dipyrromethene (BODIPY), which demonstrates high molar absorption coefficients<sup>32</sup>. Terpyridine ligands were also complexed forming M6, however, the molecules formed had very short triplet lifetimes with a maximum at 30  $\mu$ s, and did not function well as triplet photosensitisers<sup>30</sup>.

Wu et al attempted a similar process altering slightly the manner in which the BODIPY was bonded to the ligands and using bipyridine units to form the ligands. The two complexes synthesised can be seen in Figure 5 as M7 and M8. These molecules had a strong absorption of visible light showing a maximum molar absorbance coefficient ( $\epsilon$ ) of 76,700  $M^{-1}cm^{-1}$  for M7 at  $\lambda = 499$  nm. M8 had the larger triplet lifetime at 279.7  $\mu$ s. This led to an overall quantum yield of 1.2% for M6 and 0.7% for M7, calculated using perylene as the acceptor molecule<sup>31</sup>. Although this yield is quite low, the high absorption value demonstrates the improvement in absorption that the addition of dyes as ligands can provide.

## Iridium Complexes

Coumarin is a group of benzopyrone based dyes<sup>35</sup> that have been examined as a possible ligand for iridium complexes to increase their absorption of visible light. Murata et al used coumarin 6 as a ligand directly for iridium complexes and these complexes showed very high absorption values ( $\epsilon = 129,000 M^{-1}cm^{-1}$  at  $\lambda = 483$  nm)<sup>36</sup>; however, no evidence of these complexes being used for triplet photosensitisers could be found. Sun et al added a variety of coumarin derivative to a phenanthroline ligand which can be seen in Figure 8. These molecules showed strong absorption in the visible region, notably M9, had a maximum absorption value of  $\epsilon = 70,920 M^{-1}cm^{-1}$  at  $\lambda = 466$  nm, a triplet lifetime of 75.5  $\mu$ s leading to an upconversion quantum yield of 21.6% using diphenylamine (DPA) as the acceptor,

while M10 had a maximum absorption value of  $\epsilon = 64,170 \text{ M}^{-1}\text{cm}^{-1}$  at  $\lambda = 418 \text{ nm}$  and had a triplet lifetime of  $73.6 \mu\text{s}$  and a quantum yield of 23.4% using DPA as the acceptor molecule<sup>37</sup>. Despite its higher quantum yield M10 might be less useful for photovoltaic applications due to its absorption of lower wavelength light.

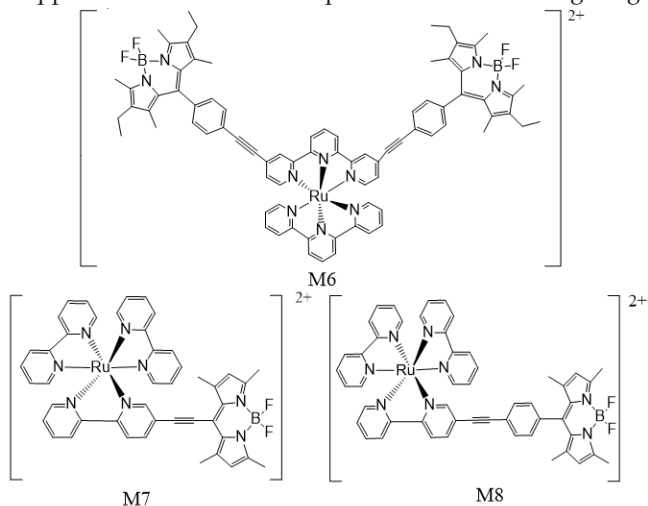


Figure 5: Ruthenium complexes, in which BODIPY units were attached to the ligand(s) in order to increase the absorption of light. M6 was synthesised by Galleta et al<sup>30</sup>, and M7 and M8 were synthesised by Wu et al<sup>31</sup>.

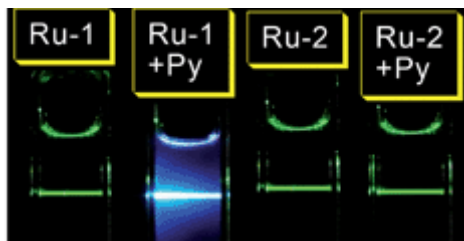


Figure 6: Image of some of the complexes in Figure 5 acting as upconverters, where Ru-1 is M7, Ru-2 is M8 and py is pyrene, which acts as an acceptor molecule. The complexes are being excited with 532 nm light<sup>31</sup>.

Yue et al synthesised the molecule which is labelled as M11 in Figure 7. The molecule had a maximum absorbance value of  $\epsilon = 50,900 \text{ M}^{-1}\text{cm}^{-1}$  at 490 nm and has a triplet lifetime of  $53.3 \mu\text{s}$ . Despite these relatively low values the molecule had an upconversion quantum yield of 28.1% using DPA as the acceptor molecule. Computational calculations showed that the triethylamine molecule made very little contribution to the photophysical properties of the molecule<sup>33</sup>. In order to further increase the upconversion yield, experiments were carried out with the

triethylamine group removed, in M12 it was not replaced and in M13 it was replaced with a pyrene molecule as can be seen in Figure 7. M13 had the larger maximum absorption value of  $52,400 \text{ M}^{-1}\text{cm}^{-1}$  at 481 nm. M12 had the larger triplet lifetime of 136.1  $\mu\text{s}$ . This led to M12 having an upconversion yield of 30.2% and M13 having a yield of 31.6% both calculated using DPA as the acceptor<sup>34</sup>. The high yield achieved by these molecules suggest that they could have potential applications as upconverters in photovoltaic cells. These ligands were also attached to ruthenium complexes, however much lower values for the upconversion yield were achieved with a maximum value of 14.7% recorded for M12, when the iridium atom replaced with a ruthenium atom<sup>39</sup>. This demonstrates the importance of matching the ligand used to the metal centre in order to achieve the maximum possible upconversion yield, which is a key concept in coordination chemistry. It also demonstrates the increase in the upconversion that can be achieved through the use of a heavier metal centre.

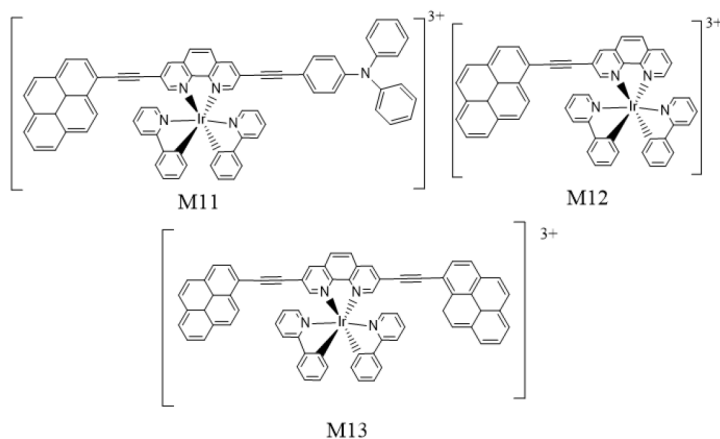


Figure 7: Iridium complexes with a variety of ligands based on 1,10-phenanthroline. Synthesised by Yue et al<sup>33, 34</sup>

## Dinuclear Complexes

It has been demonstrated that using bridged ruthenium complexes increases the triplet lifetime of the molecule<sup>41</sup>. A bridged complex is a complex in which one or more of the ligands is attached to two metal centres<sup>42</sup>. Wang et al synthesised bridged complexes using both iridium and ruthenium which can be seen in Figure 9. Both of these complexes showed have high molar absorption coefficients at higher wavelengths than the previously mentioned complexes. M14 had the largest absorption at  $\epsilon = 113,000 \text{ M}^{-1}\text{cm}^{-1}$  at 570 nm. The molecules also had very long triplet lifetimes, with M14 having a triplet lifetime of 1,316  $\mu\text{s}$ . These molecules also

showed very high upconversion yield with M14 having a yield of 19.1% and M15 having a yield of 25.5%, which was the highest yield reported for any molecule based on BODIPY, at the time of publishing<sup>38</sup>.

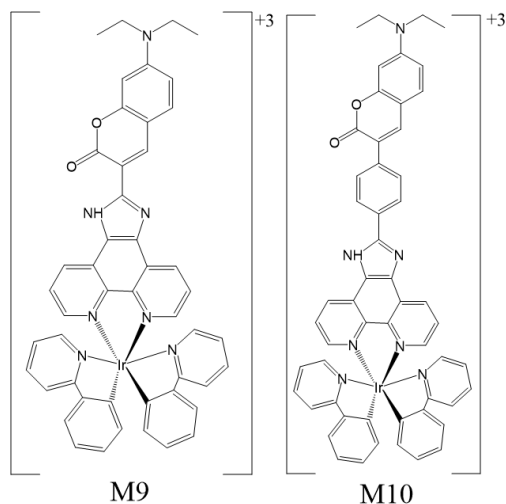


Figure 8: Iridium complexes in which coumarin was used as a ligand to increase the absorption of light. The complexes were synthesised by Sun *et al*<sup>37</sup>.

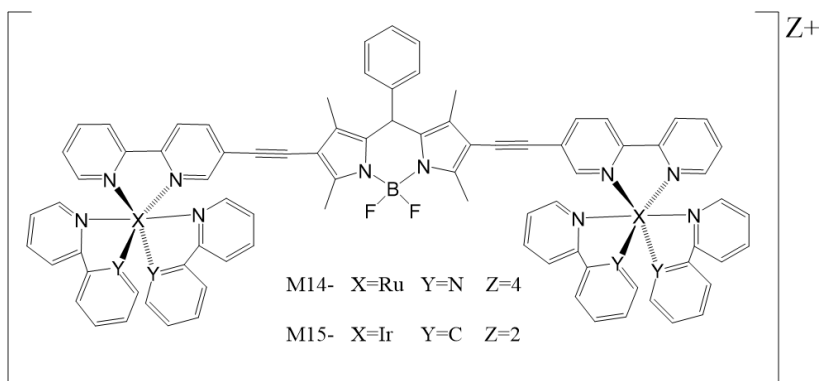


Figure 9: Dinuclear metal complexes, in which the metal centre is either ruthenium or iridium and the nature of the ligands depends on the metal centre chosen. Synthesised by Wang *et al*<sup>38</sup>.

Further tests were carried out by the Draper group to quantify the effects that bridging had on the photosensitisers, bridged complexes based on nitrogen substituted carbazole ligands were formed as were their mononuclear contemporaries, the molecules can be seen in Figure 10. The bridged complexes both had higher molar absorption coefficients and a lower triplet lifetime than

the mononuclear compounds, all of the values were lower than the previously synthesised dinuclear complexes. The bridged ruthenium complex had a higher quantum upconversion yield than the mononuclear complex, 21.6% vs 19.1% while the bridged iridium complex had a lower quantum upconversion yield than the mononuclear complex, 15.3% vs 19.0%, when the yields were measured using DPA<sup>40</sup>. This suggests that there is no well-defined relationship between the number of metal centres in a complex and its upconversion quantum yield. In all cases however the dinuclear complexes had a greater molar absorption coefficient, suggesting that dinuclear complexes can be used for highly efficient quantum upconversion if suitable ligands can be synthesised.

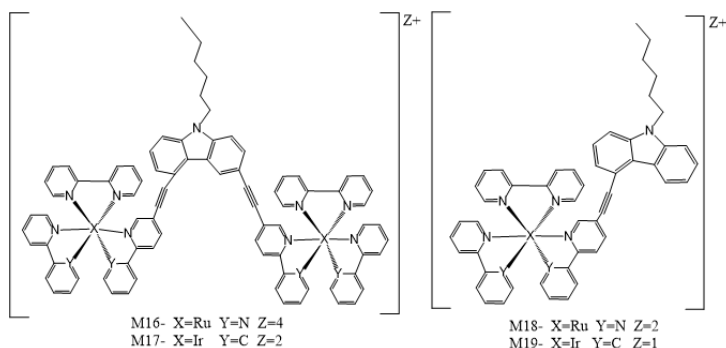


Figure 10: Dinuclear metal complexes, in which the metal centre is either ruthenium or iridium and the nature of the ligands depends on the metal centre chosen. Synthesised by Wang *et al*<sup>40</sup>.

## Conclusions

An overview of the development of metal complexes which act as triplet photosensitisers has been given in this review as well as an examination of their potential application for upconversion. There is a great deal of promising work being done in this field leading to large improvements in the efficiency of the upconverters being synthesised. It should be noted however that all reported upconversion yields are given for measurements taken in solution and that in order to use these molecules for practical applications, they must be capable of functioning in the solid state, rubbery polymers are currently being investigated for this purpose [20]. The use of coumarin based iridium complexes as well as the use of dinuclear complexes does however seem promising as both of these methods can provide high upconversion efficiency. It should be noted, however, that triplet photosensitisers not composed of expensive heavy metals are also being investigated and that future advances may lie in this area [11].

On top of the application discussed here triplet photosensitisers can also be used for singlet oxygen sensing [43], photoinduced hydrogen production from water,

photocatalytic organic reactions and photodynamic therapy [10].

## Acknowledgements

I would like to thank Prof. Draper and the members of her group. Their help was invaluable during in the writing of this review.

## References

1. Jacoby M. The future of low-cost solar cells. *CENEAR*, 94:30–35, 2016.
2. Lee C., Lin C., Wei T., Tsai M., Meng Y., Li C., Ho K., and Wu C. Economical low light photovoltaics by using the Pt-free dye-sensitized solar cell with graphene. *Nano Energy*, 18:109–117, 2015.
3. Yoon S., Tak S., Kim J., Jun Y., Kang K., and Park J. Application of transparent dye-sensitized solar cells to building integrated photovoltaic systems. *Build Environ*, 46:1899–1904, 2011.
4. Lee Y., Chae J., and Kang M. Comparison of the photovoltaic efficiency on DSSC for nanometer sized TiO<sub>2</sub> using a conventional sol-gel and solvothermal methods. *Ind. Eng. Chem. Res.*, 16:609–614, 2010.
5. Ceroni P. Energy up conversion by low polar excitation: New applications of an old concept. *Chem. Eur. J.*, 17:9560–9564, 2011.
6. Guo X., Liu Y., Chen Q., Zhao D., and Ma Y. New Bichromophoric Triplet Photosensitizer Designs and Their Application in Triplet-Triplet Annihilation Upconversion. *Adv. Opt. Mater.*, 17, 2018.
7. Goldschmidt J.C. and Fischer S. Upconversion for Photovoltaics – a Review of Materials, Devices and Concepts for Performance Enhancement. *Adv. Opt. Mater.*, 3:510–535, 2015.
8. Zhao J, Ji S., and Guo H. Triplet-triplet annihilation based upconversion: from triplet sensitizers and triplet acceptors to upconversion quantum yields. *RSC Adv.*, 1:937–950, 2011.
9. Ma L., Guo H., Li Q., Guo S., and Zhao J. Visible light-harvesting cyclometalated Ir(III) complexes as triplet photosensitizers for triplet-triplet annihilation based upconversion. *Dalton Trans.*, 41: 10680–10689, 2011.
10. Zhao J., Wu W., Sun J., and Guo S. Triplet photosensitizers: from molecular design to applications. *Chem. Soc. Rev.*, 42:5323–5351, 2013.
11. Wu W., Zhao J., Sun J., and Guo S. Light-Harvesting Fullerene Dyads as Organic Triplet Photosensitizers for Triplet Triplet Annihilation Upconversions. *J. Org. Chem.*, 77:5305–5312, 2012.
12. Lewis G. and Kasha K. Phosphorescence and the triplet state. *J. Am. Chem. Soc.*, 66:2100–2116, 1944.
13. Hehre W.J., Pople J.A., Wasserman E. Lathan W.A., and Radom L., and Wasserman Z.R. Molecular Orbital Theory of the Electronic Structure of Organic Compounds. 28. Geometries and Energies of Singlet And Triplet States of the C<sub>3</sub>H<sub>2</sub> Hydrocarbons. *J. Am. Chem. Soc.*, 98:4378–4383, 1976.
14. N.J. Turro, J. C. Sciaiano, and V. Ramamurthy. Principles of Molecular Photochemistry: An Introduction. "The University of Chicago Press", 2009.
15. Khudyakov I.V., Serebrennikov Y.A., and Turro N.J. Spin-Orbit Coupling in Free-Radical Reactions: On the Way to Heavy Elements. *Chem. Rev.*, 93:537–570, 1993.

16. Marian C.H. Spin-orbit coupling and intersystem crossing in molecules. *WIREs Comput. Mol. Sci.*, 2: 187–203, 2011.
17. Beiri O., Hellrung B. Wirz J., Schutkowski M., Drewello M., and Kieffhaber T. The speed limit for protein folding measured by triplet-triplet energy transfer. *Proc. Natl. Acad. Sci. U.S.A.*, 17: 9597–9601, 1999.
18. Soler M. and McCusker J.K. Distinguishing between Dexter and Rapid Sequential Electron Transfer in Covalently Linked Donor-Acceptor Assemblies. *J. Am. Chem. Soc.*, 130:4707–4724, 2008.
19. Monguzzi A., Tubino R., Hoseinkhani S., Campione M., and Meinardi F. Low power, non-coherent sensitized photon up-conversion: modelling and perspectives. *Phys. Chem. Chem. Phys.*, 14:4322–4332, 2012.
20. Singh-Rachford T.N. and Castenello F.N. Photon upconversion based on sensitized triplet-triplet annihilation. *Coord. Chem. Rev.*, 254:2560–2573, 2010.
21. Zhao J., Ji S., and Guo H. Triplet-triplet annihilation based upconversion: from triplet sensitizers and triplet acceptors to upconversion quantum yields. *RSC Adv.*, 1:937–950, 2011.
22. J. Wang. In search of strong light-harvesting and long-lived Ru (II) and Ir(III) triplet photosensitizer [PhD thesis]. "Trinity College Dublin. School of Chemistry. Discipline of Chemistry", 2018.
23. Zhao J., Ji S., Wu W., Wu W., Guo H., Sun J., Sun H., Liu Y., Li Q., and Huang L. Transition metal complexes with strong absorption of visible light and long-lived triplet excited states: from molecular design to applications. *RSC Adv.*, 2:1712–1728, 2012.
24. Zhao J., Wu W., Ji S., and Guo S. Triplet photosensitizers: from molecular design to application. *Chem. Soc. Rev.*, 42:5323–5351, 2013.
25. Clark W.D.K., Litt A.D., and Steel C. Triplet lifetimes of benzophenone, acetophenone, and triphenylene in hydrocarbons. *J. Am. Chem. Soc.*, 491:5413–5415, 1969.
26. Guo X, Liu Y, Zhao D., and Ma Y. New Bichromophoric Triplet Photosensitizer Designs and Their Application in Triplet-Triplet. *Adv. Opt. Mater.*, 6:1700981, 2018.
27. Kozlov D.V. and Castellano F.N. Anti-Stokes delayed fluorescence from metal-organic bichromophores. *Chem. Commun.*, 0:2860–2861, 2004.
28. Tyson D.S., Bialecki J., and Castellano F.N. Ruthenium(II) complex with a notably long excited state lifetime. *Chem. Commun.*, 0:2355–2356, 2000.
29. Mari C., Pierroz V., Ferrari S., and Gasser G. Exploitation of Long-Lived 3 IL Excited States for Metal-Organic Photodynamic Therapy: Verification in a Metastatic Melanoma Model. *Chem. Sci.*, 6: 2660–2686, 2015.
30. Galleta M., Campagna S., Quesada M., Ulrich G., and Ziessel R. The elusive phosphorescence of pyromethene-BF2 dyes revealed in new multicomponent species containing Ru(II)-terpyridine subunits. *Chem. Commun.*, 0:4222–4224, 2005.
31. Wu W., Sun J., Cui X., and Zhao J. Observation of the room temperature phosphorescence of Bodipy in visible light-harvesting Ru(II) oylimine complexes and application as triplet photosensitizers for triplet-triplet-annihilation upconversion and photocatalytic oxidation. *J. Mater. Chem. C*, 1: 4577–4589, 2013.
32. Gabe Y., Uen T., Urano Y., Kojima H., and Nagano T. Tunable design strategy for fluorescence probes based on 4-substituted BODIPY chromophore: improvement of highly sensitive fluorescence probe for nitric oxide. *Anal. Bioanal. Chem.*, 3:621–626, 2006.
33. Lue Y. and et al. Highly Efficient Triplet Photosensitizers: A Systematic Approach to the Application of Ir(III) Complexes containing Extended Phenanthrolines. *Chem. Eur. J.*, 22:11349–11356, 2016.
34. Lue Y. and et al. Iridium(III) Complexes Bearing Pyrene-Functionalized 1,10-Phenanthroline Ligands as Highly Efficient Sensitizers for Triplet-Triplet

- Annihilation Upconversion. *Angew. Chem.*, 55: 14688–14692, 2016.
35. Takiwaza S., Ikuta N., Zeng F., Komaru S., Sebata S., and Murata S. Impact of Substituents on Excited-State and Photosensitizing Properties in Cationic Iridium(III) Complexes with Ligands of Coumarin 6. *Inorg. Chem.*, 55:8723–8735, 2016.
36. Takiwaza S., Pérez-Bolívar C., Anzenbacher P., and Murata S. Cationic Iridium Complexes Coordinated with Coumarin Dyes – Sensitizers for Visible-Light-Driven Hydrogen Generation. *Eur. J. Inorg. Chem.*, 25:3975–3979, 2012.
37. Sun J., Wu W., Guo H., and Zhao J. Visible-Light Harvesting with Cyclometalated Iridium(III) Complexes Having Long-Lived  $^3\text{IL}$  Excited States and Their Application in Triplet-Triplet-Annihilation Based Upconversion. *Eur. J. Inorg. Chem.*, 21: 3165–3173, 2011.
38. Wang J., Lu Y., McGoldrick N., Zhang C., Yang W., Zhao J., and Draper S.M. Dual phosphorescent dinuclear transition metal complexes, and their application as triplet photosensitizers for TTA upconversion and photodynamic therapy. *J. Mater. Chem. C*, 4:6131–6139, 2016.
39. Lu Y., Conway-Kenny R., Twamley B., McGoldrick N., Zhao J., and Draper S.M. 1,10-Phenanthroline Ruthenium(II) Complexes as Model Systems in the Search for High-Performing Triplet Photosensitisers: Addressing Ligand versus Metal Effects. *ChemPhotoChem.*, 1:544–552, 2017.
40. Wang J., Lu Y., Conway-Kenny R., Twamley B., Zhao J., and Draper S.M. Novel ruthenium and iridium complexes of N-substituted carbazole as triplet photosensitisers. *Chem. Commun.*, 54:1073–1076, 2018.
41. Harriman A., Khatyr A., and Ziessel R. Extending the luminescence lifetime of ruthenium(II) poly(pyridine) complexes in solution at ambient temperature. *Dalton Trans.*, 0:2061–2068, 2003.
42. Shaw J.R., Webb R.T., and Schmehl R.H. Intersystem Crossing to both Ligand-Localized and Charge-Transfer Excited States in Mononuclear and Dinuclear Ruthenium(II) Diimine Complexes. *J. Am. Chem. Soc.*, 112:1117–1123, 1990.
43. Pinero M., Carvalho A.L., Pereira M.M., Gonsalves A.M.D., Arnaut L.G., and Formosinho S.J. Photoacoustic Measurements of Porphyrin Triplet-State Quantum Yields and Singlet-Oxygen Efficiencies. *Chem. Eur. J.*, 4:2299–2307, 1998.

TS  
SR



# Physics

TS  
SR

## Letter from the Editor

Today's society has been blighted by the spread of false information. Whether this stems from political motives or ignorance is to some extent irrelevant. What is more important than ever though, is the greater promotion of knowledge and opinions based on facts and evidence. With over 2.5 million scientific papers being published each year, it has become a near impossible task to filter out the good from the bad. That is why I believe that the TSSR and other student run journals like it are invaluable to our college community. Reviews are a great way of condensing down the vast amount of knowledge found in the towering number of publications.

I am proud to be a part of a journal that ensures scientific integrity. We aim to give students the opportunity to improve their writing skills, develop their critical thinking and give them their first experience of scientific journalism. Beyond this, we want to give students a platform for scientific discussion that will hopefully spread out further into the wider college community as a whole.

This year was a busy and stressful time for everyone in college due to the change in year structure. Therefore, I was especially impressed by the amount of submissions we received and I want to compliment each author on the outstanding quality of their work. No one should be discouraged by not being published; I have chosen these reviews as they fit into the vision of having an edition that covers a wide range of topics. The choice was tough as all the submissions were engaging, thorough and eloquently written.

The astrophysics submission reviews the direct detection of exoplanets through radio emissions. With the launch of the TESS telescope in 2018, excitement has grown extensively about newly found exoplanets. New methods of detecting exoplanets are on the rise, and the direct detection through radio emissions allows us to assess their habitability more easily, making this an enticing topic to explore.

This year's edition contains two material science papers as I believe that they beautifully portray the diversity of the field. The review on Vanadium Dioxide as a phase change material shows us how it is always possible to find new uses for materials which we thought we already knew everything about. This illustrates why scientists should always remain creative and keep an open mind. On the other side of the coin we have flexible electronics, a topic which should thrill anyone who has an interest in technological developments since it could open doors from wearable electronics to health care applications.

Finally, I have included a review on the use of Salt Gradients as a form of renewable energy. As this is one of the biggest problems we face in society today, I believe that striving for new developments is imperative. Although conventional renewable energy has been developing at rapid pace we should keep our mind open to alternative sources of renewable energy wherever they may come from.

I want to extend my gratitude to Dave McCloskey who went over and beyond to help me throughout this process as my academic supervisor and reviewer. Furthermore, I want to thank the peer reviewers, Hugh Manning, Robert Kavanagh and Calin Hrelescu, who were all an essential asset to this year's issue.

Maxime Deckers

Physics Editor

Trinity Student Scientific Review 2019

# FLEXIBLE ELECTRONICS AND THE PRE-STRAIN STRATEGY: A POSITIVE SIDE TO WRINKLING

Lucy Prendeville

Senior Sophister

Nanoscience, Physics and Chemistry of Advanced Materials

*The realisation of stretchable and flexible electronic devices requires the development of materials with strain-invariant electrical properties. Unsurprisingly, this is not a simple task to achieve; high conductivity and stretchability are challenging properties to combine. The pre-strain strategy is one such approach implemented to surmount this problem and fabricate deformable, electrically stable composites. This method involves the deposition of conductive materials onto pre-strained, flexible substrates. Relaxation of the substrate forces the conductive layer to buckle or wrinkle, inducing a corrugated structure with the potential to endure large deformation while exhibiting minor resistance changes. This review focuses on the pre-strain strategy as a method for generating flexible, conductive electrodes with strain-invariant electrical properties. The buckling mechanics of the deposited thin film are discussed along with the conditions required to induce wrinkle formation. Procedures implemented to control the geometry of the wrinkled pattern are considered along with various nanomaterials used in this field. This is an exciting new area of physics which will literally shape the future of electronics.*

## Introduction

In recent years, increased demand for applications such as wearable medical electronics<sup>1</sup>, flexible displays<sup>2, 3</sup>, field-effect transistors<sup>4, 5</sup> and flexible photonic devices<sup>6</sup> have resulted in a paradigm shift towards the development of stretchable electronic systems. Flexible and stretchable electronics prove a much more challenging technology to produce than foldable electronics<sup>7</sup>; as mentioned by M. Park et al., “high conductivity and stretchability seem to be mutually exclusive parameters”<sup>8</sup>. The fundamental difficulty stems from the fact that traditional electronic and optoelectronic materials are brittle and as a result tend to be

damaged upon bending<sup>9,10</sup>.

The pre-strain strategy evades this problem. This alternative approach involves the deposition of conductive nanomaterials such as silver nanowires (AgNWs), carbon nanotubes (CNTs) and graphene onto pre-strained elastomer substrates, polymers with considerable elastic properties. Release of the pre-strain and subsequent shrinkage of the substrate to its initial dimensions forces the thin conductive film to buckle<sup>11,12</sup>, forming a sinusoidal or wavy pattern which is schematically illustrated in Figure 1. As mentioned by H. Cheng et al., this procedure introduces a significant level of stretchability to the system<sup>13</sup>. The pioneering work carried out by D. Khang et al. demonstrated the preparation of stretchable silicon (Si) films by the pre-strain strategy<sup>11</sup>. They studied the buckling of thin metal films deposited on thermally expanded polydimethylsiloxane (PDMS) substrates<sup>12</sup>; a hydrophobic, silicon-based elastomer. Subsequent cooling and contraction of the compliant PDMS forced the thin film to adopt a wrinkled geometry in an effort to minimise the compressive stresses induced as a result of the mechanical instability<sup>14</sup>.

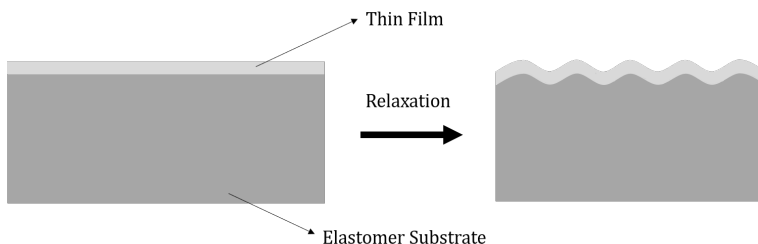


Figure 1: A diagrammatic representation of the mechanical buckling of a thin film upon release of the elastomer pre-strain. Adapted from D. Khang et al., copyright Wiley-VCH Verlag GmbH & Co. KGaA, reproduced with permission<sup>12</sup>

As mentioned by T. Cheng et al., this buckled or corrugated structure is one of the most common architectures for the design of strain-invariant thin film electrodes<sup>15</sup>. Deposition of conductive nanomaterials onto the expanded area of the substrate allows the resulting composite to tolerate higher levels of deformation in comparison to those prepared under conditions of no pre-strain<sup>16</sup>.

## Wrinkling Mechanics

Upon release of the substrate pre-strain, the type of buckled pattern formed depends on a number of factors including the degree of elastomer pre-strain<sup>17</sup> and the relative compliance of the substrate<sup>18</sup>. Two possible buckling modes include buckle delamination and wrinkling, both illustrated in Figure 2. Buckle delamination occurs when a portion of the film detaches from the substrate, forming a localised pattern<sup>18</sup>. In contrast, wrinkling is observed when the film remains in contact with the substrate surface, generating a wavy, sinusoidal pattern on release of the pre-

strain<sup>19</sup>.

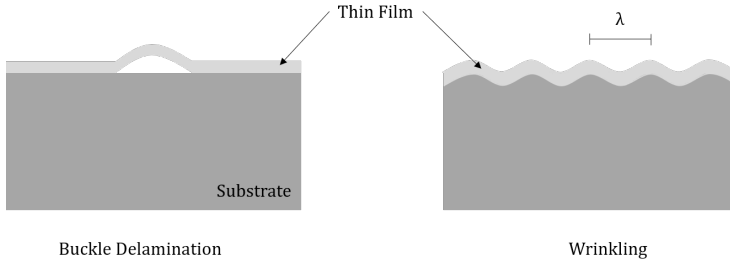


Figure 2: Schematic representation of the two main buckling modes for a thin film on a compliant, elastomer substrate; buckle delamination and wrinkling. Adapted from H. Mei et al., reproduced with permission<sup>18</sup>

Formation of a wrinkled pattern is highly desirable in the field of stretchable electronics as increasing the number of wrinkles improves the stretchability of the composite<sup>16</sup>. Surface wrinkling occurs in a film-substrate system when the compressive stress experienced by the film exceeds the critical wrinkling stress,  $\sigma_w$ <sup>20</sup>. This is governed by Equation 1 below, based on an energetic analysis<sup>18</sup>.

$$\sigma_w = \frac{\bar{E}_f}{4} \left( \frac{3\bar{E}_s}{\bar{E}_f} \right)^{2/3} = \bar{E}_f \varepsilon_c \quad (1)$$

Where  $E_f$  and  $E_s$  are the plane-strain moduli of the thin film and substrate respectively and  $\varepsilon_c$  is the critical strain for wrinkling, or the minimum strain required to induce the formation of a wrinkled pattern. The ratio of  $E_s$  to  $E_f$  is known as the stiffness ratio<sup>21</sup>. It is very clear from the above relationship that the more compliant the substrate is relative to the film, the lower the critical stress for wrinkling, favouring this type of buckling mode. In contrast, the critical stress for delamination is lower than that for wrinkling when the substrate has a high stiffness<sup>21</sup>, making delamination the more likely mode of buckling. This is further explanation as to why PDMS is usually incorporated as the elastomeric substrate in the development of stretchable electrodes; it is a compliant and flexible material whose stiffness can be tuned by varying the degree of cross-linking, thus promoting the formation of a wrinkled buckled mode which is more advantageous in this field<sup>22</sup>.

Precise control of the wrinkling wavelength and amplitude can be used to alter the mechanical properties of stretchable devices as required<sup>23</sup>.  $\sigma_w$  arises from the minimisation of the total elastic energy in the film and substrate<sup>24</sup>. The minimisation of energy method has been used to understand the mechanics of such systems and has been critical for the development of different models<sup>25,26</sup>. For systems prepared

under small substrate pre-strains (< 5%), D. Khang et al. described how energy minimisation leads to sinusoidal wrinkles with wavelength,  $\lambda_0$ , and amplitude,  $A_0$ , by:

$$\lambda_0 = 2\pi h \left( \frac{\bar{E}_f}{3\bar{E}_s} \right)^{1/3} = \frac{\pi h}{\sqrt{\varepsilon_c}} \quad (2)$$

$$A_0 = h \sqrt{\frac{\varepsilon_{pre}}{\varepsilon_c} - 1} \quad (3)$$

Where  $h$  is the film thickness and  $\varepsilon_{pre}$  is the pre-strain of the elastomeric substrate during the deposition process<sup>27</sup>.  $\lambda_0$  depends only on the film thickness and the mechanical properties of both film and substrate under small strains; there is no dependence on the substrate pre-strain<sup>12</sup>. Increasing the pre-strain does however contribute to an increase in wave amplitude. In contrast, with larger pre-strains (> 5%) the substrate becomes nonlinear and can be modelled as neo-Hookean<sup>12</sup>; a hyperelastic material model that is similar to Hooke's Law but can be used to predict the nonlinear response of materials to large deformations<sup>28</sup>. H. Jiang et al. demonstrated that the buckling of stiff thin films on compliant substrates can be described by the same mechanics as an accordion-bellows<sup>25</sup>;

$$\lambda = \frac{\lambda_0}{(1 + \varepsilon_{pre})(1 + \xi)^{1/3}} \quad (4)$$

$$A = \frac{A_0}{\sqrt{1 + \varepsilon_{pre}}(1 + \xi)^{1/3}} \quad (5)$$

Where  $\xi = 5(\varepsilon_{pre}(1 + \varepsilon_{pre})) / 32$  and  $\lambda_0$  and  $A_0$  are as given previously in Equations 2 and 3<sup>12</sup>. The factor of  $(1 + \xi)^{1/3}$  originates from the geometrical nonlinearity associated with the large applied strain<sup>29</sup> while  $\lambda_0/(1 + \varepsilon_{pre})$  and  $A_0/(1 + \varepsilon_{pre})^{1/2}$  signify their respective variations based on accordion-bellows mechanics<sup>15</sup>.

## Controlling the Geometry of Buckled Surfaces

Adjusting the mechanical properties of the system and thickness of the deposited film allows the wrinkle orientation to be controlled as desired<sup>30</sup>. The geometry

of the buckled pattern can also be precisely tailored by the presence of adhesion sites on the surface of the elastomer substrate<sup>31, 32</sup>. Y. Sun et al. used lithography, a patterning technique, to develop a PDMS substrate with highly polar  $-\text{O}_n\text{Si}(\text{OH})_{4-n}$  groups at defined positions on the surface which acted as activated surface sites<sup>31</sup>. They selectively treated areas of the surface with ozone by passing UV light over the pre-stained PDMS substrate through a UVO photomask. The PDMS surface was modified in areas exposed to ozone, becoming hydrophilic. The group transferred single-crystal Si nanoribbons to the pre-stained elastomer substrate, resulting in piece-wise chemical bonding between the PDMS and Si film at these activated, polar regions<sup>12</sup>. Under the pre-strain strategy, delamination of the film occurs with release of the substrate pre-strain unless the adhesion to the elastomer is strong enough<sup>12</sup>. This concept was exploited by Y. Sun et al. to develop a periodic buckled pattern with controlled wavelength and amplitude. Delamination of the Si film occurred at inactivated regions; areas of the substrate that had not been exposed to ozone. The width of the activated and inactivated regions can be precisely controlled by varying the mask pattern, thus allowing the buckled pattern to be adjusted as required<sup>12</sup>. The team also demonstrated the buckling of  $\text{SiO}_2$ -coated GaAs films using the same procedure<sup>31</sup>. As displayed in Figure 3 below, under this method the substrate surface layer does not buckle with the thin film upon release of the pre-strain.

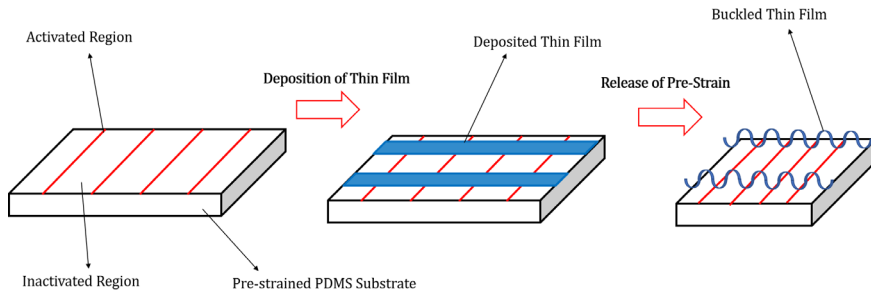


Figure 3: Schematic of the controlled delamination buckling of thin films by activating sites on the surface of pre-stained PDMS. Adapted from Y. Sun et al., reproduced with permission<sup>31</sup>

## Progress made in the Field using Nanomaterials

Indium-tin oxide is one of the most widely used materials in transparent conductors but owing to its intrinsic brittleness and rising production costs, it is unsuitable for use in the fabrication of flexible or stretchable transparent conductors<sup>33</sup>. Nanomaterials including AgNWs<sup>7, 34</sup>, CNTs<sup>35, 36</sup> and graphene<sup>37, 38</sup> have been extensively studied as potential candidates for use in this area. Nanomaterials are much more stretchable than their bulk analogues<sup>39</sup>. In particular, metal nanowires show promise owing to their ductility and high conductivity<sup>16</sup>. When assembled

into an interconnected network, the large length to diameter aspect ratio of metallic nanowires facilitates their mechanical compliance<sup>7</sup>. Silver has the highest intrinsic electrical conductivity of all metallic materials<sup>39</sup>, thus AgNWs have been at the centre of much research in this field<sup>16</sup>.

### *(1) Silver Nanowires*

In 2012, P. Lee et al. developed a novel synthesis procedure for the fabrication of long AgNWs which demonstrated superior mechanical compliance as well as robust conductivity in comparison to graphene and CNT-based composites<sup>7</sup>. They emphasised the importance of nanowire length in the preparation of materials with strain-invariant properties; longer structures easily establish percolation paths, conductive paths with long-range connectivity, and reduce the number of inter-nanowire junctions, areas at which large decreases in resistance occur<sup>7</sup>. P. Lee et al. transferred the nanowires onto a pre-strained Ecoflex substrate using suction pressure, followed by a thermal annealing step to remove the poly(vinyl pyrrolidone) surfactant and enhance the electrical properties of the network. Their composite demonstrated electrical stability under many stretching cycles and had the ability to endure strains up to 460% before significant resistance changes were observed.

F. Xu et al. also prepared a stretchable AgNW-based composite by embedding the metallic nanowires into the surface of the PDMS substrate<sup>34</sup>. They drop-casted AgNW solution onto a silicon substrate, followed by casting of liquid PDMS over the dried nanowire network and curing of the composite. When strained from 0 to 50% of its original length, their composite displayed a stable electrical conductivity by the fifth stretching-release cycle due to a buckling of the AgNW-PDMS surface layer. G. Huang et al. commented on this approach, noting that the electrical stability of such conductors is low with mechanical deformation as the embedded nanowire networks can be easily damaged under high strains<sup>40</sup>.

Therefore, with an aim of making progress in the development of wearable electronics, G. Huang et al. implemented a pre-straining and post-embedding (PSPE) process to achieve both electrical and mechanical stability in their AgNW-PDMS electrodes<sup>40</sup>. This process combined the advantages of both the pre-strain and embedding processes described above to achieve strain-invariant conductive materials. The group spray-deposited AgNW-ethanol solution onto 80% pre-strained PDMS. Liquid PDMS was cast over the nanowire network and the pre-strain was released, causing the deposited film to buckle. The composite was cured and the resulting PSPE circuit was removed from the initial PDMS substrate. The diagram in Figure 4 schematically illustrates the steps involved in the PSPE process.

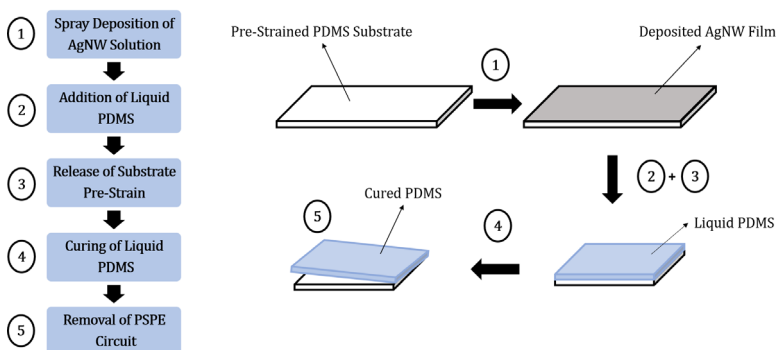


Figure 4: A schematic representation of the PSPE process with a flowchart outlining the steps in the procedure. Adapted from G. Huang et al.<sup>40</sup>

They observed minor variations in resistance with mechanical deformation of their electrodes and strong adhesion of the AgNW network to the elastomer PDMS substrate; an important factor to prevent unwanted delamination of the thin film in particular areas<sup>19</sup>. Their composites exhibited a high conductivity of  $1.52 \times 10^4 \text{ S cm}^{-1}$ , showing promise for the future of AgNW-based stretchable electronic materials prepared by the PSPE method. L. Cao et al. also developed a general strategy for the production of stretchable conductors based on both pre-strain and embedding processes<sup>33</sup>. They described the process as a ‘universal method’ that can be applied to various types of nanomaterials including nanowires and nanotubes.

## (2) Carbon Nanotubes and Graphene

In addition to AgNWs, carbon-based nanomaterials such as CNTs and graphene display promising attributes for use in the fabrication of stretchable electrodes including high carrier mobility, high mechanical strength as well as excellent thermal conductivity<sup>41</sup>. The natural curvature and ability of CNTs to easily entangle make them particularly suited for use in this field<sup>36</sup>. In comparison to AgNW-based electrodes, CNTs exhibit higher sheet resistances due to large contact resistances<sup>42</sup> and the difficulty in preparing bulk quantities of metallic CNTs with high purity<sup>15</sup>. However, much research has been carried out to improve the mechanical and electrical properties of CNTs for this field. S. Park et al. developed stretchable films by spray-depositing single-walled CNTs onto pre-strained PDMS substrates<sup>43</sup>. The resulting films displayed high conductivities of  $2200 \text{ S cm}^{-1}$  and excellent biaxial stretchability, with the ability to endure strains up to 150%. The group also performed cyclic tests on their films and observed very small, insignificant changes in resistance with strain, demonstrating the strain-invariant electrical properties of their electrode.

Structural defects or large interlayer resistances usually affect the electrical and mechanical stretchability of graphene, hindering its ability to function as required in soft electronics<sup>44</sup>. Therefore, hybrid graphene-CNTs or graphene-AgNW films have been studied, to enhance the conductivity and flexibility of graphene-coated PDMS substrates<sup>45, 46</sup>. For example, M. Lee et al. prepared graphene-AgNW hybrid nanostructures with enhanced electrical properties, low sheet resistance and mechanical flexibility<sup>47</sup>. High density percolation networks of AgNWs were integrated into graphene, forming bridges across defects in the 2D material, thus decreasing the overall resistance of the composite. The hybrid nanostructure also demonstrated enhanced mechanical stability, with an ability to endure tensile strains up to 100% without significant changes in the electrical properties.

These examples merely give a small indication of the progress made in the field of stretchable electronics to date using nanomaterials and the pre-strain strategy. Conducting polymers such as PEDOT:PSS also possess ideal properties for use in this area; high conductivity, flexibility as well as good reversibility<sup>48</sup>. The overall focus of research in this field involves the search for appropriate low-cost materials and simple, scalable methods to produce mechanically stable and robust stretchable electronic devices.

## Conclusion

The mechanical buckling phenomenon has proved to be fundamental in the advancements made on stretchable and flexible electronic systems to date. As discussed in this review, the pre-strain strategy is a simple yet effective approach for the development of materials with strain-invariant electrical properties. This method involves the deposition of conductive nanomaterials onto pre-strained, stretchable substrates. Once the critical wrinkling strain has been reached, relaxation of the substrate forces the deposited thin film to buckle, forming a wrinkled pattern with enhanced strain-invariant electrical properties. The wrinkle wavelength and amplitude can be precisely controlled by the presence of adhesion sites on the surface of the substrate, allowing the mechanical properties of the electrode to be altered as required. One-dimensional nanomaterials including AgNWs and CNTs show particular promise in this field. The high aspect ratio of metallic nanowires and nanotubes establishes effective percolation paths with low junction resistances, enabling both high conductivity and mechanical compliance; factors required of stretchable conductive materials.

The future of flexible electronics offers a wide range of opportunities and will completely revolutionise the technological world we live in. The possibilities are endless; from applications in wearable electronics<sup>40</sup> to biointegrated electronics<sup>49</sup> to high-performance flexible integrated circuits<sup>50</sup> as well as flexible displays<sup>51</sup> and energy-related devices<sup>52</sup>. It is exciting to review the advances that have been made to date; the era of stretchable electronics is rapidly approaching.

## Acknowledgements

This review was adapted from a thesis entitled 'Solution Processed Stretchable Electrodes', compiled as part of my Final Year Project for the module PYU44NP2. I would like to thank Professor Jonathan Coleman, Dr. Conor Boland, Daniel O'Driscoll, Sonia Biccai and Cian Gabbett for their help, advice and guidance throughout the 9 weeks of my project.

## References

1. Liu Y, Pharr M, Salvatore G-A. Lab-on-Skin: A Review of Flexible and Stretchable Electronics for Wearable Health Monitoring. *ACS Nano*. 2017;11(10):9614–35.
2. Yu Z, Niu X, Liu Z, Pei Q. Intrinsically Stretchable Polymer Light-Emitting Devices Using Carbon Nanotube-Polymer Composite Electrodes. *Adv Mater*. 2011;23(34):3989–94.
3. Park S, Xiong Y, Kim R-H, Elvikis P, Meitl M, Kim D-H, et al. Printed Assemblies of Inorganic Light-Emitting Diodes for Deformable and Semitransparent Displays. *Science* (80- ). 2009;325(5943):977–81.
4. Shin G, Yoon C-H, Bae M-Y, Kim Y-C, Hong S-K, Rogers JA, et al. Stretchable Field-Effect-Transistor Array of Suspended SnO<sub>2</sub> Nanowires. *Small*. 2011;7(9):1181–5.
5. Kim J, Lee M, Jeon S, Kim M, Kim S, Kim K. Highly Transparent and Stretchable Field-Effect Transistor Sensors Using Graphene-Nanowire Hybrid Nanostructures. *Adv Mater*. 2015;27(21):3292–7.
6. Liu Y, Liu Y, Qin S, Xu Y, Zhang R, Wang F. Graphene-Carbon Nanotube Hybrid Films for High- Performance Flexible Photodetectors. *Nano Res*. 2017;10(6):1880–7.
7. Lee P, Lee J, Lee H, Yeo J, Hong S, Nam KH, et al. Highly Stretchable and Highly Conductive Metal Electrode by Very Long Metal Nanowire Percolation Network. *Adv Mater*. 2012;24(25):3326–32.
8. Park M, Im J, Shin M, Min Y, Park J, Cho H, et al. Highly Stretchable Electric Circuits from a Composite Material of Silver Nanoparticles and Elastomeric Fibres. *Nat Nanotechnol*. 2012;7:803–9.
9. Dang W, Vinciguerra V, Lorenzelli L, Dahiya R. Printable Stretchable Interconnects. *Flex Print Electron*. 2017;2:013003.
10. Rogers JA. Materials for Semiconductor Devices that can Bend , Fold , Twist , and Stretch. *MRS Bull*. 2014;39(6):549–56.
11. Wang B, Bao S, Vinnikova S, Ghanta P, Wang S. Buckling Analysis in Stretchable Electronics. *npj Flex Electron*. 2017;1:5.
12. Khang DY, Rogers JA, Lee HH. Mechanical Buckling: Mechanics, Metrology, and Stretchable Electronics. *Adv Funct Mater*. 2009;19(10):1526–36.
13. Cheng H, Zhang Y, Hwang KC, Rogers JA, Huang Y. Buckling of a Stiff Thin Film on a Pre-Strained Bi-Layer Substrate. *Int J Solids Struct*. 2014;51(18):3113–8.
14. Amjadi M, Pichitpajongkit A, Lee S, Ryu S, Park I, Engineering M, et al. Highly Stretchable and Sensitive Strain Sensor based on Silver Nanowire-Elastomer Nanocomposite. *Am Chem Soc*. 2014;8(5):5154–63.
15. Cheng T, Zhang Y, Lai W, Huang W. Stretchable Thin-Film Electrodes for Flexible Electronics with High Deformability and Stretchability. *Adv Mater*. 2015;27(22):3349–76.
16. Kim A, Ahn J, Hwang H, Lee E, Moon J. Pre-strain Strategy for Developing a Highly Stretchable and Foldable One-Dimensional Conductive Cord based on a Ag Nanowire Network. *Nanoscale*. 2017;9(18):5773–8.

17. Wang S, Xiao J, Song J, Ko C, Hwang K, Rogers JA. Mechanics of Curvilinear Electronics. *Soft Matter*. 2010;6(22):5757–63.
18. Mei H, Huang R, Chung JY, Stafford CM, Yu H. Buckling Modes of Elastic Thin Films on Elastic Substrates. *Appl Phys Lett*. 2017;90(15):151902.
19. Nolte AJ, Chung JY, Davis CS, Stafford CM. Wrinkling-to-Delamination Transition in Thin Polymer Films on Compliant Substrates. *Soft Matter*. 2017;13(43):7930–7.
20. Han X, Zhao Y, Cao Y, Lu C. Controlling and Prevention of Surface Wrinkling via Size-Dependent Critical Wrinkling Strain. *Soft Matter*. 2015;11(22):4444–52.
21. Ebata Y. Bending, Wrinkling, and Folding of Thin Polymer Film / Elastomer Interfaces. PhD Thesis, University of Massachusetts Amherst; 2013.
22. Wang Z, Volinsky AA, Gallant ND. Crosslinking Effect on Polydimethylsiloxane Elastic Modulus Measured by Custom-Built Compression Instrument. *J Appl Polym Sci*. 2014;131(22):41050.
23. Nam J, Seo B, Lee Y, Kim DH, Jo S. Cross-Buckled Structures for Stretchable and Compressible Thin Film Silicon Solar Cells. *Sci Rep*. 2017;7:7575.
24. Huang R $\tilde{A}$ . Kinetic Wrinkling of an Elastic Film on a Viscoelastic Substrate. *J Mech Phys Solids*. 2005;53(1):63–89.
25. Jiang H, Khang D-Y, Song J, Sun Y, Huang Y, Rogers JA. Finite Deformation Mechanics in Buckled Thin Films on Compliant Supports. *Proc Natl Acad Sci*. 2007;104(40):15607–12.
26. Huang ZY, Hong W, Suo Z $\tilde{A}$ . Nonlinear Analyses of Wrinkles in a Film Bonded to a Compliant Substrate. *J Mech Phys Solids*. 2005;53(9):2101–18.
27. Wang Y, Chen Y, Li H, Li X, Chen H, Su H, et al. Buckling-based Method for Measuring the Strain-Photonic Coupling Effect of GaAs Nanoribbons. *ASC Nano*. 2016;10(9):8199–206.
28. Kim B, Lee SB, Lee J, Cho S, Park H, Yeom S, et al. A Comparison Among Neo-Hookean model, Mooney-Rivlin model, and Ogden model for Chloroprene rubber. *Int J Precis Eng Manuf*. 2012;13(5):759–64.
29. Yu C, Jiang H. Forming Wrinkled Stiff Films on Polymeric Substrates at Room Temperature for Stretchable Interconnects Applications. *Thin Solid Films*. 2010;519(2):818–22.
30. Schweikart A, Fery A. Controlled Wrinkling as a Novel Method for the Fabrication of Patterned Surfaces. *Microchim Acta*. 2009;165(3–4):249–63.
31. Sun Y, Choi WM, Jiang H, Huang YY, Rogers JA. Controlled Buckling of Semiconductor Nanoribbons for Stretchable Electronics. *Nat Nanotechnol*. 2006;1(3):201–7.
32. Song J, Jiang H, Huang Y, Rogers JA. Mechanics of Stretchable Inorganic Electronic Materials. *J Vac Sci Technol A Vacuum, Surfaces, Film*. 2009;27(5):1107–25.
33. Cao L, Wang Z, Liu Y, Shi R, Wang X, Liu J. A General Strategy for High Performance Stretchable Conductors based on Carbon Nanotubes and Silver Nanowires. *RSC Adv*. 2017;7(33):20167–71.
34. Xu F, Zhu Y. Highly Conductive and Stretchable Silver Nanowire Conductors. *Adv Mater*. 2012;24(37):5117–22.
35. Khang D, Xiao J, Kocabas C, Maclaren S, Banks T, Jiang H, et al. Molecular Scale Buckling Mechanics in Individual Aligned Single-Wall Carbon Nanotubes on Elastomeric Substrates. *Nano Lett*. 2008;8(1):124–30.
36. Cai L, Wang C. Carbon Nanotube Flexible and Stretchable Electronics. *Nanoscale Res Lett*. 2015;10:320.
37. Kim KS, Zhao Y, Jang H, Lee SY, Kim JM, Kim KS, et al. Large-Scale Pattern Growth of Graphene Films for Stretchable Transparent Electrodes. *Nature*. 2008;457:706–10.
38. Eda G, Fanchini G, Chhowalla M. Large-Area Ultrathin Films of Reduced Graphene Oxide as a Transparent and Flex-

- ible Electronic Material. *Nat Nanotechnol.* 2008;3:270–4.
39. Yao S, Zhu Y. Nanomaterial-Enabled Stretchable Conductors : Strategies, Materials and Devices. *Adv Mater.* 2015;27(9):1480–511.
40. Huang GW, Xiao HM, Fu SY. Wearable Electronics of Silver-Nanowire/Poly(dimethylsiloxane) Nanocomposite for Smart Clothing. *Sci Rep.* 2015;5:13971.
41. Ding J, Fu S, Zhang R, Boon E, Lee W, Fisher FT, et al. Graphene–Vertically Aligned Carbon Nanotube Hybrid on PDMS as Stretchable Electrodes. *Nanotechnology.* 2017;28(46):465302.
42. An L, Friedrich CR. Measurement of Contact Resistance of Multiwall Carbon Nanotubes by Electrical Contact using a Focused Ion Beam. *Nucl Inst Methods Phys Res B.* 2012;272:169–72.
43. Park S, Vosguerichian M, Bao Z. A Review of Fabrication and Applications of Carbon Nanotube Film-based Flexible Electronics. *Nanoscale.* 2013;5(5):1727–52.
44. Gong S, Cheng W. One-Dimensional Nanomaterials for Soft Electronics. *Adv Electron Mater.* 2017;3(3):1600314.
45. Tung VC, Chen L, Allen MJ, Wassei JK, Nelson K, Kaner RB, et al. Low-Temperature Solution Processing of Graphene - Carbon Nanotube Hybrid Materials for High-Performance Transparent Conductors. *Nano Lett.* 2009;9(5):1949–55.
46. Jeong C, Nair P, Khan M, Lundstrom M, Alam MA. Prospects for Nanowire-Doped Polycrystalline Graphene Films for Ultra-transparent, Highly Conductive Electrodes. *Nano Lett.* 2011;11(11):5020–5.
47. Lee M, Lee K, Kim S, Lee H, Park J, Choi K, et al. High-Performance, Transparent, and Stretchable Electrodes Using Graphene – Metal Nanowire Hybrid Structures. *Am Chem Soc.* 2013;13(6):2814–21.
48. Sun K, Zhang S, Li P. Review on Application of PEDOTs and PEDOT : PSS in Energy Conversion and Storage Devices. *J Mater Sci Mater Electron.* 2015;26(7):4438–62.
49. Kim D, Lu N, Huang Y, Rogers JA. Materials for Stretchable Electronics in Bio-inspired and Biointegrated Devices. *MRS Bull.* 2012;37(3):226–35.
50. Xiang L, Zhang H, Hu Y, Peng L. Carbon Nanotube-based Flexible Electronics. *J Mater Chem C. Royal Society of Chemistry;* 2018;6(29):7714–27.
51. Gelinck GH, Huitema HEA, Van Veenendaal E, Cantatore E, Schrijnemakers L, Van Der Putten JBPH, et al. Flexible Active-Matrix Displays and Shift Registers based on Solution-Processed Organic Transistors. *Nat Mater.* 2004;3:106–10.
52. Lipomi DJ, Tee BC, Vosgueritchian M, Bao Z. Stretchable Organic Solar Cells. *Adv Mater.* 2011;23(15):1771–5

TS  
SR

# AURORAL RADIO EMISSION: A POTENTIAL METHOD FOR THE DIRECT DETECTION OF EXOPLANETS

Niamh Feeney  
Senior Sophister  
Physics & Astrophysics

*Exoplanets have been theorised to emit radiation in the low frequency radio range, analogous to the magnetised solar system planets. This emission is produced as a result of the interaction between a planet's intrinsic magnetic field and the stellarwind of its host star. The detection of exoplanetary radio emission would constitute a new method for the direct detection of exoplanets, and would also allow for the characterisation of exoplanetary magnetic fields, a feat which has yet to be achieved. Various computational models have been employed to predict the flux density and frequency of emission from various confirmed exoplanets. Though some studies have produced results suggesting that exoplanet radio emission could be detected using ground-based radio telescopes, such radio emission remain to be detected. This review highlights recent works and potential future work concerning planetary auroral radio emission.*

## Introduction

The search for and characterisation of planets orbiting stars outside our solar system is central to a large fraction of astrophysical research and space exploration. There has been rapid progress in the field of exoplanet detection in recent years; although the first exoplanet was detected only 26 years ago<sup>1</sup>, there are now over 3,800 confirmed exoplanets on record.

Currently, the most widely used methods of exoplanet detection are the radial velocity and transit methods. The radial velocity method measures the Doppler shift in the spectrum of a star which moves in an orbit due to the gravitational pull of an orbiting planet, while the transit method uses photometry to detect the apparent drop in visual brightness of a star as an orbiting planet transits the disk of the star<sup>2</sup>. The transit method was utilised by NASA's Kepler Space Telescope<sup>3</sup>,

which detected over 2,600 confirmed exoplanets in its 9 years in operation (2009-2018), according to the NASA exoplanet archive. Both of these methods are indirect methods of exoplanet detection, which infer the existence of an exoplanet from the effect it has on various properties of its host star.

Direct imaging of exoplanets is a direct method of exoplanet detection which relies on detecting the light from the planet, which is extremely faint in contrast to that of its host star. The current limit on the direct detection of exoplanets is the high contrast ratio between the intensity of electromagnetic radiation of the planet and its host star in the visible and infrared ranges (the ranges within which direct imaging is done); approximately  $10^9$  in the visible and  $10^6$  in the infrared<sup>4</sup>. However, there may exist a direct detection method in the low frequency radio range (between ten and a few hundred MHz<sup>5</sup>), given that planets within the solar system are known to emit radiation within this range.

The first observation of planetary radio emission was made by Burke & Franklin (1955), who detected intense emission from Jupiter in the decametre radio range. Earth's auroral kilometric radiation was observed from space in 1970<sup>6</sup>, and radio emission has since been detected from the three other magnetised planets of the solar system; Saturn<sup>7</sup>, Uranus<sup>8</sup> and Neptune<sup>9</sup>. Below 40 MHz, the magnetised solar system planets produce auroral radio emission via the interaction between their magnetic fields and the solar wind<sup>10</sup>. The solar wind compresses the planet's magnetosphere, causing "reconnection" events between the planet's magnetic field lines in the nightside magnetopause. This energises electrons, accelerating them along high-latitude field lines towards the planet's auroral region. The precipitation of these energetic electrons in the auroral region produces electromagnetic radiation in the radio range. For all the magnetised solar system planets, this radiation is only 1-2 orders of magnitude less intense than the radiation produced by the sun in the low frequency radio range<sup>11</sup>, thus making it favourable for direct detection.

It has been theorised that magnetised exoplanets may emit at radio frequencies, analogous to the aforementioned solar system planets<sup>12, 13</sup>. The detection of radio emission from exoplanets would not only be a revolutionary method of exoplanet detection, but a measurement of planetary radio emission would be indicative of the presence of an intrinsic planetary magnetic field, which is a key factor in determining planetary habitability.

This work reviews recent research done on the estimation and observation of planetary auroral radio emission based on solar system analogies, and discusses future work that could be done in this field.

## The Origins of Planetary Radio Emission

Planetary radio emission occurs when the stellar wind of the host star interacts

with a magnetised planet in its path<sup>14, 4</sup>. Stellar winds are dened as the outflow of material from stars<sup>15</sup>. In the case of the Sun, the solar wind is a flow of magnetised plasma originating from the Sun's corona<sup>16</sup> - an extremely hot region of the Sun's upper atmosphere. Stellar winds have a significant effect on their orbiting planets; they can cause planetary atmospheric mass loss, and are a key factor in determining planetary habitability<sup>17</sup>. The magnetic field of the planet can detect harmful particles from the stellar wind. For example, Mars' lack of intrinsic magnetic field leaves it exposed to the harsh eects of the solar wind, stripping it of its atmosphere and thus making it unsuitable for the evolution of life<sup>18</sup>.

Dynamo theory states that planets with a rotating, convective, conducting liquid core, such as Earth, generate a planetary-scale magnetic field<sup>19</sup>, which can be approximated as a dipole magnet as shown in Figure 1. A planet's magnetosphere is the region of space surrounding the planet that is aected by the planet's magnetic field, and can extend to up to 100 times the radius of the planet itself<sup>20</sup>, depending on the strength of the planet's magnetic field. A planet's magnetosphere acts as an obstacle to the stellar-wind plasma, causing the wind to flow around the planet's magnetosphere, conning the planet's magnetic field to a cavity surrounding the planet<sup>21</sup>. This is illustrated in Figure 1.

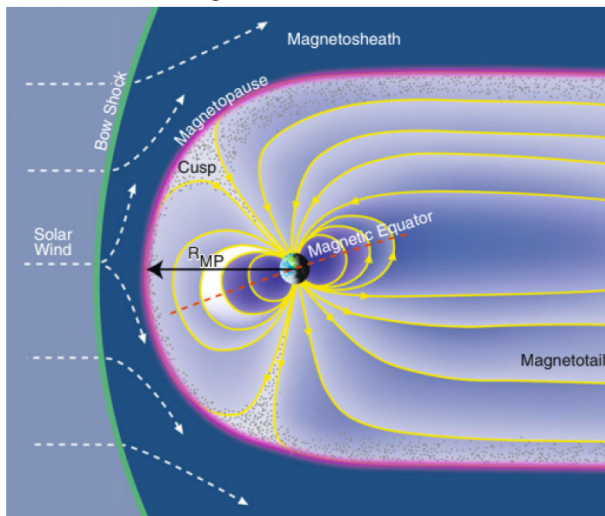


Figure 1: *Illustration of the interaction between the solar wind and the Earth's magnetic field<sup>20</sup>.*

The magnetosphere extends to the magnetopause, which occurs where there is a static pressure balance between the dynamic pressure of the stellar wind and the planet's outward magnetic pressure. The nightside is the area where the magnetic field lines are elongated and extend into the magnetotail, whereas the dayside is defined as the side of the planet facing the star where magnetic field lines appear compressed. The distance between the centre of the planet and the dayside magnetopause is referred to as the planet's magnetospheric size ( $r_m$ ), and is given

by equation (1):

$$\frac{r_m}{R_p} = \xi \left[ \frac{B_p^2}{8\pi \rho_{sw} u_{sw}^2} \right]^{\frac{1}{6}} \quad (1)$$

$R_p$  is the radius of the planet,  $B_p$  is the equatorial magnetic field strength of the planet,  $\rho_{sw}$  and  $u_{sw}$  are the density and velocity of the solar wind at the orbital radius of the planet, and  $\xi$  is a numerical factor that has been determined observationally that corrects for the effects of electrical current that flow along the magnetopause<sup>20</sup>.

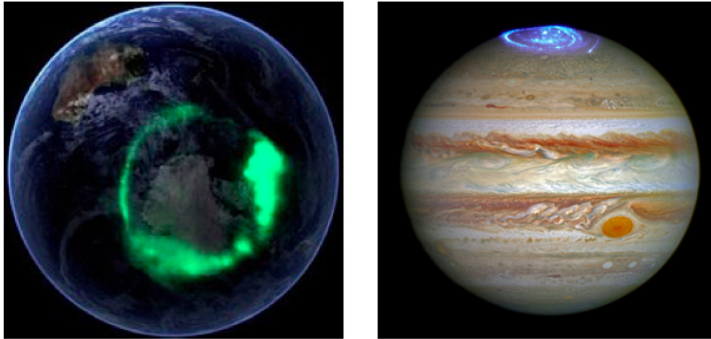


Figure 2: Left: Image of Earth's Aurora Australis. Right: Image taken by the Hubble space telescope of Jupiter's aurora, demonstrating the polar cap boundary from which the radio emission originates.

Images: NASA

Auroral radio emission originates from strongly magnetised annular rings around the planet's poles<sup>19</sup>, as seen in Figure 2. The boundary of a planet's auroral ring is thought to occur approximately where a planet's closed and open magnetic field lines meet<sup>2</sup>, and is also referred to as the planet's polar cap<sup>22</sup>. Planetary aurorae (e.g. Aurora Borealis and Aurora Australis on Earth) are powered by magnetospheric currents that cause the precipitation of energetic electrons in the polar regions of the upper atmosphere<sup>23</sup>. Alongside this emission at visible wavelengths, the energetic electrons lead to radio emission via the cyclotron-Maser instability mechanism<sup>4</sup>.

## Planetary Radio Power and Flux Density

Though the specific details of the process of planetary radio emission differ from planet to planet depending on the topology of the planet's magnetic field among other factors<sup>13</sup>, it is clear that there is a link between the power of the planetary radio emission and the incident solar wind power on each planet<sup>24</sup>. This link is described by the "radiometric Bode's law", which relates the emitted radio power of each planet to the dissipated kinetic power of the incident solar wind and the

planet's magnetic field strength<sup>10</sup>. This relation has been extrapolated to extrasolar systems<sup>25</sup>. From this, a planet's radio power is given by:

$$P_{\text{radio}} = \eta_K \rho_{\text{SW}} u_{\text{SW}}^2 \pi r_m^2 \quad (2)$$

where  $\eta_K$  is the efficiency ratio, which has been determined empirically for solar system planets to be  $1 \times 10^{-5}$ <sup>4</sup>.

The two most important characteristics of auroral radio emission to be considered when assessing whether they are detectable from Earth are the frequency and flux density of emission. The frequency of the radio emission is determined by the magnetic field strength of the planet:

$$\Delta f = 2.8 \left( \frac{B(\alpha_0)}{1G} \right) \text{MHz} \quad (3)$$

where  $B(\alpha_0)$  is the planetary magnetic field strength at the polar cap boundary where emission originates.

The planetary radio flux density ( $\Phi_{\text{radio}}$ ), which is the strength of the signal that is detected on Earth, is related to the emitted frequency and planetary radio power by

$$\Phi_{\text{radio}} = \frac{P_{\text{radio}}}{d^2 \omega \Delta f} \quad (4)$$

where  $d$  is the distance to the system, and  $\omega$  is the solid angle of the hollow cone of emission. The inverse dependence on the square of the distance tells us that the radio flux drops off rapidly as we move out of the solar system.

## Radio Astronomy

Radio telescopes operate in the low frequency range of approximately 10 MHz-100 GHz. Below 10 MHz, incoming radiation is reflected by the Earth's ionosphere, and therefore is not detectable from the ground<sup>26</sup>. Jupiter, with an intense maximum magnetic field strength of ~14 G, is the only planet that produces radio emission that can be detected from the ground with current radio instruments. In the case of the earth ( $B_p \approx 0.3$  G), emission frequency is in the range of 50-500 kHz<sup>27</sup>. Radio astronomy is conducted using large radio telescopes that consist of antennae which act as collectors of radio waves. The size of radio telescopes required keeps growing in order to obtain high intensity observations at increasingly low frequencies<sup>28</sup>. Radio arrays which operate using principles of interferometry consist of a collection of large radio telescopes all observing the same object at the same frequency. Telescopes such as the Low Frequency Array (LOFAR) have

extremely long baselines which gives them a high sensitivity.

The unit of intensity/sensitivity used in radio astronomy is the Jansky (Jy), which measures the flux density of a radio source. 1 Jy is given as

$$1 \text{ Jy} = 10^{-26} \frac{W}{\text{m}^2 \cdot \text{Hz}} = 10^{-23} \frac{\text{erg}}{\text{s} \cdot \text{cm}^2 \cdot \text{Hz}} \quad (5)$$

## Models of Planetary Radio Emission

Thus far, radio emission from exoplanets remain undetected, however, much work has been done in estimating the frequency and flux density of this radio emission computationally, using solar system analogies. These estimations have been used to guide radio telescope observations and select candidates which are likely to produce intense radio emission.

Estimates have been computed by a number of researchers in the field using a variety of computational methods. Stellar winds are simulated using 3D magnetohydrodynamic equations<sup>29</sup>, and then combined with models of exoplanetary magnetic fields to predict the size of the planetary magnetosphere, planetary radio power, and the frequency and flux density of emission. The results obtained in these studies should be considered as providing a range of radio flux densities and frequencies of emission from exoplanets, rather than providing exact estimations. Exact values require knowledge of planetary magnetic field strengths, which are not yet known for exoplanets. In their computation of predicted radio emission from V830 Tauri b, Vidotto & Donati (2017) found that the flux density of emission is weakly dependent on planetary magnetic field strength, however, there is a strong dependence on the frequency of emission on planetary magnetic field strength. Increasing the planet's magnetic field strength by a factor of 10 decreases the flux density by a factor of 1.8, but increases the frequency of emission by a factor of 13<sup>22</sup>.

Radio emission from planets which orbit their stars at orbital radii over 4x shorter than that of the Earth (close-in planets) are predicted to produce radio emission several orders of magnitude greater than those of Jupiter<sup>13</sup>. This is due to the extremely high densities of stellar winds at short distances from the star, which causes the planets to emit increased radio power. Models also show that the radio power scales with planetary radius, therefore Jovian-like planets (such as Jupiter) are expected to produce intense emission. According to equation (3), a magnetic field strength >4 G is required to produce emission >10 MHz (Earth's ionospheric cutoff frequency). Given that the planetary magnetic field strength scales with the planetary radius, giant planets are most likely to produce emission which is detectable from Earth. Combining these 3 results, it is clear that hot Jupiters (giant planets orbiting at short distances from their host stars) are strong candidates in

the search for exoplanet radio emission<sup>30</sup>.

Lazio et. al. (2004) computed the predicted fluxes of the 118 exoplanets known at the time of writing, and obtained a maximum flux density of emission of 300 mJy. Griessmeier (2011) did so for 547 exoplanets, and obtained a flux density range of  $10^{-4}$ - 610 mJy. According to this study, HD 410004 b is predicted to produce the most intense emission with a flux density of 610 mJy. Vidotto & Donati (2017) suggest that not only should we look towards close-in planets in the search for exoplanet radio emission, but towards close-in planets which orbit stars which may host powerful winds, i.e. pre-main sequence stars. Radio emission from V830 Tauri b, a close-in pre-main sequence giant planet, was estimated by Vidotto & Donati (2017). They found the flux density of emission to be between 6-24 mJy, and the frequency of emission to be 18-240 MHz, depending on the assumed planetary magnetic field strength.

A common conclusion of research done in this field is that due to the inverse square dependence of flux density on distance to the system from Earth, the strongest candidates for observation are planets of close proximity to the solar system<sup>13, 5</sup>. This is what makes the work done by Burkhart & Loeb (2017) on the predicted radio emission from Proxima Centauri b particularly interesting. Proxima Centauri, the closest star to the Sun, has a confirmed planet in its orbit; Proxima Centauri b<sup>31</sup>. This planet orbits 20 times closer to its star than the earth orbits the Sun<sup>31</sup>, and is the closest exoplanet to the solar system, making it one of the most likely candidates for producing radio emission which is detectable from Earth. It is predicted to produce radio emission of flux density >100 mJy in a frequency range of 0.02 - 3 MHz.

## **Is the Predicted Emission Detectable?**

There are a number of radio arrays operating in the low frequency range (e.g. UTR-2, GMRT, LOFAR). Currently, LOFAR offers the best frequency of operation - sensitivity combination. The Low Frequency Array (LOFAR), operates in the frequency range of 10-60 MHz, at a theoretical sensitivity limit of 21 mJy<sup>32</sup>.

Though the predicted flux density of emission of exoplanets in several studies done in this field lies above 21 mJy, attempts at observing this emission have returned no results. This could be due to a number of reasons. Vidotto & Donati (2017) theorise that the hot plasma of the host star's wind, which also may emit in the radio range, could absorb emissions from the planet embedded in it, thus preventing radiation from escaping. It is also likely that the frequency of the majority of the emissions is below that of the earth's ionospheric cutoff point. Until more information about exoplanet magnetic fields is known, the exact frequencies of exoplanetary radio emission remain uncertain.

The Square Kilometre Array (SKA) will outperform LOFAR in sensitivity, however

it is set to operate at frequencies above 50 MHz<sup>30</sup>. For planets with magnetic field strengths  $<4$  G, as is likely in the case of Proxima Cen b given its Earth-sized radius, radio emission is unlikely to be detectable with ground-based radio telescopes.

Perhaps inspiration should be taken from successful space-based exoplanet detection missions such as NASA's Kepler telescope in the quest for the detection of exoplanetary radio emission. In recent years, there has been discussion of the potential construction of a radio array on the lunar surface; Radio Observatory on the Lunar Surface for Solar Studies<sup>33, 34</sup>. This would have an enormous impact on the search for exoplanetary radio emission, allowing signals from low frequency sources, such as exoplanets, to be detected and characterised. The results found in the studies mentioned in this review should provide motivation for the building of a lunar array.

## Conclusion

Exoplanets of close proximity to the solar system are the strongest candidates for future observations in the search for detectable planetary radio emission. Proxima Cen b is of particular interest, given its close proximity to the solar system (1.3 pc). Should it have a planetary magnetic field  $>4$  G, it may produce radio emission within the frequency and sensitivity range of LOFAR ( $f > 10$  MHz,  $> 21$  mJy). However given its Earth-sized radius, it is unlikely to have a magnetic field strength  $> 1$  G, which means its emission frequency would be below the Earth's ionospheric cutoff point of 10 MHz.

The potential future construction of a radio array on the Lunar surface would be great news in the field of exoplanet radio emission. This would allow weak low frequency radio signals (such as those from exoplanets) to be detected. The detection of emission from exoplanets in the radio range would open a new path for the direct detection of exoplanets, and would also allow their magnetic fields to be characterised; a feat which has not yet been achieved.

## References

1. A. Wolszczan and D. A. Frail. A planetary system around the millisecond pulsar PSR1257 + 12. , 355:145(147, January 1992.
2. M. Perryman. The Exoplanet Handbook. May 2011.
3. W. J. Borucki, D. Koch, G. Basri, N. Batalha, T. Brown, D. Caldwell, J. Caldwell, J. Christensen-Dalsgaard, W. D. Cochran, E. DeVore, E. W. Dunham, A. K. Dupree, T. N. Gautier, J. C. Geary, R. Gilliland, A. Gould, S. B. Howell, J. M. Jenkins, Y. Kondo, D. W. Latham, G. W. Marcy, S. Meibom, H. Kjeldsen, J. J. Lissauer, D. G. Monet, D. Morrison, D. Sasselov, J. Tarter, A. Boss, D. Brownlee, T. Owen, D. Buzasi, D. Charbonneau, L. Doyle, J. Fortney, E. B. Ford, M. J. Holman, S. Seager, J. H. Steen, W. F. Welsh, J. Rowe, H. Anderson, L. Buchhave, D. Ciardi, L. Walkowicz, W. Sherry, E. Horch, H. Isaacson, M. E. Everett, D. Fischer, G. Torres, J. A. Johnson, M. Endl, P. MacQueen, S. T. Bryson, J. Dot-

- son, M. Haas, J. Kolodziejczak, J. Van Cleve, H. Chandrasekaran, J. D. Twicken, E. V. Quintana, B. D. Clarke, C. Allen, J. Li, H. Wu, P. Tenenbaum, E. Verner, F. Bruhweiler, J. Barnes, and A. Prsa. Kepler Planet-Detection Mission: Introduction and First Results. *Science*, 327:977, February 2010.
4. P. Zarka, J. Queinnee, B. P. Ryabov, V. B. Ryabov, V. A. Shevchenko, A. V. Arhipov, H. O. Rucker, L. Denis, A. Gerbault, P. Dierich, and C. Rosolen. Ground-Based High Sensitivity Radio Astronomy at Decameter Wavelengths. In H. O. Rucker, S. J. Bauer, and A. Lecacheux, editors, *Planetary Radio Emission IV*, pages 101{127, 1997.
5. J.-M. Griemeier, P. Zarka, and J. N. Girard. Observation of planetary radio emissions using large arrays. *Radio Science*, 46:RS0F09, December 2011.
6. N. Dunckel, B. Ficklin, L. Rorden, and R. A. Helliwell. Low-frequency noise observed in the distant magnetosphere with OGO 1. , 75:1854, 1970.
7. M. L. Kaiser and M. D. Desch. Radio emissions from the planets earth, Jupiter, and Saturn. *Reviews of Geophysics and Space Physics*, 22:373{384, November 1984.
8. M. D. Desch, M. L. Kaiser, P. Zarka, A. Lecacheux, Y. Leblanc, M. Aubier, and A. Ortega-Molina. Uranus as a radio source, pages 894{925. 1991.
9. J. W. Warwick, D. R. Evans, G. R. Peltzer, R. G. Peltzer, J. H. Romig, C. B. Sawyer, A. C. Riddle, A. E. Schweitzer, M. D. Desch, M. L. Kaiser, W. M. Farrell, T. D. Carr, I. de Pater, D. H. Staelin, S. Gulkis, R. L. Poynter, A. Boischof, F. Genova, Y. Leblanc, A. Lecacheux, B. M. Pedersen, and P. Zarka. Voyager planetary radio astronomy at Neptune. *Science*, 246:1498{1501, December 1989.
10. M. D. Desch and M. L. Kaiser. A radio-metric Bode's Law: Predictions for Uranus. *NASA STI/Recon Technical Report N*, 84, March 1984.
11. P. Zarka. Plasma interactions of exoplanets with their parent star and associated radio emissions. , 55:598{617, April 2007.
12. P. Zarka. Radio Emissions from the Planets and their Moons. Washington DC American Geophysical Union Geophysical Monograph Series, 119:167{178, 2000.
13. T. J. Lazio, W., W. M. Farrell, J. Dietrick, E. Greenlees, E. Hogan, C. Jones, and L. A. Hennig. The Radiometric Bode's Law and Extrasolar Planets. , 612:511{518, September 2004.
14. P. Zarka. The auroral radio emissions from planetary magnetospheres - What do we know, what don't we know, what do we learn from them? *Advances in Space Research*, 12:99{115, August 1992.
15. E. N. Parker. The Hydrodynamic Theory of Solar Corpuscular Radiation and Stellar Winds. , 132:821, November 1960.
16. E. N. Parker. Dynamics of the Interplanetary Gas and Magnetic Fields. , 128:664, November 1958.
17. H. R. Johnson, F. R. Querci, S. Jordan, R. Thomas, L. Goldberg, and J.-C. Pecker. The M-type stars. *NASA Special Publication*, 492, 1986.
18. M. H. Acuna, J. E. Connerney, R. P. Lin, D. Mitchell, H. Reme, C. Mazelle, D. Vignes, N. F. Ness, and P. Cloutier. The Magnetic Field of Mars - A Window into Mars' Past. *AGU Fall Meeting Abstracts*, pages P41A{06, December 2001.
19. I. de Pater and J. J. Lissauer. *Planetary Sciences*. December 2001.
20. F. Bagenal. *Planetary Magnetospheres*, page 251. 2013.
21. S. Chapman and V. C. A. Ferraro. A new theory of magnetic storms. Terrestrial Magnetism and Atmospheric Electricity (*Journal of Geophysical Research*), 36:77, 1931.
22. A. A. Vidotto and J.-F. Donati. Predicting radio emission from the newborn hot Jupiter V830 Tauri b and its host star. , 602:A39, June 2017.

- [23] C. S. Wu and L. C. Lee. A theory of the terrestrial kilometric radiation. , 230:621{626, June 1979.
- [24] H. O. Rucker. Solar wind influence on non-thermal planetary radio emission. *Annales Geophysicae*, 5:1{11, February 1987.
- [25] W. M. Farrell, M. D. Desch, and P. Zarka. On the possibility of coherent cyclotron emission from extrasolar planets. , 104:14025{14032, June 1999.
- [26] J. D. Kraus. *Radio astronomy*. 1966.
- [27] D. A. Gurnett. The earth as a radio source - Terrestrial kilometric radiation. , 79:4227{4238, October 1974.
- [28] W. N. Christiansen and J. A. Hoegbom. *Radiotelescopes*. 1969.
- [29] A. A. Vidotto, R. Fares, M. Jardine, J.-F. Donati, M. Opher, C. Moutou, C. Catala, and T. I. Gombosi. The stellar wind cycles and planetary radio emission of the Boo system. , 423:3285{3298, July 2012.
- [30] J.-M. Griessmeier. The search for radio emission from giant exoplanets. *Planetary Radio Emissions VIII*, pages 285{299, 2017.
- [31] G. Anglada-Escude, P. J. Amado, J. Barnes, Z. M. Berdi-nas, R. P. Butler, G. A. L. Coleman, I. de La Cueva, S. Dreizler, M. Endl, B. Giesers, S. V. Jeers, J. S. Jenkins, H. R. A. Jones, M. Kiraga, M. Kourster, M. J. Lopez-Gonzalez, C. J. Marvin, N. Morales, J. Morin, R. P. Nelson, J. L. Ortiz, A. Or, S.-J. Paardekooper, A. Reiners, E. Rodriguez, C. Rodriguez-Lopez, L. F. Sarmiento, J. P. Strachan, Y. Tsapras, M. Tuomi, and M. Zechmeister. A terrestrial planet candidate in a temperate orbit around Proxima Centauri. , 536:437{440, August 2016.
- [32] J. D. Turner, J.-M. Griessmeier, P. Zarka, and I. Vasylieva. The search for radio emission from exoplanets using LOFAR low-frequency beam-formed observations: Data pipeline and preliminary results for the 55 Cnc system. *Planetary Radio Emissions VIII*, pages 301{313, 2017.
- [33] T. J. W. Lazio, R. J. MacDowall, J. O. Burns, D. L. Jones, K. W. Weiler, L. Demaio, A. Cohen, N. Paravastu Dalal, E. Polisensky, K. Stewart, S. Bale, N. Gopalswamy, M. Kaiser, and J. Kasper. The Radio Observatory on the Lunar Surface for Solar studies. *Advances in Space Research*, 48:1942{1957, December 2011.
- [34] P. Zarka, J.-L. Bougeret, C. Briand, B. Cecconi, H. Falcke, J. Girard, J.-M. Griessmeier, S. Hess, M. Klein-Wolt, A. Konovalenko, L. Lamy, D. Mimoun, and A. Aminaei. Planetary and exoplanetary low frequency radio observations from the Moon. , 74:156{166, December 2012.

# RECENT RESEARCH ON PHASE CHANGE MATERIAL VANADIUM DIOXIDE

Jill Ivers  
Senior Sophister  
Physics

*Since its discovery in 1959, interest has grown in vanadium dioxide ( $\text{VO}_2$ ) due to its fast and reversible metal-to-insulator transition (MIT) which, unlike for most MIT materials, occurs concurrently to a structural phase transition<sup>1</sup>. This transition takes place at  $T_c = 340$  K ( $68^\circ\text{C}$ ) and can be triggered by varying temperature and other external stimuli. The phase transition is accompanied by changes in its physical properties, especially its conductivity and hence its optical properties<sup>1</sup>. Recent research on this phase change material reflects its diversity. In this review, a range of scientific articles published in the previous year are examined; articles published prior to 2018 are excluded in order to focus on the most current findings on  $\text{VO}_2$ . Modern research is concentrated on the development of simple, cost-effective and highly productive fabrication techniques of  $\text{VO}_2$ -based optical metamaterials, engineered substances with properties which are not naturally occurring. These metamaterials will allow the potential applications of this phase change material to be realised and incorporated into daily life<sup>5</sup>. Furthermore, research has been performed in order to determine the suitability of  $\text{VO}_2$  for a wide range of future applications such as use in smart optical solar reflectors as a temperature control system<sup>11</sup>,  $\text{VO}_2$ -based nanostructures for dynamic plasmonic colour generation, plasmonic-photonic actuatable waveguide modulators<sup>14</sup>. Some other applications of  $\text{VO}_2$  are; tunable optical metamaterials<sup>5</sup>, modern programmable metasurfaces<sup>4</sup>, terahertz communication and imaging applications<sup>9</sup> and the production of active terahertz chiral metamaterials based on  $\text{VO}_2$ <sup>3</sup>.*

## Introduction

Vanadium dioxide ( $\text{VO}_2$ ) is a phase change material which promises both challenges and opportunities<sup>1</sup>. Since its discovery in 1959, interest has grown in  $\text{VO}_2$  due to its fast and reversible metal-to-insulator transition (MIT). This multi stimuli-induced transition takes place at an accessible critical temperature of  $T_c = 340 \text{ K}$  ( $68^\circ\text{C}$ ) and, unlike for most MIT materials, it occurs concurrently with a structural phase change<sup>1</sup>. This review summarizes the key theory related to the structure of  $\text{VO}_2$ , its properties, the mechanism of its phase change and its various types of fabrication. We will conclude with a discussion of recent research undertaken on this phase change material and its potential applications.

## Theory

At atmospheric pressure and temperatures above  $T_c$ ,  $\text{VO}_2$  exhibits metallic properties due to an increase in the free carrier concentration<sup>4</sup>. Metallic  $\text{VO}_2$  has a tetragonal (rutile) structure: its Bravais lattice consists of a rectangular prism with a square base (length  $a$  and width  $b$ ) and height ( $c$ ), shown in Figure 1 (a)<sup>5</sup>. The lattice constants of  $\text{VO}_2(\text{R})$  are  $a=b \approx 4.55 \text{ \AA}$  and, along the  $C_R$  axis, the single V-V distance is  $c \approx 2.88 \text{ \AA}$ . This is shorter than the critical V-V interaction distance of  $2.94 \text{ \AA}$ <sup>1</sup>. Thus, the d-orbitals are shared by all vanadium atoms and therefore metallic properties are exhibited.

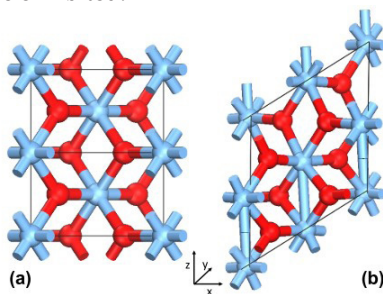


Figure 1: *Crystal structure of (a) metallic  $\text{VO}_2(\text{R})$  and (b) insulating  $\text{VO}_2(\text{M1})$* <sup>5</sup>.

Below the critical temperature, this phase change material undergoes a structural phase transition to monoclinic structure (M1)<sup>1</sup>, shown in Figure 1(b)<sup>5</sup>. The three defining lattice constants are of unequal lengths:  $a \approx 5.75 \text{ \AA}$ ,  $b \approx 4.53 \text{ \AA}$  and  $c \approx 5.38 \text{ \AA}$  and the third vector encounters the other two at an angle  $\beta=122.6^\circ$ <sup>1</sup>. Due to the two different V-V distances, the formation of a dimer and the localisation of d-orbitals occurs<sup>5</sup>. As a result, semiconducting properties are exhibited. The unit cell doubles in size and chains of vanadium atoms at the edges of the cell show zig-zag behaviour<sup>2</sup>.

Below the critical temperature an indirect energy band gap of  $0.45 \text{ eV}$  is exhibited

by  $\text{VO}_2$ <sup>5</sup>, resulting in insulating or semiconducting behaviour. This is evident in Figure 2<sup>5</sup>, the electronic band structure plots for the semiconducting and metallic phases respectively.

However, when  $\text{VO}_2$  undergoes a phase transition its electronic properties change, which has piqued the interest of the scientific community. In the electronic structure for metallic  $\text{VO}_2$ <sup>2,5</sup>, the energy bands are shift upwards and overlap with the Fermi energy. However, the electronic properties of  $\text{VO}_2$  are highly anisotropic<sup>5</sup> and are dependent on the substrate on which the film is grown. They are also susceptible to the addition of dopants<sup>2</sup>. Furthermore, during the phase transition abrupt changes occur to the lattice structure and constants, accompanied by significant changes in electrical and thermal conductivity, emissivity, optical properties, i.e. dielectric function and magnetic susceptibility<sup>2</sup>.

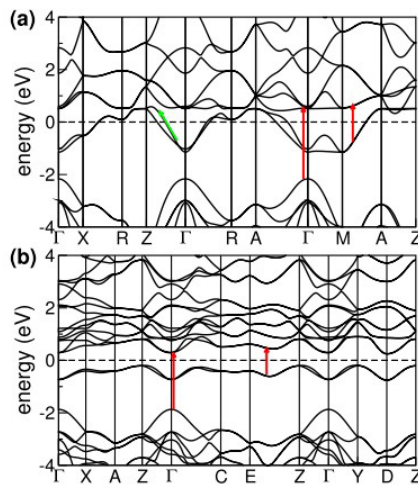


Figure 2: Electronic band structure of (a) metallic  $\text{VO}_2$  and (b) insulating  $\text{VO}_2$ . The Fermi level is denoted by the dotted lines. Red arrows indicate interband and green arrows mark intraband transitions respectively<sup>5</sup>.

For example, Liu et al. described a step-like decrease in magnetic susceptibility as metallic  $\text{VO}_2$  cools to semiconducting  $\text{VO}_2$ <sup>1</sup>. This material's behaviour follows the Curie-Weiss law above  $T_c$ ; below the critical temperature the magnetic susceptibility has a small, constant value<sup>1</sup>. With increasing temperature, the electrical conductivity increases of up to five orders of magnitude due to the overlapping of the energy band in the crystal<sup>2</sup>. As  $\text{VO}_2$  transitions from an insulator to metal, the complex refractive index of  $\text{VO}_2$  undergoes a wavelength-dependant modification. While in the UV and visible spectral range the changes are rather small, moderate significant changes are observed in the near IR during the MIT<sup>6</sup>.

When  $\text{VO}_2$  is in its metallic phase, there is an interaction between light irradiated

upon it and the collective oscillation of conductive electrons, so-called plasmons. This leads to mixed electromagnetic waves and surface-charges<sup>8</sup>. Consequently, this phase change material has interesting plasmonic components which play an important role in its properties.

Due to the fast phase change, the debate concerning the mechanism of the structural phase transition is ongoing and more than one model is needed to explain it. Goodenough et al. theorized the reorganization of the band structure during the MIT<sup>1</sup>. Peierls believed the transition was the result of lattice distortion; Mott indicated that the transition was electron correlation driven<sup>1</sup>. It is likely an intermediate between the two, 'Mott-assisted Peierls' can most accurately describe the process to date.

There are a number of types of fabrication of VO<sub>2</sub> including pulsed laser deposition, sol-gel method, chemical vapour deposition, molecular beam epitaxy, reactive-based target ion beam deposition, electron beam evaporation and crystallization<sup>9</sup> to name just a few. In order to use this material in large-scale productions, a simple but highly productive fabrication technique needs to be developed first and a number of issues must be overcome such as the mild toxicity of VO<sub>2</sub><sup>2</sup>.

## Recent Research on VO<sub>2</sub>

Due to its fast and reversible MIT, VO<sub>2</sub> has been key to multiple research articles published in 2018. In this section, a review of a potential large-scale fabrication method of VO<sub>2</sub> will be discussed, followed by developments on optical solar reflectors, plasmonic colour generation, waveguide modulators, VO<sub>2</sub> metamaterial junctions, modern programmable metasurfaces, VO<sub>2</sub> in the use of THz waves in communication and imaging and finally, chiral metamaterials.

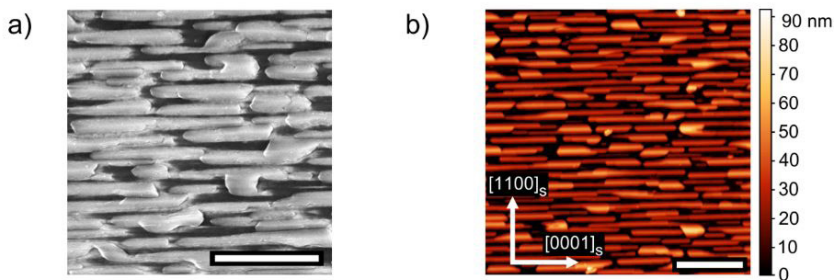


Figure 3: a) Scanning electron microscope and (b) atomic force microscopy images of VO<sub>2</sub> film. Scales bars are 0.5 and 1 μm respectively. The labels in (b) denote the crystallographic directions of the surface of the sapphire substrate<sup>10</sup>.

Whilst thermally-induced phase transition has dominated previously, interest is now turning to alternative stimulus responses of the MIT of  $\text{VO}_2$  and new fabrication methods. The development of a simple but highly productive method of fabrication is needed; a concept tackled by Ligmajer et al., who proposed a route to the large-scale production of switchable dielectric metasurfaces using  $\text{VO}_2$  nanostructures<sup>10</sup>. Improving upon the previous fabrication of tunable materials with top-down nanostructuring, this paper discussed the epitaxially growth of nanobeams of  $\text{VO}_2$ . Using pulsed laser deposition, the thin films were produced in a one-step epitaxial growth process. Figure 3<sup>10</sup> shows scanning electron microscope and atomic force microscopy images of the  $\text{VO}_2$  surface grown epitaxially on a sapphire substrate. Ligmajer et al. reported that the nanobeams supported plasmonic components in metallic  $\text{VO}_2$ , such as localized surface plasmons. Thus, it was concluded that large-scale anisotropic nanostructures of  $\text{VO}_2$  can be produced using this method and may prove to be useful in transmission control due to the recorded modulation depth of greater than 9 dB in the telecommunications wavelength bands<sup>10</sup>.

Sun et al. used the  $\text{VO}_2$  MIT to produce a smart optical solar reflector for future use as a passive thermal control system in spacecrafts<sup>11</sup>. A patterned thermochromic metasurface consisting of  $\text{VO}_2$  nanoboxes on top of an optical solar reflector was fabricated. As a spacecraft or satellite orbits the Earth, thermal fluctuations may be damage the electronic devices, reducing their lifetime. Hence, an internal temperature control system is necessary to maintain reduced emittance at low temperatures to prevent the devices becoming too cold, and increased emittance at high temperatures to avoid overheating. It follows a unique, switchable material with a thermally-induced MIT is a possible solution for improving the emittance tunability. Sun et al. lowered the critical temperature of  $\text{VO}_2$  to room temperature by doping the metamaterial with tungsten. An enhanced emittance tunability of 0.48 was observed, a 30% improvement upon the corresponding unstructured film<sup>11</sup>.

Recently  $\text{VO}_2$  has been used for structural colour generation, i.e. dynamic plasmonic colour generation. Shu et al. discussed the advantageous MIT of  $\text{VO}_2$  and the combination of  $\text{VO}_2$  with noble metal plasmonic nanostructures to tune their optical properties<sup>12</sup>. This involved the fabrication of silver nanodisks arrays on a thin film of  $\text{VO}_2$ . Different colours across the visible spectrum could be produced by tuning the spatial periodicity of the arrays and the diameter of the nanodisks<sup>12</sup>. Furthermore, Song et al. proposed the similar combinations of  $\text{VO}_2$  with noble metal plasmonic nanostructures for plasmonic tunable colour filters and photodetectors<sup>13</sup>. Their numerical simulations indicate broadband multifunctional properties, such as multiple resonant modes, by the integration of  $\text{VO}_2$  into a so called metamaterial absorber. Due to the advantageous multi-functionally, flexibility and high efficiency of the dynamic plasmonic colour tuning by making use of the MIT of  $\text{VO}_2$ , future possible applications include plasmonic colour filter and printing, and imaging technologies<sup>12</sup>.

Clark et al. investigated the creation of an optically pumped hybrid plasmonic-

photonic actuatable waveguide modulator using the phase change of  $\text{VO}_2$ , shown in Figure 4<sup>14</sup>. The construction of this device involved the combination of a subwavelength  $\text{Au}/\text{VO}_2$  nanostructure with a silicon waveguide. An optical pump signal propagating in the silicon waveguide was focused into the phase change material and thus the MIT was optically induced. Due to its metallic properties, metallic  $\text{VO}_2$  could restrict light to subwavelength dimensions. An extinction ratio of 26.85 dB/ $\mu\text{m}$  and length 440 nm was recorded<sup>14</sup>.

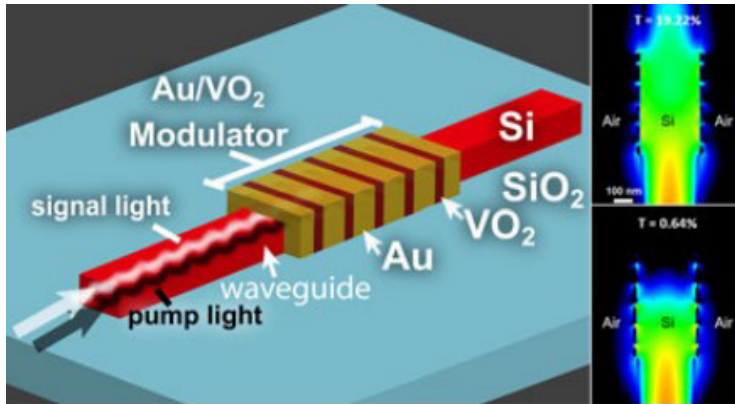


Figure 4: An illustration of a hybrid  $\text{VO}_2$  all-optical modulator<sup>14</sup>

An interesting paper by Eaton et al. discussed the concept of a  $\text{VO}_2$  junction metamaterial, a metamaterial sample with a mixture of metallic and insulating  $\text{VO}_2$  gave optical properties different from those of either of the separate materials. The resulting rigid-structured junction sample had tunable optoelectronic properties and anisotropic permittivity<sup>5</sup>, which has the potential to excite propagating volume plasmon polaritons, a fundamental excitation of light-matter interactions on the nanoscale<sup>5</sup>. Thus, the optical properties at a given wavelength could be controlled by varying the amount of insulating  $\text{VO}_2$  in a device, which potentially leads to a new class of metamaterials<sup>5</sup>.

Liu et al. included  $\text{VO}_2$  in the discussion of modern programmable metasurfaces and the multiple functionalities that can be controlled by external stimuli in phase change materials<sup>4</sup>. Reference was made to the thermally-induced MIT and its potential to shift the optical resonance frequency, alter the transmission amplitude and control the polarization of the transmitted electromagnetic wave<sup>4</sup>.

Zhao et al. discussed the photoinduced controlling of the phase shift of terahertz waves in  $\text{VO}_2$  nanostructures<sup>9</sup>. In order to use terahertz (THz) waves in communication and imaging, phase modulation devices must be developed. A ring-dumbbell composite resonator with  $\text{VO}_2$  nanostructures was fabricated. Figure 5<sup>9</sup> shows an X-ray diffraction pattern and a scanning electron microscope image of  $\text{VO}_2$  on a quartz substrate. In order to produce a large phase shift, a hybrid resonant mode coupled by L-C and dipole resonance was produced. A noticeable

improvement was recorded in the resonant frequency peak<sup>9</sup>. A phase shift of 138° was observed near 0.6 THz. Within 55 GHz bandwidth, the phase shift exceeded 130°. Thus, the fabricated compact nanostructure produced a significant switching property during the MIT.

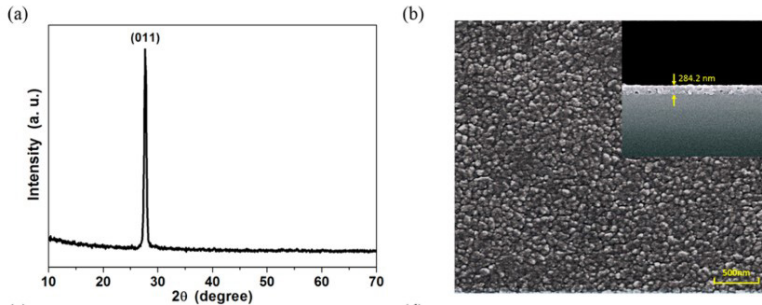


Figure 5: (a) X-ray diffraction pattern of VO<sub>2</sub> with peak at (001) and (b) scanning electron microscope image of VO<sub>2</sub> showing its thickness of 284.2 nm on a quartz substrate<sup>9</sup>

Finally, Wang et al. investigated the production of active terahertz chiral metamaterials based on VO<sub>2</sub><sup>3</sup>. It was observed that large controllable chiroptical responses could be generated by a fabricated VO<sub>2</sub>/gold twisted fishnet metamaterial. This hybrid metamaterial allowed for dynamically tuneable chiroptical responses at THz frequencies. A circular dichroism of 40° and polarization rotation of 200°/λ were observed at 0.7 THz<sup>3</sup>. It was suggested that the active control of polarization states of a transmitted THz wave could be invaluable in potential applications such as plasmon-enhanced biosensing<sup>3</sup>.

## Discussion and Conclusion

This review presented some of the recent progresses on the research and applications of phase change material VO<sub>2</sub>. This material is unique with its multi stimuli-responsive structural and metal-to-insulator phase transition at a conveniently attainable temperature of 68°C. Resulting changes in a wide range of physical properties make this phase change material a valuable resource for many applications.

Advances in the epitaxially growth of nanobeams of VO<sub>2</sub> may lead to an effective technique for the large-scale production of anisotropic nanostructures of VO<sub>2</sub><sup>10</sup>. This in turn will enable this material to be considered for an even wider range of applications<sup>1</sup>. VO<sub>2</sub> may be used in smart optical solar reflectors as a temperature control system<sup>11</sup>. VO<sub>2</sub>-based nanostructures may be used in dynamic plasmonic colour generation. Additionally, the fabrication of VO<sub>2</sub> in an optically pumped hybrid metamaterial leads to applications such as a plasmonic-photonic actuable waveguide modulators<sup>14</sup>. A junction of both metallic and insulating VO<sub>2</sub> has been

fabricated and its potential to excite propagating volume plasmon polaritons has been investigated<sup>5</sup>. VO<sub>2</sub> may be used in the production of modern programmable metasurfaces<sup>4</sup>. Lastly, the photoinduced controlling of the phase shift of terahertz waves in VO<sub>2</sub> nanostructures is used for communication and imaging<sup>9</sup> and production of active terahertz chiral metamaterials based on VO<sub>2</sub><sup>3</sup>.

It is possible to conclude from this review that the research taking place on this phase change material is diverse and interdisciplinary with applications ranging from biosensing to solar reflectors. Further development of simple, cost-effective and highly productive fabrication techniques of VO<sub>2</sub>-based metamaterials will allow the potential applications of this phase change material to be realised and incorporated into daily life<sup>5</sup>.

## Acknowledgements

This work was adapted from a research report “Dynamic Tuning of Plasmonic Components Based on Phase Change Materials” for course PYU4PP2 submitted in January 2019.

## References

1. Liu K, Lee S, Yang S, Delaire O, Wu J. Recent progresses on physics and applications of vanadium dioxide. *Mater Today* [Internet]. Elsevier Ltd; 2018;xxx(xx):1–22.
2. Ke Y, Wang S, Liu G, Li M, White TJ, Long Y. Vanadium Dioxide: The Multistimuli Responsive Material and Its Applications. *Small* [Internet]. 2018;1802025:1802025.
3. Wang S, Kang L, Werner DH. Active Terahertz Chiral Metamaterials Based on Phase Transition of Vanadium Dioxide (VO<sub>2</sub>). *Sci Rep* [Internet]. Springer US; 2018;8(1):1–9.
4. Liu F, Ptilakis A, Mirmoosa MS, Tsilipakos O, Wang X, Tasolamprou AC, et al. Programmable Metasurfaces: State of the Art and Prospects. 2018;
5. Eaton M, Catellani A, Calzolari A. VO<sub>2</sub> as a natural optical metamaterial. *Opt Express* [Internet]. 2018;26(5):5342.
6. Cormier P, Son TV, Thibodeau J, Doucet A, Truong V Van, Haché A. Vanadium dioxide as a material to control light polarization in the visible and near infrared. *Opt Commun* [Internet]. Elsevier; 2017;382:80–5.
7. Su V-C, Chu CH, Sun G, Tsai DP. Advances in optical metasurfaces: fabrication and applications [Invited]. *Opt Express* [Internet]. 2018;26(10):13148.
8. Giannini V, Fernández-Domínguez AJ, Heck SC, Maier SA. Plasmonic nanoantennas: Fundamentals and their use in controlling the radiative properties of nanoemitters. *Chem Rev*. 2011;111(6):3888–912.
9. Zhao Y, Zhang Y, Shi Q, Liang S, Huang W, Kou W, et al. Dynamic Photoinduced Controlling of the Large Phase Shift of Terahertz Waves via Vanadium Dioxide Coupling Nanostructures. *ACS Photonics*. 2018;5(8):3040–50.
10. Ligmajer F, Kejik L, Tiwari U, Qiu M, Nag J, Konečný M, et al. Epitaxial VO<sub>2</sub>Nanostructures: A Route to Large-Scale, Switchable Dielectric Metasurfaces. *ACS Photonics*. 2018;5(7):2561–7.

11. Sun K, Riedel CA, Urbani A, Simeoni M, Mengali S, Zalkovskij M, et al. VO<sub>2</sub> Thermochromic Metamaterial-Based Smart Optical Solar Reflector. *ACS Photonics*. American Chemical Society; 2018;5(6):2280–6.
12. Shu FZ, Yu FF, Peng RW, Zhu YY, Xiong B, Fan RH, et al. Dynamic Plasmonic Color Generation Based on Phase Transition of Vanadium Dioxide. *Adv Opt Mater*. 2018;6(7).
13. Song S, Ma X, Pu M, Li X, Guo Y, Gao P, et al. Tailoring active color rendering and multiband photodetection in a vanadium-dioxide-based metamaterial absorber. *Photonics Res*. 2018;6(6):492–7.
14. Clark JK, Ho Y-L, Matsui H, Delaunay J-J. Optically Pumped Hybrid Plasmonic-Photonic Waveguide Modulator Using the VO<sub>2</sub> Metal-Insulator Phase Transition. *IEEE Photonics J* [Internet]. 2018;10(1):1–9.

TS  
SR

# WORTH ITS SALT? A STUDY OF SALINITY GENERATED ENERGY AND ITS (ELECTRICAL) CURRENT CHALLENGES

Pierce Sinnott

Junior Sophister

Nanoscience, Physics and Chemistry of Advanced Materials

*Salinity Gradient Energy (SGE) refers to the Gibbs free energy dissipated by the mixing of two solutions of different concentrations, typically of salt (sodium chloride), as such solutions are readily available in low concentration in fresh/river water and higher concentration in sea water or brine. Harvesting this energy was first proposed by Pattle in 1954. Mechanisms to achieve this through pressure retarded osmosis or reverse electrodialysis were set forth by Pattle in 1973 and Loeb in 1977 respectively<sup>1, 2</sup>. Recent development in polymer and material physics necessary to create cost-efficient, mechanically and chemically suitable membranes have led to a recent revitalisation of the field<sup>3</sup>, including new techniques proposed as recently as 2009 such as BattMix and CapMix<sup>4</sup>. In this review, the basis of pressure retarded osmosis and reverse electrodialysis are discussed, alongside their advantages and current boundaries to implementation.*

## Introduction

In 2018, the United Nation's Intergovernmental Panel on Climate Change released a special report warning that urgent and unprecedented action must be undertaken within the next 12 years to limit global warming to a maximum of 1.5°C<sup>5</sup>. This dire message contrasts with the US Department of Energy's expectation of a global increase in energy consumption of 48% between 2012 and 2040, with a corresponding 46% increase in anthropogenic carbon dioxide emissions<sup>6</sup>. This clearly necessitates increased emphasis, development and support for renewable energy sources. While a number of these are commonplace and widely known, namely solar, wind, hydro-, geothermal and biomass, Salinity Gradient Energy (SGE) is a lesser known though promising complement to existing energy production.

There are few studies of CapMix and BattMix technologies as they have only come about recently. Consequently, the scope of this review shall be limited to Pressure Retarded Osmosis (PRO) and Reverse Electrodialysis (RED).

## Osmosis: Physical Effects and Mathematical Description

Osmosis describes the flow of a solvent through a semipermeable membrane in order to equalise concentrations of two solutions separated by this membrane (here denoted with more saline/salt water or high concentration, HC and freshwater or low concentration, LC). This gives rise to an osmotic pressure defined by the van't Hoff equation, whereby

$$\pi = i c R T \quad (1)$$

where  $\pi$  is osmotic pressure,  $i$  is the van't Hoff factor,  $c$  is the molar solute concentration,  $R$  and  $T$  are the gas constant and absolute temperature respectively<sup>7</sup>. This osmotic pressure represents the pressure that, if applied to the HC solution, would cause the osmotic transfer of water across the membrane to become thermodynamically unfavourable and cease<sup>8</sup>. Applying greater pressures than the osmotic is referred to as reverse osmosis, where instead water flux is from HC to LC solution, and is widely applied in desalination<sup>9</sup>.

The maximum flux through such a semi-permeable membrane,  $J$ , is described by

$$J = A (\Delta\pi - \Delta P) \quad (2)$$

with permeability coefficient of the membrane  $A$ ,  $\Delta\pi$  the difference in osmotic pressure across the membrane and  $\Delta P$  the difference in hydrostatic pressure between the two solutions<sup>10</sup>. Consequently, flow rate of water across the membrane,  $\Delta V$ , can be defined by

$$\Delta V = J A_m \quad (3)$$

with  $A_m$  membrane area. Hence, the maximum ideal work obtainable is

$$W_{net}^{max} = P_D \Delta V \quad (4)$$

Where  $P_D$  is the constant applied pressure. This is achieved at 100% efficiency. In reality, we must include an efficiency factor,  $\eta$ , in order to account for imperfect mechanical efficiency giving  $\eta P_D \Delta V$ . A membrane power density,  $D$ , the power obtainable per unit area of membrane is defined by

$$D = J P_D, \text{ or } D = A (\Delta\pi - \Delta P) P_D \quad (5)$$

and setting  $\Delta P$  as  $P_D$ , we see through differentiation with respect to  $P_D$  that

membrane power density is maximised where

$$P_D = \frac{\Delta\pi}{2} \quad (6)$$

Hence, the optimal operating pressure for the HC solution is half of the osmotic pressure difference across the membrane<sup>8</sup>.

## Free Energy of Mixing

Mixing two solutions of different concentration releases energy described by Gibbs' free energy of mixing,  $\Delta G_{mix}$ . This describes the energy that is lost to entropy where the two solutions are directly mixed.  $\Delta G_{mix}$  represents the maximum theoretical amount of energy available, under a reversible, isothermal process<sup>4</sup>.

This mixing occurs in nature where freshwater rivers meet saltwater bodies, and these sites could be adapted for salinity gradient energy production<sup>11</sup>. Here, the Gibbs' energy can be calculated by

$$\Delta G_{mix} = G_B - (G_{HC} + G_{LC}) \quad (7)$$

with  $G_B$  being the brackish water (a mixture of saltwater and freshwater) resulting from the recombination of the HC and LC.  $G_{HC}$  and  $G_{LC}$  are the Gibbs free energy of the high and low concentrations respectively. Assuming ideal solutions, for an aqueous solution where the solute has completely dissociated, as occurs with highly ionic salt such as sodium chloride, the  $\Delta G_{mix}$  is given by

$$\frac{-\Delta G_{mix}}{RT} = \left[ \sum x_i \ln(i x_i) \right]_B - \phi \left[ \sum x_i \ln(i x_i) \right]_{LC} - (1 - \phi) \left[ \sum x_i \ln(i x_i) \right]_{HC} \quad (8)$$

where  $x_i$  is the mole fraction of the  $i$ -th species,  $\phi$  is the ratio of moles of LC to the total moles in system, and these species have activity  $i$ . The rest is as defined as before<sup>4</sup>.

Greater salinity gradients result in greater  $\Delta G_{mix}$ . The mixing of  $1\text{m}^3$  of seawater with  $1\text{m}^3$  of river water dissipates approx. 2.6 MJ, which accounts for about 1 MJ at the suggested feasible 40% efficiency<sup>7</sup>. For hypersaline sources (taken here as 5.3 M NaCl solutions), this value is multiplied by up to 11<sup>2</sup>. The global osmotic pressure gradient energy has been estimated to be 1750 – 2000 TWh/year, or half of current hydropower energy generation<sup>9</sup>. However, harnessing this energy has proven difficult.

The two most prominent and promising techniques to harness this energy through salinity gradient power generation are pressure-retarded osmosis (PRO) and reversed electrodialysis (RED). Both methods emit zero carbon emissions in energy generation and are abundant, while also suffering from none of the

problems of periodicity of supply of some other renewable energies<sup>8</sup>.

## Pressure Retarded Osmosis

The simplest PRO system consists of a pressurised HC solution and LC solution at ambient pressure separated by a semipermeable membrane. Water permeates from less to more concentrated solution by osmosis. The more saline solution becomes less concentrated as this process continues. This increased volume of the HC is a form of mechanical energy<sup>12</sup>. The HC solution is passed through a pressure exchanger to increase pressure to a constant applied pressure  $PD$ . This must be less than the osmotic pressure difference to avoid reverse osmosis as per equation 1. Furthermore, equation 6 shows that a total pressure of half of the osmotic pressure maximises efficiency. Pressure is also applied to the HC solution to reduce and ensure flow rate is steady, and to cause the eponymous osmotic pressure retarding<sup>4</sup>. In the hydro turbine,  $PD$  is reduced to zero and the mechanical work converted to useful electrical work.

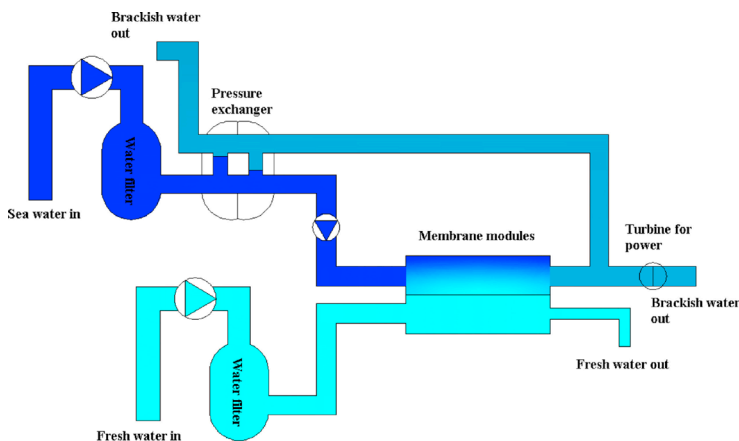


Figure 1: A simple demonstration of the workings of a PRO system, featuring the main processes performed on each input solution<sup>13</sup>.

## Reverse Electrodialysis

RED consists of a series of repeating units, where a HC solution is bounded on either side by an anion exchange membrane and cation exchange membrane (AEM, CEM), with LC solution upon the opposite sides of either membrane. Donnan exclusion ensures that only the appropriate type of ion can pass through their respective ion exchange membranes (IEM)<sup>12, 14</sup>. Hence, ion selectivity and mass transportation capacity are important aspects of membrane design<sup>1</sup>. These

IEMs consist of fixed-charged groups attached to a polymer backbone<sup>3</sup>. The CEM and AEM contain electrical equilibriums of fixed negative charges and mobile cations, and fixed positive charges and mobile anions respectively. The concentration gradient applied across the IEM attracts counterions and repels coions. As counterions can more easily pass through their respective IEM, a net ionic flow and hence electrochemical potential is set up with oppositely charged ions travelling in opposite directions<sup>16</sup>. A number of these cells are connected into a single RED stack with a redox couple or capacitive electrodes converting this ion flow to electric current<sup>4,14</sup>. A representative sample of this is seen in figure 2 below.

The total circuit force, or Open Circuit Voltage (OCV) is derived from the Nernst equation as

$$OCV = \frac{NRT}{F} \left( \frac{\alpha_{CEM}}{z_{ca}} \ln \frac{\gamma_{HC} \cdot C_{HC,ca}}{\gamma_{LC} \cdot C_{LC,ca}} + \frac{\alpha_{AEM}}{z_{an}} \ln \frac{\gamma_{HC} \cdot C_{HC,an}}{\gamma_{LC} \cdot C_{LC,an}} \right) \quad (9)$$

with N membrane pairs, cathode and anode denoted by subscripts ca and an respectively, ion permselectivity  $\alpha$  and activity coefficients  $\gamma$ <sup>17</sup>. Permselectivity describes the ability of the IEM to transport only their named type of counter-ion: cations in the CEM and anions in the AEM. Clearly, an increased concentration gradient, as seen in the argument of the natural logarithm, increases this OCV, as well as increased permselectivities.

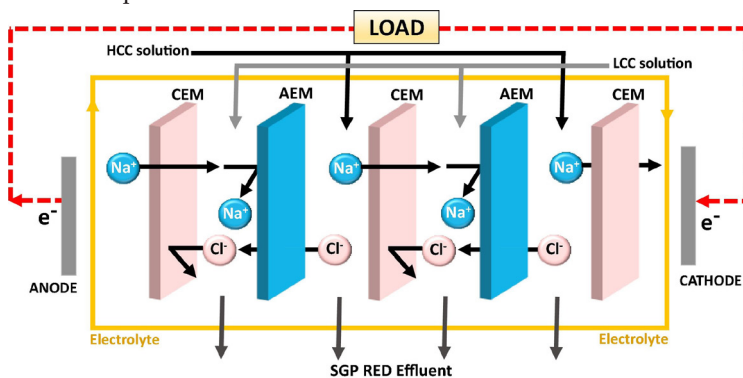


Figure 2: A reduced representation of the overall RED stack formed by connecting a number of RED cells. Ion flow, ion exchange membranes (IEMs) and alternating positions of HC and LC solutions are highlighted<sup>17</sup>.

## Analysis of the Membrane

The main barrier to widespread implementation of these SGE processes lies with the membranes. In RED, the requirements for commercially available IEMs include high permselectivity, low electrical resistance, resistance to fouling, suitable

mechanical and chemical stability to ensure a long lifetime and low production cost.

These and other essential properties such as ion exchange capacity depend greatly on the IEM's chemical structure and polymer basis. Existing IEMs used in fuel cells and electrolyzers prove unsuitable for the purpose of SGE, as those membranes are designed for operation under strongly acidic environments and often using divalent ions rather than monovalent sodium and chloride ions<sup>17</sup>. A number of IEMs have been tested in a laboratory setting, including by Długolecki et al, who in 2008 recorded power densities of 5 W/m<sup>2</sup> and 4 W/m<sup>2</sup> for AEMs and CEMs respectively, with densities of 6W/m<sup>2</sup> anticipated with membranes specifically designed for RED<sup>3</sup>. Differences in properties of Na<sup>+</sup> and Cl<sup>-</sup> ions, such as mobility, diffusion and ion radius result in these different interactions with their IEMs and hence power densities. No membrane has yet distinguished itself as a clear favourite and development continues. Nonetheless, the most recent available research from 2018 indicates that IEMs based on sulfonated polyetheretherketone (SPEEK) and polyvinyl alcohol (PVA)<sup>17</sup> and polymer/metal-organic framework (MOF) hybrid membranes show high promise. These two materials boasted maximum membrane power densities of 1.3 and 2.87 W/m<sup>2</sup> respectively in practical settings<sup>14</sup>,<sup>17</sup> with the greatest potential to be economically viable. Their nanosized pores and asymmetric ion channels perform the necessary roles of selective filters and ion rectifiers, while also being readily customisable<sup>15</sup>.

## Sources of High and Low Concentration Solutions

While it has previously been estimated by Logan et al<sup>18</sup> that total global SGE arising from mixing of fresh and seawater at estuaries is 2.6 TW, the extractable amount is estimated at 2000 TWh/year<sup>18</sup>. Development of this technology could become profitable earlier by exploiting certain sources of hypersaline water: whether anthropogenic in desalination plants or natural such as the Dead Sea, Great Salt Lake or salt domes, natural underground solid salt reservoirs. The concentrations of salt in seawater and river water are broadly accepted as 35 g/L and 88 mg/L respectively<sup>4</sup>. Such hypersaline sources can provide salinity gradients up to 11 times greater than that of typical seawater sources. Such hypersaline sources are more suited towards RED than PRO. However, as optimal applied pressure for PRO is approximately half of the osmotic pressure, this is much more likely to strain or damage PRO membranes than RED which require lower pressures for hypersaline sources. Usage of hypersaline water from desalination plants and the potential usage of urban wastewater as the freshwater input would allow for a greater number of sites, while also potentially incorporating current waste water treatment, to avoid fouling of the membranes<sup>19</sup>. Permselectivity also decreases with increasing concentration, requiring IEMs with greater fixed charge densities to maintain Donnan exclusion<sup>4</sup>.

Increasing concentration gradient also results in concentration polarisation. This refers to varying concentration profile across the system, for example with lower concentration near incoming water flux and greater at the LC-membrane interface<sup>9</sup>. Therefore, a salt build-up at the membrane interfaces can occur, which reduces effective osmotic pressure, necessitating a careful balancing act. Small leakages of sodium chloride through the membrane is also inevitable and contributes to this concentration polarisation<sup>8, 19</sup>. Increased turbulence and flow rate have been found to be generally ineffective in remedying this, though changes in support layer morphology and water permeation flux can prove effective<sup>9</sup>.

The usage of seawater as the HC solution or wastewater/grey water as the LC solution exacerbates the problem of fouling. Dissolved organic matter, microbes forming biofilms and colloids can reduce efficiency in PRO and RED by up to 60%. Pre-treatment of the input water can resolve such fouling, though naturally increases expense and limits practicability of these systems<sup>4</sup>.

While these methods of SGE are lauded for their environmentally friendly design and zero carbon emissions, some environmental impacts are unavoidable, as with all anthropogenic endeavours. These include land modification, potential habitat disruption and discharge of pollutants, potentially including brackish water. However, these can be minimised through implantation of pilot schemes and rigorous site-specific analysis and are substantially less harmful than any form of fossil fuel<sup>20</sup>.

## Concluding Remarks

The theory of Salinity Gradient Energy is well established, and put to practice in a number of labs and test sites worldwide. The current challenges are largely material based, with a number of active research groups across Spain, Singapore, Japan, the Middle East, Australia, Norway, China and South Korea developing solutions<sup>21</sup>.

Statkraft, a Norwegian state power company and Europe's largest single generator of renewable energy<sup>22</sup>, operated a 10 kW PRO plant in Norway from 2009 until 2012. The project was discontinued due to cost inefficiencies stemming from the expense of the necessary membranes<sup>20</sup>. While this project not being resumed indicates that is not yet commercially viable, the three-year testing period nonetheless clearly showed the validity of the fundamental mechanisms and design, requiring only the final puzzle piece of a suitable and cost-effective membrane.

Skillhagen estimates a minimum membrane energy density of 5 W/m<sup>2</sup> for commercial viability of whole system<sup>23</sup>. Although theoretical and indeed lab values far surpass this, commercial values have yet to. With the often unsteady rate of material development, estimates for the time scale of implementation of these technologies are vague at best in the accompanying literature. As such, these SGE

techniques require further study, especially promising newer methods including CapMix as part of a holistic approach towards sustainable energy development.

## References

1. R.E. Pattle. "Production of Electric Power by Mixing Fresh and Salt Water in the Hydroelectric Pile". *Nature*, 174 (1954), pp. 660.
2. S. Loeb. "Method and apparatus for generating power utilizing reverse electrodiolysis". US Patent 4,171,409.
3. P. Długołęcki; K. Nymeijer; S. Metz and M. Wessling. "Current status of ion exchange membranes for power generation from salinity gradients". *J Membr Sci*, 319 (2008), pp. 214-222.
4. Ngai Yin Yip, Doriano Brogioli, Hubertus V. M. Hamelers, and Kitty Nijmeije. "Salinity Gradients for Sustainable Energy: Primer, Progress, and Prospects". *Environ. Sci. Technol.* 2016, 50, pp. 12072-12094. October 10, 2016.
5. [V. Masson-Delmotte, P. Zhai, H. O. Pörtner, D. Roberts, J. Skea, P. R. Shukla, A. Pirani, W. Moufouma-Okia, C. Péan, R. Pidcock, S. Connors, J. B. R. Matthews, Y. Chen, X. Zhou, M. I. Gomis, E. Lonnoy, T. Maycock, M. Tignor, T. Waterfield (eds.)]. "IPCC, 2018: Summary for Policymakers. In: Global warming of 1.5°C. An IPCC Special Report on the impacts of global warming of 1.5°C above pre-industrial levels and related global greenhouse gas emission pathways, in the context of strengthening the global response to the threat of climate change, sustainable development, and efforts to eradicate poverty". *World Meteorological Organization*, Geneva, Switzerland, pp 1-32 .
6. U.S. Energy. "Information administration, international energy outlook". U.S Department of Energy (2016).
7. Uri Lachisha. "Osmosis and thermodynamics". *Am. J. Phys.* 75, 11, November 2007 pp. 997-998.
8. Fernanda Helfer and Charles Lemkert. "The power of salinity gradients: An Australian example". *Renewable and Sustainable Energy Reviews*. Volume 50, October 2015, pp 1-16.
9. Gang Han; Sui Zhang; Xue Li and Tai-Shung Chung. "Progress in pressure retarded osmosis (PRO) membranes for osmotic power generation". *Progress in Polymer Science*. Volume 51, December 2015, pp 1-27.
10. C Fritzmann; J Löwenberg; T Wintgens and T. Melin. "State-of-the-art of reverse osmosis desalination". *Desalination*, 216, pp. 1-76. 2007.
11. Caitlin Seyfried; Hannah Palko and Lindsay Dubbs. "Potential local environmental impacts of salinity gradient energy: A review". *Renewable and Sustainable Energy Reviews*. Volume 102, March 2019, pp 111-120.
12. Zhen Lei Cheng; Xue Li and Tai-Shung Chung. "The forward osmosis-pressure retarded osmosis (FO-PRO) hybrid system: A new process to mitigate membrane fouling for sustainable osmotic power generation". *Journal of Membrane Science*. Volume 559, 1 August 2018, pp. 63-74.
13. Zhijun Jia; Baoguo Wang; Shiqiang Song and Yongsheng Fan. "Blue energy: Current technologies for sustainable power generation from water salinity gradient". *Renewable and Sustainable Energy Reviews*, Volume 31, March 2014, pp 91-100.
14. IUPAC. "Compendium of Chemical Terminology, 2nd ed." (the "Gold Book"). Compiled by A. D. McNaught and A. Wilkinson. Blackwell Scientific Publications, Oxford (1997). XML on-line corrected version: <http://goldbook.iupac.org> (2006-) created by M. Nic, J. Jirat, B. Kosata; updates compiled by A. Jenkins.
15. Ruirui Li; Jiaqiao Jiang; Qingqing Liu; Zhiqiang Xie and Jin Zhai. "Hybrid nano-

channel membrane based on polymer/MOF for high-performance salinity gradient power generation". *Nano Energy*, Volume 53, November 2018, pp. 643-649.

16. Shiojenn Tseng; Yu-Ming Li; Chih-Yuan Lin and Jyh-Ping Hsu. "Salinity gradient power: Optimization of nanopore size". *Electrochimica Acta*, Volume 219, 20 November 2016, pp 790-797.

17. Ramato Ashu Tufaa et al. "Progress and prospects in reverse electrodialysis for salinity gradient energy conversion and storage" *Applied Energy*. Volume 225, pp 290-331. 1 September 2018.

18. B.E. Logan and M. Elimelech. "Membrane-based processes for sustainable power generation using water". *Nature*, 488 (2012), pp. 313-319.

19. A. Cipollina; M. L. Di Silvestre; F. Giacalone; G. M. Micale; E. Riva Sanseverino; R. Sangiorgio; Q. T. T. Tran; V. Vaccaro and G. Zizzo. "A methodology for assessing the impact of salinity gradient power generation in urban contexts". *Sustainable Cities and Society*, Volume 38, April 2018, pp. 158-173.

20. AP Straub; NY Yip and M. Elimelech. "Raising the bar: increased hydraulic pressure allows unprecedented high-power densities in pressure-retarded osmosis". *Environ Sci Technol Lett*, 1 (2014), pp. 55-59.

21. David Acuña Mora and Arvid de Rijck. "Blue Energy: Salinity Gradient Power in Practice". *GSDR 2015 Brief*. 2015.

22. Caitlin Seyfried; Hannah Palko and Lindsay Dubbs. "Potential local environmental impacts of salinity gradient energy: A review". *Renewable and Sustainable Energy Reviews*. Volume 102, March 2019, pp 111-120.

23. S. E. Skilhagen. "Osmotic power—a new, renewable energy source". *Desalin Water Treat*, 15 (2010), pp. 271-278.

TS  
SR